ESTIMATING INDIVIDUAL MUSCLE FORCES IN HUMAN MOVEMENT

by
JOHN HENRY CHALLIS

A Doctoral Thesis

Submitted in partial fulfilment of the requirements for the award of

Doctor of Philosophy of the Loughborough University of Technology

July, 1991

ABSTRACT

Estimating Individual Muscle Forces in Human Movement

J.H.Challis

If individual muscle forces could be routinely calculated in vivo, non invasively, considerable insight could be obtained into the etiology of injuries and the training of muscle for rehabilitation and sport. As there are generally more muscles crossing a joint than there are degrees of freedom at the joint, determining the individual forces in the muscles crossing a joint is a non-trivial problem. This study focused on the development of the procedures necessary to estimate the individual muscle forces during a dumbell curl, and the measurement procedures required for the determination of the necessary input parameters. The procedures developed could easily be applied to other body movements.

A subject was filmed at 200 Hz performing a number of dumbell curls. The coordinates of significant body landmarks were reconstructed in a three-dimensional inertial reference frame using the direct linear transformation. Local reference frames were defined for the subject's forearm and upper arm. Measurements were made on a dry bone specimen with similarly defined reference frames, of the locations of the locations of the origins and insertions of the three modelled elbow flexors: the biceps, brachialis, and brachioradialis. Osteometric scaling was used to define the origins and insertions of the three elbow flexors on the experimental subject. Using a straight line model the length, rate of change of length, and the moment arms of the elbow flexors were determined throughout the filmed movements. Data smoothing and differentiation were performed using generalised cross-validated splines.

A model of each muscle consisted of a contractile component representing the muscle fibres, in series with an elastic component representing the tendon. The force produced by the contractile component was dependent on the length and velocity of the muscle fibres, and the active state of the motor units. These were modelled using non-linear relationships with the active state dynamics model based on calcium activity. Tendon elasticity was modelled using Hooke's Law.

Parameters for the force-length model for each of the muscles were determined using a non-linear optimization algorithm. The model parameters were systematically varied until a best fit was obtained to a number of experimentally determined joint torques measured during maximal isometric contractions at different degrees of elbow flexion. Parameters for the force-velocity relationship were obtained from the literature.

A number of different procedures were used to estimate the individual muscle forces during the activities studied. Individual muscle forces were most successfully estimated during maximal activity. During sub-maximal activity a new objective function, which minimised energetic cost, estimated muscle forces which were physiologically realistic.

STATEMENT OF RESPONSIBILITY

I hereby certify that I am responsible for the work within this thesis. The original work is my own, and has not been submitted to this or any other institution for a higher degree.

John Henry Challis
Loughborough University of Technology
July, 1991

Aspects of this work have been published as follows:-

Articles in refereed journals

Challis,J.H.,and Kerwin,D.G. (1991) Accuracy assessment, and control point configuration when using the DLT for photogrammetry. **Journal of Biomechanics** (in press)

Challis,J.H., and Kerwin,D.G. (1991) Calculating upper limb inertial parameters. ***Journal of Sports Sciences*** (in press)

Challis,J.H. and Kerwin,D.G. (1989) The selection of filtering and differentiation techniques for biomechanical data. ***Journal of Sports Sciences*** 7:2;175-177.

Articles in books

Challis, J.H., Kerwin, D.G., Ramsbottom R. and Boobis L. (1987) Muscle fibre composition, isometric leg strength and endurance in man. In: ***Biomechanics: Basic and Applied Research***, (Editors Bergmann,G., Kolbel,R., and Rohlmann,A.), pp613-618, Developments in Biomechanics Series, Martinus-Nijhoff Publishers, Dordrecht, Holland.

Challis,J.H., and Kerwin,D.G. (1988) An evaluation of splines in biomechanical data analysis. In: ***Biomechanics XI-B***, (Editors de Groot,G., Hollander,A.P., Huijing,P.A., and van Ingen Schenau,G.J.), pp1057-1061, Free University Press, Amsterdam.

Abstracts in refereed journals

Challis,J.H., and Kerwin,D.G. (1988) Quintic spline functions. ***International Journal of Sports Biomechanics, Research Digest*** 4:180.

Challis,J.H. and Kerwin,D.G. (1988) Optimal filtering and differentiation of biomechanical data using cross-validated splines. ***Journal of Sport Sciences*** 6:2;152.

Challis,J.H., and Kerwin,D.G. (1989) An evaluation of cine-photogrammetric techniques. ***Journal of Sports Sciences*** 7:1;72.

Challis,J.H., and Kerwin,D.G. (1990) An examination of the accuracy of anthropometric techniques. ***Journal of Sports Sciences*** 8:1;73-74.

Challis,J.H., and Kerwin,D.G. (1991) The experimental determination of muscle model parameters in vivo. ***Journal of Sports Sciences*** (in press)

Challis,J.H., and Kerwin,D.G. (1991) Estimation of individual muscle forces during a dumbell curl. ***Journal of Biomechanics*** (in press)

Conference presentations

Challis,J.H., and Kerwin,D.G. (1987) Numerical data management using quintic spline functions. Proceedings of the Sports Biomechanics Section, British Association of Sports Science No. 12, (Editor Bartlett,R.).

Challis,J.H., and Kerwin,D.G. (1990) The force-velocity relationship and isokinetics. AISEP International Conference, Loughborough, England, July 20-25.

Challis,J.H., and Kerwin,D.G. (1987) Optimal filtering and differentiation of biomechanical data using cross-validated splines. Proceedings of the British Association of Sports Science Conference, (Editors Alderson,J., Hale,T., and White,J.), pp136-145.

Challis,J.H., Yeadon,M.R., and Kerwin,D.G. (1991) Numerical differentiation of biomechanical data. Proceedings of the Sports Biomechanics Section, British Association of Sports Science No.16, (Editor Yeadon,M.R.).

ACKNOWLEDGEMENTS

I would like to express my thanks to:-
David Kerwin for acting as my supervisor, and for his advice and support over more years than we both care to remember,
Professor H.Thomason my Director of Research, for his support during the execution of the research contained in this thesis,
Fred Yeadon for his advice, and for reading the manuscript of this thesis,
my parents for their financial and moral support.

Finally for her continued support and encouragement, and for helping in ways I cannot begin to describe, I would like to express my sincere gratitude to my wife, Sue.

The financial support necessary to complete this thesis was due to a Studentship from Loughborough University of Technology.

DEDICATION

To Sue

TABLE OF CONTENTS

CHAPTER I

INTRODUCTION

INTRODUCTION

The works of Aristotle (384-322 B.C.), Leonardo da Vinci (1452-1519), and Giovanni Borelli (1608-1679) all contain reference to the need to relate the structure of muscle to the mechanical events which it initiates. In one of his many note books Leonardo da Vinci advised that when studying muscle one must "Make the rule and give the measurement of each muscle, and give the reasons of all their functions, and in which way they work and what makes them work."

Such an understanding of the function of muscle must include details of how the different muscles acting at a joint contribute to the net muscle moment they produce at the joint. Since the 15th century there have been many scientific and technological developments which have facilitated the measurement of human movement, but it is still very difficult to understand and explain human movement, particularly at a neuro-muscular level.

Kinematic and kinetic analyses facilitate mechanical descriptions of activities, but although it is well established that muscles are stimulated by electrical impulses from the nervous system, the way in which muscles are recruited to perform a given task is still unknown. If individual muscle forces could be routinely calculated in vivo, non invasively, considerable insight could be obtained into the etiology of injuries and the training of muscle for rehabilitation and sport. Such analyses may also provide insight into the muscular constraints which may limit athletic performance, and the optimization of performance in both sporting activities and the work place. This study focussed on the development of the procedures necessary to estimate the individual muscle forces during a dumbell curl, and the measurement procedures required for the determination of the necessary input parameters and variables. The procedures developed could easily be applied to other body movements.

It is hoped that this study will contribute to knowledge and understanding in the area of estimating individual muscle forces, and help to stimulate further research and developments that may eventually lead to individual muscle forces being calculated in vivo, on a routine basis.

1:1 THE PROBLEM AREA

The musculo-skeletal system consists of muscle and the linked skeletal system. Muscles comprise active muscle fibres and passive tendon; they move the skeleton in response to input from the nervous system. The action of a muscle is determined by the locations of the origin and insertion of the muscle and the line of action of the muscle relative to the joint or joints it crosses. To produce coordinated movement the nervous system must control the timing, sequencing, and degree of activation of a muscle crossing a joint. Not only must this recruitment take account of the contractile properties of the muscle fibres but allowance must also be made for the elasticity of the tendon in series with these fibres, and for any other muscles crossing that joint which may be capable of producing or contributing to the desired joint moment.

This study examined the methodology necessary to estimate the individual forces in the muscles causing

elbow joint flexion. There were various reasons for examining this particular joint. The joint is easy to isolate, and the musculo-skeletal geometry is relatively simple, making analysis easier, and hopefully providing greater insight. As well as these experimental consideration the elbow joint is interesting as it has a key function in many everyday movements and sports activities.

1:2 MODELLING

Eykhoff (1974) defined a model as

"...a representation of the essential aspects of an existing system (or a system to be constructed) which presents knowledge of that system in a usable form." (page 1)

All except the simplest models are collections of smaller units which could themselves be called models. The major model developed in the study is that for the estimation of the forces in the muscles causing elbow flexion. This model is a necessary conglomeration of smaller models, and the procedures required to provide input to this model also incorporated models. Many accepted experimental protocols are based on certain assumptions and simplifications which comprise a model, for example computing resultant joint moments and forces using inverse dynamics.

In the 18th century many philosophers and scientists (e.g. Lagrange and Laplace) believed in determinism, that is that the universe could be completely defined in terms of the mechanical concepts of force, matter, and motion. Kline (1953) has argued that it was this philosophy that lead to the belief in scientific perfectability. Pierre Simon Laplace (1749-1827) claimed that

"An intellect knowing at any given instant of time, all forces acting in nature, as well as the momentary positions of all things of which the universe consist, would be able to comprehend the motions of the largest bodies of the world and those of the smallest atoms in one single formula, provided it were sufficiently powerful to subject all the data to analysis.."

Such a modelling attempt is very unlikely, at least in the near future! The full potential power of modelling is still untapped and the limit of the modelling process to allow man to understand the world and all its aspect further has yet to be reached.

It is important that the model developed is detailed enough to consider all the pertinent aspects of the system being studied. Conversely the fewer parameters the easier they are to determine, and often the easier the model is to understand and apply. In developing models in this study, model complexity and the number of parameters were both considered, and a compromise sought between the two before a model was developed or adopted.

In the development of the models in this study, various simplifying assumptions have been made. Some of these simplifications are justified in terms of model validity, others are justified because the models are limited by the current state of knowledge in biomechanics, or other relevant disciplines. Paul and Berme (1985) highlighted this problem with reference to biomechanics

"...modelling of human mechanical function must be considered as an idealization as not yet supported by real data. It continues in the hope that solutions will be formulated to allow the elucidation of the very complex phenomena associated with body movement..." (page 49)

The criticism that certain simplifying assumptions lead to some factors being neglected can be made of most modelling studies, but this does not devalue this as an area of study. To counter these criticisms the model must be developed in such a way that all the pertinent knowledge is incorporated. In the area of the estimation of muscle forces, one of the chief shortcomings is the difficulty in acquiring subject specific data, e.g. the moment arms, the physiological cross-sectional areas, and the optimal lengths of the muscles involved in the activity. As a consequence it is the duty of the biomechanician to develop models in such a way that future knowledge can be easily incorporated. Hopefully these models can be updated and improved as new information is gathered and more advanced measuring techniques become available.

1:3 DETERMINATION OF THE INPUT DATA

Various parameters and variables were required as inputs for the different models used in this study. For example to compute the resultant joint moment at the elbow, the following were required: the location of the centre of mass, the moments of inertia, and the kinematics of the distal segment. To determine these and other required values, a number of techniques were employed. The techniques and models adopted are all discussed in the relevant chapters. To try and facilitate increased accuracy, comparison of techniques has been undertaken, and the most accurate technique used for subsequent analyses. Where possible the accuracy of the technique has been reported.

The methods used to determine the input data include: three-dimensional cine-photogrammetry, three-dimensional kinematics and kinetics, anthropometric modelling of body segments, and osteometric scaling.

1:4 MODEL VALIDATION

Hay (1987) claimed with direct reference to model validation that

"....failure to validate a model makes the results obtained when it is used suspect - and possibly even worthless." (page 1200)

Obviously some of the research literature is suggesting a possible avenue of study, and therefore the model is merely a suggestion of what could be attempted or of use. But if a modelling approach is to be of practical use, rather than a theoretical consideration, it is necessary to validate the model.

Model parameters are often determined using a least-squares technique, by minimising the difference between the model predicted values and some "real" values from the system being modelled. The validity of the model is often assessed by calculating the residual error between the model estimates and the "real" values. Although this is a test of the model, such a procedure does not give an independent measure of the model. An independent measure would give a clearer indication of the accuracy of the model. It is not always possible to get an independent measure, in which case a sensitivity analysis can be used. Here the elements making up the model are varied and the effect on the model predictions assessed.

By performing numerical checks on the various inputs to the models used and comparing results with the

published literature, it is hoped that these values are as accurate as possible. Where comparisons were not possible, models were examined using sensitivity analyses.

1:5 COMPUTERISATION

Many of the solutions to problems used in this study would not have been possible without the use of a computer, and the volume of data processed would have been reduced considerably without the use of a computer. Except where otherwise stated the computer programs were written in FORTRAN 77. They were initially implemented on a PRIME 750 mainframe using the Salford University FORTRAN compiler. They were then transferred to an Archimedes 440, and compiled and run error free, using the Acornsoft FORTRAN 77 compiler. All programs were portable, i.e running using the ANSI specification of FORTRAN 77, not using any extensions to that set.

1:6 STATEMENT OF PURPOSE OF STUDY

The purpose of this study was to develop and examine the methodology necessary to estimate the individual muscle forces contributing to elbow flexion. This methodology included the procedures used to determine input variables and parameters for the models used to estimate the muscle forces.

1:7 OVERVIEW OF THE STUDY

The study was performed in two basic phases. The first phase concentrated on the methodology required to derive the kinematic and kinetic data required as input to the model to estimate muscle forces. The second phase was devoted to this model and the application of it to investigate a basic movement, and to examine the muscle forces involved.

The methodology for the validation of these muscle force estimation procedures were examined and discussed. Before the muscle force estimation procedures could be implemented a number of input parameters were required for each of the models. The methods to determine these input parameters were also assessed. A number of estimation procedures were examined, and results compared.

Within each of the following chapters reference will be made to two experiments. The "static data capture" was used to initialise data in the muscle model, and to examine muscle forces in static (isometric) activity. The "dynamic data capture" was used to collect the data necessary for the analysis of a series of dumbell curls, so that dynamic activity could be investigated.

1:8 ORGANISATION OF THE CHAPTERS

Chapters II to VII were organised as follows:-

CHAPTER II - this chapter reviews some of the photogrammetric techniques used in biomechanics to obtain the position of points in space, and details the technique used in the present study. The accuracy of the technique adopted is assessed. The sources of error in the recording process are discussed. All the analyses undertaken in the present study were three-dimensional.

CHAPTER III - this chapter details the techniques used to determine the limb kinematics. As the reconstructed body landmarks contain noise, the reduction of noise in a signal is discussed and examined. For the determination of limb kinetics, derivative information is required; the calculation of derivatives is also examined in this chapter. Estimates are made of the errors associated with these state variables. The accuracy of the spline technique used to smooth and differentiate the data is compared with other commonly adopted techniques.

CHAPTER IV - this chapter is concerned with calculating the muscle moments acting about a joint. To determine the resultant joint moments and forces, the inertial properties of the distal rigid body must be known. Therefore this chapter contains details of the computation of the inertial properties of the subject's forearm and hand, and of the dumbell which the subject grasped. A sensitivity analysis is performed to estimate the accuracy of the resultant joint moments. The assumptions made in order to estimate the net moments caused by the muscles crossing a given joint are also discussed.

CHAPTER V - the purpose of this chapter is to present the model used to represent the muscles causing elbow flexion. The chapter is divided into six sections each dealing with some aspect of muscle modelling. The property to be modelled is first reviewed then modelling approaches are discussed before a model is adopted. The procedures for the determination and validation of the model parameters are also detailed.

CHAPTER VI - in this chapter the procedures used to estimate the individual muscle forces causing elbow flexion are detailed. There have been a number of techniques used to estimate muscle forces and these are reviewed. Procedures for determining muscle forces using static optimization procedures are discussed and compared. The final five sections present a new procedure for the estimation of individual muscle forces.

CHAPTER VII - here the results and findings from the previous chapters are summarised, and discussed. Recommendations for further study are made.

CHAPTER II

CINE-PHOTOGRAMMETRIC PROCEDURES

INTRODUCTION

Photogrammetry is the science and art of obtaining accurate measurements from photographic images. It is the purpose of this chapter to review some of the photogrammetric techniques used in biomechanics to obtain the position of points in space, and to detail the technique used in the present study. All the analyses undertaken in the present study were three-dimensional.

The analysis procedures in cine-photogrammetry can be divided into three stages:-

DATA PRODUCTION	filming
DATA REDUCTION	digitizing
DATA MANAGEMENT	reconstruction of points in space

Each stage will be dealt with in this chapter. The final stage includes the reduction of errors in the sampled signals, these errors will include random noise. The reduction of the amount of noise in the measurements will be covered in detail in the next chapter. The sources of error in the recording process are discussed.

2:1 LITERATURE REVIEW : CINE-PHOTOGRAMMETRIC TECHNIQUES

There are various techniques which purport to analyse human movement in three-dimensions. For this review these techniques were categorised into four main groups:-

- techniques in which the cameras optical axes have to intersect
- techniques in which the cameras' are in known positions
- techniques which incorporate the Direct Linear Transformation
- alternative techniques to the Direct Linear Transformation offering similar flexibility in camera positioning

Techniques falling into each of these groups will be discussed in detail with particular reference being made to their accuracy. In considering the accuracy of any of these techniques it is important to consider the dimensions of the space in which the measurements have been taken. These dimensions were not explicitly mentioned in some of the papers reviewed, in which cases it was not possible to fully assess the accuracy of these techniques.

2:1.1 HISTORICAL PERSPECTIVE

Attempts to analyse human movement in three-dimensions have only been reported in volume since the late sixties, but attempts were made to perform such analysis nearly one century earlier. Braune and Fischer (1987) in their work performed at the turn of the last century reported the trajectories of joint

centres in three-dimensions to within a few millimetres, using a four camera technique. Bernstein (1967) reporting work carried out in 1930, used appropriately placed mirrors so that one camera could record two views of the same activity, as if the cameras were orthogonally placed. He reported an accuracy of 1 mm in locating points in an analysis of punching.

The efforts that these early pioneers must have made to achieve an analysis of movement in three-dimensions without sophisticated projection and digitization systems and high speed digital computers, demonstrates the value that they must have placed in knowledge of the three-dimensional movement of the human body.

2:1.2 INTERSECTING OPTICAL AXES

Noble and Kelley (1969) used a technique which incorporated three cameras placed along three orthogonal axes, with their optical axes intersecting. Each camera was used to give the position of a point in an object space plane parallel to the camera image plane. Therefore a point was only accurately located if it was in all three of the primary object space planes simultaneously. This is only possible for one point: the origin of the object space coordinate system. They reported a mean error in the location of a sphere going down a helical slide; the mean deviation was 0.51 inches, with a range of 0.09 - 1.16 inches. Any movement away from each of the primary planes reduced the accuracy of the estimation of that point, as perspective error was introduced. There was no discussion of how to ensure that the optical axes of cameras intersected.

Miller and Petak (1973) suggested a multiple camera technique in which two or more cameras could be used. The optical axes had to intersect and cameras had to be set at specified angles to one another. Points were located in real space by using a basic image-object distance relationship. No report was made as to the accuracy of this technique.

Martin and Pongratz (1974a, 1974b) presented a technique involving two cameras placed orthogonally with their optical axes intersecting. Martin and Pongratz (1974a) outlined a series of equations based around simple geometric relationships which would correct for perspective error. Their equations were equivalent to those of Miller and Petak (1973) but employed less redundant data. Martin and Pongratz (1974b) compared the results of measuring points in three-dimensional space with and without correction for perspective error. The mean error along all three axes without correction was 1.1917 inches, and with correction for perspective error was 0.7644 inches; the means were calculated from Table I of Martin and Pongratz (1974b). The dimensions of the calibrated space were approximately 42 * 25 * 47 inches. These figures were not very accurate compared with techniques reviewed in later sections, but demonstrate the need to correct for perspective error. The incorporation of more redundant data should improve the accuracy of the reconstructions with this technique.

Bergemann (1974) advanced a technique in which the optical axes of the cameras had to intersect, and a common origin had to be in view of all cameras. Utilising certain geometrical relationships between real points in space and the image created in two cameras it was possible to locate points in space. Using this

technique Bergemann found a mean absolute error in locating points of a quarter of an inch. The dimensions of the test area were not explicitly stated in the paper.

The preceding techniques required the optical axes of the cameras to intersect, but the cameras also had to be positioned in certain configurations relative to one another. To overcome this problem van Gheluwe (1974), presented a technique in which the optical axes of the cameras had to intersect but the cameras could be positioned to suit the problems of the activity under investigation. He claimed an accuracy in locating points of better than 1 cm, but did not explicitly state the dimensions of the calibrated space.

Cappozzo (1983) advanced a technique in which the optical axes of two cameras had to intersect at the origin of the reference system, and lie in the X-Y plane of that reference system, but the angle between the cameras was not restricted. Using simple geometry and with as few as three control points, it was possible to reconstruct points in real three-dimensional space. Cappozzo estimated that the maximal systematic error with this technique was 0.44 mm in the X and Z directions and 1.3 mm in the Y. The calibrated space was not mentioned, although planar grids of 3.2 m by 1.5 m were used to calibrate the cameras.

The problem with these techniques is the positioning of the cameras so that the optical axes intersect. To allow for the difficulty and often resulting failure in correctly aligning the optical axes of the cameras, van Gheluwe (1975) proposed a series of equations that corrected for small errors in axes alignment. This would appear to be a very worthwhile contribution to this area but unfortunately the author does not present any figures for the resulting increase in accuracy. No other authors have acknowledged the adoption of this technique.

One final problem with such techniques is that in aligning the cameras it is assumed that the optical axis of the camera is perpendicular to the image plane of the camera. This is not strictly the case and as such must be seen as a source of systematic error that should be quantified.

2:1.4 CAMERAS IN KNOWN POSITIONS

Although for some of the techniques in the previous section it was necessary for the cameras to be in known positions, this section will deal with techniques that require the accurate positioning of the cameras, and measurement of their positions, but do not require the optical axes of the cameras to intersect.

Many of the techniques in this area rely on techniques originally developed in stereo-photogrammetry. Stereo-photogrammetry predominantly uses specially designed metric cameras that have precisely known internal geometry. Ayoub, Ayoub, and Ramsey (1970) used two metric cameras aligned so that their optical axes were parallel, the two photographs produced (a stereo-pair) when viewed through a stereo-comparator gave a three-dimensional image. In a static assessment of their technique they found the maximum percentage difference between the true and measured lengths was less than 2 percent of the length being measured, with a mean of 1 percent. The maximum length measured was 20 inches. To be able to produce the coordinates in three-dimensions, they required accurate details of the geometry of the

test field.

Lippert (1973) used standard stereo-photogrammetric techniques to study human movement in three-dimensions. A stereo-pair with a base distance of 0.40 m were used (Zeiss SMK - 40). Control points were reconstructed with a standard error of 0.07 μm, 0.07 μm, and 0.50 mm in the X, Y, and Z directions respectively, but he claimed to be able to measure translations of the human tibia to within 5 mm.

Penrose, Wood, and Blanksby (1976) assessed three techniques for three-dimensional cine-analysis, one with the cameras' optical axes intersecting at a common origin point, the second with the optical axes intersecting at a common target, and finally with the axes not aligned. For all three techniques the positions of the cameras had to be determined. The three techniques used the same principles as Bergemann (1974) to perform the three-dimensional reconstruction. Of the three techniques compared, that with optical axes intersecting at a common origin was marginally most accurate in locating known points in space. The mean errors for this technique were 0.0052 m ± 0.0047, 0.0064 m ± 0.0033, and 0.0041 m ± 0.0038 in the X, Y, and Z directions respectively. The dimensions of the space calibrated were not mentioned.

All of these techniques have removed the need for optical axes to intersect, and replaced it with the need to know precisely where the cameras are. Both these restrictions provide experimental problems.

2:1.5 THE DIRECT LINEAR TRANSFORMATION

Photogrammetric techniques predominantly use metric cameras. To obtain the three-dimensional information about points of interest with metric cameras two transformations are usually performed. The first transforms from some form of comparator coordinates to image coordinates, and the second transforms from image coordinates to object space coordinates. Non-metric cameras do not have a known image coordinate system so the first transformation is not possible. Abdel-Aziz and Karara (1971) showed that it is possible to combine these two transformations into one linear transformation, they called this the direct linear transformation (DLT). As only one transformation is used it is possible to use this technique with non-metric cameras. The DLT equations are:-

$$Ud + \Delta Ud = \frac{AX + BY + CZ + D}{IX + JY + KZ + 1.0} \qquad [2.1]$$

$$Vd + \Delta Vd = \frac{EX + FY + GZ + H}{IX + JY + KZ + 1.0} \qquad [2.2]$$

Where:-

Ud, Vd - are the digitizer coordinates of a point

ΔUd, ΔVd - are the errors associated with the coordinates

X, Y, Z - are the object space coordinates of a point

and A-K are the calibration coefficients.

To determine the calibration coefficients it is necessary to have at least six control points in the field of view of the camera. To locate a point in three-dimensional space using this technique, there must be two images of this point, usually produced by two cameras. A computer program was produced by Marzan and Karara (1975) to perform the DLT. In this paper the DLT was extended to incorporate a model of lens distortion. The full lens distortion model required a further five calibration coefficients to be added to the 11 used in the basic model. In testing the technique they reported a standard deviation in locating static points in space of 0.07 mm, the dimensions of the calibrated space were not mentioned.

The DLT is a technique which has been adopted by many researchers in biomechanics. The primary advantages of this technique are:-

non-metric cameras may be used
the optical axes of the cameras do not need to intersect
the positions of the cameras are arbitrary, and do not need to be measured
only two images of the object are required
more cameras are easily accommodated

Although the DLT technique was originally specified for still cameras, it is now used for cine-cameras. Various implementations of the DLT will now be reviewed with reference to the accuracy of this technique.

Van Gheluwe (1978) used his own derivation of the DLT equations to examine the accuracy of measuring seventeen lengths on a transparent cylinder. The mean deviation in calculating these distances "..fluctuated around 0.1 cm". The dimensions of the calibrated space were not given.

Shapiro (1978) using twenty control points showed an average deviation in locating points in space of 0.43 cm in the X direction, 0.51 cm in the Y direction and 0.44 cm in the Z direction, but did not give the dimensions of the space within which this accuracy was achieved.

Miller, Shapiro, and McLaughlin (1980) examined the DLT using ten control points for calibration. They reported root mean square (RMS) errors for the reconstruction of the control points of 0.176 cm for the X axis, 0.428 cm for the Y axis, and 0.468 cm for the Z axis. They did not explicitly mention the dimensions of the calibrated space but it can be estimated to be 0.25 m * 0.3 m * 0.3 m. They showed that if the positions, relative to a member reference frame, were available about three or more non-collinear markers affixed to a rigid body, it was possible to obtain the position and orientation of the rigid body, without first computing the position of the markers in the object space reference frame. When eight markers were affixed to the rigid body in a two camera condition the RMS errors for locating the origin of the member reference frame were 0.073 cm for the X axis, 0.096 cm for the Y axis, and 0.149 cm for the Z axis. They also reported results for the estimation of three-dimensional coordinates using one camera only with their modified DLT procedure. Analysis of their equations suggests that the results obtained from the one camera condition may not be unique. The authors did not find this a problem, as they provided results for the one camera condition. The one camera condition did not provide results as accurate as the two

camera conditions. In attempting to further increase the accuracy of the reconstruction they employed five extra calibration coefficients to allow for lens distortions; they reported that this resulted in no increase in accuracy. Using the initial estimates obtained from the DLT, Miller et al. (1980) used a similar procedure to Hatze (1988) (discussed later in this section) to improve the accuracy of the calibration coefficients by adjusting them in relation to the cameras internal and external parameters. They reported no increase in accuracy.

Marchand, Thiry, Sirois, Drouin, and Allard (1983) compared two techniques for three-dimensional cinematography. One technique was the DLT using 12 calibration coefficients, and the other was "...a classical reconstruction algorithm based on geometrical optics.". No further details of the second technique were given, and the use of the extra term in the DLT parameters was to allow for lens distortion although which aspect of lens distortion was not stated. The techniques were assessed by comparing their accuracy in predicting a series of lengths ranging from 176 mm to 252 mm. In addition to using two cameras, a mirror was used in a series of trials, so that one camera recorded two images. The dimensions of the calibrated space were not mentioned although the mirror used was 0.6 m * 0.9 m. Using the "classical technique" the mean error in predicting the lengths was 10 mm with two cameras, and 40 mm with a mirror and one camera. The DLT method produced an error of 7 mm in both cases.

In an attempt to examine in more detail how different aspects of the DLT technique affected accuracy, Wood and Marshall (1986) examined a total of sixteen conditions. They set up their cameras in two ways: one gave a camera base to object distance ratio of 2:1, the other gave a ratio of 1:1. Using a calibration structure containing 43 known points, four different combinations of control points were examined. These were: 30 control points evenly distributed over the calibration structure; 11 control points evenly distributed over the calibration structure; seven control points evenly distributed over the calibration structure; and 11 control points clustered around the central vertical axis of the calibration structure. Sets of both 11 and 12 calibration coefficients were calculated, with the extra coefficient being used to correct for symmetrical lens distortion. Accuracy for the sixteen conditions was assessed by calculating the RMS error between known points on the calibration structure and their calculated locations. Three way analysis of variance was used to compare the conditions. The authors made three conclusions based on their results: results were poor if extrapolation occurred outside the range of the control points; a 1:2 camera base to object distance was superior to a 1:1 ratio, and 11 calibration coefficients were better than 12. The lowest average RMS error for all three axes was 5.7 mm, for the 30 control point condition with a ratio of 2:1. They employed a calibration structure of 3.5 m * 2.5 m * 1.5 m with the control points being located to within ±1 mm.

Hatze (1988) presented a modified version of the DLT in which the DLT calibration coefficients were constrained so that the orientation matrix of the object coordinate system to image coordinate system was guaranteed to be orthogonal. This matrix should be orthogonal although Hatze suggested that in the conventional solution the resulting matrix is not. Analysis by Walton (1981) showed that the orthogonality condition was preserved in this matrix for his analysis; even so Hatze's Modified DLT (MDLT) produced more accurate results than the conventional solution. A calibration structure of 0.425 m * 2.04 m * 2 m was used on which 30 control points were measured to an accuracy of "better than ±1 mm". A number of

different calibration structure configurations and lens distortion models were examined. The lowest RMS errors were reported for the MDLT with correction for radial and asymmetrical lens distortion, these were 0.7 mm, 0.7 mm, and 0.8 mm in the X, Y, and Z directions respectively. For the same condition the basic DLT produced errors of 5.3 mm, 4.2 mm, and 4.8 mm. This represents a significant improvement.

Hatze (1988) used the computer programme of Marzan and Karara (1975) to perform the DLT; this programme solves a system of normal equations to arrive at a solution. This linear least squares technique can result in significant rounding errors which directly affect results (see section 2:2.3). In his MDLT another least squares technique was used which Hatze claimed was "numerically stable". This different linear least squares technique could account for some of the differences in the two techniques, rather than Hatze's new formulation of the DLT.

The accuracy reported by Hatze (1988) for the location of the points is better than the accuracy reported in measuring the control points. In contemporary photogrammetric practice (e.g. Brown, 1978) the positions of the control points are only considered as approximations and are adjusted along with parameter estimation. The DLT was not designed as a technique to do this, and it has yet to be proved that it can. Hatze (1988) and others (e.g. Wood and Marshall, 1986), used the estimated positions of the control points to assess accuracy in their papers. This is not an independent measure, and cannot be considered a real test of the accuracy of these techniques as the control points were used to calibrate the system initially. Reconstruction of control points reflects the accuracy of the mathematical techniques employed and any unaccounted for aspects of the photogrammetric process (including noise); it does not necessarily reflect the accuracy of the technique in locating unknown points in space.

Ball and Pierrynowski (1988) addressed the need for a calibration object which fills all of the space in which the activity is to take place. They used a calibration object smaller than the total volume to be calibrated and calibrated the total space by moving the calibration structure. The calibration structure was placed in a master position and calibration coefficients calculated. The calibration structure was then moved and its position calculated with reference to the master position, this resulted in twice the number of control points being available. Given the larger number of control points the calibration coefficients were recalculated. This procedure was repeated for all calibration structure positions. As movement of the calibration frame was not constrained so that each new position overlapped with the old position a non-linear least squares technique was used to reduce extrapolation errors. In a volume of 2 m * 2 m * 2 m a smaller calibration structure was moved around to 125 different positions, the lowest mean error in locating a point was 10.2 mm. The authors did not mention explicitly the size of the calibration structure used, but it is presumed that there was some overlapping of the images of the calibration structure (which the authors claim is not required). Information on the errors arising when no overlap occurs would have been of value in assessing this technique. In a slightly larger calibrated space Wood and Marshall (1986) reported errors in locating points of around half the magnitude of those reported by Ball and Pierrynowski (1988). The technique of Ball and Pierrynowski is of interest, but the paper does not give a complete analysis. If an image has three non-collinear control points overlapping with the original position, it should then be possible to locate all the remaining points on the control structure in the object space. This would

seem to be a simpler solution to the problem than that recommended. The analysis was performed using WATSMART (Northern Digital, Canada) which is a light emitting diode (LED) opto-electronic movement measurement system.

2:1.6 ALTERNATIVE TECHNIQUES

Fioretti, Germani, and Leo (1985) presented a technique for "very close-range" photogrammetry. Rather than recourse to the principles of photogrammetry they used a black box technique where the digitizer coordinates were related to the object space coordinates by a third order Taylor series. There were 35 parameters associated with each object space coordinate, and 105 to identify a point in three-dimensions. The calibration object had to contain at least 35 control points. A calibration structure of 0.5 m * 0.5 m * 0.5 m containing 126 control points was used. Model coefficients were determined using 63 control points. A second set of control points, which were not used for calibration, were located with a mean RMS error for all axes of 0.2388 mm.

The DLT method requires a three-dimensional calibration structure. This presents some problems. Accuracy is reduced if points are considered outside of the calibration structure (Wood and Marshall, 1986). This being the case the structure must occupy at least the same space as the activity, therefore for one running stride a volume of around 9 m^3 (2 m * 1.5 m * 3 m), would be required. A structure of this size causes many restrictions particularly as it would be very large for field work. Ideally the structure should be mechanically very stable to ensure accuracy and yet be portable. To circumvent these problem some researchers have calibrated cameras another way, by using the technique of "analytical self-calibration" (Kenefick, Gyer and Harp, 1972). Brown (1956) was the first to utilize such a technique, in which all the necessary variables (eg. control points) are carried in the computations as constrained parameters. By doing this, any errors in the control points and any parameters can be accounted for. This work has been significantly developed by Duane C. Brown (eg. Brown, 1956, 1968, 1978). Using this technique it was discovered that it is not necessary to view a three-dimensional distribution of control points, but that multiple views of a two-dimensional distribution of control points is sufficient. The problems of manufacture and transportation of a calibration structure are greatly reduced when a two-dimensional structure is required rather than a three-dimensional one.

Woltring (1978, 1980) developed a technique which did not have the full flexibility of "analytical self-calibration", but only needed multiple views of a two-dimensional calibration structure to perform a three-dimensional calibration. The calibration structure needed to contain only four control points. Woltring (1980) assessed this technique, using a suitably placed mirror so one camera could obtain two views of the same image, to estimate intermarker distances on a 1.27 m rod placed in the field of view. A sample standard deviation of the estimation of the lengths was found of 1.4 mm in the centre of the calibrated volume, and 2.3 mm at the upper and lower edges. When the data was subjected to a 5 Hz Butterworth filter (in both forward and reverse directions to eliminate phase lag) the errors were reduced to 0.8 mm and 1.0 mm respectively. The dimensions of the calibrated space were 1.2 m * 1.2 m * 1.2 m. The author commented that some of this error could be accounted for by the mirror not being perfectly flat.

Woltring, McClay, and Cavanagh (1989) extended this technique so that calibration could be performed from a group of markers on the body. In the reported study, which examined human walking, four markers in known relative positions were placed on each segment. Model parameter initialisation was performed using a constrained DLT with the DLT parameters being estimated from the groups of markers. Once parameter initialisation had been performed the procedure of Woltring (1978,1980) was implemented. Measurement noise was estimated to be less than 0.5 mm. This paper used SELSPOT-II (Selcom, Sweden), a LED based opto-electronic movement measurement system.

Dapena, Harman, and Miller (1982) also advanced a technique which irradicated the need for a three-dimensional calibration structure. The internal camera parameters were calculated by taking measurements from the image of two planar calibrated crosses. Using an object of known length in the field of view of the camera they calculated the external camera parameters. If the internal and external camera parameters are known for two cameras it is possible to locate in three-dimensions any points viewed in both cameras. In a space of 37.5 m^3 (5 m * 5 m * 1.5 m) the root mean square errors in locating fifteen known control points were 15 mm, 13 mm, and 6 mm, these represented relative errors in length of 0.5 percent, 0.7 percent, and 0.5 percent in the X, Y, and Z directions respectively. The major advantage of this technique was that to calibrate a large volume, all that was needed were two suitably measured crosses and an object of known length in the space where the activity was to take place.

2:1.7 CONCLUSION

There have been a variety of techniques used to measure the locations of points in three-dimensions. It is hard to make a direct comparison of accuracy of the different techniques because of variations in the dimensions of the spaces studied. The method of assessing accuracy also varies between researchers with some comparing estimated with known lengths (e.g. van Gheluwe, 1978; Woltring, 1980), whilst others use known points (e.g. Wood and Marshall, 1986; Hatze, 1988). A problem of the validity of accuracy levels arises if control point reconstruction is used as the measure of accuracy.

2:2 THE DIRECT LINEAR TRANSFORMATION

The preceding literature review illustrates that the DLT gives accuracy levels comparable to, if not better than, many of the other techniques available. The modification proposed by Hatze (1988) offers even greater accuracy. Its chief limitation is that control points must be distributed throughout the space in which the activity is anticipated to take place. An analysis of the dimensions of the human arm and the movements to be studied revealed that a space of 1.0 m by 0.6 m by 1.0 m would be sufficient to record all the information required. It was therefore feasible to adopt the DLT technique for the acquisition of the three-dimensional data in this study, as it was not a problem to manufacture a calibration frame of suitable size to provide the control points.

A derivation of the DLT equations is given in Appendix A, including details of the lens distortion model. In the following sections further details of the DLT are presented.

2:2.1 THE CALCULATION OF THE CALIBRATION COEFFICIENTS

As well as filming the activity in question, a suitable distribution of control points must also be filmed; these are normally located on a calibration structure. Digitization of the control points (known three-dimensional locations on the calibration structure in the field of view) enables them to be used as inputs to the equations detailed in the Appendix A. The resulting system of equations can be represented as:-

$$A.x = B \qquad [2.3]$$

where:-

A - is an m * n matrix composed of the object space coordinates of the control points, and the digitizer coordinates of the control points

m - is twice the number of control points

n - is the number of calibration coefficients (11)

x - is an unknown column vector containing the camera specific calibration coefficient

and B is a column vector containing the digitizer coordinates of the calibration points.

To make this system of equations determinant it is necessary to film and digitize at least 6 control points. Given this information the system of equations can be solved giving the calibration coefficients. This procedure has to be performed for each camera. The solution of this system of equations is performed using singular value decomposition, details of which are given in section 2:2.3.

2:2.2 SPACE INTERSECTION

Once the calibration coefficients have been calculated they can be combined with the digitizer coordinates of the points of interest to obtain the object space coordinates of those points. This gives:-

$$A.x = B \qquad [2.4]$$

where:-

A - is an m * n matrix containing the digitizer coordinates of the unknown point, and the calibration coefficients

m - is 2 * the number of images recorded

n - is three, the number of unknown object space coordinates

x - is an unknown column vector containing the object space coordinates of the digitized point

and B is column vector containing the digitizer coordinates of the unknown point and the calibration coefficients.

To make this system of equations determinant for a three-dimensional analysis it is necessary to combine data from at least two images, obtained from different views. For cine-photogrammetric analysis these images must be synchronised, see section 2:3.5. This system of equations is solved using the singular value decomposition for every digitized point.

2:2.3 LINEAR LEAST SQUARES

For both the calculation of the calibration coefficients, and space intersection, the general problem is to

find a vector x which satisfies:-

$$A.x = B \qquad [2.5]$$

In a least squares sense the problem is to minimise the residual (r):-

$$r = |A.x - B|^2 \qquad [2.6]$$

To solve the least squares problems specific to the DLT, Marzan and Karara (1975) and Walton (1981), have used normal equations, where the problem is reformulated as:-

$$(A^T.A).x = A^T.B \qquad [2.7]$$

Where ^{T} refers to the transpose of a matrix.

Given this reformulation the system can be solved using one of the forms of Gaussian elimination. The matrix resulting from the product of A and its transpose often has a very high condition number, which can result in very high round-off errors in the solution (Golub and van Loan, 1983). Indeed if the matrix is near singular the routine is guaranteed to fail.

Golub and Reinsch (1971) presented a method for factorizing a real matrix A into three matrices U, E, and V:-

$$A = U.E.V^T \qquad [2.8]$$

Where:-

A - is an m * n real matrix

U - is an m * m orthogonal matrix

V - is an n * n orthogonal matrix

and E is an m * n diagonal matrix where for $i \neq j$ $e_{ij} = 0.0$, and the diagonal contains the singular values of A.

This factorization is called the singular value decomposition (SVD).

The singular values contained along the diagonal of matrix E permit the calculation of the rank and condition of matrix A; these give an indication of the strength of the solution to equation 2.5.
The condition number is:-

$$cond(A) = \frac{e.max}{e.min} \qquad [2.9]$$

Where e.max and e.min are the maximum and minimum values of e_{ij} respectively.

This value will give an indication of the anticipated error magnification in solving equation 2.5 (Forsythe, Malcolm, and Moler, 1977). To improve the accuracy of the solution any e_{ij} which falls below a certain tolerance (estimated from the precision of the data) is set to zero. The rank is the number of non-zero

terms along the diagonal of E. If there are not many, matrix A is said to be rank deficient, in which case a high condition number is expected. The solution of normal equations for estimating linear least squares will fail if the matrix is rank deficient. If the matrix A is rank deficient this is a reflection on the input data. This is unlikely to occur during space intersection. If it occurs during the calculation of the calibration coefficients there are three solutions: attempt to identify and remove erroneous control points; attempt to improve the accuracy of the data by digitizing more or new control points and see if the rank increases; if the digitized values of the control points contain stochastic errors, averaging of multiple digitizations of these points may improve the solution. If this fails the activity will have to be re-filmed.

An orthogonal matrix has the following properties:-

$$U.U^T = I \qquad [2.10]$$

$$U^T = U^{-1} \qquad [2.11]$$

Therefore assuming adjustments have been made to E, a solution to equation 2.5 would be:-

$$U.E.V^T.x = B \qquad [2.12]$$

by substitution:-

$$V.(\text{diag } 1/e_{ij}).U^T.B = x \qquad [2.13]$$

which would minimise equation 2.6.

This solution has a number of advantages over the normal equations used by Marzan and Karara (1975) and Walton (1981). The SVD will work even when matrix A is near singular: although the solution to equation 2.5 will not be very accurate, normal equations would fail under these conditions. Also compared with other least squares techniques the SVD is less susceptible to rounding errors (Golub and van Loan, 1983).

2:2.4 ACCURACY ASSESSMENT

There have been two techniques used to assess the accuracy of photogrammetric techniques. One is to reconstruct known points and evaluate the difference between their true value and estimated value (e.g. Fioretti et al., 1985; Wood and Marshall, 1986). The other is to look at the difference between known lengths in the calibrated space and their estimated lengths (e.g. van Gheluwe, 1978; Woltring, 1980). With the first technique it is possible to separate the inaccuracies associated with each axis, with the second technique these inaccuracies are grouped together. Using the DLT researchers have reconstructed control points to assess accuracy, but these results can be flattering as these points were used to perform the calibration (Wood and Marshall, 1986; Hatze, 1988). An improved procedure is to have a second set of points with which to test the technique. This is difficult to achieve when the researcher is trying to incorporate as many redundant points in the model as possible. These methods of estimating accuracy are now compared.

The protocol used in this investigation was the same as for the static data capture unless otherwise stated. The mean values of ten digitizations of the control points on the calibration structure were used as inputs to the DLT. Three procedures were used to assess the accuracy and to look at the problems associated with different assessment procedures. These were:-

1. Relocation of control points
2. Location of a group of known points (digitized only once)
3. Estimation of a number of lengths

To obtain a set of known points with which to assess the DLT the calibration structure was rotated through 180 degrees about a central vertical axis, the calibration structure is shown in figure 2.1. The frame occupied the same space but as the positions of the control points on the calibration structure were not symmetrical, they did not occupy the same positions as they had prior to rotation. The locations of the control points on the rotated calibration structure were then calculated, giving a second set of control points. This rotated frame was also used for estimating lengths. This was done by computing the distances between all the control points, giving a total of 1275 lengths. Two frame configurations were used: the full structure containing 51 control points; and a "Christmas tree" like structure which gave 11 control points. The accuracy of the known measured locations of the control points, on both the calibration structure and rotated calibration structure are discussed in section 2:4.1.

The results are presented in table 2.1. Both calibration structures produced high accuracies when evaluated by the reconstruction of their own control points. When subjected to the more rigorous assessment of the second set of control points the accuracy of both was reduced. The lowest RMS error was found in the reconstruction of the 11 control points of the "Christmas tree" like structure. With so few points the DLT could map directly onto these points. This could not be done with the 51 control points on the calibration structure. When accuracy was assessed using the second set of control points the full structure was twice as accurate as using the "Christmas tree" configuration. The estimation of the lengths also shows the error arising when using reconstruction of control points to evaluate accuracy. These results illustrate the error that can arise in evaluating accuracy by reconstructing the control points, particularly when there are only a few control points. To get a true estimation of the accuracy, an alternative assessment criteria to that of reconstruction of the control points used in the calibration is necessary.

For the dynamic data capture only the reconstruction of control points was available for accuracy assessment. The results in table 2.1 indicate that the more control points used, the closer the reconstruction of control points comes to giving a true estimation of reconstruction accuracy. Accuracy figures for the dynamic data capture must be considered in this light. The RMS errors for the reconstruction of the control points were 0.0012 m, 0.0033 m, and 0.0013 m for the X, Y, and Z axes respectively.

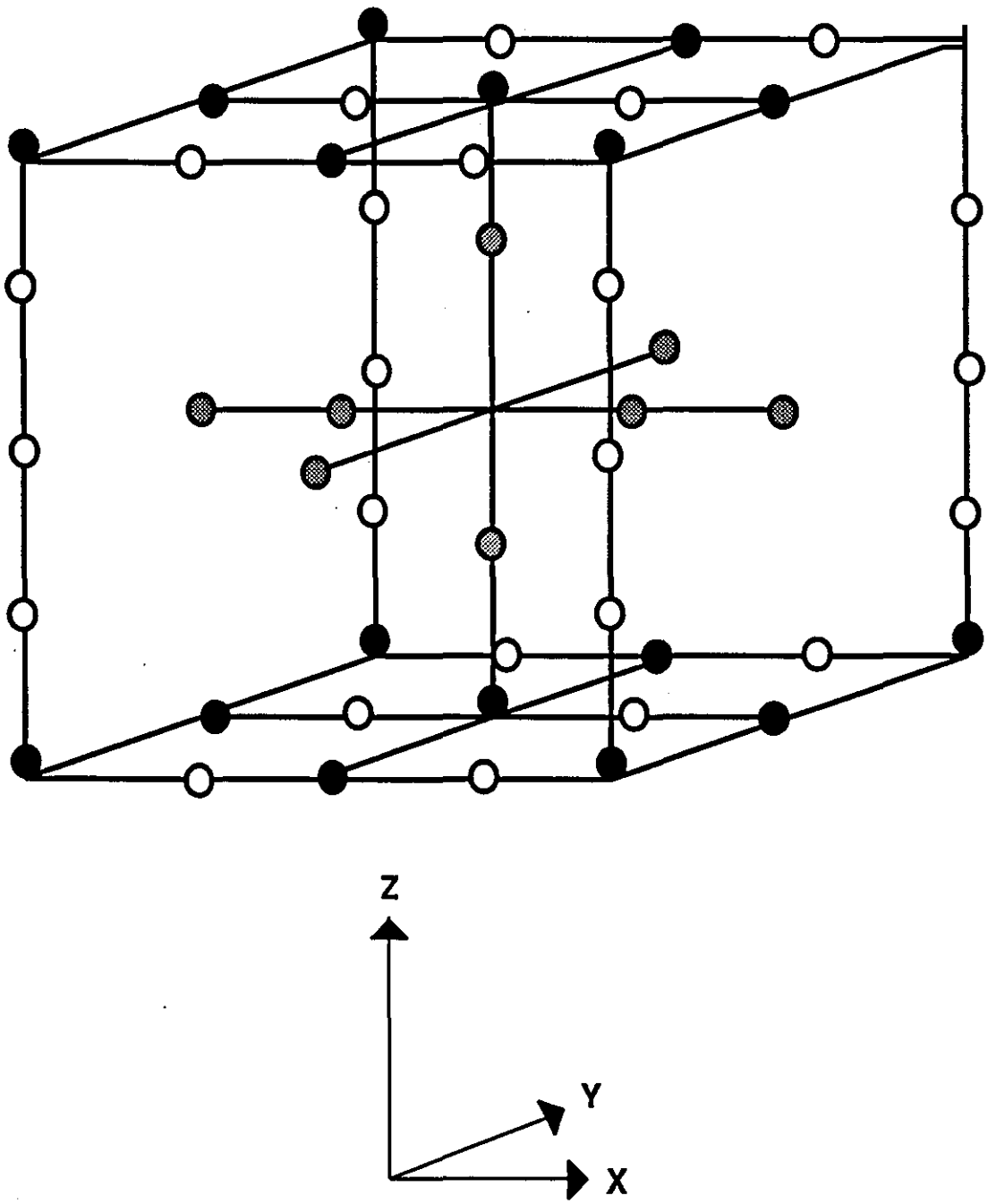

FIGURE 2.1 - A diagram of the calibration frame.

TABLE 2.1 - The root mean square errors in locating points in three-dimensions for the static data capture.

NUMBER OF CONTROL POINTS	AXIS	CONTROL POINTS	SECOND SET OF CONTROL POINTS	INTER CONTROL POINT DISTANCES
	X	0.0012 m	0.0043 m	
11	Y	0.0008 m	0.0055 m	0.0082 m*
	Z	0.0021 m	0.0043 m	
	X	0.0016 m	0.0025 m	
51	Y	0.0016 m	0.0021 m	0.0038 m*
	Z	0.0019 m	0.0023 m	

(N.B. - * RMS error for the intercontrol point distances compares the estimated lengths with the actual lengths, these measures are not specifically associated with one axis.)

2:2.5 THE DISTRIBUTION OF CONTROL POINTS

Control points must be contained in the field of view of each camera. This can be done by measuring the positions of various points naturally occurring in the field of view, but it is more common to place a calibration object which contains a number of control points in the space to contain the activity of interest, take some film of it, remove it and perform the activity in that space. Van Gheluwe (1978) constructed a calibration object containing 21 control points. It consisted of three perpendicular rods that intersected at a common origin giving a three-dimensional cross like structure. This configuration has become known as a "Christmas tree" (Wood and Marshall, 1986; Hatze, 1988). Walton (1981) hung spheres from the ceiling to provide control points. Wood and Marshall (1986) used a wedged shaped structure with diagonal struts, on which there was 43 control points. Hatze (1988) used a three-dimensional rectangle with two vertical struts in the front and back of the rectangle, providing 30 control points.

In the manufacture of a calibration structure there are a number of points which must be considered. The structure should fill all of the space in which the activity is to happen. The control points should be viewable from all camera positions, and they must be measured accurately. The accuracy of the location of points in the object space must be considered limited by the accuracy with which the control points have been measured. Other issues regarding the mechanical stability of the calibration structure are dealt with in section 2:4.1. To further examine the influence of the distribution of control points on the resulting data, two experiments were performed. The protocol used in these studies was the same as in the static data capture unless otherwise stated.

Experiment 1.

Both Wood and Marshall (1986) and Hatze (1988) grouped a set of control points so that they had a "Christmas tree" type structure. They found that this design of structure produced a less accurate calibration than when points were selected from all over their control objects. In neither study was it possible for them to precisely mimic the "Christmas tree" structure with the calibration structure used. The calibration structure used in this study was shown in figure 2.1. This structure was effectively the rectangle of Hatze (1988), albeit with smaller dimensions, with a "Christmas tree" inside, which allowed both types of structure to be examined. The calibration structure of Hatze (1988) did not contain any control points inside the structure; the influence of this is also examined.

Five different calibration structure configurations were examined. These were:-

Frame Configuration A - this was the "Christmas tree" like structure comprising the central cross structure of the calibration structure. It contained 11 control points.

Frame Configuration B - this structure used the four vertical corner posts of the calibration structure. This mimicked using four marked poles to provide the control points. It contained 20 control points.

Frame Configuration C - this used the corner balls of the calibration structure only. This represents the minimum case if a rectangular or cuboid frame was used, or if balls were suspended from the ceiling. It contained only 8 control points.

Frame Configuration D - was a "kite" like structure comprising the "Christmas tree" structure of A with a horizontal cross on the top and bottom orientated the same as the central cross of the "Christmas tree". It

contained 23 control points.
Frame Configuration E - was composed of all the points on the outer three-dimensional rectangle of the calibration structure. This is similar to the frame used by Hatze (1988). It contained 36 control points. These different control point configurations are shown in figure 2.2.

In light of the investigation reported in the previous section the accuracy associated with these frames was assessed by locating the points on the rotated frame, and by estimating of the distances between the points on the rotated frame.

The results are presented in table 2.2. The results for the reconstruction of the control points confirms that the fewer control points that are used, the more flattering is the reconstruction of control points as a measure of photogrammetric accuracy (see previous section). Frames A and D gave the least accurate results, with the remaining frames giving very similar results. Frame C with only eight control points gave very good results compared with Frame E which contained over four times the number of points, distributed throughout the calibrated space.

To assess where the deficiencies in these frame configurations occur, a further analysis was undertaken. Calibration was performed using the points from one of the frame configurations, then the digitizer coordinates of the rotated frame for another frame configuration were input and these points had to be estimated. As the true locations were known, the root mean square error could be calculated and this was averaged for all three axes.

The results for this analysis are presented in table 2.3. For frame configurations B, C and E there were no points included on the inside of the calibrated space. Frame configuration A included some of the inside points, so calibration was performed using frames B,C, and E which then had to locate the points making up frame configuration A. Results show that the more control points used in these configurations the better the accuracy, although these increases were very small.

Frame configurations A and D did not have any control points around the sides, so they could be evaluated for these points using the other frame configurations. Results for both of these frame configurations show that configuration D is more accurate for these side points than configuration A. The inaccuracies for estimating the control points on the side of the calibration frame using frame configurations not containing these points, are greater than the inaccuracies for the location of the inside control points with calibration frames only containing the outer control points. Frame configuration E was marginally more accurate than the full calibration structure in all cases.

On this analysis the "Christmas tree" style frame was much less accurate than frame configurations which surrounded the space to be calibrated. The "Christmas tree" style frame was less accurate at estimation around the sides than those frames which had "sides" were at estimating internal points. These results indicate that it is more important to surround the space in which the activity is to take place than to have control points inside the space, although there may exist other control point configurations which

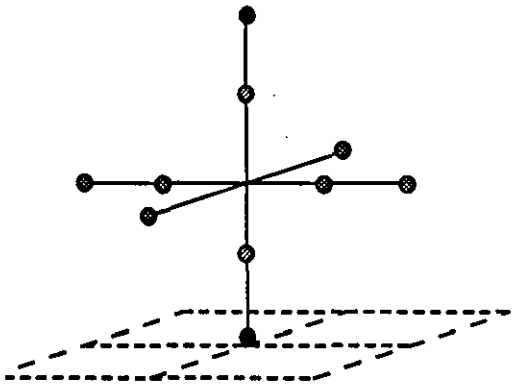

Control Point Configuration A

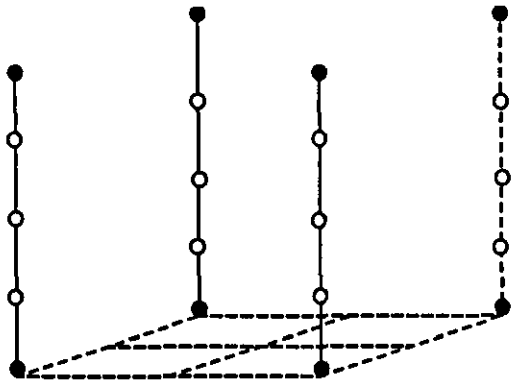

Control Point Configuration B

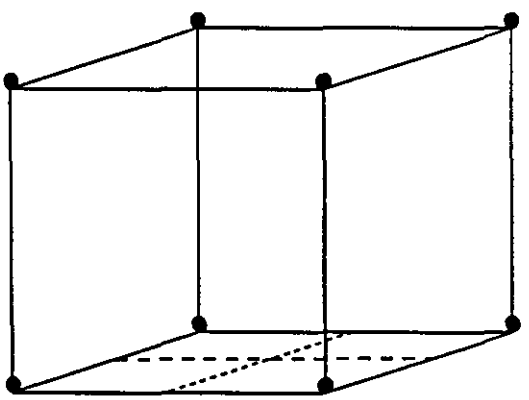

Control Point Configuration C

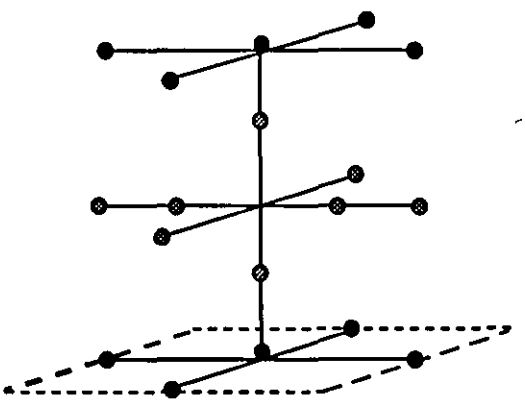

Control Point Configuration D

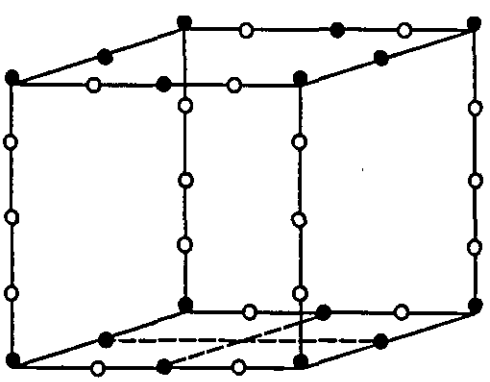

Control Point Configuration E

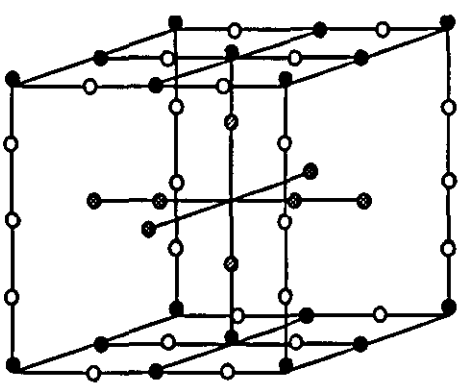

The Complete Frame

FIGURE 2.2 - Different control point configurations, using the calibration frame.

TABLE 2.2 - The root mean square errors in locating points in three-dimensions using different calibration frame configurations for static data capture.

CONTROL POINT CONFIG -URATION	AXIS	CONTROL POINTS	SECOND SET OF CONTROL POINTS	INTER CONTROL POINT DISTANCES
	X	0.0012 m	0.0043 m	
A	Y	0.0008 m	0.0055 m	0.0082 m*
	Z	0.0021 m	0.0043 m	
	X	0.0009 m	0.0023 m	
B	Y	0.0011 m	0.0019 m	0.0034 m*
	Z	0.0008 m	0.0022 m	
	X	0.0006 m	0.0023 m	
C	Y	0.0008 m	0.0020 m	0.0035 m*
	Z	0.0008 m	0.0022 m	
	X	0.0012 m	0.0033 m	
D	Y	0.0014 m	0.0031 m	0.0055 m*
	Z	0.0023 m	0.0026 m	
	X	0.0016 m	0.0024 m	
E	Y	0.0013 m	0.0020 m	0.0035 m*
	Z	0.0012 m	0.0022 m	

(N.B. - * RMS error for the inter-control point distances compare the estimated lengths with the actual lengths, these measures are not specifically associated with one axis.)

TABLE 2.3 - The root mean square errors, averaged for all three axes, in locating points in three-dimensions using different calibration frame configurations (static data).

CALIBRATION FRAME	CONFIGURATION OF POINTS ON SECOND FRAME				
	A	B	C	D	E
A	0.0027 m	0.0056 m	0.0068 m	0.0028 m	0.0051 m
B	0.0022 m	0.0019 m	0.0023 m	0.0020 m	0.0020 m
C	0.0024 m	0.0018 m	0.0019 m	0.0022 m	0.0020 m
D	0.0021 m	0.0036 m	0.0045 m	0.0022 m	0.0032 m
E	0.0021 m	0.0021 m	0.0027 m	0.0020 m	0.0021 m
COMPLETE FRAME	0.0023 m	0.0024 m	0.0030	0.0021 m	0.0023 m

may give superior accuracy.

Experiment 2.
If the activity occurs outside of the space that has been calibrated, errors will be introduced due to extrapolation. Wood and Marshall (1986) reported a 50 to 100 percent increase in the error associated with locating a point when it was outside the calibrated space. The distance of the points from the outside of the calibrated space was not reported. The errors associated with extrapolation outside of the calibrated space are investigated here.

The data used were from the static data capture. The frame was considered in two halves. The bottom half of the frame was used for calibration and then the top half of the frame was used to estimate the errors of extrapolating out of the calibrated space. Using the data from the rotated calibration structure, the RMS errors in locating points in the calibrated half of the frame were 0.0024 m, 0.0019 m, 0.0024 m along the X, Y and Z axes respectively, whilst for the uncalibrated space they were 0.0032 m, 0.0034 m, and 0.0015 m. Surprisingly the accuracy in locating points for the Z axis was better, but for the other two axes the error was approximately 50 percent greater.

In any three-dimensional analysis of movement to maintain measurement accuracy every effort should be made to ensure that the whole of the space in which the activity is to take place is calibrated.

2:2.6 CAMERA POSITIONING

Wood and Marshall (1986) examined DLT accuracy when the cameras had different angles of convergence. Rather than express the angle of convergence they used a distance:base ratio (distance from the mid-point between the cameras to the object: intercamera distance). They used two ratios: 1:1 which (assuming that the optical axes of the cameras intersected at the object) gave an angle of convergence of 90 degrees, and 1:2 which gave an angle of 53 degrees. Analysis of variance between these two conditions showed that the vertical axis showed no significant difference between conditions, but there was a significant difference for the other two axes with an angle of convergence of 90 degrees giving greater accuracy than 53 degrees.

In a theoretical analysis Abdel-Aziz (1974) examined the accuracy of object space reconstruction in a two camera condition. He showed that assuming the positioning of the cameras was symmetrical, the accuracy of reconstruction depended on the outer orientation parameters of the cameras. These parameters were the intercamera distance, the angle of convergence, and the distance from the mid-point between the cameras to the point of convergence. When varying the angle of convergence whilst keeping the distance of the cameras to the point of convergence constant, his analysis confirmed the results of Wood and Marshall (1986), that 90 degrees of convergence would give greater accuracy than 53 degrees. The greatest accuracy under these conditions was reported for an angle of convergence of 80 degrees, or using the ratio of Wood and Marshall (1986) this would be 1:1.7. This analysis by Abdel-Aziz (1974) indicates that the greatest inaccuracies are expected for the depth axis, which is an axis perpendicular to the line between the two cameras.

Although the preceding discussion has shown that appropriate camera positioning can result in improved accuracy, camera positioning must also reflect the need for a clear view of all the control points and the need to identify the marked body landmarks to be digitized. For the static data capture an angle of convergence of 85 degrees was used with both cameras being placed the same distance from the point of convergence. According to the formulae developed by Abdel-Aziz (1974), this angle gives good accuracy although not the maximum possible. For the analysis undertaken, 85 degrees permitted viewing of the markers from both cameras for more of the activity than any of the other camera configurations tested.

For the dynamic analysis one camera was used which recorded two views of the same subject due to the appropriate placement of a mirror. A pilot study using a still camera was undertaken to determine the camera position. The camera position selected allowed all control points on the calibration structure to be clearly visible in both views. It also permitted better viewing of the markers on the subject from both views for more anticipated arm positions than any other camera position. The DLT treated the digitizer coordinates resulting from the mirror image as if from another camera. Using the DLT it was therefore possible to estimate that the angle of convergence between the two "cameras" was 130 degrees. Using the analysis of Abdel-Aziz (1974) with this experimental configuration the accuracy for the X and Z axes should be two orders of magnitude greater than that for the Y axis. This analysis was confirmed by the reported RMS errors for the reconstruction of the control points for the dynamic data capture, as the RMS error for the Y axis was over two and half times greater than it was for the other two axes. For the dynamic data capture the Y axis was approximately parallel with the depth axis.

2:2.7 COMPUTER PROGRAMMING

The algorithm was coded in FORTRAN 77 using double precision variables. The programme was initially checked using artificial data from the theoretical observations of a cube with a number of known locations on it. To solve the system of linear equations the SVD was used. The SVD algorithm was based on that of Golub and Reinsch (1971). A number of numerical checks were included in the code, including relocation of the control points and estimation of the perspective centre of the cameras.

2:2.8 NUMERICAL CHECKS

To confirm that the process was working properly, a number of numerical checks were performed. The first and most obvious was to reconstruct the location of the control points. If the programme was working correctly this should be very accurate as the model was fitted directly to these points. The second check was to locate any points on the calibration structure which had not been used for the calibration. The third was to estimate the positions of the cameras: given the information contained in the DLT calibration coefficients it is possible to estimate the object space coordinates of the cameras' perspective centres. These positions could be compared with measurements made in the field.

2:3 PHOTOGRAMMETRIC ERRORS

There are many potential errors which may impinge on the true value of the coordinates derived from a photogrammetric technique. It is the purpose of this section to identify these errors and to examine how they may be removed or reduced. The removal of these errors can be performed directly, by removing the

source of the error, for example by relocating incorrectly placed markers. In some cases the direct approach is not applicable, in which case if possible the error source should be modelled, and then the error reduced using this model. In other cases the size of the error will be small enough that it can be ignored.

It is important that the errors are removed or reduced in the order in which they occur, according to Ghosh (1979)
"Analogically applied corrections and the computational refinement of data should give appreciably correct photo coordinates. It is imperative that the corrections are applied sequentially in the order reverse to their occurrence during the data acquisition procedure, unless all could be contained in a single mathematical model." (page 85)
If such a sequence is not followed these errors may be magnified and or correlated with the underlying signal in which case they will be very hard to remove or reduce, requiring complex models.

In the following sections the sources of error are discussed and methods for their removal or reduction examined. It is assumed that the projected image is of good quality.

2:3.1 FILM MOVEMENT

It is assumed that during the filming of the calibration structure and the activity to be studied that the film frames have all been orientated identically. This may not occur if the camera vibrates significantly during filming. By placing markers (reference points) in the background of the activity which are viewable during calibration and during the activity, it is possible to correct for these small movements. Given at least two markers the film frame can be re-orientated back to the orientation during filming of the calibration structure. In this study this was done using a linear least squares algorithm which was the two-dimensional equivalent of the routine described in section 3:1.3. This type of re-orientation can also compensate for the incorrect registration of the film in the projector (this is discussed in section 2:3.3). These corrections only apply if the film remains flat in both the camera and the projector.

For the static data the film was mounted in slides; special attention was paid to trying to ensure the film was aligned identically in all the slide mounts. However it was not possible to precisely align the film in the slide mounts, therefore correction was made for the different orientations of the film in the slide mounts. Four reference markers were visible in the projected image of each slide. The digitizer coordinates of these reference points as measured for the slides containing the calibration frame were used as the criterion. By comparing the digitizer coordinates of the reference points of the criterion with those of other slides a transformation matrix was calculated. The transformation matrix permitted the images from all the slides to have the same orientation. The effects of this re-orientation are shown in table 2.4 where accuracy measures for the location of points on the rotated calibration frame are compared, with and without image re-alignment.

For analysis of the film from both the static and dynamic data capture these re-orientations were performed, when required.

TABLE 2.4 - The root mean square errors in locating points in three-dimensions with and without correction for incorrect alignment of film images (static data).

	AXIS	RMS ERRORS FOR LOCATING NEW CONTROL POINTS
NO CORRECTION	X	0.0157 m
	Y	0.0044 m
	Z	0.0078 m
WITH CORRECTION	X	0.0025 m
	Y	0.0021 m
	Z	0.0023 m

2:3.2 FILM DEFORMATION

The image is carried in the emulsion which is on the film; both of which may undergo deformations. These deformations are dependent upon the material, temperature, aging, and chemical treatment of the film, and can be affected by transportation at high framing rates. The changes can be categorised as follows:-

1. Uniform deformation - shrinkage or expansion, which produces a simple scaling error, along one axis.
2. Differential deformation - when there is a systematic distortion along the length of the film, and across the width. This can be corrected for using an affine transformation.
3. Irregular distortion - these are complex changes in the film or emulsion which are hard to model, and therefore hard to reduce. It can be caused by emulsion creep, stretching of the film, and lack of flatness of the emulsion.

Non-metric cameras generally do not have fiducial markers, so it is not possible to correct for irregular distortion. The other two distortions are comparatively easy to correct for and are implicit within the DLT formulation.

2:3.3 DIGITIZER RELATED ERRORS

Digitizer errors can arise from three sources: the digitizing tablet, the projection system, and from the actions of the person doing the digitizing.

The DLT incorporates the transformation of digitizer coordinates to image coordinates. There are two assumptions implicit in this transformation. These are:-

1. Projector distortions are negligible.

There are three potential problems with the use of the projection system. It is another lens based system which may distort the image; the film may not always register the same in the gate of the projector every time; and the heat produced by the projector may affect the film or its emulsion. This first problem can be circumvented by the DLT which can account for this distortion at the same time as accounting for the lens distortion of the camera. By digitizing constant points of the projected image of the film (e.g. images of the sprocket edges) it is possible to check that the film is registering the same in the gate of the projector each time, by checking that these points are in the same position each time. If they are not then the registration of the film in the gate of the projector can be corrected. Small errors of this type can be corrected using the procedure described in 2:3.1, as long as the film remains flat. Finally, when in operation the projector gives off heat which may have an effect on the film and its emulsion. The projector used was fitted with a fan and it is assumed that once the projector had "heated-up" it maintained a constant temperature, therefore digitization was not performed until after a 10 minute "warm-up" period.

2. Image and its projection are parallel.

It was checked that the image and its projection were parallel by ensuring that the aspect ratios of the image and its projection were the same.

It is possible that the accuracy of the digitizing tablet may limit the accuracy of point location in the three-dimensional object space. The digitizing tablet used in this study had a resolution of 0.025 mm. This resolution is greater than the accuracy to which the operator could identify points, and less than the diameter of the cross hairs of the cursor. The digitizer coordinates of the points on the calibration frame were randomly perturbated by 0.025 mm over a number of runs. Using these perturbated values to perform camera calibration made no difference to the reconstruction accuracy.

The final consideration in this section is the accuracy of the person performing the digitization. The accuracy depends on their ability to locate points, and the consistency with which this is performed. Locating points is relatively simple if those points are clearly marked. For example the centre of a sphere is easy to locate, providing its image is not too big, as the image is the same from any camera view. Markers placed on key body landmarks are not so easy to locate. For any particular camera these markers may not be clearly visible, or they may not be visible at all at certain times. The position of markers used in the present study was constrained by the fact that these markers were placed with reference to bony landmarks underlying the skin. Small black ink marks were placed on the skin. For each body segment under study at least three non-collinear markers had to be visible. To help locate these markers, two perpendicular lines were drawn through the marks, so if the marker could not be seen a line associated with that mark gave an indication of its position. For the static data capture the images from both cameras were projected at the same time; this was not necessary for the dynamic data capture as both images were recorded on one film.

Assuming the operator can clearly see the point to be digitized there will still be some variation in the digitization of points. To reduce this variation the digitization of the control points on the calibration structure was performed 10 times, and the average value calculated. Section 3:5.2 discusses the effect of signal averaging. The differences in reconstruction accuracy for the static data, using different numbers of digitizations, are presented in table 2.5. For the dynamic data capture the averaging of the multiple digitizations of the calibration frame had no effect on the accuracy of the calibration. For calculation of the calibration coefficients for the static data capture the means of 10 digitizations were used.

For the film images of movement there were at least 150 frames to digitize. It was not practical to perform multiple digitizations of all frames. To examine the accuracy of digitizing this data, four frames were chosen at random and both views digitized 10 times. This gave an estimation of the noise for each marker, and the variation in locating the different points. This analysis is discussed in detail in section 3:5.2. Following the recommendation of Ghosh (1979) it was necessary to reduce this noise from the digitized projected image coordinates before any further operation was performed on the data. This was done using the Generalised Cross-validated Spline. Details of this technique, and the justification for using it, are presented in the next chapter.

2:3.4 LENS DISTORTION

Lens distortion deforms the image and therefore invalidates the assumption that the image is a central projection of the object space. There are two major types of lens distortion. The first is radial distortion,

TABLE 2.5 - The root mean square errors in locating points in three-dimensions after averaging repeat digitizations of image co-ordinates of control points, for the static data capture.

NUMBER OF DIGITIZ -ATIONS	AXIS	CONTROL POINTS	SECOND SET OF CONTROL POINTS	INTER CONTROL POINT DISTANCES
	X	0.0021 m	0.0028 m	
1	Y	0.0017 m	0.0022 m	0.0044 m*
	Z	0.0022 m	0.0025 m	
	X	0.0018 m	0.0026 m	
3	Y	0.0017 m	0.0021 m	0.0040 m*
	Z	0.0019 m	0.0024 m	
	X	0.0018 m	0.0025 m	
5	Y	0.0017 m	0.0021 m	0.0038 m*
	Z	0.0019 m	0.0023 m	
	X	0.0017 m	0.0025 m	
8	Y	0.0016 m	0.0021 m	0.0038 m*
	Z	0.0019 m	0.0023 m	
	X	0.0016 m	0.0025 m	
10	Y	0.0016 m	0.0021 m	0.0038 m*
	Z	0.0019 m	0.0023 m	

(N.B. - * RMS error for the inter-control point distances compares the estimated lengths with the actual lengths, these measures are not specifically associated with one axis.)

which causes the displacement of an image relative to the optical axis of the camera. An outward displacement results in "pin-cushion" distortion and an inward distortion causes "barrel" distortion. The second type of distortion is asymmetrical or de-centering distortion, which is caused by imperfect centering of lenses. This can result in either radial or tangential distortion. Both of these types of distortion can be modelled, allowing their influence to be reduced before digitized points are used to locate points in the object space.

Marzan and Karara (1975) incorporated a lens distortion model into their DLT formulation, increasing the number of parameters to 16. This model permitted correction for radial and asymmetrical lens distortions. They used standard models of lens distortion, although they only used three terms in their model of radial distortion, whereas Ghosh (1979) recommended at least five or six terms.

Miller et al. (1980) used the lens distortion model of Marzan and Karara (1975) and reported no improvement in accuracy when results were compared with the standard eleven parameter solution. They did not report the differences. Walton (1981) also used this model but found that it reduced the accuracy of the reconstruction of the control points. Wood and Marshall (1986) used one correction term for radial lens distortion; for the conditions they examined this lens distortion model reduced the accuracy of point reconstruction. Hatze (1988) examined his modified DLT in the three conditions incorporating the lens distortion model of Marzan and Karara (1975), and found that the lens distortion model only gave increased accuracy in one condition. The condition which gave the improved results used the most control points, and this lead Hatze to suggest that the lens distortion model should only be used where 30 or more control points are available.

To implement the lens distortion model of Marzan and Karara (1975) the basic eleven DLT parameters must be calculated. These are then used to estimate the principal point location in digitizer units which is required for the lens distortion models. Information about the control point locations in the object space and in digitizer units are combined to estimate the lens distortion model parameters. Once these have been obtained it is possible to reduce the systematic errors caused by lens distortion. The corrected coordinates are then used for locating digitized points in the object space. This procedure can be performed iteratively until no change in accuracy is achieved. Marzan and Karara (1975) performed the procedure once, whilst Walton (1981) performed the procedure iteratively until there was no improvement in the location of the control points. As Walton did not find an increase in accuracy, his routine only performed one iteration.

To assess the value of incorporating a lens distortion model in the photogrammetric model, a number of different lens distortion models were compared. These were:-

1. One radial distortion term.
2. Two radial distortion terms.
3. Three radial distortion terms
4. Four radial distortion terms.
5. Five radial distortion terms.

6. Six radial distortion terms.
7. Two terms to correct for asymmetrical distortion.
8. Two terms to correct for asymmetrical distortion, and three terms to correct for radial distortion.
9. Two terms to correct for asymmetrical distortion, and six terms to correct for radial distortion.

The programme was sequentially run with each one of the lens distortion models listed. The programme ran iteratively until 10 successive adjustments had been made with no improvement in accuracy, or until there was a decrease in accuracy. Accuracy was assessed by reconstructing the control points. The results from the static data capture will be discussed first.

Option one was the same as that used by Wood and Marshall (1986) and after 10 iterations this resulted in no change in reconstruction accuracy. In his photogrammetric model Woltring (1980) reported that accuracy of reconstruction was only increased when incorporating one radial distortion term, and not when using more terms or correcting for asymmetrical distortion. Option two resulted in a decrease after three iterations as did option three. Options four, five, and six all resulted in a small increase in accuracy of 0.1 mm along one axis only. This supports the recommendation of Ghosh (1979) that four or five radial distortion terms should be included in a lens model. Option seven resulted in no change in accuracy after 10 iterations. Option eight was the model proposed by Marzan and Karara (1975) and used by Hatze (1988), but after 10 iterations there was no increase in reconstruction accuracy. Finally option nine resulted in an increase in reconstruction accuracy of 0.1 mm along the X axis only.

The increases in accuracy with the lens distortion models only occurred when using more than the three radial distortion terms usually used with the DLT (Marzan and Karara, 1975; Hatze, 1988). The recommendation of Hatze (1988) that lens distortion models should only be used when there are at least 30 control points available has not been validated. With 51 control points and the same lens distortion model as used by Hatze (option eight) there was no increase in accuracy. Presumably the lens distortion model gave Hatze (1988) an increase in reconstruction accuracy as a consequence of being used in conjunction with his modified DLT, and not as a consequence of the number of control points.

The effect of the nine lens distortion models on the dynamic data was also examined. In none of the cases did it result in an increase in reconstruction accuracy. Option eight was the only option not to decrease accuracy. These results are worse than those for the static data capture, but confirm the findings that these lens distortion models do not increase the accuracy of the DLT. These models were applied for both images from the dynamic data capture to see if any one of the models could account for any distortion that the mirror may have introduced into the image. The was no increase in accuracy using this approach.

As there was no increase in reconstruction accuracy with the dynamic data, no lens distortion model was used. The increases in accuracy with the lens distortion model for the static data capture were very small and occurred at the precision limit of the system used to measure the calibration frame. Therefore no lens distortion model was incorporated for the static data reconstructions.

2:3.5 TEMPORAL MATCHING OF DATA

At least two images from different angles are required to locate the digitized points in the object space. Exposures made with two different cameras are not automatically simultaneously exposed. There are three ways in which two images can be synchronised. The cameras can be phase locked so the opening and closing of the shutters occurs at the same time. With the LOCAM II the Redlake Corporation claim that when phase locked the shutter of one camera would be out of phase with the other camera's shutter by a maximum of 18 degrees. Alternatively two images can be recorded on the same piece of film by the appropriate placement of a mirror in the field of view of the camera (e.g. Woltring, 1980). This presents a number of problems: the size of the image is effectively reduced, the mirror can introduce distortions, and for many activities a large mirror would be required. The final technique is to interpolate the data sets over the same time base. Walton (1981) used a timer in view of both cameras to establish frame times. He then interpolated the data of the faster camera over the time base of the slower, this was done using linear interpolation. Dapena (1979) used a timer to obtain the start and end times of the activity then assumed that the framing rate was constant between these two points. This gave frame times for each camera, he then used an interpolating cubic spline to time match the data.

The process of interpolating the data creates a few problems. There must be some way of measuring the time interval between frames. It cannot be guaranteed that the cameras are running at a consistent framing rate. The manual for the LOCAM II ("Operating instructions and illustrated parts list", Redlake Corp., Campbell, Calif) claims that the camera takes 0.53 seconds to get up to 200 frames per second (fps). No claims are made about how consistently that framing rate is held. If the activity is filmed during this run-up period the framing rate cannot be used as a measure of time. If the framing rate is assumed constant then a time base can be calculated for each camera. It is then necessary to synchronise the cameras by estimating the time of an event which can be clearly seen in both cameras, and then interpolating using this moment as a reference. It is possible to have the time printed directly onto the film. This allows interpolation of the film without recourse to an event in the field of view (assuming the same timing device is used for all cameras). The other option is to have a timing device in view of the cameras. When using such a device it is necessary that the shutter speed is quick enough to be able to distinguish the time to the desired accuracy.

The temporal matching of the data was not necessary in this study as a mirror was used for the dynamic data capture so two images could be recorded simultaneously onto each film frame, which is a clear advantage of the mirror technique. As mentioned in section 2:3.2, digitizer coordinates of the projected image were smoothed prior to reconstruction. This also permitted an examination of the possible effects of incorrect data synchronisation. Using the data from one of the dumbell curls (trial #3), the data from the mirror image were interpolated over a new time base at the same time as being smoothed, see section 3:4.5. The phase locking of two cameras would maximally produce only an 18 degree mismatching of shutters. At a framing rate of 200 fps and a shutter opening of 1/3, this would produce images temporally offset by 0.00025 s. The reconstructed locations of the points from the synchronised images were used as the criterion with which the reconstructed locations from the non-synchronised images were compared. The results gave the root mean square error between the two measures over the total number of frames

for the trial examined (n = 232) for the 10 points digitized, eight on the subject, and 2 on the dumbell.

The results are presented in table 2.6. The largest error was 3.2 mm for the Y coordinate digitized point 9 which was one end of the dumbell. This error is less than the precision of the reconstruction accuracy along that axis. For the other two axes the errors are not as large as the precision of the reconstruction accuracy along the axis. Therefore the error that would have been associated with synchronisation of the images had phase locking cameras been used would not have been significant in the present study. The velocity of the markers has an effect on the accuracy due to synchronisation; if the movement is very fast there is more movement between the exposure of images and the associated errors are increased. Analysis of the velocity of the movement of the points digitized in the dumbell curl (trial #3), using the techniques described in Chapter 3, showed that the markers with the highest velocities (numbers 9 and 10) had th e largest inaccuracies associated with synchronisation of the non-synchronised images.

2:3.5 OTHER ERRORS

There will be other errors which will corrupt the final signal produced by the photogrammetric technique. These will arise from a number of sources, for instance imperfections in the photogrammetric model. Not all of the noise in the digitized coordinates can be removed, and some will transfer to the final signal, but will have been operated on by all computations involved in obtaining object space coordinates from digitized image coordinates. The mathematical techniques used to estimate various parameters are subject to limitations, some imposed by the restriction of computers operating to a finite precision. Given these factors it must be anticipated that the final object space coordinates will be corrupted with noise, albeit at at lower signal to noise ratio than would have been achieved if the precautions mentioned had not been used.

Systematic error may be present in the data. This can arise from any part of the photogrammetric process. On the calibration structure some of the control points may have been incorrectly measured, or the person doing the digitizing may consistently identify a marker incorrectly. Vigilance by the experimenter should keep these and other such systematic errors to a minimum.

2:3.6 SUMMARY

This section has detailed the errors which may arise in the photogrammetric process. Methods for reducing some of these errors have been investigated. Any systematic errors remaining are assumed to be small enough to be considered insignificant. The random noise affecting the sampled data is assumed to be white, the details for its reduction are given in the next chapter.

2:4 EXPERIMENTAL DETAILS

In the preceding sections the discussion ignored the quality of the image resulting from the filming process. This is influenced by the focus and aperture of the lens, shutter speed, available light, the quality and ASA rating of the film, and the processing of the film. Wherever possible those factors which were under the control of the experimenter were optimized. Details pertinent to the two filming sessions are now given.

TABLE 2.6 - The root mean square errors in locating points in three-dimensions when the digitized images were not synchronised, compared with their locations estimated from synchronised images. (Difference between frames was 0.00025 s).

NUMBER OF MARKER	ROOT MEAN SQUARE ERROR		
	X AXIS	Y AXIS	Z AXIS
1	0.0008 m	0.0025 m	0.0003 m
2	0.0010 m	0.0028 m	0.0003 m
3	0.0008 m	0.0022 m	0.0001 m
4	0.0009 m	0.0024 m	0.0002 m
5	0.0007 m	0.0021 m	0.0001 m
6	0.0007 m	0.0019 m	0.0002 m
7	0.0011 m	0.0032 m	0.0006 m
8	0.0011 m	0.0030 m	0.0004 m

(N.B. - the points to which the markers correspond are listed in section 2:4.4)

2:4.1 CALIBRATION STRUCTURE

This section details the design and manufacture of the calibration structure. A diagram of the structure was reproduced in figure 2.1.

Analysis of the activities to be studied showed that a structure of 1.0 m * 0.6 m * 1.0 m would be sufficient to record all the information required. The structure was not particularly large so portability was not a problem.

The calibration structure was designed so that there were control points throughout the structure. The outside of the structure formed a rectangular reference frame (Hatze, 1988), and the inside gave a "Christmas tree" reference frame (van Gheluwe, 1978). This design was selected for two purposes: to ensure that there were control points throughout the calibrated space, and to permit a study of the influence of control point distribution on reconstruction accuracy (2:2.5).

It is important that the position of the control points to be digitized are precisely identifiable. A control point in the form of a two-dimensional marker may not be viewable from all camera positions. To circumvent this problem spheres were used since the centres are identifiable from whatever perspective they are viewed. The spheres were large enough to be clearly identified but small enough to facilitate accurate identification of their centres in the projected image. Golf balls were used as they are manufactured to a consistent size, and met the desired criteria.

During manufacture of the frame emphasis was placed on stability. Twelve millimetre diameter steel tubing was used for the frame and the centrally drilled spheres were hammered onto the frame, where they remained firmly fixed. The frame was painted matt-black to reduce reflections. The spheres were of four different colours to allow for coding of the positions of the spheres. The spheres were placed at approximately 0.20 m intervals vertically, and 0.30 m intervals horizontally. Their precise locations were determined by surveying the calibration frame.

A heavy metal base was manufactured on which the calibration structure rested. All measurements were made assuming that the base was horizontal. The calibration structure would only fit onto the base in one configuration. The base was adjusted until it was horizontal as indicted by a spirit level.

The locations of the control points were determined using a surveying system developed in the Department of Civil Engineering, Loughborough University of Technology. The system incorporated two theodolites: a Sokkisha DT4 and a Zeiss Elta 40. This system used a laser which was aimed through the eyepiece of the Zeiss Elta 40 onto the object to be measured, giving a common target for both theodolites. The combination of the information from both of the theodolites gave the three-dimensional coordinates of the point in an inertial reference frame. When the calibration frame was measured, a Kern sub-tense bar with a calibrated length of 2 m was measured as being 2.00001 m long using this system.

Although the measurement system was accurate, the accuracy of the measurements depended on how

well the centres of the spheres were located. There was no way to directly assess this but repeat measures were taken of the positions of the spheres on the frame in order to assess how consistently these estimates were made. The RMS error when comparing the first measurement of the spheres on the calibration frame with the second was 0.0008 m. Both theodolites independently measured the location of points on the vertical axis, so it was possible to get an estimate of the accuracy in identifying the target by calculating the difference between the two measures. The mean difference was 0.58 mm (± 0.45 mm), indicating that the spheres were consistently located.

To assess the accuracy of the DLT the calibration frame was rotated to a new orientation, see section 2:2.4 for details. To obtain this new position the calibration structure was rotated approximately 180 degrees about the central vertical axis of the structure. To determine the new positions of the control points, the new positions of four of the control points were measured, given the original and new positions of these four points it was possible using the procedures described in section 3:1.4 to determine the angle through which the frame had been rotated. Given this angle the locations of the remaining control points could be determined.

2:4.2 EXPERIMENTAL SET-UP - STATIC DATA CAPTURE

Two 35 mm cameras were used. The camera designated number one was a Canon EOS 750, camera two was a Canon EOS 620. The lens on each camera was set to a focal length of 35 mm. Both cameras were loaded with Kodacolor Ektrachrome 400 ASA film, and their F-stop and shutter speeds were selected automatically by the cameras. Both cameras were mounted at the same height, which was approximately level with the centre of the calibration frame. The cameras were then directed so the calibration frame was central to both of their fields of view. They were both 2.55 m away from the centre of the frame with an angle of convergence of 85 degrees. These camera positions were selected after a pilot study. The selected positions allowed all control points on the calibration structure to be clearly visible in both views. It also permitted viewing of the markers on the subject from both views for more anticipated arm positions than other camera positions examined. Two 1.25 kW halogen lamps were used. These were positioned approximately behind each camera and aimed at the centre of the activity. A white background was selected for the activity as this increased the contrast for the black markers on the subject. In the background of the field of view of each camera four markers were placed which served as reference markers (see section 2:3.1).

During the static data capture the subject performed a number of maximum isometric elbow flexions at different joint angles. Photographs were also taken of a dry bone specimen of an upper limb, so measurements required for osteometric scaling could be made (see section 5:1.2).

2:4.3 EXPERIMENTAL SET-UP - DYNAMIC DATA CAPTURE

A mirror was used so that two images could be recorded of the same object by one camera. A LOCAM II (Model 51) was used, fitted with a Schneider Kreuznach Variogen 1.8/10-100 lens, the focal length of which was set at 20 mm. It was loaded with Eastman Ektachrome 7250 film (tungsten 400 ASA). For filming the calibration frame and timing lights the F-stop was 5.6 and for the subject it was set to 4.0.

Initially the shutter on the LOCAM was set to 1/12 which when the camera ran at 200 fps gave an exposure time of 1/2400 of a second. This was done so that the camera framing rate could be calibrated. With this exposure time it was possible to identify the time of each exposure to a millisecond using a timing device. The interval between exposures gave the framing rate. A number of frames were examined to ensure that the framing rate remained constant once the camera was up to speed. The shutter was then opened up to 1/3 and the remainder of the filming performed at the nominal framing rate of 200 fps. Analysis of the initial sequence of film showed that at a nominal speed of 200 fps the camera was running at 200 fps, a rate which was consistently maintained.

A pilot study was performed to select the camera position. The position selected allowed all control points on the calibration structure to be clearly visible in both views. It also permitted viewing of the markers on the subject from both views for more anticipated arm positions than other camera positions examined. The camera position and its orientation to the mirror are shown in figure 2.3.

To illuminate the experimental area six halogen lamps were used giving 5.5 kW of light. These had to be positioned so they were not visible in the mirror and did not shine into the mirror. As a consequence the lights were placed in a straight line perpendicular to the mirror as close as possible to the activity without being in shot of the camera. They were aimed across the area of interest to avoid reflections in the mirror and the consequent reduction in the quality of the mirror image. A white background was selected for the activity as this increased the contrast for the black markers on the subject. In the background of the field of view four markers were placed which served as reference markers (see section 2:3.1).

The timing mechanism used consisted of four columns of ten LEDs, giving seconds, tenths, hundredths and thousands of a second respectively.
During the Dynamic data capture a number of different elbow flexions were filmed:-
TRIAL #1 - elbow flexion with the forearm in a neutral position throughout movement
TRIAL #2 - a maximum dumbell curl with 17.5 kg
TRIAL #3 - first of five repetitions of dumbell curls with 15 kg
TRIAL #4 - a dumbell curl with 15 kg executed as fast as possible
This order was selected to reduce the effects of fatigue. The movements involved in a dumbell curl are illustrated in figure 2.4.

2:4.4 DIGITIZING DETAILS

The digitizer used throughout the present study was a Terminal Display Systems HR 48. This has an active area of 1.20 m by 0.90 m, with a resolution of 0.025 mm. The influence of this degree of accuracy has been discussed in section 2:3.3.

For the static data the film negatives were placed on glass slide mounts and projected onto the digitizing tablet using a Kodak S-AV 2010 Projector fitted with an 85 mm lens. This resulted in a projected image which was half life size for both images. For analysis of the dynamic data the 16 mm projector used was an NAC Analysis Projector, fitted with 50 mm lens. This resulted in a projected image which was

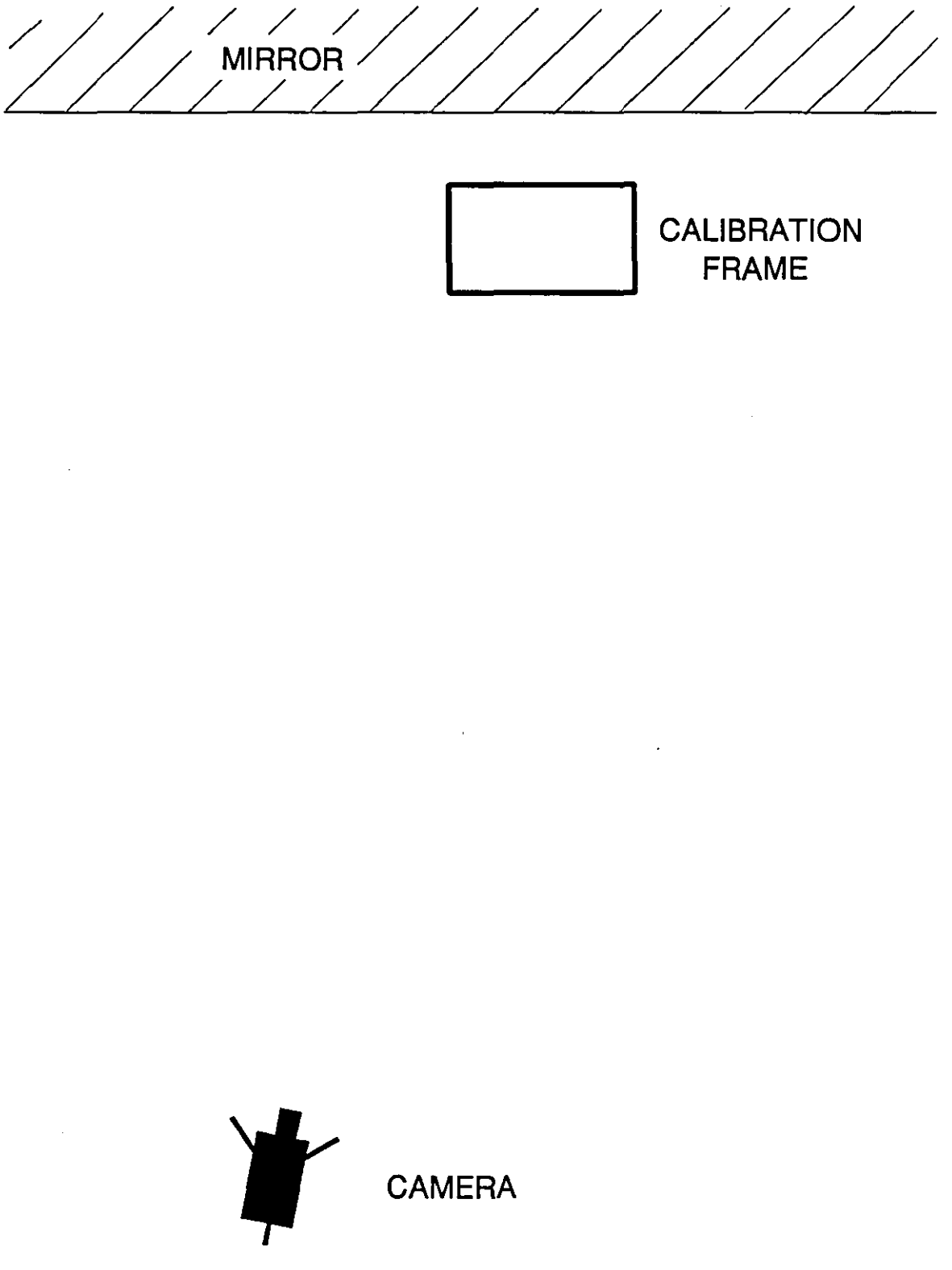

FIGURE 2.3 - The experimental set-up for the dynamic data capture.

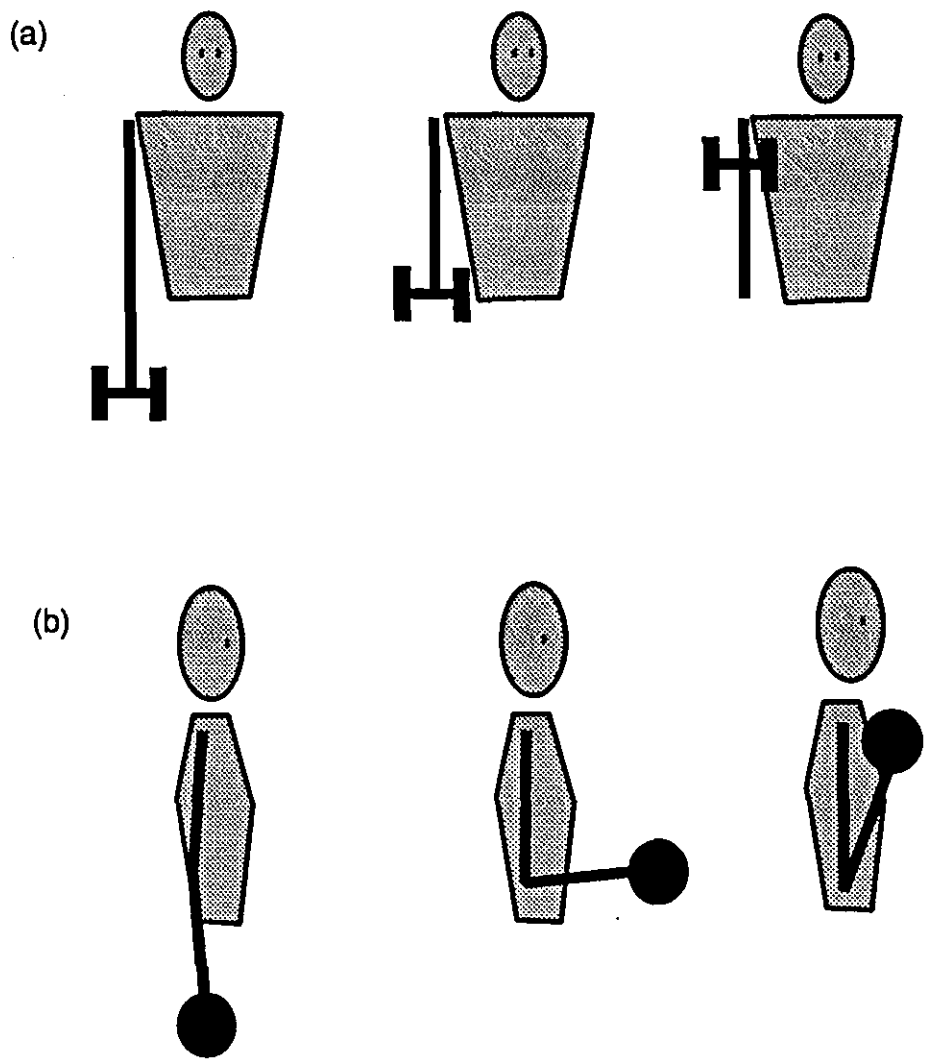

FIGURE 2.4 - A diagram illustrating a dumbell curl. (a) Anterior view. (b) Lateral view.

approximately half life size for both images. To allow for any change in the film and the emulsion that may arise due to the change in temperature caused by the projectors, they were allowed to "heat up" for 10 minutes before any digitizing took place. After this time it was assumed that no temperature changes occurred.

The digitizer was interfaced to an Archimedes A3000 Acorn computer which logged all the digitized data using software already available in the Department of Physical Education and Sport Science. After digitizing the data was converted into ASCII format and transferred either to the PRIME 750 (University mainframe) or the Archimedes 440 microcomputer. Here the raw image data were graphically inspected to check for any incorrectly digitized points. Where "outliers" occurred, the frame was re-digitized immediately and the new values substituted for the old values including the formerly incorrect point.

The digitizing of each sequence of film was performed in one session. The length of any one of these sessions did not exceed 3 hours. The following points were digitized during the dynamic data capture:-

1. Styloid process of the ulna
2. Styloid process of the radius
3. Olecranon of the ulna
4. Medial epicondyle of the humerus
5. Lateral epicondyle of the humerus
6. Lesser tubercle of the humerus
7. Marker on the radial end of the dumbell
8. Marker on the ulna end of the dumbell

The first six points were marked superficially onto the skin at the sites believed to correspond to the bony landmarks. Target like markers were placed on the ends of the dumbells. The same points were digitized for the static data capture except ends of a handle attached a force plate were digitized rather than the dumbell ends. For the osteometric scaling additional sites were digitized on a dry bone specimen of the upper limb (see section 5:1.2).

2:4.5 ACCURACY

A detailed account of the reconstruction accuracy was given in section 2:2.4, and is summarized in this section. For the static data capture the RMS errors in locating a group of control points, distributed throughout the calibrated space were 0.0025 m, 0.0021 m, and 0.0023 m for X, Y, and Z axes respectively, these control points were not used for determining the calibration coefficients. For the dynamic data capture the RMS errors in locating a group of control points were 0.0012 m, 0.0033 m, and 0.0016 m for X, Y, and Z axes respectively. The accuracy for the dynamic data capture was assessed by reconstructing the positions of the control points, used to determine the calibration coefficients, the limitations of this approach were discussed in section 2:2.4. These accuracy values were for a clearly identified point within the object space. It cannot be anticipated that the location of all the markers on the subject were as accurate as this. The problem of marker identification is covered in more detail in the next chapter.

CHAPTER III

DETERMINATION OF LIMB KINEMATICS

INTRODUCTION

The last chapter detailed how points are located in a three-dimensional object space. Although these reconstructed marker positions refer to significant body landmarks, the locations of these points do not describe limb kinematics. This chapter details the techniques used to determine the limb kinematics. As the reconstructed body landmarks contain noise, the reduction of noise in a signal is discussed and examined. Derivative information is required for the determination of limb kinetics; the calculation of derivatives is also examined in this chapter. Estimates are made of the errors associated with the state variables necessary to compute resultant joint moments.

3:1 POSITION AND ATTITUDE DETERMINATION

The location of a rigid body in three-dimensional space is specified by the position and attitude (orientation) of that body. It is the purpose of the following sections to detail how the position and attitude can be calculated.

3:1.1 OVERVIEW OF TECHNIQUES

Consider a set of three non-collinear points pi (i=1,2,3), fixed to a rigid body. The locations of these points are known in an inertial reference frame. Assuming that there is also an orthogonal reference frame fixed to the rigid body (called the member reference frame), the locations of the three points in this reference frame are qi. The following relationship exists:-

$$qi = [R].pi + V \qquad [3.1]$$

Where:-

[R] - is an attitude matrix (sometimes called the rotation matrix)

and V is a position vector.

The attitude matrix contains the direction cosines between the axes of the inertial and member reference frames, therefore suitable rotations and a translation are performed to bring the axes of one reference frame into line with the other. The attitude matrix can be used to compute the orientation angles (see section 3:1.4). The relationship expressed in equation 3.1 does not only apply in moving from an inertial reference frame to a member reference frame. It can be used in moving from any orthogonal reference frame to any other. An important property of the attitude matrix [R] is that it is orthogonal, therefore:-

$$[R]^T.[R] = [R].[R]^T = [R]^{-1}.[R] = I \qquad [3.2]$$

Where:-

I - is the identity matrix.

Relationship 3.1 can also be used to describe the movement of a rigid body from one position to another, given the points measured in position one (pi), and then in position two (qi). It is possible to determine the attitude matrix and translation vector which would result in such a displacement. Given these two parameters it is possible to compute the helical or screw axis parameters which are often used in the kinematic analysis of joints.

There are various techniques used to determine [R] and V, given that at least three non-collinear points have known locations in both reference frames. The majority of these techniques are concerned with the determination of helical axis parameters, whilst in the present study they are required for the computation of the position vector and the orientation angles. As this distinction only exists with regard to how these parameters are used, it is necessary to examine both sources of literature to review the techniques for [R] and V determination. Three different groups of techniques will be considered: direct; unweighted least-squares; and iterative cine-photogrammetric.

The direct techniques are those where [R] and V are calculated assuming that the coordinate data are free from error. These techniques make no assumptions about the rigidity of the body under study. Angeles (1986) and Friberg (1988) both advanced techniques to compute [R] and V which fall into this category.

In the least-squares techniques, the points are not considered error free and the techniques minimise the difference between the measured coordinates and the calculated locations of those points. All of these techniques use unweighted least-squares. Selvik (1974) used a least-squares technique which required an initial approximation of [R] and V. Spoor and Veldpaus (1980) proposed a least-squares method which minimised the same function as Selvik (1974) but did not require an initial approximation of the parameters. Its chief disadvantage was that it required the calculation of the eigenvectors of a three by three matrix. Veldpaus, Woltring, and Dortmans (1988) presented a technique similar to Spoor and Veldpaus (1980), but their technique did not require the calculation of eigenvectors, and relied on a Newton-Raphson procedure to solve a system of non-linear equations. The technique also produced a figure of merit which reflected inaccuracies in the measurement data, and in the rigidity of the bodies to which the markers defining the member reference frame were fixed. A similar technique which also provides a least-squares estimate of [R] and V is that of Siegler, Chen, and Schneck (1988). They employed a non-linear optimization algorithm to find [R] and V. All of these techniques were optimal in a least-squares sense.

There are two iterative cine-photogrammetric techniques, both of which obviate the need to compute the location of the points in the inertial reference frame as an intermediate step in the computation of [R] and V. Direct estimates of the position vector and the orientation angles of the rigid bodies are obtained from the image coordinates. The technique of Miller, Shapiro, and McLaughlin (1980) used the DLT parameters reformulated using a Taylor series approximation for the determination of the orientation angles and position vector. The resulting system of equations was solved using linear least-squares implemented via Normal equations. The procedure required an initial approximation of the parameters. They presented the results for a number of conditions, all using the same basic formulation, and showed

that increased accuracy was achieved when the largest number of markers (eight) defined the member reference frame. Woltring (1982) combined the collinearity equations of photogrammetry with the relation which transforms points from one reference frame to another, in this case object space reference frame to member reference frame, equation 3.1. The resulting relationship was modelled using a second order Taylor series approximation, and solved given a suitable initial approximation by a Newton-Raphson iterative procedure. There was no report on the accuracy of this technique. As cine-photogrammetric techniques tend to have larger errors associated with measurements along one axis, see section 2:2.6, these approaches where the object space coordinates are not directly reconstructed may result in greater accuracy than techniques where the object space coordinates of all points are calculated.

Woltring and Huiskes (1985) used a theoretical model to examine the accuracy of the estimation of the parameters describing the helical axis under a number of conditions. They employed different combinations of the following operations: prior smoothing of data; smoothing of resulting data; iterative adjustment calculus; and incorporation of a rigid body model. The filter used considered the data to be contaminated with stationary, uncorrelated noise with a mean value of zero. The most significant result was that more accurate estimates of the helical axis parameters were obtained when the raw data were smoothed prior to the determination of these parameters, rather than smoothing the computed parameter values. The lower accuracy as a result of smoothing the computed parameters is not surprising as the determination of the helical axis parameters involves non-linear transformations; these transformations would change the nature of the noise contaminating the signal, making conventional low-pass filtering inappropriate for removal of this noise. The determination of orientation angles involves similar non-linear transformations.

3:1.2 MARKER MOVEMENTS

The position vector and attitude matrix are determined from the positions of markers fixed to a theoretically rigid body. As the body may not be rigid there may be movement of markers relative to the genuine reference frame which they are intended to define. A consideration of the movement of these markers is necessary. The three-dimensional cine-photogrammetric procedures described in Chapter II located the positions of these markers but made no allowance for the markers moving from their ordained positions. Macleod and Morris (1987) examined the amount of marker movement using rigid markers during three activities: walking, stamping, and landing. Using a video based system they assessed the accuracy to which they could locate the markers to be 0.002 to 0.003 m. Shank length was measured during the activity by reference to a pair of appropriately placed markers. Variations in the inter-marker distances were compared with the shank length measured before the activity. The markers used weighed 3 g. During walking there was a variation in shank length of 0.01 m, and 0.02 m during landing. Using heavier markers (10 g) there was a variation of 0.015 m during walking, and 0.023 m during landing. This type of error must be considered systematic as it is correlated with the movement. An increase in reconstruction accuracy has little effect if these systematic errors are not reduced as they are much greater than the reconstruction errors.

The movement of the markers in the study of Macleod and Morris (1987) was due to the movement of the

underlying skin. In a study of horses, the effect of skin movement was assessed. Van den Bogert, van Weeren, and Schamhardt (1990) examined horses walking normally. The researchers either embedded LEDs into the bones of the horses or used transcutaneous pins. This permitted quantification of skin movement. The peak to peak amplitude of skin displacement was 0.15 m. To illustrate the errors due to skin movements the moment arm of the gastrocnemius was calculated with skin effected marker positions and direct bone measurements. Errors of up to 30 percent were found at both the knee and tarsal joints. A two-dimensional model was developed to correct for marker movements due to skin movement. The authors concluded that

"...when using skin marker-based kinematic data of the horse for the calculation of biomechanical parameters, correction for skin displacement is nothing but a must. Furthermore, although the absolute values of skin displacement in human gait analysis will be substantially smaller resulting in a smaller error due to this artifact, there is no reason to believe that the situation is substantially different." (Page 100)

The study of Macleod and Morris (1987) highlighted the influence of the mass of the markers on marker movements, no mention is made in the report of van Den Bogert et al. (1990) of the mass of their markers. Their study was only two-dimensional. The implicit assumptions of such an analysis could disguise the true nature of skin movement, and its influence on marker movement.

Both studies indicate the need to study the influence of skin movement on marker movement. Until more information is available the researcher must:-

1. Place markers where they will be least influenced by the movement of skin.
2. Use markers which are as light as possible.
3. Attempt to quantify the movement of these markers.

The second consideration is circumvented by marking the skin directly with an appropriate marker. The last recommendation is hard to achieve, but one simple partial indication of the amount of marker movement is to plot the variation of distance between the positions of pairs of markers, measured before the activity and calculated from the cine-photogrammetric data during the activity. Pairs of marker may be equally effected by skin movement, but this will not be the case for all pairs of markers. Such an analysis has been undertaken in the present study. The results are reported in section 3:5.3.

3:1.3 DETERMINATION OF POSITION AND ATTITUDE

For the determination of [R] and V an unweighted least-squares technique was adopted in this study. By using an unweighted least-squares based technique some of the errors in the measurements of the points in the inertial and member reference frames are accounted for. The technique used was that of Hanson and Norris (1981) which computes the singular value decomposition of a cross-dispersion matrix to compute [R] and V.

[R] and V were computed as follows:-

$$qi = [R].pi + V \qquad \text{(3.1 restated)}$$

Compute the cross-dispersion matrix:-

$$[C] = \frac{1}{k} \sum_{i=1}^{K} (qi - \bar{q})(pi - \bar{p})^T \qquad [3.3]$$

Where:-

$$\bar{q} = \frac{1}{k}\sum_{i=1}^{K} qi \qquad \bar{p} = \frac{1}{k}\sum_{i=1}^{K} pi \qquad [3.4] \text{ and } [3.5]$$

and k is the number of non-collinear points on the rigid body, $k > 3$.

The singular value decomposition of the cross-dispersion matrix was computed:-

$$[C] = [U].[S].[V]^T \qquad [3.6]$$

Section 2:2.3 gives more details of the computation of the singular value decomposition of a matrix. The attitude matrix is computed from:-

$$[R] = [U].[V]^T \qquad [3.7]$$

The position vector is computed from:-

$$V = \bar{q} - [C].\bar{p} \qquad [3.8]$$

Matrix [S] contains the singular values of the cross-dispersion matrix. The rank of this matrix can be used to determine errors in the rigid body model. If the rank is three then the distribution of the reference points on the rigid body is three-dimensional, if the rank is two then the distribution is planar, and if the rank is one then all the points are collinear.

This technique is computationally similar to that of Veldpaus et al. (1988). Their routine requires the inversion of a three by three matrix (see their equation 4.10), the most robust technique with which to perform such an inversion is the SVD (see section 2:2.3). The technique of Hanson and Norris (1981) employs the SVD of a three by three matrix but fewer additional calculations than Veldpaus et al. (1988).

In light of the findings of Woltring and Huiskes (1985) the coordinates of the reference points on the rigid bodies measured in the inertial reference frame were smoothed prior to the computation of [R] and V. Because these points had been smoothed and a least-squares algorithm was used the angles computed from [R] were not smoothed further. As [R] is used to transform coordinates from one reference frame to another, filtering these angles may cause the matrix to become non-orthogonal in which case its use would be limited as the inverse of the matrix would not be so easily determinable. This assumes that the filtered angles are used to reconstruct the transformation matrix.

3.1.4 ANGLE DETERMINATION

The attitude matrix [R] is considered to consist of a sequence of three rotations, given by three rotation matrices. There is one angle associated with each matrix. The following may be stated:-

$$[R] = [R3].[R2].[R1] \qquad [3.9]$$

Where:-

$$[R1] = \begin{bmatrix} 1 & 0 & 0 \\ 0 & \cos\phi & \sin\phi \\ 1 & -\sin\phi & \cos\phi \end{bmatrix} \qquad [3.10]$$

$$[R2] = \begin{bmatrix} \cos\theta & 0 & -\sin\theta \\ 0 & 1 & 0 \\ \sin\theta & 0 & \cos\theta \end{bmatrix} \qquad [3.11]$$

$$[R3] = \begin{bmatrix} \cos\psi & \sin\psi & 0 \\ -\sin\psi & \cos\psi & 0 \\ 0 & 0 & 1 \end{bmatrix} \qquad [3.12]$$

Where:-
ϕ, θ, and ψ are angles.

In this case Cardan angles (also known as Bryant angles) have been used. In the case of Eulerian angles matrix [R1] is the same in format as matrix [R3], but with a different associated angle, because these two rotations occur about the same axis (Wittenburg, 1977). As matrix multiplication is generally not commutative the values of the angles are dependent on the sequence of these multiplications. The sequence of these rotations varies with different definitions of these angles. Eulerian or Cardan angles have most commonly been adopted to define body orientations, although the former term is often used as a generic term for all types of orientation angles (e.g. Greenwood, 1965 page 332).

Eulerian angles can be calculated from the following formulae:-

$$\cos\theta = [R]_{33} \qquad [3.13]$$

$$\cos\phi = -[R]_{32} / \sin\theta \qquad [3.14]$$

$$\cos\psi = [R]_{23} / \sin\theta \qquad [3.15]$$

The angles are not defined for $\theta = n.\pi$ (n=0,1,...), as the first and third axes cannot be distinguished: this is the gimbal lock condition. Therefore this definition of orientation angles is most useful when θ remains non-zero and less than 180 degrees.

Cardan angles can be calculated from:-

$$\sin\theta = [R]_{31} \qquad [3.16]$$

$$\sin \phi = - [R]_{32} / \cos \theta \qquad [3.17]$$

$$\sin \psi = - [R]_{21} / \cos \theta \qquad [3.18]$$

For $\theta = 0$ the three axes are still orthogonal unlike the Euler angles under this condition. Gimbal lock occurs when $\theta = \pi/2 + (n.\pi)$ $(n=0,1,...)$, as here the rotation of the axes by ϕ and ψ are identical. It can be seen that if anticipated rotations about the Y axis fluctuate around zero degrees, and never achieve an angle ± 90 degrees then Cardan angles are appropriate. Whereas if the angles are anticipated to be larger than ± 90 degrees then Euler angles are more suitable, as long as angles of zero do not occur.

For the determination of limb kinetics the angular velocity of the rigid body is also required. For Cardan angles this is expressed in matrix form:-

$$\begin{bmatrix} \omega_x \\ \omega_y \\ \omega_z \end{bmatrix} = \begin{bmatrix} \cos\theta.\cos\psi & \sin\psi & 0 \\ -\cos\theta.\sin\psi & \cos\psi & 0 \\ \sin\theta & 0 & 1 \end{bmatrix} . \begin{bmatrix} \phi' \\ \theta' \\ \psi' \end{bmatrix} \qquad [3.19]$$

Where:-

ω_x, ω_y, and ω_z - are the angular velocities
and ϕ', θ', and ψ' are the derivatives with respect to time of ϕ, θ, and ψ.

Verstraete and Soutas-Little (1990) proposed a new technique for the determination of the angular kinematics of a rigid body. Given two points on a rigid body the relative velocity between the two must be perpendicular to the position vector between the two points and the angular velocity. If it is assumed that linear velocity has already been calculated then the only unknown is angular velocity. If more than two points are measured on the rigid body it is possible to formulate a series of equations relating the known variables to the angular velocity, the resulting system of equations can be solved using a linear least-squares technique. By using this approach the authors claimed that allowance was made for marker movement when computing limb angular kinematics. As this technique requires the determination of linear velocity of the rigid body landmarks, or linear acceleration if angular acceleration is required, the errors due to marker movement have not been completely eliminated from these variables so marker movement is only partially accounted for with this technique. The authors present some results for this technique but have no criterion with which to compare their results, so its accuracy is hard to assess.

The rotation occurring at a joint is normally described by the rotations necessary to align a proximal segment member reference frame with that of a distal segment. There are three possible types of rotatory motion permitted at a joint. These can be described as flexion-extension, abduction-adduction, and internal-external rotation. Reference to figure 3.1 illustrates how the angles associated with these rotations can be obtained, by comparing the two member reference frames. In the figure rotations about the Xp axis corresponds to flexion extension, the Yp axis to abduction-adduction, and the Zp axis to internal-external rotation. There are no commonly accepted definitions of joint axes, so researchers must choose those they feel are the most appropriate for the activity and joint being studied. If member reference frames are fixed to both distal and proximal segments, and the locations of at least three

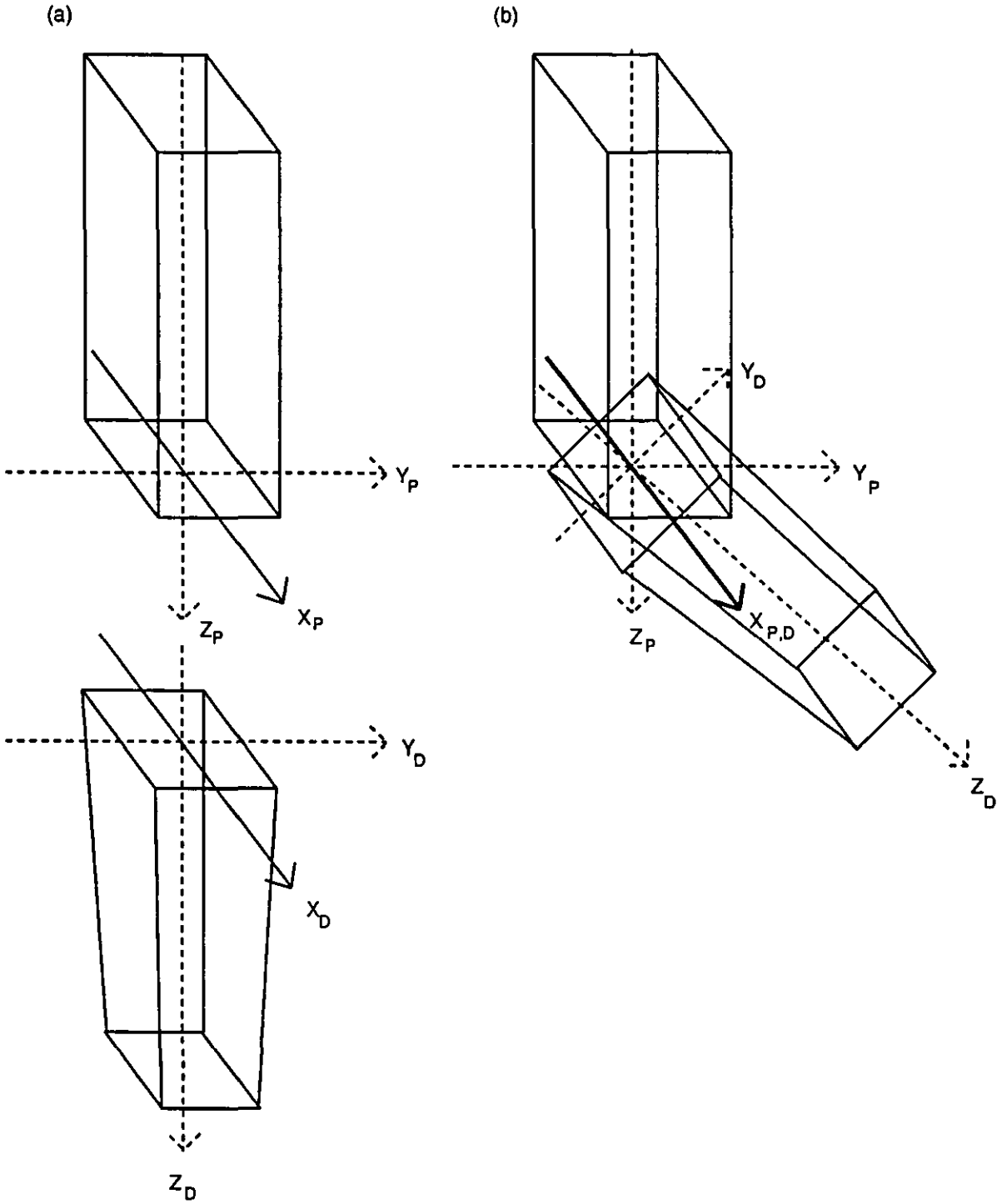

FIGURE 3.1 - a) Two rigid bodies and their member reference systems.

b) Two rigid bodies, showing the effect of rotation of the distal segment about the X axis.

non-collinear points are measured in an inertial reference frame for both frames, the attitude matrices and position vectors which transform points from the inertial reference frame to these member reference frames can be calculated using the procedures already discussed. The angles describing joint movement are then obtained from the attitude matrix produced from the product of the attitude matrix for the distal segment and the inverse of the attitude matrix for the proximal joint. This can be stated as follows:-

$$[R]_j = [R]^T_{ip}.[R]_{id} \qquad [3.20]$$

$$V_j = [R]^T_{ip}.(V_{id} - V_{ip}) \qquad [3.21]$$

Where:-
$[R]_j$ - is the attitude matrix defining joint orientation, or the orientation of the distal reference frame with reference to the proximal
$[R]_{ip}$ - is the attitude matrix for the inertial reference frame to the proximal member reference frame
$[R]_{id}$ - is the attitude matrix for the inertial reference frame to the distal member reference frame
and V_j, V_{id}, V_{ip} - are the position vectors.
The transpose of an attitude matrix is its inverse, see equation 3.2.

Alternative axes systems have also been defined, for example Chao (1980), and Grood and Suntay (1983). Grood and Suntay demonstrated their system on the knee with flexion occurring about a femoral medial-lateral axis, an axis for internal-external rotation embedded in the tibia, and the abduction axis defined by a floating axis. This alternative type of joint axis definition gives three axes which are not necessarily orthogonal. In examining joint motion a more appropriate system is the use of the helical axis, which is discussed in the next section.

3:1.5 HELICAL AXES

A joint is the connection between two rigid bodies. Chalses theorem of the motion of a rigid body states that the motion of a rigid body can be considered to be a translation along, and a rotation about a suitable axis in space. In light of this theorem the motion between two rigid bodies can be defined by the screw or helical axis parameters. The helical axis parameters therefore describe the whole body motion as a combination of a translation along, followed by a rotation about a directed line in space (the axis). The four helical axis parameters therefore are the rotation about the axis, the translation along the axis, the location of a point on the axis, and the direction of the axis. Reference is often made to finite helical axis (FHA), and instantaneous helical axis (IHA). The former represents the helical axis as defined by the initial and final positions only, whilst the latter is considered continuous and therefore is evaluated over small movement steps using the FHA as the approximations to the IHA. The way in which joint angles are defined varies between researchers. This makes it difficult to compare studies. The FHA and the IHA are not dependent on the way in which joint angles are defined, so are very useful in examining joint function.

Helical axes are most often calculated from the data resulting from Roentgen stereo-photogrammetry. This is the science of obtaining measurements from radiographic images. These measurements are

normally made on metallic markers placed in the skeleton. Selvik, Alberius, and Aronson (1983) reported an accuracy of 10 μm in measuring lengths using this technique. Siegler et al. (1988) used a three-dimensional digitizing system to measure the position of bones, this system had a reported accuracy of 0.0001 m in locating points. Both of these techniques demonstrate a high accuracy compared with cine-photogrammetric techniques. As the helical axis is an appropriate way to define joint motion, the accuracy of its estimation with the present quality of data is examined here.

Woltring, Huiskes, de Lange, and Veldpaus (1985) presented formulae for the estimation of the error variance associated with estimating the helical axis parameters. These formulae are presented here in a slightly simplified form:-

$$\sigma_\theta = \frac{\sigma}{p} \cdot \sqrt{\frac{2}{n}} \qquad [3.22]$$

$$\sigma_t = \sigma \cdot \sqrt{\frac{2}{n}} \qquad [3.23]$$

$$\sigma_n = \frac{2.\sigma}{\left(p.\theta.\sqrt{n}\right)} \qquad [3.24]$$

$$\sigma_s = \frac{2.\sigma}{\left(\theta.\sqrt{n}\right)} \qquad [3.25]$$

Where:-

p - is the effective landmark distribution radius

n - is the number of landmarks

θ - is the amount of helical rotation

σ - is the standard deviation of error in marker location

σ_θ - is the standard deviation of error in helical rotation

σ_t - is the standard deviation of error in helical translation

σ_n - is the standard deviation of error in direction of helical axis

and σ_s is the standard deviation of error in location of point on the helical axis

$$p^2 = \frac{2}{3} \cdot r^2 \qquad [3.26]$$

Where:-

r - is the root mean square distance of landmarks to mean position

There are a number of assumptions associated with these formulae which are discussed later. These formulae are now examined assuming that the IHA is computed in vivo using cine-photogrammetric data. An initial look at these formulae shows that the error of the calculated translation along the axis is proportional to the error in the marker locations, and inversely proportional to the square root of the number of markers. The number of markers is constrained by the number of bony landmarks visible

beneath the skin, some of these landmarks may not be used because the skin movement may be so great that the marker position does not accurately reflect the position of the bony landmark. The rotation about the axis is similar to the translation error term except it is also inversely proportional to the landmark distribution. The landmark distribution is limited by the size of the limb, and by the number of bony landmarks visible beneath the skin. The accuracy of the location of a point on the helical axis and the direction of the axis are both proportional to the accuracy of marker location, and inversely proportional to the angle of helical rotation, and the number of landmarks. These formulae indicate that a better estimate is achieved by a larger rotation angle, but the IHA is approximated by the FHA and the assumption is that the smaller the rotation the closer the FHA comes to approximating the IHA. The angle of helical rotation used in these formulae must also be considered in light of the error associated with the estimation of the helical rotation.

A sample calculation was performed to examine the anticipated accuracy of IHA parameters estimated for the elbow joint in vivo. The standard deviation of the noise affecting marker locations was assumed to be 0.002 m, which represents slightly better quality data than that obtained in the present study. Table 3.8 in section 3:5.4 presents an estimate of the standard deviations of noise affecting data sampled in this study. Additional assumptions were that n=4, P=0.10 m, and the joint was assumed to rotate 3 degrees. The results were: σ_θ = 0.81°, σ_t = 0.00141 m, σ_n = 21.9°, σ_s = 0.0382 m.

The error in the helical rotation was approximately a quarter of the total amount of rotation assumed. To improve this the accuracy of marker reconstruction would have to be increased significantly. The error in locating a point on the axis was nearly 0.04 m, but for most of the joints investigated the location of the helical axis after a finite rotation has been shown to vary by only a few millimetres (e.g. Siegler et al., 1988; Youm, Dryer, Thambyrajah, Flatt, and Sprague, 1979). The standard error in the estimation of the attitude of the helical axis was 21.9 degrees which is another significant error. Given these error estimates there are two options which would increase the accuracy of the IHA estimation: either increase the angle of rotation, or the accuracy of marker location. If the angle of rotation was increased this invalidates the IHA assumptions. Therefore the only practical option is to improve the accuracy of the marker locations. From the preceding analysis it can be concluded that in the present study the accuracy in locating the markers was too low to make IHA estimation practical.

To arrive at the error formulae Woltring et al. (1985) had to make a number of assumptions about the data. These are now discussed:-

1. Marker distribution was considered to be isotropic, which means that there are no preferential directions or planes in the distribution of the markers. This effectively means that the markers are placed at the vertices of a regular polyhedron. Spoor (1984) further examined these formulae and showed that if this condition was only slightly violated the results of the formulae still applied.
2. These formulae assumed that the noise contaminating the marker locations is zero mean, uncorrelated, and with the same standard deviation for each axis. With cine-photogrammetric data these conditions are hard to achieve, particularly that of having the same error associated with each axis, as shown in section 2:2.6. Depth errors are normally greater than those of the other axes. It may also be difficult to

have the same error in all coordinates as points may be obscured in one or more cameras views at various times during the activity.
3. They assumed that the helical axis parameters had been estimated using a statistically optimal procedure. Such procedures were discussed in section 3:1.1.
4. The error terms used here also assumed that one rigid body (normally the proximal) was fixed in relation to the measurement apparatus. If both are moving as is the case in the present study, the error terms are more complicated.
Although these assumptions could not be upheld in the present investigation, the general trends reflected in these formulae still apply, although the actual errors would be higher than those estimated.

De Lange, Huiskes, and Kauer (1990) examined the increase in accuracy obtained when noisy positional data obtained from Roentgen stereophotogrammetry were smoothed using generalised cross-validated spline procedures. Using a physical model on which the helical axis parameters were known they found that the accuracy in the description of the FHA improved when the noisy data were operated on using a spline procedure. Their results confirmed the computer simulation model of Woltring and Huiskes (1985), and the error propagation formulae of Woltring et al. (1985).

Studies of the helical axis on various joints (e.g. the knee, van Dijk, Huiskes, and Selvik, 1979; the wrist, Youm and Yoon, 1978; the ankle, Siegler et al., 1988) show that the IHA is non-stationary. As in vivo techniques normally rely upon Roentgen stereo-photogrammetric procedures, the helical axis is not estimated in normal loading situations when measurements are made on live subjects. If the measurements are made on cadavers, no indication is given of the influence on helical axis estimation of muscular contraction. The influence of such approximations on the variation in helical axis parameters is an area worthy of further investigation, as is the effect of the helical axis in the study of in vivo joint kinematics and kinetics.

3:1.6 SUMMARY

In the preceding sections a procedure has been adopted for the estimation of the attitude matrix and position vector of the rigid body in space. The orientation angles of rigid bodies are defined by Cardan angles. Using the formulae of Woltring et al. (1985) it was shown that given the quality of data available in this study it was inappropriate to compute the IHA of the elbow joint.

3:2 THE HUMAN ELBOW JOINT

To describe the motion of the forearm in relation to the upper arm it is necessary to define an appropriate set of member reference frames. To facilitate this the bones of the upper arm and forearm and their articulations are described in the following sections. No knowledge is required of the wrist and the hand as they were considered an extension of the forearm with no individual movement. In order to compile this section in addition to the observation of dry bone specimens details have been extracted from Steindler (1970), Kapandji (1970), and Hay and Reid (1982).

3:2.1 THE BONES OF THE ARM

An anterior view of the bones of the upper limb is shown in figure 3.2, a posterior view is shown in figure 3.3.

The head of the humerus is hemi-spherical, it is offset medially from the axis of the long shaft of the bone. Much of the humeral head lies outside the joint capsule, and this area is used for the attachment of various muscles. The tendon of the long head of the biceps runs between the greater and lesser tuberosities, which form the bicipital groove of the head of the humerus.

The long shaft of the humerus narrows at the top to form the surgical neck. The shaft bulges in the mid-shaft area to form the deltoid tuberosity. Distally the bone becomes wider and flatter. The distal end consists of two round condyles - the lateral and medial epicondyles, which are superseded by the medial and lateral supracondylar ridges. From these ridges many of the muscles of the forearm originate. Between these two epicondyles lie the articular surfaces of the humerus, the trochlea. Lateral to the trochlea is the hemi-spherical cartilage; the capitulum.

The forearm is composed of two bones the radius and the ulna. When the arm is supinated the radius and ulna lie parallel to one another, with the ulna being on the medial side of the forearm. It is possible for the forearm to rotate to a pronated position where the forearm has rotated about an axis along the length of the bones. In this movement the radius moves across the ulna. The axis of rotation passes distally through the head of the ulna, and proximally through the head of the radius.

The radius is the shorter of the two bones in the forearm. The head is cylindrical with the upper surface being concave and cup-shaped for articulation with the capitulum of the humerus. The sides of the radial head are covered by articular cartilage. It is these side heads which rest in the radial notch of the ulna. The neck is distal to the head and is much thinner; the radial tuberosity lies on the antero-medial aspect of the neck. The bone shaft has a sharp border, which is the line of attachment of the interosseous membrane, which connects the shafts of the radius and ulna. The larger end is the distal end, which has two articular surfaces. There is a small notch on the medial aspect which is for articulation with the ulna. The end-face is concave and angled medially.

The proximal articular surface of the ulna has a trochlear notch, for the articulation with the trochlea of the humerus. The base of the trochlear notch is known as the olecranon, and it forms the olecranon process, onto which the triceps tendon inserts. On the distal side of the trochlea notch is the coronoid process which fits into the coronoid fossa in full flexion. Distal to the coronoid process is the ulnar tuberosity. As the ulna tapers towards the wrist, its lateral border is sharp and is the origin for the interosseous membrane. At its distal end it articulates with the notch of the radius.

3:2.2 ARTICULATIONS OF THE JOINT

The elbow joint has been described as a trochogiglymus joint (Steindler, 1970) due to the three articulations at the joint. The humero-radial articulation between the capitulum of the humerus and the

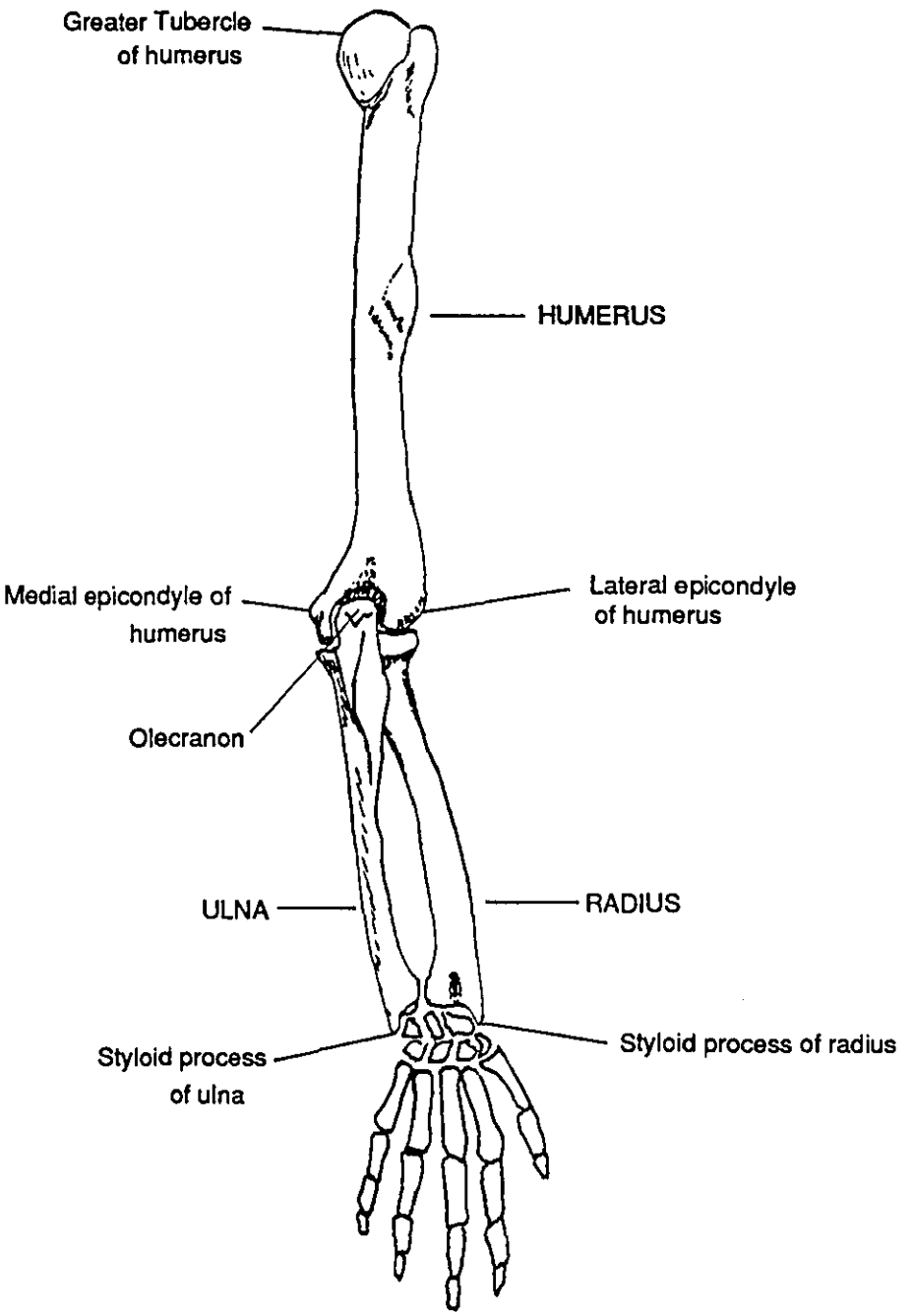

FIGURE 3.2 - Posterior view of the bones of the right arm.

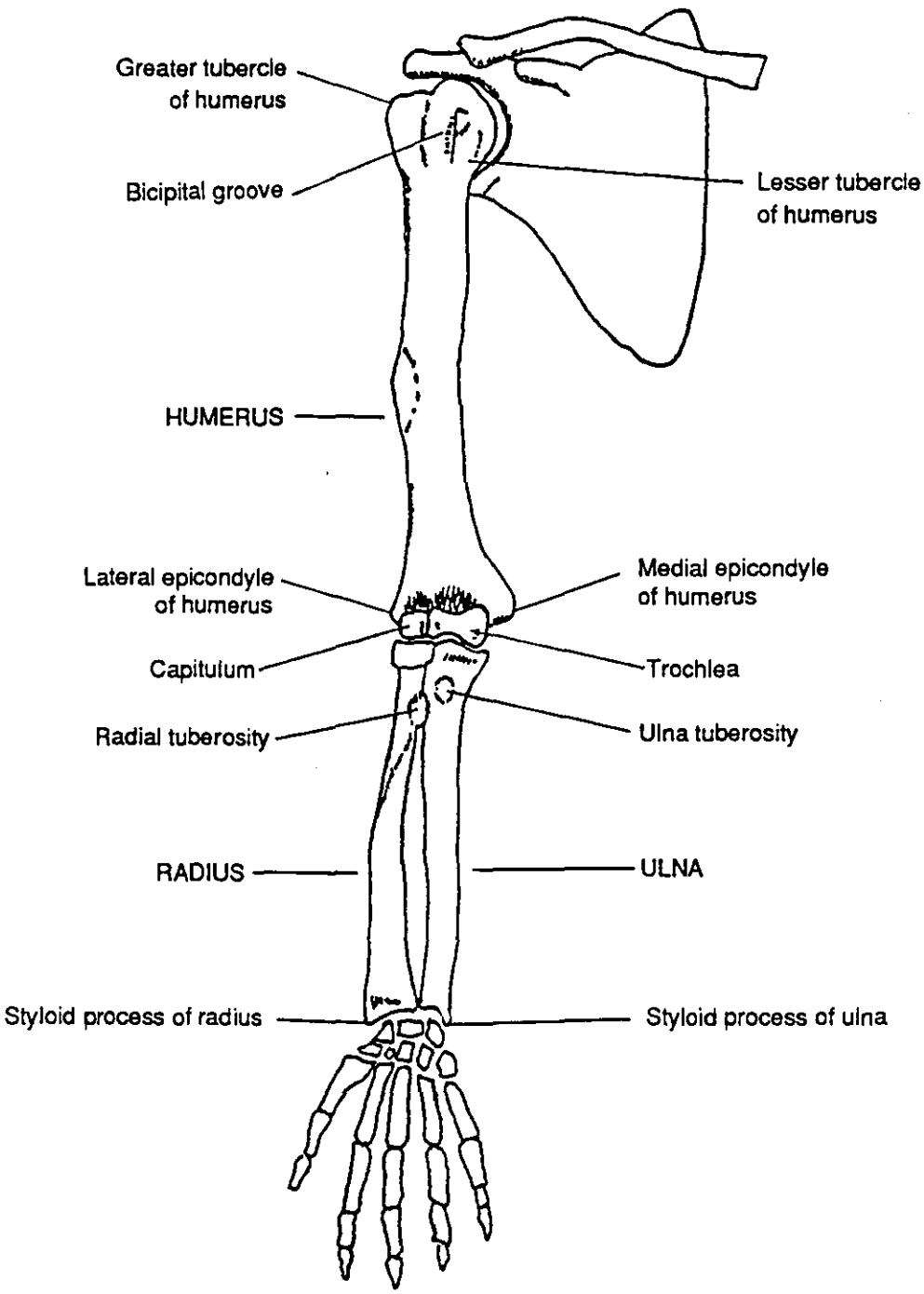

FIGURE 3.3 - Anterior view of the bones of the right arm.

head of the radius, permits the rotation of the radius about its long axis. The humero-ulnar articulation between the trochlea and trochlear notch of the ulna is a hinge like joint which permits flexion-extension of the forearm. The radio-ulnar articulation is between the head of the radius and the radial notch of ulna; during pronation-supination the radius rotates around the ulna about this joint. Due to the geometry of these articulations and the ligamentous structures of the elbow joint there is little translatory movement at the joint (Morrey and An, 1983), and for the purposes of the present investigation none is assumed.

3:2.3 MOVEMENT OF THE FOREARM

The joint has two major degrees of freedom permitting flexion-extension, and pronation-supination. Supination is the rotation of the forearm so that the thumb moves laterally, pronation moves the thumb medially. The geometry of the joint and its ligamentous constraints result in the additional motion of abduction-adduction. The abduction-adduction angle of the elbow joint is generally called the carrying angle. This third angular component is passive in nature. The precise definition of the carrying angle varies between researchers. Some researchers have defined the carrying angle as the angle by which the long axis of the ulna deviates from the long axis of the humerus (e.g. Chao and Morrey, 1978). Whereas others have defined a longitudinal axis for the forearm and measured carrying angle in relation to this axis (e.g. Amis, Dowson, Unsworth, Miller, and Wright, 1977). The three angular orientations of the forearm are illustrated in figure 3.4.

Kapandji (1970) measured the range of flexion-extension to be 145 degrees, with flexion being stopped as the flexor muscles meet the forearm. Whilst for supination and pronation he reported angles of 90 degrees and 85 degrees respectively. Steindler (1970) investigating the carrying angle reported a range of 10 to 15 degrees for men, and 20 to 25 degrees for women, with the carrying angle zero at full flexion. Youm et al. (1979) examined the arms of eight cadavers and reported a range of flexion of 140 degrees (standard deviation 5 degrees), a range of pronation of 70 degrees (S.D. of 5 degrees), and finally for supination a range of 85 degrees (S.D. of 4 degrees).

Chao and Morrey (1978) performed an extensive analysis of the movements of the forearm of two cadavers. During flexion both specimens showed the same pattern of change in carrying angle; these changes were 16 and 20 degrees through out the full range of flexion. The change in carrying angle was independent of the position of the forearm which was in either a supinated, neutral, or pronated position. They also showed 5 degrees of axial rotation during flexion, independent of the starting position of the limb.

Chao and Morrey (1978) claimed that supination-pronation was due to the rotation of the radius about the radio-ulnar joint with the ulna showing no movement, whilst the radius deviates medially from its position. Youm et al. (1979) also showed that supination-pronation involves no movement of the ulna, with the radius performing the rotation. They demonstrated that during supination-pronation axial rotation of the ulna occurred distally, but not proximally.

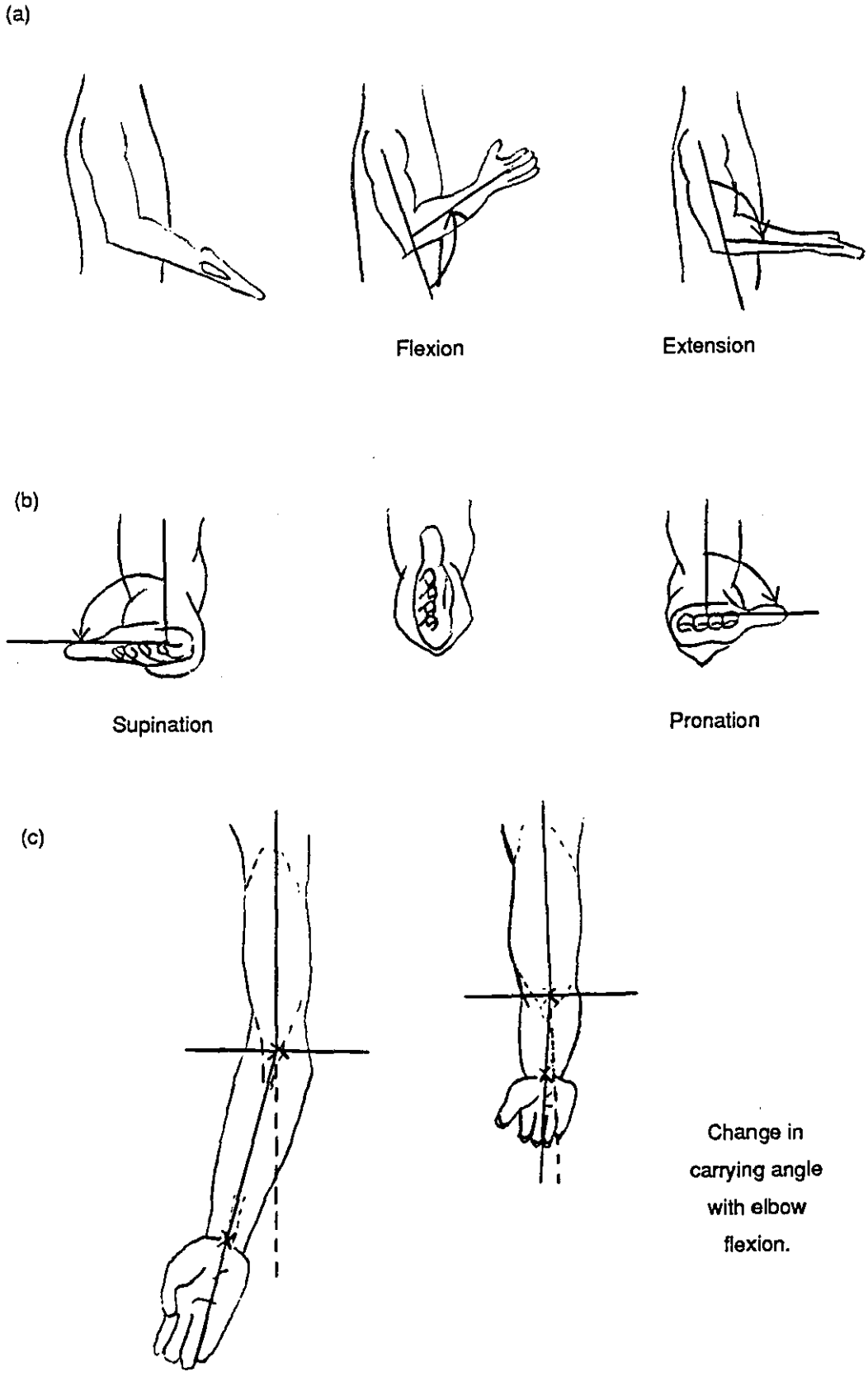

FIGURE 3.4 - The three angular motions of the elbow joint.

There have been many contradictory reports as to how the carrying angle varies during flexion. Dempster (1955) examined the carrying angle and claimed that it changed in an oscillatory pattern with flexion. Amis et al. (1977) examined the variation in carrying angle during elbow flexion and claimed that the range of movement was the same when the hand was adducted and abducted, and that the carry angle changed throughout flexion. Youm et al. (1979) also showed that the variation in the carrying angle varied with amount of flexion as a sinusoidal function, but claimed it remained constant after 100 degrees of flexion. London (1981) claimed that it remained constant during flexion, whilst Chao and Morrey (1978) showed that it varied linearly during flexion with it being maximum at full extension and minimum at full flexion.

In an attempt to clarify the variation of the carrying angle An, Morrey, and Chao (1985) examined how the carrying angle was affected by two different definitions of the carrying angle. The first technique measured the angle between long axis of the humerus and the long axis of the ulna in the plane containing the axis of joint flexion-extension and the humerus. The second defined the angle as the abduction-adduction angle of the long axis of the ulna to the long axis of the humerus using Eulerian angles. These definitions gave different results, but the authors did not attempt to evaluate their relative merits. This variation in results illustrates the effect of using different measuring techniques. It must also be remembered that given the small number of cadaver elbow joints which have been investigated to date, it may be possible that much of this variation can be accounted for by the naturally occurring differences in human elbow joints.

Fischer (1909) calculated the instant centre of rotation of the elbow during flexion, and found that it was located in the centre of the trochlea, and its location only varied by 2 to 3 mm during flexion. Similar results were found by Chao and Morrey (1978). Youm et al. (1979) measured the IHA of the elbow during flexion-extension and showed that the axis was located through the centre of the trochlea. For supination-pronation the axis passed distally through the ulna and proximally through the centre of the capitulum. In both cases there was little variation in the locations of the IHA in different limb positions.

3:2.4 MARKER POSITIONING

Markers were positioned based on the discussion in section 3:1.2. Instead of using rigid markers, the points of interest were marked directly onto the skin. This was done using a black marker pen, making a target of 2 cm in diameter which gave an image size large enough to be easily recognised when digitizing but small enough so its centre could easily be estimated. Ink lines were extended from these markers so that if the marker was not directly visible a line associated with the marker gave an indication of the location of the marker.

Points on the arm were chosen so that skin movement would be as small as possible whilst still defining meaningful bony landmarks. Three landmarks were identified for the humerus; these were the lateral and medial epicondyles, and the lesser tubercle of the humerus. The landmarks used for the forearm were the styloid process of the radius, the styloid process of the ulna, and the olecranon process (ulna). Other marker positions were considered but disregarded as it was either too difficult to clearly identify them, or they were too affected by skin movement. The ends of the dumbells were also marked defining a line that

passed centrally through the handle of the dumbells, so that when the forearm was supinated this line was approximately parallel to the flexion-extension axis.

3:2.5 DEFINITION OF MEMBER REFERENCE FRAMES

For the analyses undertaken in this study it was necessary to define sets of member reference frames which permitted description of the movements of the forearm relative to the upper arm, and had physical significance to the bones of the arm. The measurements of these frames were made during the static data capture.

The axes were defined so that they were meaningful with reference to the angular orientations of the joint. The flexion-extension axis (X axis) was defined perpendicular to the common longitudinal axis, and orientated in the medial lateral direction. The abduction-adduction axis (Y axis) was defined perpendicular to the longitudinal axis, and orientated in the anterior-posterior direction. The supination-pronation axis (Z axis) was defined parallel to the longitudinal axis of the rigid body.

Chao and Morrey (1978), when studying the motion of the elbow joint, defined four sets of member axes. One was fixed to the upper arm, one to the forearm, and one to each of the radius and the ulna. The latter pair of axes were used to define the rotation of the ulna relative to the radius during supination-pronation. For the study of forearm motion in this study the humeral and forearm axes were defined similarly to those of Chao and Morrey (1978). For the humeral reference frame the Z axis was defined as the long axis of the shaft of the humerus, the X axis was defined as a line through the centre of the trochlea perpendicular to the Z axis, and the Y axis was perpendicular to these two axes. The origin of this system was in the centre of the trochlea. This location corresponds with the location of the centre of rotation as determined by Fischer (1909) and Chao and Morrey (1978) during flexion. The locations of the axes also correspond well with the location of the IHAs during flexion-extension and supination-pronation calculated by Youm et al (1979). To give the angular orientation of the forearm a reference frame was then defined in this segment. The Z axis passed through the centre of the styloid process of the ulna distally, and through the radial head proximally, the X axis passed through the centre of the radial neck perpendicular to the Y axis, the Y axis was orthogonal to these two axes. These reference frames were also used to describe the origins and insertions of the muscles examined in this study. (The origins of the biceps were assumed to be onto the head of the humerus, removing the need to model the scapula, see section 5.1.3).

To determine the resultant joint moment a reference frame was defined which modelled the forearm, hand, and dumbell as a single rigid body. The humeral reference frame was modelled as described for the other analyses. The origin of the distal member reference frame was located at the centre of mass of the rigid body, see section 4:3.2 for how the location of the centre of mass was computed. A longitudinal axis (Z axis) was defined which passed through the olecranon of the ulna proximally, and centre of the dumbell distally. As the dumbell was grasped so the hand was central to the handle of the dumbell this axis passed approximately through the mid point between the styloid processes of the ulna and radius. The X axis was defined as being parallel to an axis centrally through the handle of the dumbell, when the forearm was supinated this axis was approximately parallel to the X axis of the humeral reference frame. The Y

axis was orthogonal to these two axes.

There is a final choice of whether to use Eulerian angles or Cardan angles. From previous studies it was possible to anticipate the range of motion that would be measured. In no case was any angle expected to exceed 180 degrees. Using the notation from section 3:1.4 Eulerian angles are not defined if θ is 0 degrees or 180 degrees, whereas the Cardan angles are undefined when θ is 90 degrees. As in this study the Y axis was associated with abduction-adduction (carrying angle) the expected range of movement was approximately from 0 degrees to 25 degrees. Euler angles would be undefined if θ, the carrying angle, was 0 degrees, whereas the range of movement was not great enough to limit the Cardan angles. Therefore Cardan angles were used to describe the orientation of the forearm in relation to the humerus.

3.3 LITERATURE REVIEW : SMOOTHING AND DIFFERENTIATION OF DATA

Photogrammetrically derived human movement data is contaminated with noise as a result of the nature of the recording process. Noise can generally be defined as the undesirable parts of a signal. In the case of the photogrammetrically derived data in the present study the sampled signal was considered to consist of three parts:-

SAMPLED SIGNAL = TRUE SIGNAL + SYSTEMATIC NOISE + RANDOM NOISE

It is generally assumed that the sources of systematic noise have been identified and removed from the signal. The remaining sources of systematic noise are then assumed so to be small that they can be ignored, and of low enough frequency that they will have little effect on the derivatives.

Unfortunately random noise cannot be directly identified. Noise can arise from many sources, as discussed in section 2:3. Winter, Sidwall, and Hobson (1974) analysed data from a television tracking system, which gave two dimensional coordinates of body landmarks, to ascertain the frequency characteristics of the noise from the data capture system. During one phase of gait the "heel and ball markers" were stationary therefore any signal measured during this period was due to the system. The noise was of a predominantly higher frequency than the biomechanical signal. Lesh, Mansour, and Simon (1979) performed multiple digitizations of the same sequence of data, to examine the frequency content of human gait data. The averaging of these five digitizations was assumed to have effectively eliminated the noise due to the digitization procedure. Analysis of the resulting signal suggested that the noise impinging on the signal was generally of a higher frequency than the frequency components of the signal. They also used the same technique as Winter et al. (1974) to quantify the noise and found that compared with the results from averaging, the noise levels were underestimated.

Although the noise introduced in the measuring procedure probably occurs across the whole spectrum, its influence will be most significant in those parts of the frequency spectrum where there are no frequency components from the true signal, and when the amplitude of the noise and the signal frequency components are similar. The techniques reviewed in the following sections attempt to remove this higher frequency noise. It is technically very difficult to ascertain how much of the signal within the bandwidth of

the true signal is noise. The amplitude of any noise occurring in the lower range of frequencies in the estimated signal bandwidth is considered to be insignificant compared with the amplitude of the true signal. The way in which the data is differentiated is also very important as this has an affect on the accuracy of estimated derivatives (see section 3:4).

The terms smoothing and filtering are used interchangeably in the biomechanical literature. When smoothing a signal this normally involves the removal of the high frequency components from the signal; in which case it is equivalent to low-pass filtering. In this review the term filter will be used when referring to digital filters and the term smoothing used for other techniques which remove the high frequency components of a signal. To aid in the structure of this review the techniques have been placed in three categories: digital filters, truncated Fourier series, and splines. As some of the papers deal with a number of techniques, these are reviewed under the category of the technique which the author(s) favoured.

3:3.1 DIGITAL FILTERS

A digital filter operates on a set of data to produce an output in which selected frequencies contained in the input signal have been removed. The implementation of these filters can be in hardware or software form, in biomechanics the software option is most often used. The data has to be equidistantly sampled (equal sample intervals) and after operation by the filter a suitable differentiator has to be applied to obtain signal derivatives. Digital filters are commonly classified as being either low-pass, band-pass, or high-pass. These refer to the frequency components of the original signal which are allowed to pass unaffected by the filter (see figure 3.5). Low-pass filters are used for the removal of noise from film derived data.

Digital filters are also classified as being recursive or non-recursive filters. The output of a recursive filter is determined from the weighted sums of past output values as well as past and or present input values. The output of a non-recursive filter is determined from the sum of weighted past and present input values. Recursive filters tend to require fewer terms to obtain the desired frequency response of the filter, but introduce phase lag into the signal. Recursive filters are normally applied in forward and reverse directions to cancel phase lag. All the techniques reviewed here are attempts to implement an ideal low-pass filter; this is never realised and the various phases of the frequency response of a typical low-pass filter are given in figure 3.5.

One of the first smoothing techniques suggested for biomechanical data was the recursive Chebyshev filter (Plagenhoef, 1968). Plagenhoef presented a computer program for the kinetic analysis of human movement using data derived from photogrammetric techniques, using the Chebyshev filter for noise reduction. The frequency response of this filter has a ripple in the pass-band, which means that some of the frequencies of interest will be attenuated (Stearns, 1975). Ideally a low-pass digital filter with a flat frequency response in the pass-band would produce superior results. An example of such a filter is the Butterworth filter, which has been adopted by many researchers in biomechanics (e.g. Winter et al., 1974; Bobbert, Huijing, and van Ingen Schenau, 1986).

Winter et al. (1974) obtained data from a computer-television system, and filtered the data with a

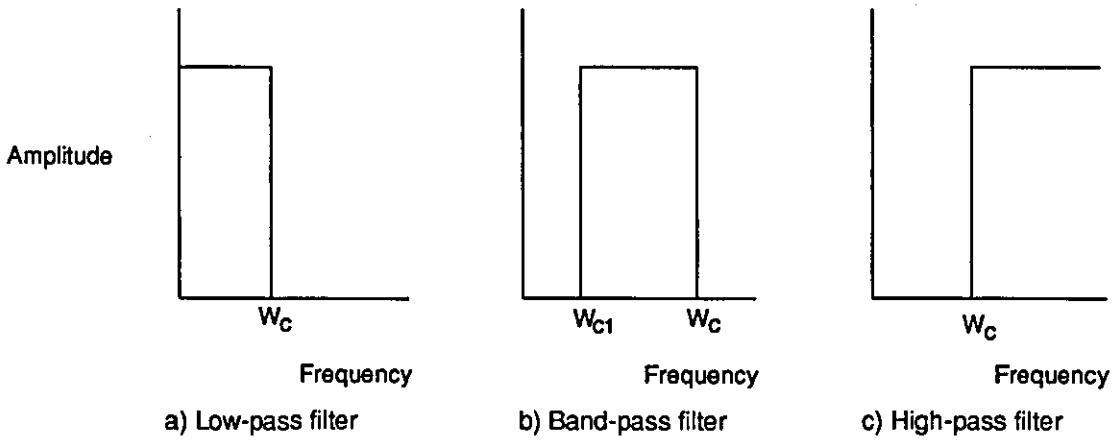

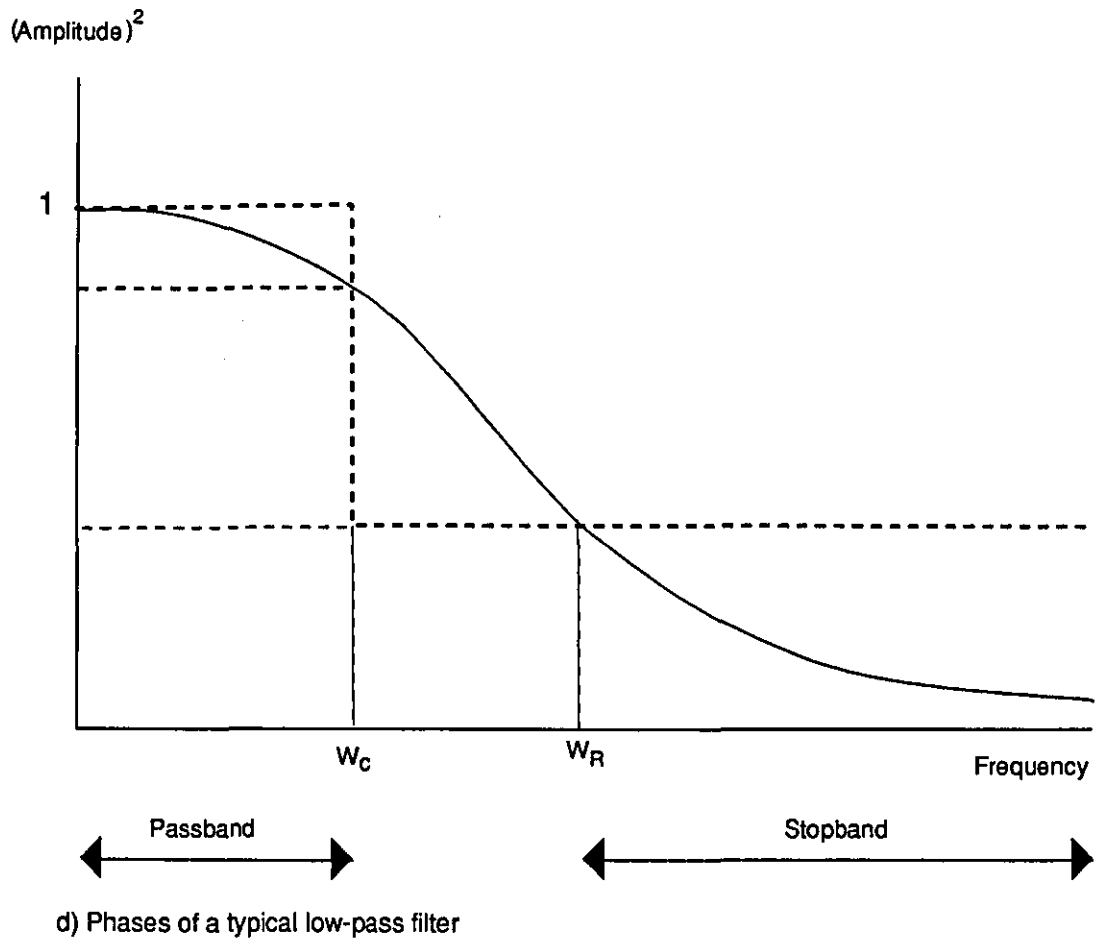

FIGURE 3.5 - Three types of digital filters (a,b,c), and the phases of a typical low-pass filter (d), where W_C is the cut-off frequency for the filter, and W_R is the rejection frequency for the filter.

Butterworth filter (an example of a recursive filter). The cut-off frequency was set after analysis of the frequency characteristics of the sampled signal. Later work by Winter and colleagues (Pezzack, Norman, and Winter, 1977) evaluated a number of filters. An aluminium arm fitted with an accelerometer was filmed as it rotated. The film was digitized to obtain angular displacement data, which was reproduced in the paper so that others could evaluate smoothing and differentiating techniques with these data. These data were then analysed using three separate techniques to estimate angular displacement and velocity values, which were compared with the criterion accelerometer data. The three techniques used were: the Chebyshev filter with derivatives calculated by direct differentiation of the resulting polynomial; no filtering of signal but differentiation with the second order finite difference differentiating formulae; and a second Butterworth filter, applied in forward and reverse directions followed by first order finite difference differentiating formulae. By inspection of the resulting curves they concluded that the Butterworth filter was superior to the other techniques. A spline fitting technique was not examined but was criticised because of knot placement 'encumbering the procedure': this shows ignorance of the work of Dierckx (1975) and Reinsch (1967) both of whom advanced spline fitting techniques which obviate the need for the manual placing of knots. The paper of Pezzack et al. (1977) led to a number of other researchers examining various techniques for data smoothing in biomechanics using the published data (e.g Soudan and Dierckx, 1979; Wood and Jennings, 1979; Hatze, 1981a). Unfortunately this was not an ideal approach as the data used was a poor approximation to data sampled from a real photogrammetric study of human movement. Although the data in question had been digitized and this is a source of error in most studies, many of the other sources of error were not present (e.g. skin movement, marker movement, problems in joint centre location). The second derivative values of this signal at both the beginning and end of the data set were zero, which does not provide an adequate test of many differentiating techniques, as will be discussed later.

Recursive filters require filtered and non-filtered data points to produce the output. At the beginning of the data set there are no prior raw or filtered values. To eliminate phase lag these filters are applied in forward and reverse directions which means that this problem occurs at either end of the data set. Smith (1989) examined the effect of adding extra data points at the beginning and end of the data set to overcome the problems at the end points when using the Butterworth filter. Four data padding techniques were assessed: digitizing extra points at the beginning and end of the data set; duplication of the end points; linear extrapolation; and reflection of the data end points. The effect of this data padding was assessed by computing the mean residual difference between the estimated second derivative values and the criterion values. The middle of the data set of Pezzack et al. (1977) was used, leaving extra data for the padding operations. The number of padding points was varied from five to 30. Although the Butterworth filter was used to filter the displacement data, the data padding techniques were assessed by examining their estimates of the second derivative of the signal, which was computed from the Butterworth filtered displacement data which was then processed using the first order central difference differentiating formulae. Therefore the direct effects of the data padding techniques on the output from the Butterworth filter were masked by also using the differentiating formulae. Using extra digitized points either side of the data gave the most accurate results, reflection of the data points gave the next best. Padding with more than 10 points made no difference to the increase in accuracy with any of the padding techniques.

Lesh et al. (1979) reported the use of a non-recursive finite impulse response (FIR) filter, for noise reduction in displacement data and differentiation of data (first and second derivatives). They used the algorithm of McClellan, Parks, and Rabiner (1973) to derive the filter coefficients for the FIR filter. In this program the number of filter coefficients, pass-band, and cut-off must all be specified. Frequency analysis of an averaged signal provided them with the required cut-off frequencies.

A recursive filter incorporating a dynamic programming filter was advanced by Busby and Trujillo (1985); Trujillo and Busby (1983) gave a more detailed description of this filter. Two data sets from Andrews, Cappozzo, and Gazzini (1981) were used to assess this technique. Busby and Trujillo (1985) used the same criterion measure as Andrews et al. (1981) used when assessing five data smoothing and differentiation techniques, and so it was therefore possible to compare results. Displacement data results were comparable, but second derivative results were superior using the dynamic programming filter for both data sets. The technique was also tested on data from Anderssen and Bloomfield (1974a), from Lanczos (1967), and the data of Pezzack et al. (1977). The technique performed well for all these data sets.

Jetto (1985) used a Kalman filter to smooth noisy data derived from the measurement of haemodynamic signals. This technique was extended by Fioretti and Jetto (1989) so that derivatives could also be estimated: they applied this technique to biomechanical data. The Kalman filter is a recursive filter with an infinite impulse response. In this case the Kalman filter minimised the noise remaining in the signal by assuming the measurement noise was Gaussian. On a noisy test data set this technique produced accurate estimates of the true displacement, first derivative, and second derivative values.

3:3.2 TRUNCATED FOURIER SERIES

A Fourier series is a representation of a signal by the weighted sum of a number of sine and cosine terms of increasing frequency. If enough of these terms are included in the series then a tight fit to the signal is obtained. By adjusting the number of terms the tightness of the fit and therefore the amount of smoothing is adjusted. Once the appropriate fit is made to the raw displacement data the series can be directly differentiated to give the derivatives of the signal. To fit a Fourier series to a finite data set the Discrete Fourier Transform (DFT) is used giving the Discrete Fourier series (DFS). An alternative to the DFT is the Fast Fourier Transform (FFT) (Cooley and Tukey, 1965). The FFT fits a DFS to a set of data: it is computationally much quicker than the DFT and is less sensitive to computer round-off errors. The only drawback is that FFT algorithms impose restrictions on the number of data points, the most common being that the number of data points be a power of two (e.g. Cooley and Tukey, 1965). Another FFT algorithm requires that the number of data points be prime, (Burrus and Eschenbacher, 1981).

Probably the first person to fit a Fourier series to human movement data was Bernstein (1967), reporting work he performed in 1929. Cappozzo, Leo, and Pedotti (1975) also advanced the use of fitting a trigonometric series to displacement data. To determine the number of Fourier coefficients to be used, the residual (between sampled signal and filtered signal) was plotted against the number of terms retained. Visual inspection was then used to determine the highest coefficient to be retained. In 1983 Cappozzo

and Gazzani presented a comparison of four techniques used to determine the coefficients of a DFS. Two of the techniques calculated the DFS coefficients directly from the data, one using a standard DFT algorithm (Cappozzo et al., 1975), the other using a simplified DFT. The other two techniques evaluated used splines; one derived the coefficients using the routine of Dierckx and Piessens (1977). The other spline technique used the spline to smooth the data and then calculated the DFS coefficients using the simplified DFT. The simplified DFT performed least well, with the other three techniques producing better results, all three being equally accurate in computing the DFS coefficients. The greater the sampling rate the closer the simplified DFT came to the accuracy of the other three techniques. The technique of using the spline followed by the simplified DFT required the second lowest amount of computer time (the simplified DFS required the least). Consequently it was this technique the authors recommended. FORTRAN code was provided for the implementation of their simplified DFT.

Cappozzo and Gazzani (1983) used the algorithm of Dierckx and Piessens (1977) to compute Fourier coefficients. Soudan and Dierckx (1979) examined this technique at greater length. Splines were fitted to the data and then the underlying functions were integrated using the technique advanced by Piessens (1971) to derive Fourier coefficients. The technique was assessed by visual inspection of the real and calculated second derivatives using the data of Pezzack et al. (1977). The authors were aware that this data had a low noise content compared with normal biomechanical data so more noise was added to the signal. Visual inspection of the graphical representation of the results showed this technique to be successful.

Jackson (1979) proposed the use of a Fourier series to smooth biomechanical data. This paper focussed on the number of terms necessary in the Fourier series to accurately produce the desired signal. The residual was considered a function of the number of terms making up the Fourier series. A discrete Fourier series was fitted to the data using the maximum number of coefficients (this is limited by the rate at which the signal was sampled), the second derivative of this function was calculated. The second derivative was evaluated with each subsequent assessment ignoring the highest Fourier coefficient remaining. When the value of the second derivative fell below a certain prescribed level for the removal of three consecutive coefficients, this was considered to be the optimal number of coefficients with which to smooth the function. The work of Jackson is hard to assess as the prescribed level below which the second derivative must fall was not defined. In addition details were not given as to why the second derivative values were selected as being a criterion.

Hatze (1979a, 1981a) presented a DFT based technique to filter and differentiate biomechanical data. A Fourier sine series was fitted to the data. The data were initially linearly detrended. Hamming (1983) warned against such an operation as he claimed it adversely affects the low order frequency components of the signal. This process may have introduced errors into Hatze's processed signal but they were not evident in his analysis of this technique. This technique was based on the work of Anderssen and Bloomfield (1974a, 1974b), which employed a form of optimal regularization to select the degree of smoothing. The accuracy of this technique was examined by calculating the first and second derivatives of the data of Pezzack et al. (1977). Additional noise was added to this data, and the technique still

produced good estimates of the derivatives.

Hatze claimed that the process could have been speeded up if an FFT had been employed. As an FFT places restrictions on the number of data points (e.g. the number must be a power of two, or prime) and the number of samples cannot be guaranteed to adhere to such restrictions, the data may have to be further manipulated. One solution to this would be to reflect the data about a vertical axis, making it cyclical, until a suitable number of data points are obtained. This solution would add to the number of data points and increase the amount of computation: one of Hatze's criteria for selecting this technique. An alternative solution to this problem would be to add data points to either end of the sample. This would effectively add a discontinuity to the data resulting in the approximating trigonometric function becoming oscillatory at these discontinuities (the Gibbs effect, Stearns, 1975) making signal estimates poor at these end points.

Sprigings, Burko, Watson, and Laverty (1987) in an anthropometry study, examined the optimally regularized Fourier Series of Hatze (1981a) (which is commercially available), for analysing the data of the vertical displacement of a metal ball dropping under the influence of gravity. The results for the second derivative showed very poor prediction for the end points, where the curve tended towards zero. The technique of Hatze (1981a) is based around a Fourier sine series: a sine series automatically has values of zero at both ends of the curve, this would also apply to the second differential of a sine series. It is therefore not surprising that this technique behaves in the way reported by Sprigings et al. (1987). The data of Pezzack et al. (1977) which Hatze used to test his technique has values of zero at both ends of the second derivative so this data did not provide an adequate test of this technique.

3:3.3 SPLINES

A spline is a series of polynomials joined together to represent a signal; a piece-wise polynomial. The polynomials are all of the same order (2m) and join at positions called knots. There are certain conditions imposed on the spline which are detailed in section 3:4.5. There are various differences between the ways in which researchers have implemented spline techniques. These differences arise from the order of the polynomials making up the spline, the number and positions of the knots, and finally how the degree of smoothing is selected. The natural spline fitting routine of Reinsch (1967) has been often used in biomechanics (see following review for references). A significant feature of this spline technique is that the end points are constrained to be zero for the k th derivative of the spline where k=m,...2m-2; as the Reinsch spline was a cubic, k was equal to two.

Zernicke, Caldwell, and Roberts (1976) compared the vertical force generated in a kick measured on a force plate with that estimated from film data. The Reinsch (1967) cubic spline was fitted to the film displacement data and differentiated permitting calculation of the velocities and accelerations. The spline routine of Reinsch (1967) has knots at all data points. The degree of smoothing of this spline is adjusted using a smoothing parameter 'S' which controls the tightness of fit of the spline to the raw data. In this study 'S' was determined by visual inspection of the fitted curve. Combining the segmental acceleration data with the anthropometric data of Dempster (1955) the vertical ground reaction force was calculated.

The difference between the criterion values (force plate value for vertical reaction force) and the calculated values (from film using the spline) were numerically assessed. In addition to using a spline, an orthogonal polynomial was fitted to the data. The mean percent differences between force plate measured reaction force and film derived force estimations were 4.75 percent for the spline and 10.27 percent for the polynomial. As both of these techniques require the specification of the closeness of the fit, these results indicate either the superiority of the spline, or the more appropriate choice of the tightness of the fit of the spline over the polynomial. The force data was recorded from four channels on a chart recorder and this trace was then digitized and summed to derive vertical force. The accuracy of this method of determining ground reaction force must be questioned. The smoothing and differentiating techniques were assessed in conjunction with anthropometric data, which means it is difficult to know which to apportion the inaccuracies to. Finally, the activity was assumed to be planar but to be sure of this a three-dimensional study should have been undertaken initially. Even with these deficiencies this paper does represent a structured attempt to assess the value of splines in smoothing biomechanical data.

McLaughin, Dillman, and Lardner (1977) used a variety of sets of data to attempt to evaluate a cubic spline. The cubic spline of Reinsch (1967) was used with the standard deviation of each point being estimated so it could be used as a weighting factor in the spline routine. The degree of smoothing, 'S', was set equal to the number of data points. The first evaluation was the comparison of the vertical ground reaction force of a vertical jump measured by a force plate, with the value predicted using acceleration values calculated using the cubic spline. A graphical comparison with the force plate recording of the vertical acceleration, showed that the spline gave a good approximation. This evaluation of the spline using a force plate is very similar to that of Zernicke et al. (1976) and suffers from all the same problems. The spline was then compared with a least-squares polynomial technique. Both techniques were used to compute the angular acceleration of the lower leg during running. There was no criterion with which to compare the data, yet the least-squares polynomial was criticised for giving unrealistic end point values. In this case the spline gave end point values of zero which could also be considered unrealistic, but no mention was made of this. The spline was then compared with first order finite difference differentiating formulae for determining angular velocity for forearm flexion. Again no criterion was available for comparing the techniques. Finally the spline was used to derive the vertical acceleration of a weight falling freely to the ground, the spline at either end of the sample gave acceleration values of zero. To remedy these end point problems McLaughin et al. (1977) suggested that 20 points be added at either end of the sample, or that the corresponding number of points be ignored. This differs from the recommendations of Zernicke et al. (1976) who for the same procedure suggested only three points. The lack of criterion measures on which to base the comparisons between the different techniques examined in this study means that the results are not enlightening.

The limitations placed on the second derivative in the case of the cubic spline mean that unrealistic values are produced at either end of the data range when estimating second derivatives (see section 3:5.5). This is not the case with quintic or higher order splines. It was one of the purposes of the paper of Wood and Jennings (1979) to compare the cubic with the quintic spline. They graphically compared the vertical acceleration curve of a vertical jump with the curve produced by a force plate. The graphical

representation showed that the second derivative of the quintic spline had greater accuracy than the cubic in calculating accurate second derivative data, especially at the end points. To further advance the use of the quintic spline they used the spline on the data of Pezzack et al. (1977). As with all of the other published studies using this data set the quintic spline produced an accurate estimate of the true second derivative.

Dierckx (1975) presented a spline algorithm which fitted a spline of variable order using an automatic knot placement technique. The Butterworth filter followed by central difference equations to differentiate the filtered data were compared with the spline of Dierckx (1975), by Pettett and Budney (1981). The details given of the implementation of their work with the spline were limited, as the selection of the smoothing parameter 'S' was not outlined. Using displacement data from the motion of a golf club they evaluated the accuracy of the techniques using the same signal but two different sampling rates. Their results showed that greater accuracy was achieved in the calculated second derivative with the higher sampling rate. In addition they highlighted the fact that the spline was more effective than the digital filter in regions of rapid acceleration. These results have useful implications if sampled data is expected to contain regions of high acceleration. Unfortunately the authors did not establish how they derived their criterion data for the first and second derivative values, making it difficult to evaluate these results.

Miller et al. (1980) filmed a motor driven 'spatial linkage'. The resulting three-dimensional data were used to assess five techniques for filtering and differentiating the data. The five techniques were: second-order finite difference differentiating formulae; least-squares polynomial fitting; digital filtering using a Butterworth filter followed by finite difference equations to obtain derivatives; fitting of a Fourier series and then differentiating this series to find derivatives; and finally fitting a cubic spline. Criterion values were obtained from knowledge of the rate at which the 'spatial linkage' was driven. The RMS errors were calculated. The first two techniques did not perform well, but the last three all produced very similar RMS errors for the first and second derivatives of the sampled signal.

As mentioned previously the second derivative of a Reinsch cubic spline is constrained to have end point values of zero. Zernicke et al. (1976) and McLaughin et al. (1977) both suggested solutions to this problem. Phillips and Roberts (1983) proposed that when a cubic spline is used, one data point should be added at either end of the data set to reduce the effect of the constrained second derivative values on the estimated second derivative values. They compared a digital filter, a cubic spline, and an 'augmented spline' (a normal cubic but with one data point added to either end of the data set). The Reinsch cubic spline was used with the smoothing parameter 'S' set equal to the number of data points. Phillips and Roberts used two sets of artificial data and looked at the deviation of the second derivative of the last five data points from a criterion. In both cases the 'augmented spline' performed better than the digital filter and the standard cubic spline. Using the data of Pezzack et al. (1977), the digital filter produced an error in the last acceleration value of 38 percent, the cubic spline 28 percent, and the 'augmented spline' 4.3 percent. This problem with inaccuracy in estimating end point second derivative values is less acute with quintic splines where the same restrictions are not placed on the second derivative.

Andrews et al. (1981) presented a comparative study of five techniques for the smoothing and differentiation of film derived displacement data, including a cubic spline. The techniques compared (which included some of those already discussed) were: a fourth order low-pass Butterworth filter followed by a Sterling differentiating formula; the cubic spline of Dierckx and Piessens (1977); a truncated Fourier series based technique (Cappozzo et al., 1975), and a non-parametric technique after Anderssen and Bloomfield (1974b). To evaluate these techniques two mathematically generated signals were used, both with Gaussian noise added to the signal. The first signal was a trigonometric series, and the second a fourth order polynomial. The technique was assessed by evaluating the mean square error as a percentage of the mean of the absolute values of the true signal. In all cases the various parameters in the filters were manipulated, to give optimal results. The authors reported that no one technique proved superior overall to the other techniques. Examination of the results revealed that the approach based in the frequency domain (Anderssen and Bloomfield, 1974b) gave the best results with the trigonometric series data, and best results for data generated from the polynomial series were obtained with the spline. This highlights the problem of using mathematically generated functions to test smoothing and differentiating techniques if the technique to be assessed has a similar underlying function to the test function.

Vaughan (1982) filmed a golf ball dropping vertically and then tested the ability of three techniques to correctly predict the acceleration due to gravity (g). A quintic spline was more accurate than both a cubic spline and a Butterworth filter combined with finite difference differentiating formulae. The amount of smoothing was adjusted manually for all the techniques. These results are somewhat false, as it is very rare to know the values of the second derivatives when adjusting the amount of smoothing.

Woltring (1985) circumvented the problem of having to manually adjust the amount of smoothing by using the Generalised Cross-Validated Spline (GCVS) routine of Utreras (1980), which automatically determines the tightness of the spline fit. He compared both the cubic and quintic GCVS's with the FFT based routine of Hatze (1981a). They were tested on the data of Vaughan (1982), the data of Pezzack et al. (1977), and some data generated from a mathematical function. For the constant acceleration data neither the cubic spline nor the FFT method performed very well. The quintic GCVS predicted a constant acceleration value very close to the value of 'g' at the site of the measurements of Vaughan (1982). With the data of Pezzack et al. (1977) the quintic GCVS and the FFT technique both performed well, but when additional noise was added to the signal the FFT technique's performance deteriorated with particular problems at the end points. Using the mathematically generated function Woltring also demonstrated that the end point restriction placed on the m^{th} and higher derivatives of a 2m order natural spline, affects the prediction of the m^{th} derivative throughout the signal as well as at the end points. This problem had previously been highlighted for the cubic spline (e.g. Wood and Jennings, 1979), but was shown to exist generally for natural splines. For example a jerk (third derivative) would be poorly predicted by a quintic spline.

3:3.4 SUMMARY

The preceding review of literature shows that a variety of techniques have been suggested to process biomechanical data. Comparison of these techniques is difficult because researchers have used different

and in some cases inappropriate assessment techniques. It has been shown that the data of Pezzack et al. (1977) without additional noise added to the signal does not represent a typical biomechanical signal. The zero end point values of this data set also make its use inappropriate for the assessment of some techniques. Mathematically generated data cause problems since a filtering technique whose underlying function is similar to that of the function generating the data can be predisposed to perform well. Even if a technique has been shown to produce accurate results there is still one very important consideration; how is the amount of smoothing selected ? In many of the assessments undertaken in the literature the true signal is known and the degree of smoothing adjusted until a good result is obtained. Once a technique has been shown to produce good results under these conditions the researcher is still left with the problem of selecting the degree of smoothing for a real data set.

3:4 EXAMINATION OF SMOOTHING AND DIFFERENTIATION TECHNIQUES

The following sections examine various filtering and differentiation techniques, to determine which is the most suited to the removal of noise from a film derived signal.

3:4.1 SELECTION CRITERIA

When selecting filtering and differentiating techniques, (a single technique may not necessarily be employed for both purposes), a number of preliminary criteria must be examined.

1. Memory Size : Does the computer on which the software is to be run provide a limitation in terms of memory size ?

2. Execution Time : Is the time in which the data are processed of prime concern ? Is filtering to be carried out on line ?

3. Sample Interval : Are the data equidistantly sampled in time ? (Some filters and differentiators will only operate with constant sample intervals in which case prior interpolation is required).

Once limitations imposed by these criteria have been identified, the technique which provides the most accurate estimate of the required variables should be selected. In the present context these preliminary criteria did not limit the selection of techniques. Indeed execution time for a data filtering and differentiation technique was insignificant compared with the time required to manually digitize the film data.

3:4.2 ASSESSMENT CRITERIA

When trying to assess the accuracy of smoothing and differentiating techniques it is virtually impossible to obtain data from a biomechanical system where one knows the true signal underlying the noisy sampled signal. A number of approaches have been taken in trying to establish successful criteria for assessing filtering and differentiation techniques. Pezzack et al. (1977) used an accelerometer to provide criterion data against which the film data, once suitably filtered and differentiated, were compared. Analysis of this data (eg. Lanshammar, 1982), showed that it contained far less noise than would normally be expected from genuine film data. In addition these data had end point second derivative values of zero, which do not serve as a suitable test of the abilities of some techniques. During free flight the centre of mass of the body has a constant acceleration. Data derived from such situations can be of use when assessing smoothing and differentiating techniques. There are two major problems with using such data. The need

to employ anthropometric data to determine the centre of mass of the whole body clouds the assessment of the data smoothing and differentiation techniques because the accuracy of anthropometric data must also be assessed. Also, as the acceleration of the centre of mass of the body is constant, this does not test the technique's ability to estimate acceleration values which do not remain constant. Often the most practical solution is to use some mathematical function which approximates some aspect of human movement, to which noise can be added. The function can be differentiated directly to yield the true values of the first and second derivatives, which can then be compared with the estimated values produced by the techniques under investigation from the noisy data. In the selection of these functions the frequency profiles of the signal with and without noise must be examined to ensure that in both the time and frequency domains the data are similar to real biomechanical data. All techniques should be evaluated over a suitable range of data sets, avoiding any unique predisposition to favour the characteristics of each technique's underlying function. Once suitable data sets have been obtained a method is required with which to evaluate the accuracy of the techniques used to filter and differentiate the data. Often a graphical representation of both the noisy and filtered data is used, but this does not provide an easily comparable criterion. A better option is to evaluate the percentage root mean square error between the true and estimated values of the signal. This is computed as follows:-

$$MSE = \left[\frac{1}{n-1} \sum_{i=1}^{n} (E_i - C)_i^2 \right]^{\frac{1}{2}} \qquad [3.27]$$

Where:-

MSE - is the mean square error

n - is the number of data points

E_i - is the estimated value of point i

and Ci is the criterion value of point i.

$$MV = \left[\frac{1}{n-1} \sum_{i=1}^{n} C_i^2 \right]^{\frac{1}{2}} \qquad [3.28]$$

Where:-

MV - is the mean value of the criterion values

$$\%RMSE = 100.\left(\frac{MSE}{MV}\right) \qquad [3.29]$$

Where:-

%RMSE - is the percentage root mean square error

By comparing results using a percentage value it is easier to compare results across different data sets.

3:4.3 SELECTING THE AMOUNT OF FILTERING

The problem is how to select the amount of filtering that a signal requires. This is equivalent to finding where the frequency components of the signal are insignificant compared with the frequency components of the noise impinging on the signal. For many of the digital filtering techniques this requires the

specification of a cut-off frequency and the number of filter terms which will effectively specify the width of the pass-band. Truncated Fourier series are usually fitted by adjusting the number of terms until the difference between the input signal and the output signal is the same as some predetermined error estimate for the sampled signal. For a spline, unless an automated technique is used, the degree of smoothing is normally specified by varying the 'S' value in accordance with the anticipated error in the signal.

If the true underlying signal of a sampled biomechanical signal were known, optimal filters (for example Wiener) could be used to process the data. Unfortunately this is seldom the case in biomechanical studies.

There are a number of commonly adopted options for selecting the amount of filtering, including:-
1. Visual inspection of curves, before and after implementation of the filter.
2. Use of previously published criteria.
3. Use of alternative experimental evidence.
4. Multiple digitization of data to give an estimate of the error variance in the signal.
5. Adoption of some form of optimal regularization.

The first technique requires operator interaction and is unlikely to be highly repeatable. It has been employed, for example by Wood (1975), and Vaughan (1982) when using spline routines.

The second option assumes that some previously established smoothing parameter applies across a number of conditions. In fact it may be erroneous to use the same smoothing parameter repeatedly for different trials for the same subject. This approach was used by Winter et al. (1974) who determined the appropriate cut-off frequency for a digital filter for one body landmark and then used this for other body landmarks in the study, and recommended it for other gait studies.

The third option relies on data collected using different equipment. The most common method is to find the signal bandwidth from a force plate recording of the ground reaction forces during some phase of the movement being examined (e.g. Antonsson and Mann, 1985). Although an indication of the signal bandwidth can be obtained this is insufficient information with which to determine the amount of smoothing a signal requires. It is more important to know the ratio of signal to noise amplitude. Although signal bandwidth may be known, when sampling information from film the noise at the upper range of the signal bandwidth may have a larger amplitude than the signal, in which case a lower cut-off frequency is required for a filter.

The fourth method results in a sequence being digitized a number of times and so is time consuming. Information derived from the mean of the samples is then used to select the amount of filtering, such a procedure was adopted by Lesh et al. (1979). If sufficient multiple digitizations of a sequence of film are performed computing the mean is an effective way of filtering the data, see section 3:5.2. Yeadon (1984) performed two digitizations of film sequences to obtain an estimate of local noise variance. This

information was then used as a weighting factor in a spline routine. Such an approach although it uses information from multiple digitizations still requires the selection of the degree of smoothing performed by the spline routine.

The final option, optimal regularization, relies upon setting constraints on the properties of the resulting filtered signal, and often the signal's derivatives. To be of use these constraints must relate to the expected properties of the signal; such schemes can normally be automatically implemented. These features have a number of advantages: operator interaction is reduced, results are reproducible, and if the same technique is adopted by two researchers data can be more profitably compared. This does not mean that techniques employing optimal regularization should be applied without thought to the effect on the signal. Irrespective of the technique selected, the examination of the frequency spectra of both the processed and unprocessed data should be considered a basic step in ensuring the correct operation of the filtering and differentiating techniques employed.

Two techniques have been adopted in biomechanics which allow automatic selection of the degree of filtering via optimal regularization: the use of optimally regularized Fourier series (Hatze, 1981a), and the Generalised Cross Validated Spline (GCVS) (Woltring, 1986). Both of these techniques seek a balance between the closeness of fit by the Fourier series or spline and the smoothness of the signal represented by the fit and its derivatives. In comparing the two it should be mentioned that the technique of Hatze (1981a) will only handle equidistantly sampled data, and has second derivative end point values which are equal to zero. The shortcomings of the spline are dealt with in more detail in section 3:4.5.

3:4.4 EXPERIMENTAL ASSESSMENT

Three groups of techniques were investigated: splines, truncated Fourier series (TFS), and digital filters. In most biomechanical situations given genuine photogrammetrically derived data it is not possible to know the true signal underlying the noisy sampled signal. To overcome this problem mathematical functions were used to generate data to investigate these techniques. By analytical differentiation of these functions it was possible to find the true value of the first and second derivatives. Noise was added to the original data so that it would be similar to that normally found in biomechanical data. As indicated in the literature review techniques tend to perform well on data generated from mathematical functions with similar underlying functions. Therefore a number of data sets were chosen from a variety of sources. By comparing across these data sets it was hoped a clearer assessment would be obtained. The mathematical functions used to generate these data sets are presented in Appendix B. The techniques were evaluated by computing the %RMS error between the estimated signal and its true value.

The techniques were:-

Spline Techniques

As outlined earlier a variety of techniques have been advanced for the use of splines in data analysis. Splines have been fitted to noisy data by estimating the 'S' value manually. To circumvent this problem the ordinary cross-validated spline (OCVS) technique of Wahba and Wold (1975) was used. In this technique a model of the data is made, by assuming an initial value of "S'. The validity of this model is

then assessed by removing one of the data points from the noisy data set and fitting the model and then using this model to predict the missing point, this is done for each data point in turn. The value of 'S' is systematically varied until the model gives the best prediction of each data point by means of the model and the other data points. This fit is then used to evaluate the first and second differential of the signal. The algorithm used was an adaptation of the routine of L.S.Jennings (University of Western Australia) which basically implements either a Reinsch cubic or quintic spline. Both cubic and quintic OCVS were investigated.

Truncated Fourier Series

A DFT was fitted to the data using the formulae presented by Cappozzo et al. (1975). The number of Fourier terms was then adjusted until the lowest %RMS error was obtained. The data derived from recording human movement is not always strictly periodic, but the Fourier series should ideally be fitted to periodic data. For this reason four different approaches were tried:-

Operation A) null operation (i.e. the original data set was used)

Operation B) data set increased by reflecting the data about a vertical axis

Operation C) double reflection of data

Operation D) data detrended (Hatze, 1981a) so the data started and ended at the same value.

These operations are illustrated in figure 3.6.

Butterworth Filter

The data were filtered in forward and reverse direction with a second order Butterworth filter. (The application of the filter in forward and reverse direction effectively makes the Butterworth filter a fourth order filter, and eliminates phase lag.) The cut-off of the filter was varied by 0.25 Hz from 0.25 Hz up to the Nyquist frequency of the signal, and the lowest %RMS error found. To differentiate the data both first and second order finite difference differentiating formulae were used (Miller and Nelson, 1973).

For all of the techniques except the OCVS the degree of smoothing was varied iteratively until the lowest %RMS errors were found. This was done for the displacement, and the first and second derivatives of the signal separately. Therefore for the truncated Fourier series and Butterworth filter the same degree of smoothing may not have been applied to calculate the smoothed displacement data, and the first and second derivatives. The OCVS performed this tuning automatically and the degree of smoothing was the same for the displacement data and its first and second derivatives.

The results for the estimation of displacement data from the noisy data sets are presented in Table 3.1. Data set a was a noisy cosine wave, for this data set the truncated Fourier series (A, B, and C) and the Butterworth filter produced better estimates of the displacement data than the spline techniques. This was to be anticipated for the truncated Fourier series because the underlying function of the test function and the smoothing technique are similar. On the other data sets the Butterworth filter performed well. The truncated Fourier series did not perform as well, and showed varying results for the different operations on the data sets, with operation C appearing to produce the best results overall. The quintic OCVS produced marginally better results that the cubic OCVS. The results for the quintic OCVS were not as good as those

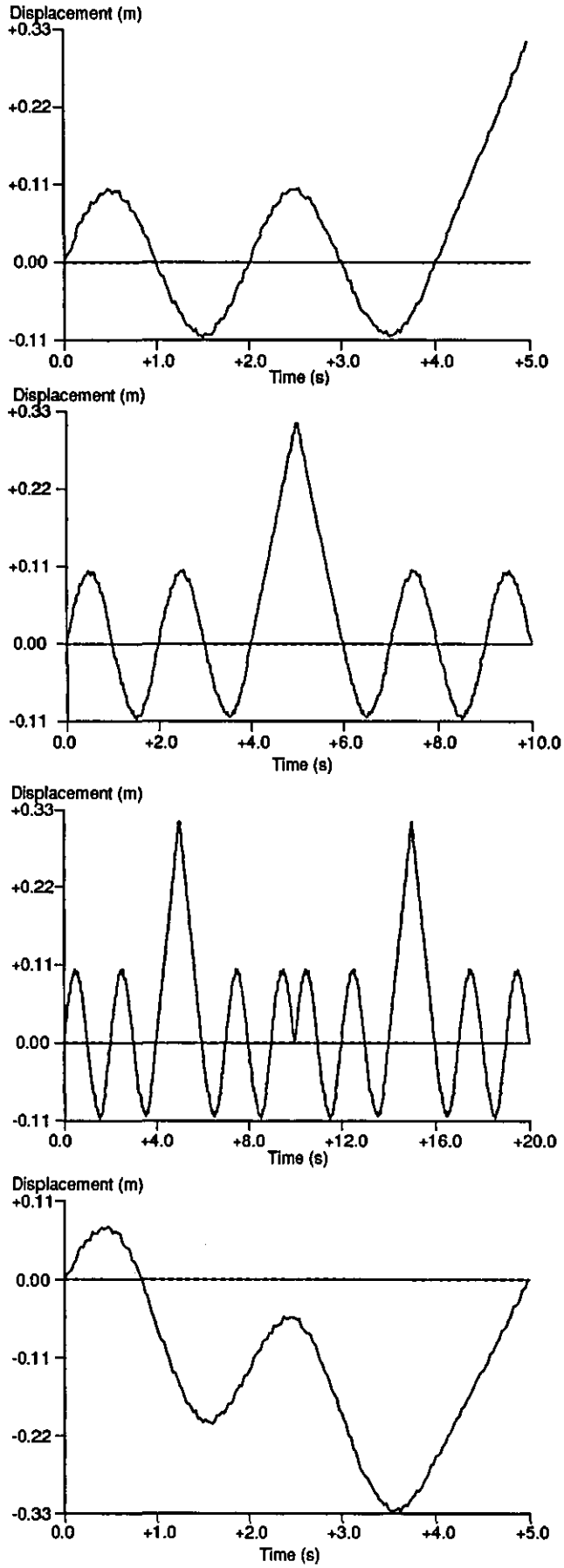

Data Operation A
Original data set

Data Operation B
Reflection

Data Operation C
Double Reflection

Data Operation D
Detrending

FIGURE 3.6 - Graphs illustrating three data operations used prior to use of truncated Fourier series.

TABLE 3.1 - The percentage root mean square errors between estimates and true values of artificial displacement data using different smoothing techniques.

	DATA SET			
TECHNIQUE	a	b	c	e
CUBIC OCVS	1.26	1.90	0.57	1.63
QUINTIC OCVS	1.24	1.052	0.78	1.30
TFS OPERATION A	0.54	1.65	2.74	1.51
TFS OPERATION B	0.91	2.04	1.23	1.80
TFS OPERATION C	0.80	2.02	1.17	1.80
TFS OPERATION D	3.23	3.81	0.63	3.27
BUTTERWORTH FILTER	0.35	0.15	0.61	0.77

(N.B. - data set **d** was not used for this analysis.)

for the Butterworth filter. It must be noted that the amount of smoothing performed by the Butterworth filter was determined by comparing the filtered values with the true values, whereas the quintic OCVS estimated its degree of smoothing automatically. Given genuine photogrammetrically derived data the degree of smoothing of the Butterworth filter would have to be estimated, and as accurate results could not be guaranteed.

As the second differential is the highest derivative required in this study, it was also used as a criterion for comparing the techniques. These results are presented in table 3.2. For data **a** the TFS (A,B, and C) again gave the best results, the reason for this has already been discussed. The Butterworth filtering technique followed by central difference differentiating formulae estimated the second derivative of the noisy signals with poor accuracy compared with other techniques. An examination of the transfer function of the central difference differentiating formula illustrates the reason for this (see section 3:4.8).

The quintic OCVS gave the lowest %RMS errors for three data sets (**b, c, d**) and had the second lowest for data set **e**. The cubic gave %RMS error values comparable with the quintic spline for the smoothed displacement data, but the corresponding values for the second derivative were poorer. This was due to the end point restrictions placed on the second derivative of a cubic spline. The same restrictions are placed on the third derivative of the quintic spline so were not evident in the present analysis. Further analysis of the spline is presented in section 3:4.5.

Overall on the data sets investigated the quintic OCVS gave the best results. It had a number of other advantages over the other techniques. It automatically selected the degree of smoothing. The other techniques required that the data were over an equidistant time base before they could be applied. The OCVS does not require equidistantly sampled data, and if a new time base is required, for example to synchronise signals, the OCVS can output smoothed values, and the derivatives of that signal, over a new time base. Computationally the OCVS was the slowest of the techniques investigated. Craven and Wahba (1979) introduced a computationally more complex but faster alternative to the OCVS: the generalised cross-validated spline (GCVS) (see section 3:4.4 for details). This quicker alternative is still not as quick as the Butterworth filter or TFS techniques but does appreciably decrease processing time. On the data sets investigated the quintic OCVS took over one hour of CPU time to process the data, whereas the other two techniques completed their computations in a few seconds. The OCVS was compared with the GCVS using the GCVS package of Woltring (1986). The results are presented in table 3.3. The OCVS produced slightly more accurate results than the GCVS, on the same data sets that were used for the earlier analysis of filtering and differentiating techniques. The quintic GCVS was several orders of magnitude faster at processing these data sets than the quintic OCVS. In light of the analyses performed in this section the GCVS was used for the smoothing and differentiating of data in this study, as it was significantly quicker than the OCVS and only slightly less accurate.

3:4.5 SPLINES

The cubic and quintic GCVS that were used in this study to interpolate, smooth, and differentiate the data, are detailed in this section.

TABLE 3.2 - The percentage root mean square errors between estimates and true values of second differential data estimated from noisy displacement data using different smoothing and differentiation techniques.

	DATA SET				
TECHNIQUE	a	b	c	d	e
CUBIC OCVS	41.99	25.11	27.80	15.86	24.92
QUINTIC OCVS	15.96	17.99	12.82	10.90	17.99
TFS DATA SET A	1.62	20.98	84.94	67.88	23.45
TFS DATA SET B	2.46	32.99	48.73	52.73	31.75
TFS DATA SET C	2.56	32.29	48.63	52.39	34.19
TFS DATA SET D	32.44	52.66	17.59	34.19	6.87
BUTTERWORTH FILTER 1ST ORDER C.DIFF	67.84	42.56	31.89	115.53	50.78
BUTTERWORTH FILTER 2ND ORDER C.DIFF	75.41	49.59	33.28	132.64	59.09

TABLE 3.3 - Comparison of the percentage root mean square error for smoothing and differentiating data using the ordinary cross-validated spline and the generalised cross-validated spline.

	DATA SET			
TECHNIQUE	a	b	c	e
		Displacement Data		
CUBIC OCVS	1.26	1.90	0.57	1.63
CUBIC GCVS	1.32	1.90	0.77	1.63
QUINTIC OCVS	1.24	1.052	0.78	1.30
QUINTIC GCVS	1.10	1.84	0.81	1.58
		Second Derivatives		
CUBIC OCVS	41.99	25.11	27.80	24.92
CUBIC GCVS	41.58	32.59	33.21	32.48
QUINTIC OCVS	15.96	17.99	12.82	17.99
QUINTIC GCVS	14.72	23.94	24.99	23.92

(N.B. - data set **d** was not used for this analysis.)

The spline is defined as a function P(ti) where the spline is composed of a series of piece-wise polynomials. These polynomials are joined at positions called knots which must fall within the data interval (t1,tn). The polynomials are of order 2.m and must be continuous at the knots up to and including the (2m-2) derivative. The order of the spline is limited by the number of data points so that $n \geq 2m$. Certain boundary conditions are imposed on the record ends. These conditions vary with the type of spline: for periodic splines the K^{th} derivative of P(ti) must be equal at the end points i.e. $P^k(t1) = P^k(tn)$ K=0,...,(m-1); for complete splines the derivatives of the boundary values are measured constraints for k=1,m-1(eg. Hu and Schumaker, 1986); and for natural splines the end points are set to zero for the K^{th} derivative for k=m,...2m-2 (e.g. Reinsch, 1967). Early spline routines required the user to select the number of points as knots (Wold, 1974). Dierckx (1975) presented an automated knot fitting technique, but it is now customary to treat all data points as knots as recommended by Reinsch (1967).

Given the noisy data set (ti,yi) for i=1,n where n is the number of samples, the natural cubic spline of Reinsch (1967) required the minimisation of the following function:-

$$\int_{t1}^{tn} \left[P^m(ti)\right]^2 dt \qquad [3.30]$$

subject to

$$\sum_{i=1}^{n} \frac{\left(P(ti) - Yi\right)^2}{\sigma Yi} \leq S \qquad [3.31]$$

Where:-

P(ti) - is the polynomial fitted to sample point ti

$P^m(ti)$ - the m^{th} derivative of the polynomial P(ti) fitted to point ti, for a cubic spline m=2

S - is the smoothing parameter

and σYi is the standard deviation of the error associated with point Yi.

In equation 3.4.1 the integral of the squared m^{th} derivative of the spline is considered to be a roughness penalty function. This effectively minimises the roughness of the signal whilst keeping the weighted root mean square error equal to or below the 'S' value. If the variance associated with each sampled point is known, Reinsch recommended that 'S' be selected in the range:-

$$n - (2.n)^{0.5} \leq S \leq n + (2.n)^{0.5} \qquad [3.32]$$

In 1975 Wahba claimed this approach would lead to systematic over smoothing of the signal. Wold (1974) suggested that 'S' should be set so that

$$0.7\,n < S < 0.95\,n \qquad [3.33]$$

The other approach is to adjust 'S' after visual inspection of the fitted curve. From equation 3.31, if an interpolating spline is required the value of 'S' is set to zero.

To overcome the problem of estimating 'S' researchers have used the cross-validation procedure, which is a form of optimal regularization. Essentially this procedure fits a spline to a data set where a number of points have been omitted. The 'S' value is then varied to minimise the residual between estimated and sampled values of these omitted points. Such a procedure for splines, the OCVS, was initially advanced by Wahba and Wold (1975). The OCVS has two major drawbacks: it is costly in terms of computer time, and it can be numerically unstable under certain conditions (Woltring, de Lange, Kauer, and Huiskes, 1987). Golub, Heath, and Wahba (1979) suggested a generalised cross-validation procedure, which circumvented these two problems. Craven and Wahba (1979) presented details of a GCVS. The procedure they proposed would find the optimal smoothing parameter for equidistant data with uniform weighting. Utreras (1980) also presented a routine which approximated to the GCVS, which was computationally faster then that of Craven and Wahba (1979). Both of these routines are available in computer numerical libraries, but permit only cubic splines to be computed. The two shortcomings (only equidistant data and uniform weighting) reduce the general applicability of these routines. Hutchinson and de Hoog (1985) presented details of a routine which would compute the cubic GCVS for non-equidistant, non-uniformly weighted data. Execution times were given for this routine, and two others. For 100 data points their spline fitting routine took 11 seconds, as did the routine of Utreras. The routine of Craven and Wahba (1979) took 1358 seconds.

Woltring (1985) combined aspects of the Fortran routines of Lyche, Schumaker, and Sepehrnoori (1983) for the determination of natural splines, with those for the generalised cross-validation procedure of Hutchinson and de Hoog (1985), to produce a GCVS package written in Fortran 77 which permits the determination of a GCVS of any even order spline for non-equidistant, non-uniformly weighted data sets, for $n > 40$. The function which has to be minimised is:-

$$\lambda \int_{t1}^{tn} [P^m(ti)]^2 \, dt + \sum_{i=1}^{n} wi(P(ti) - Yi)^2 \qquad [3.34]$$

Where:-

wi - is the positive weight factor (which is inversely proportional to the local noise variance) of data point i and λ adjusts the smoothness of the spline fit.

A potential drawback is that this automatic spline fitting technique is a "black box" technique, and the experimenter must take care not to use it thoughtlessly.

3:4.6 FURTHER ANALYSIS OF SPLINES

a. EFFECT OF SPLINE ORDER

Consideration must be given to the order of the spline selected. Lyche et al. (1983) claimed, given that m is the half order of the spline

"Higher values of m will give splines with a greater tendency to oscillate." (page 5)

Any unwarranted oscillations in a spline fit could result in inaccuracies in values estimated from the spline. This potential problem was examined by comparing GCVS of three different degrees: cubic, quintic, and

heptic (m = 2,3, and 4 respectively) using the noisy data sets in Appendix B. The results for the accuracy of such an analysis are presented in table 3.4.

With increasing order of the spline there is very little difference in the accuracy of the estimation of the true signal underlying the noisy data sets. For the second derivative data the cubic spline gave the poorest values but this was anticipated because of the restrictions placed on the second derivative of this order spline. The heptic spline produced more accurate results for all except one data set (set **c**) compared with the quintic spline.

As all data points were considered to be knots it is important to see what the data does between the knots. A second analysis was performed, here the GCVS was fitted to the data from the various data sets and then the function was evaluated at the mid-points between the knots. The true mid-point values could be evaluated by reference to the functions used to generate the data. Splines from the fourth to the tenth order were used. The results for the estimation of the displacement data are presented in table 3.5.

For four of the data sets (**a**, **b**, **c**, and **d**) the quintic spline gave the most accurate results. For the remaining two data sets (**e** and **f**) there was a small increase in accuracy with increasing order of spline. The increase in accuracy for data sets **e** and **f** using the splines of order eight and 10 was very small in comparison to the spline of order six. These results show that if interpolation between data points is to be undertaken the order of the spline has a significant effect. It should be noted that direct comparisons cannot be made between the results in tables 3.4, 3.5 and 3.1, 3.2, because the analyses were performed on different computers. These differences exist because of the differences in the random number generators used to add noise to the data, and in the precision limits of the computers.

b. THE EFFECT OF THE CONSTRAINED DERIVATIVES

The analysis in section 3:4.2 showed that the cubic spline estimates of second derivatives are not as accurate as those of the quintic spline. An analysis of a cubic polynomial illustrates why. For the cubic spline m = 2. If P(ti) is the polynomial for the interval i, then:-

$$P(ti) = A_i + B_i ti + C_i ti^2 + D_i ti^3 \qquad [3.35]$$

$$\dot{P}(ti) = B_i + 2.C_i ti + 3.D_i ti^2 \qquad [3.36]$$

$$\ddot{P}(ti) = 2.C_i + 6.D_i ti \qquad [3.37]$$

Where:-

Aj, Bj, Cj, Dj - are polynomial coefficients

$\dot{P}(ti)$ - is the first derivative of the polynomial P(ti)

and $\ddot{P}(ti)$ is the second derivative of the polynomial P(ti)

TABLE 3.4 - The percentage root mean square errors for the estimation of true displacement and second derivative values from noisy data using different order generalised cross-validated splines.

	DATA SET					
TECHNIQUE*	**a**	**b**	**c**	**d**	**e**	**f**
			Displacement Data			
CUBIC (4)	1.32	1.90	0.77	1.81	1.63	1.28
QUINTIC (6)	1.10	1.84	0.81	1.50	1.58	1.22
HEPTIC (8)	0.76	1.80	1.01	1.50	1.54	1.05
			Second Derivatives			
CUBIC (4)	41.58	32.59	33.21	15.86	32.48	22.89
QUINTIC (6)	14.72	23.94	24.99	10.90	23.92	20.71
HEPTIC (8)	5.63	20.83	39.60	7.68	20.82	16.22

(N.B. - * the figure in brackets refers to the order of the spline.)

TABLE 3.5 - The percentage root mean square errors for the estimation of true displacement values from noisy data at the mid-points between knots using different order generalised cross-validated splines.

	DATA SET					
ORDER OF SPLINE	a	b	c	d	e	f
4	1.06	1.58	0.74	2.00	1.87	1.15
6	0.85	1.50	0.64	1.83	1.78	0.99
8	0.94	1.56	0.70	1.92	1.74	0.95
10	1.51	1.59	1.26	2.02	1.73	0.92

As can be seen the cubic spline only uses linear polynomials between the knots when estimating the second derivative. This may not be appropriate for many biomechanical applications were acceleration is not linear in these regions. In addition natural splines force the end points of the spline to go through zero for the m^{th} derivative, which means that incorrect estimates of the end points of the second derivatives will be given.

To illustrate these problems figure 3.7 shows the graph of the second derivative of the data set A estimated using a cubic spline. The end point values of the derivative should be equal to one but the spline has constrained these end points to be zero. To further illustrate this end point problem a quintic spline was used to estimate the third derivative of a signal. The same procedure used to generate data set **a**, was used to generate a noisy sine wave. The third derivative of this signal also has non-zero end points, the quintic spline is constrained to have zero end point values for its third derivative, the graph is also shown in figure 3.7. Therefore the order of the spline used must be selected by considering which derivatives are required. Ragozin (1983) highlighted further problems in acquiring high order derivatives from low order splines.

Dohrmann, Busby, and Trujillo (1988) presented a generalised cross-validated cubic spline routine which does not constrain the second (m) derivative to zero at the end points but constrains the third derivative. Dohrmann (1986) presented details of this technique when used with higher order splines.

3:4.7 SAMPLE RATE

Sampling theorem states that a signal should be sampled at a rate which is greater than twice the highest frequency component in the sampled signal. If this theorem is not followed the sampled signal will be aliased, which means that any frequency components higher than the Nyquist frequency (half of the sampling rate) will be folded back into the sampled frequency domain. This theorem only states what the minimum should be and does not provide any indication of the benefits of sampling at higher rates. To examine the effect of different sampling rates, data set **b** was used but only up to the tenth term so that the signal had no frequency components above 10 Hz. The sample interval was kept the same for this data set but the sampling rate was varied from 40 to 200 Hz. A quintic GCVS was used to smooth and differentiate the data. The %RMS errors were evaluated between the true signal values and their estimated values at different signal sample rates. The effective cut-off for the spline was also calculated as was the rejection frequency. The results are presented in table 3.6.

Analysis of these results shows that as the sample rate increased so did the accuracy with which displacement and first and second derivatives were estimated. Analysis of the cut-off frequency showed that it increased as the sample rate increased. This means that less of the true signal underlying the noisy sampled signal was lost when a higher sampling rate was used. At a sample rate four times the maximum frequency component of the signal the cut-off frequency was 6.82 Hz, and the rejection frequency was 7.90Hz, which means that over 20 percent of the sample bandwidth was rejected. At 200 Hz which is twenty times the maximum frequency component of the signal the spline had a cut-off frequency at 8.16 Hz rejecting all frequencies above 9.45 Hz. The noise added to the original signal was white, which is

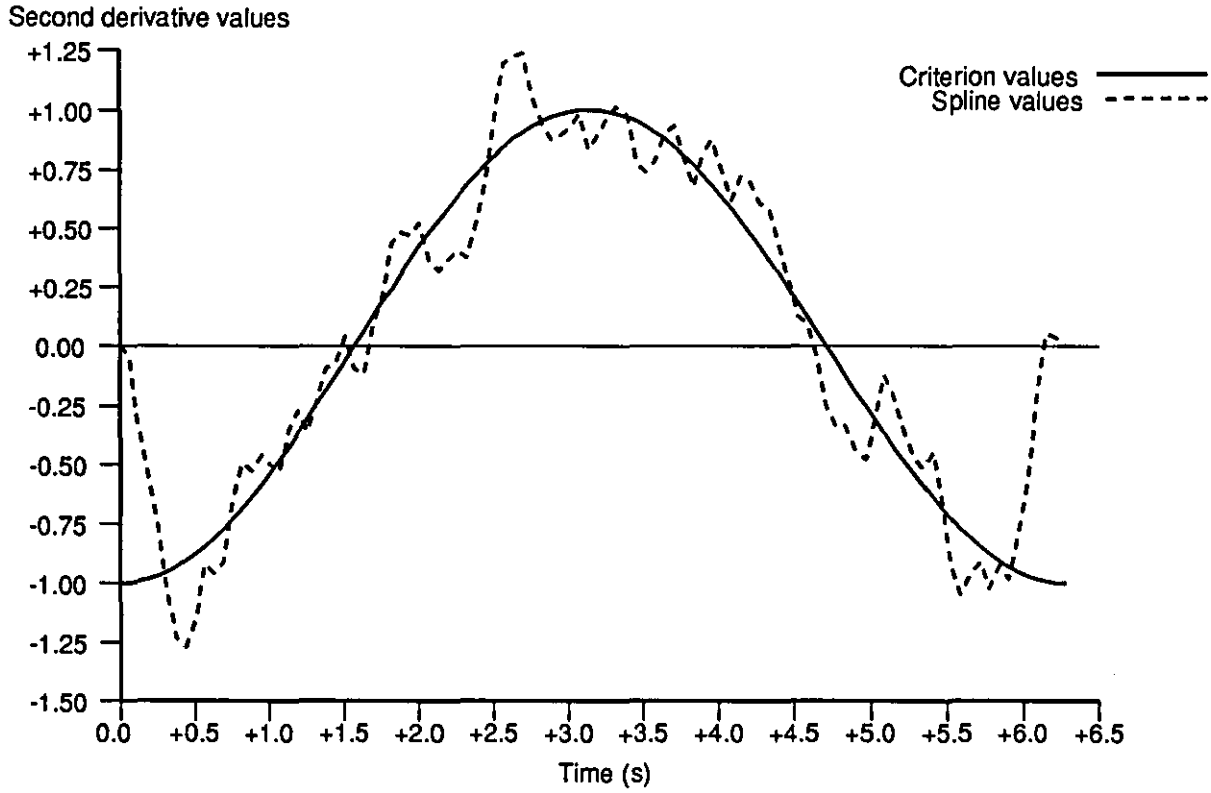

FIGURE 3.7a - Cubic spline approximation to the second derivative of a noisy cosine wave.

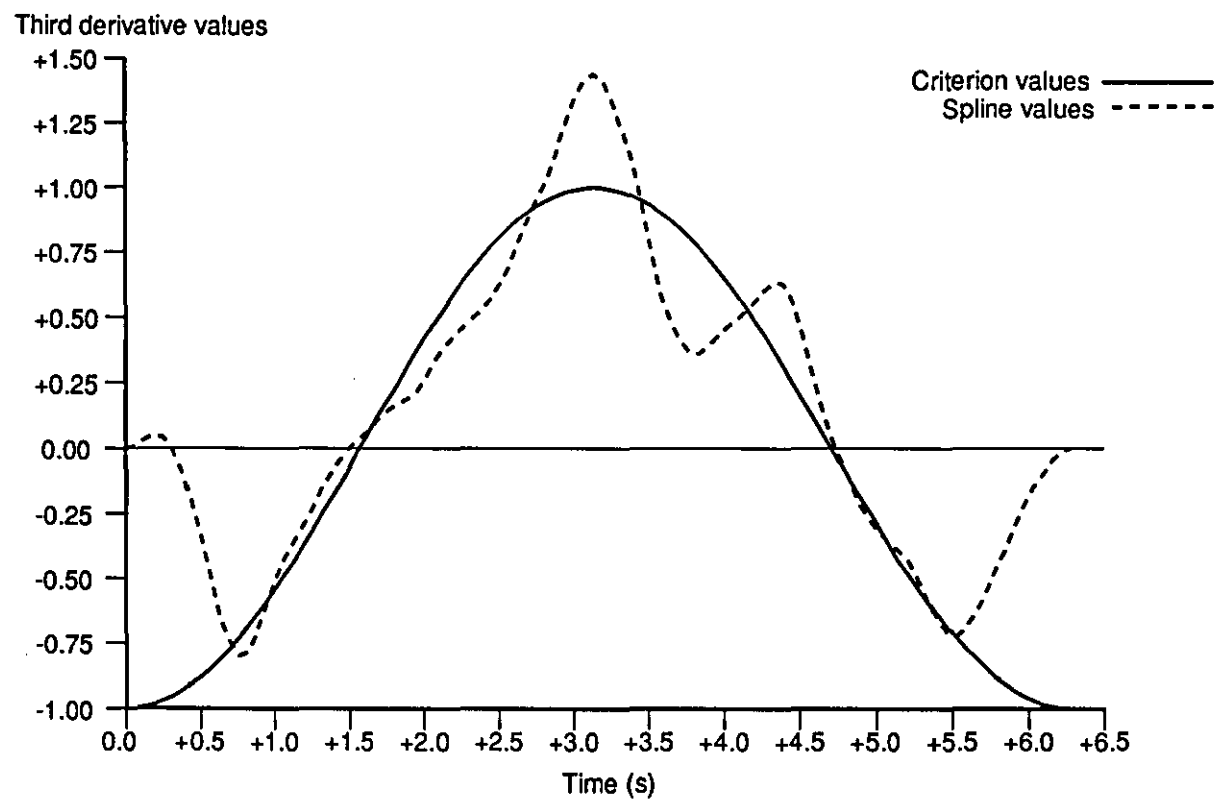

FIGURE 3.7b - Quintic spline approximation to the third derivative of a noisy sine wave.

TABLE 3.6 - The percentage root mean square errors arising when comparing true values with those estimated using the generalised cross-validated quintic spline, for data set **b** sampled at different rates.

	SAMPLE RATE				
	200 Hz	100 Hz	67Hz	50 Hz	40 Hz
DISPLACEMENT %RMSE	1.19	1.60	1.95	2.03	2.82
1ST DERIVATIVE %RMSE	5.13	7.35	7.95	8.28	10.87
2ND DERIVATIVE %RMSE	20.13	26.50	27.96	28.14	31.52
CUT-OFF FREQUENCY (Hz)	8.16	7.98	7.37	7.27	6.82
REJECTION FREQUENCY (Hz)	9.45	9.25	8.53	8.42	7.90

assumed to be wide-band. Therefore the increases in sample rate led to the true signal underlying the sampled signal and white noise becoming better defined making the noise easier to remove.

The frequency components of a signal and more significantly the highest frequency component of a signal are not known before the sampling process. Sample rate must therefore be set at a rate greater than twice the anticipated highest frequency of a signal. Using too high a sampling rate may be considered wasteful in terms of film and time but can result in more accurate definition of the displacement data and its derivatives.

3:4.8 TRANSFER FUNCTIONS

The behaviour of a filter can be described in terms of its frequency response (also known as transfer function). For a low-pass filter ideally all frequencies up to a given frequency should pass unattenuated and all frequencies above that level should be rejected. In practice such a filter is not realizable. Analysis of the frequency response of a filter is a good way of examining the effect of the filter on the signal. The transfer function of a filter is found by calculating the ratio of the amplitude spectra of the output signal to the amplitude spectra of the input signal. This is normally done by looking at the effect of the filter on a signal containing varying sinusoidal frequencies. Craven and Wahba (1979) highlighted the similarity of the transfer function of the GCVS in the uniformly weighted equidistantly sampled case with the Butterworth filter. The transfer function of a quintic GCVS and a 4 th order Butterworth filter are plotted in figure 3.8.

Following low-pass filtering, to obtain first and second derivative information the smoothed signal must be differentiated. An ideal differentiator acts as a ramp function up to the signal bandwidth and allows no frequency components above this to pass. Following the use of the Butterworth filter the first order central difference differentiating formulae have been used to differentiate data (e.g. Vaughan, 1982). The frequency response of this filter is shown in figure 3.9. As can be seen the filter amplifies all frequencies up to one fourth of the sample rate, but the cut-off is not sharp. A similar shape curve is obtained for the second order central difference differentiating formulae which were also examined in section 3:4.4. When the signal is low-pass filtered some frequency components beyond the cut-off frequency will remain, and unless the cut-off is one quarter of the sampling rate these components will be amplified by the action of the first order finite difference formulae. To obtain more accurate derivative estimation a differentiator must be selected which has a suitable frequency response with a cut-off at the same point as the low-pass filter employed. Analysis of the GCVS shows it fulfils these criteria for derivatives up to the m-1th where 2m is the order of the spline.

3:5 ANALYSIS OF KINEMATIC DATA

In this section the data collected in this study are examined, predominantly to ascertain the accuracy of derived variables.

3:5.1 FREQUENCY ANALYSIS OF DATA

The frequency components of the signal describing movement of the centre of mass, and the signal

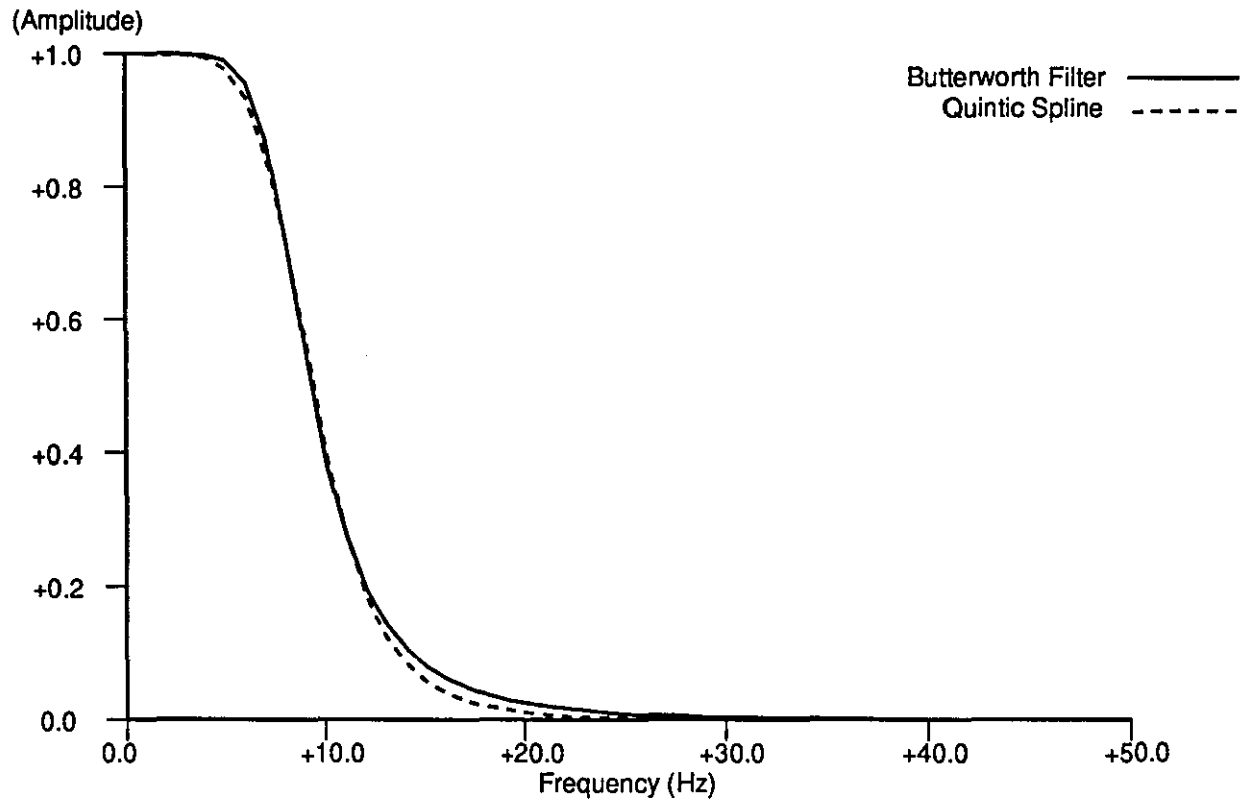

FIGURE 3.8 - The transfer functions of a generalised cross-validated spline, and a Butterworth filter, both with a cut-off frequency of 8.16 Hz.

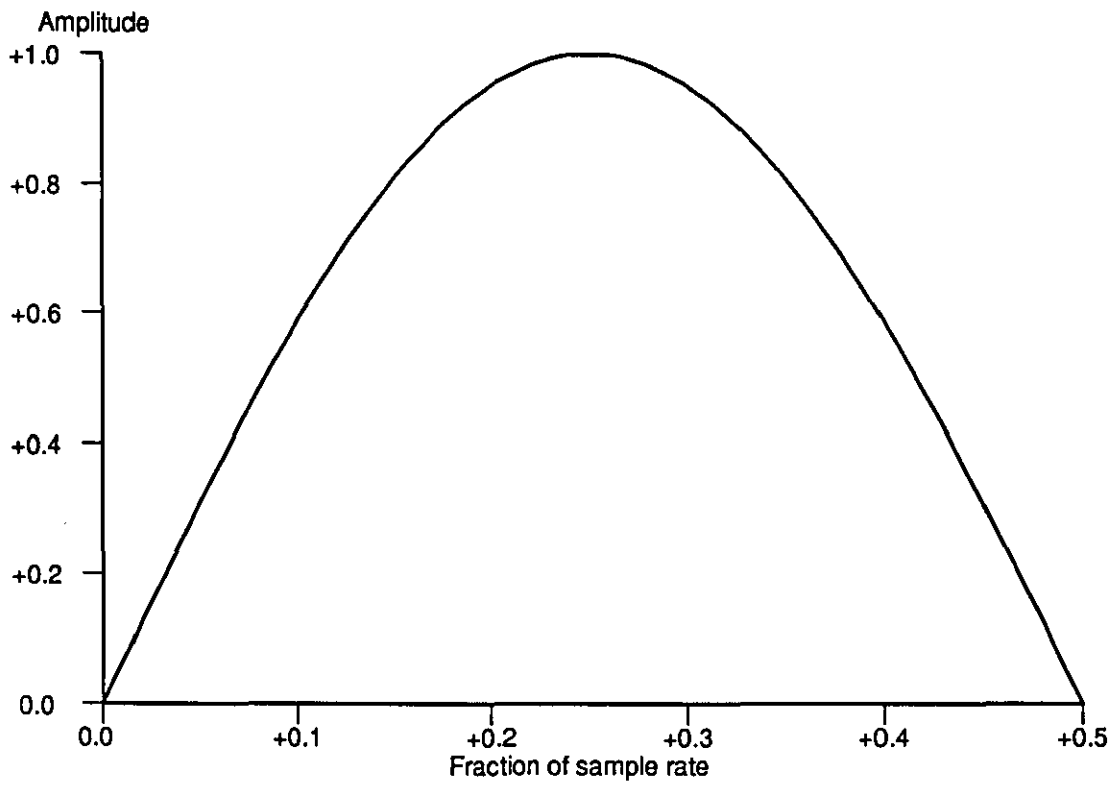

FIGURE 3.9 - The transfer function of a first order finite difference differentiating formulae.

describing the orientation of the forearm in relation to the upper arm were all determined, and the bandwidth of the signals computed for all film trials. These bandwidths were used in the analyses performed in section 3:5.4, with the values reported in the table 3.8 being the highest of those determined.

Trial #3 was representative of all the trials, so to illustrate the effect of smoothing, the amplitude spectrum of the Z coordinates describing the path of the centre of mass of the distal segment before and after smoothing is shown in figure 3.10. This analysis shows that the sampling rate of 200 Hz was over 20 times higher than the highest frequency components in the sampled signal. This over sampling has an advantage as shown in section 3:4.7.

3:5.2 SIGNAL AVERAGING

If the noise contaminating a signal is white, this means the noise is not correlated between samples and has a mean value of zero. On summing repeat measures the true underlying signal is additive, the noise is statistically independent so it tends to average out to a constant value equal to the mean value of the random noise. Therefore by taking the average of a number of repeat samples the signal to noise ratio is improved. If n repeat measures are taken, the true signal size is increased by a factor n, the variance of the noise is increased by the same factor, while the standard deviation of the noise is increased by a factor equal to the square root of n. On taking the average the signal amplitude to noise standard deviation ratio is increased by the square root of n.

To analyse the random noise introduced in the digitizing process four frames were randomly selected and digitized 10 times from trial #3. The maximum variance in digitizing a point in any one of these frames was 0.6416 mm. To quantify the noise added to the points, all the points for each frame were relocated using the digitizer coordinates from one digitization, and the mean of ten digitizations. The maximum difference between locating a point with one digitization and the mean of ten was 8.3 mm.

These data were then used to examine the effectiveness of the spline smoothing routine. The absolute error was calculated for locating the points with one digitization and the mean of ten digitizations. These errors were then averaged for each axis and across all four frames. This gave an indication of the noise that may occur across all the frames. These figures were compared with the results from smoothing. For trial #5 all the points were reconstructed with and without smoothing using the quintic GCVS. The mean absolute differences between these two estimates of the signal were computed. These differences were then averaged for all frames and for the three axes. Table 3.7 presents the absolute error estimates obtained from the averaging of multiple digitizations, and the mean absolute difference between smoothed and non-smoothed data.

In table 3.7 the noise levels estimated from the mean data compare favourably with the amount of noise removed from the whole sampled signal using the spline. This indicates that for this analysis the spline was effective in removing much of the noise from the signal. The highest error estimates were for points number 2 and 6. Point 2 was the styloid process of the ulna which during the studied movements was periodically hard to locate as it was partially obscured by the dumbell, (this landmark was not actually

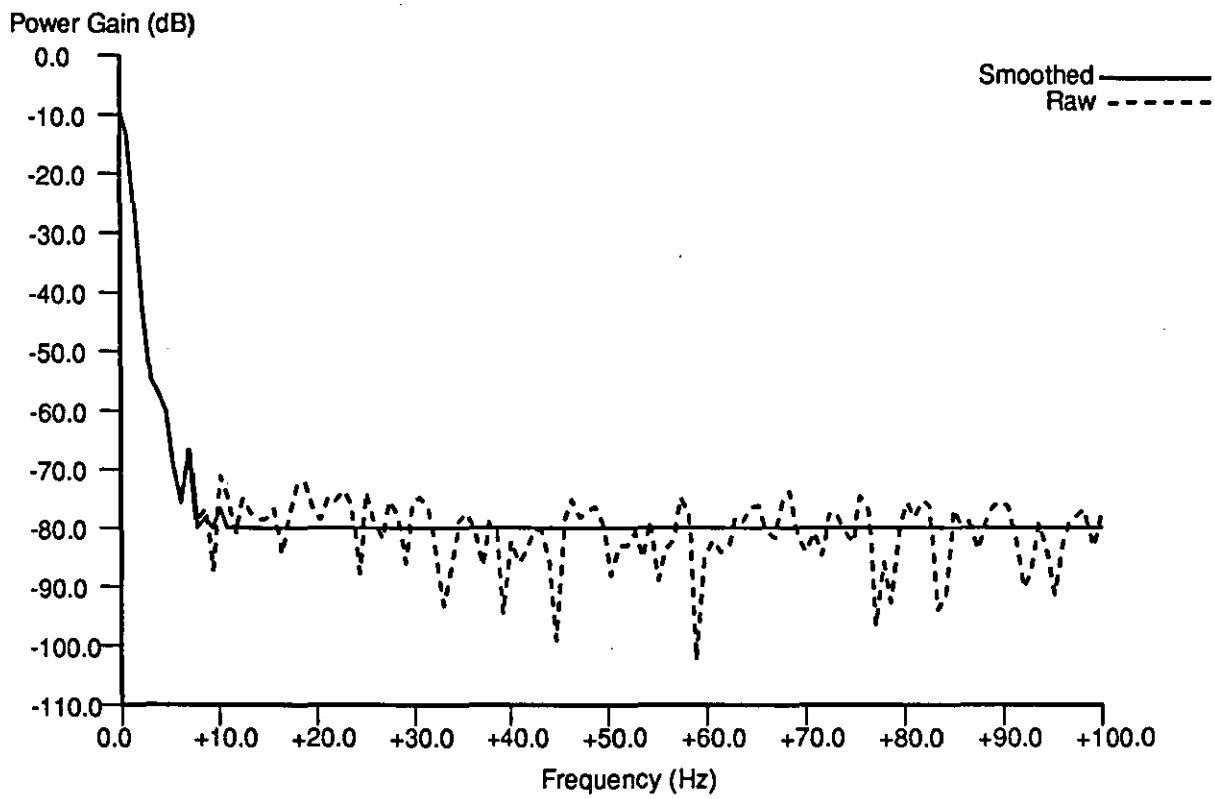

FIGURE 3.10 - The amplitude spectrum for the path of the centre of mass (Z coordinate) of the distal segment before and after smoothing.

TABLE 3.7 - The root mean square error for the mean of ten digitizations compared with the results for one digitization, and the root mean square error for all frames between the smoothed and non-smoothed signal.

	ROOT MEAN SQUARE ERRORS	
DIGITIZED POINT	MEAN DATA	SMOOTHED DATA
1	0.0016	0.0019
2	0.0040	0.0030
3	0.0033	0.0021
4	0.0030	0.0017
5	0.0029	0.0010
6	0.0042	0.0034
7	0.0021	0.0021
8	0.0029	0.0021

Notes:-

a) The root mean square errors are in metres.

b) The digitized points correspond to:-

1. Styloid process of radius
2. Styloid process of ulna
3. Medial epicondyle
4. Olecranon process of ulna
5. Lateral epicondyle
6. Lesser tubercle of humerus
7. Medial end of dumbell
8. Lateral end of dumbell

used to form the member reference frame for the distal segment during the dynamic analysis). Point 6 was the lesser tubercle of the humerus which also became partially obscured by the dumbell during part of the movement. The smoothed results compared with the mean results showed that the spline was in most cases removing most of the random noise as indicated by the mean data. The largest discrepancy was the 1.9 mm for point 5 the lateral epicondyle of the humerus. This analysis suggests that the random noise associated with the digitization process resulted in a mean error of 1.6 mm to 4.2 mm.

In the preceding analysis the assumption has been made that the noise calculated for the four randomly selected frames gave an indication of the random noise present in the whole of the film sequence. The digitized points all have different amounts of random noise associated with them, as indicated by the absolute differences between the mean of ten digitizations and one digitization shown in table 3.7. This provides a rationale for the use of the GCVS separately for each landmark, as opposed to using it for one landmark, determining the amount of smoothing and then applying this to the signal from all other landmarks.

To reduce the effect of noise contaminating the digitizer coordinates of the points on the calibration frame, these points were digitized ten times and the mean used to calculate the calibration coefficients. The effect of this procedure was analysed in section 2:2.4.

The data from the repeat digitizations of four randomly selected frames was used again to estimate the variance of the noise, see section 3:5.4.

3:5.3 MARKER MOVEMENTS

The distance between the markers was measured on the subject using a caliper. The distances between the markers was also calculated during the filmed activity from the reconstructed three-dimensional coordinates of the digitizer coordinates of these markers. The differences between the film estimated distances and their measured distance gave an indication of the effect of reconstruction accuracy and marker movement.

Analysis of trial #3 was undertaken to examine marker movements. To evaluate the error in length estimation without marker movement the distance between the two markers rigidly fixed onto the dumbell was considered. The ends of the dumbell were clearly marked, and the markers could not change their positions on the dumbell during the movement. For all the film frames the standard deviation in comparing known length with actual length was 0.0035 m for the smoothed data. This error is in keeping with the error associated with locating points in space using the cine-photogrammetric procedures adopted in this study (see section 2:2.4). To examine marker movement due to skin movement two markers were selected which were on the same bone and that were sufficiently far apart so that the errors associated with estimating their positions were independent. The markers considered were the marker on the lesser tubercle of the humerus and the marker on the lateral epicondyle of the humerus, the measured distance between which was 0.3005 m. The standard deviation over all the trials in comparing the calculated length with actual length was 0.0078 m when the data were not smoothed and 0.0064 m when the data were

smoothed. Figure 3.11 shows how the estimated length varied throughout the course of the movement.

Figure 3.11 shows that the estimated length varied throughout the movement. Van den Bogert et al. (1990) showed that during horse locomotion skin movement was correlated with the movement patterns of the horses. There is no clear indication in the present data whether the differences were correlated with the movement. This analysis does not fully quantify the amount of marker movement. If the markers both move in the same direction then the error is reduced, equally the opposite case may apply. Some of these errors may be due to digitizer operator errors both random and systematic, and include errors due to the precision and accuracy of the measurement system. The maximum error in the length estimation was 0.0173 m. The errors associated with marker movements impose an additional limit on the accuracy of calculated variables. It was not possible to further quantify marker movement or the effect of this movement on the calculated parameters.

3:5.4 LANSHAMMAR ANALYSIS

Lanshammar (1980) presented a formula which gives an estimate of the noise which can be expected to remain in a noisy signal after smoothing and or differentiation. The formula is:-

$$\sigma_K^2 = \frac{\sigma^2.\tau.\omega_s^{(2.K+1)}}{\pi.(2.K+1)} \qquad [3.38]$$

Where:-

K - is the order of the derivative

σ^2_K - is the variance of the noise contaminating the K^{th} derivative after processing

σ^2 - is the variance of the additive white noise

τ - is the sample interval

ω_B - is the bandwidth of the signal in radians ($\omega_B = 2.\pi.f_B$)
and f_B is the sample band-width in Hertz.

There are three major assumptions in this formula.

1. The signal is band-limited.
2. The noise contaminating the signal is white.
3. The frequency response of the filter or differentiator is ideal.

Slepian (1976) has shown that from a mathematical point of view no signal is band-limited. Effectively frequencies above the Nyquist frequency have to be ignored. It is not possible for the noise contaminating a signal to be perfectly white, for example the noise may be correlated between samples. The assumption that the filter is ideal means that the signal passes unattenuated up to the specified filter cut-off, after which all of the remaining signal is removed irrespective of whether it is noise or true signal. For a differentiator to be ideal means that the signal is suitably amplified up to the cut-off frequency after which no signal is allowed to pass. Such filters and differentiators are not practically realizable. These assumptions mean that the formula gives only a minimum estimate.

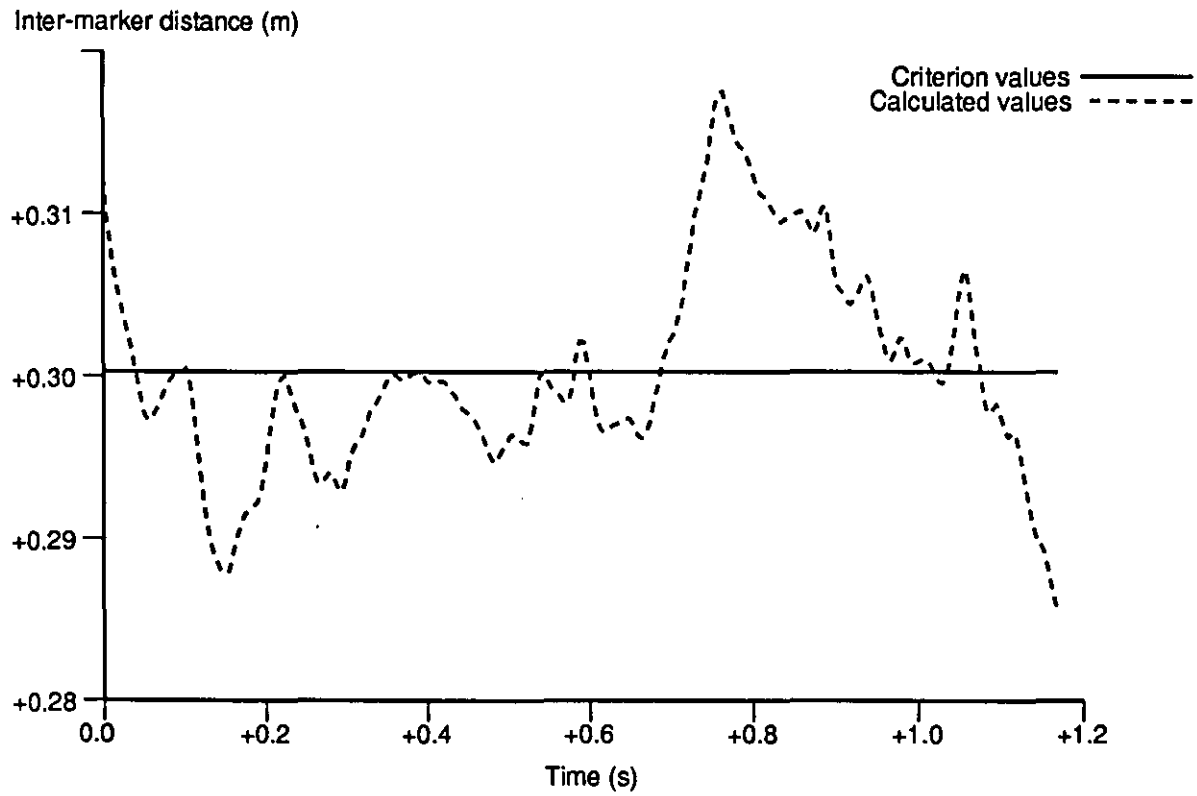

FIGURE 3.11 - The variation in calculated length between markers on the humerus: lateral epicondyle and lesser tubercle.

Re-arrangement of the formula shows how the sample rate should be adjusted to give acceptable derivative estimates:-

$$\frac{1}{\tau} = f_s = \frac{\sigma^2.\omega_o^{(2.K+1)}}{\sigma_K^2.\pi.(2.K+1)} \qquad [3.39]$$

This illustrates that the noise level of rigid body position and attitude estimates, and their derivatives can be significantly reduced by sampling at rates much greater than twice the Nyquist frequency, even if the variance of the additive white noise remains constant.

To estimate the errors in the sampled signal a Lanshammar analysis was performed on the data. To determine the variance of the noise added to the sampled signal the information from the four frames which were digitized 10 times was used. Using the procedures already described the position of the origin of the distal segment's member reference frame (the centre of mass) and the Cardan angles were determined. For each of the four frames 10 estimates of these variables were made. The variances of these variables were estimated for each frame, and then the mean variances for the four frames calculated. The highest estimated bandwidth of the sampled signal from section 3:5.1 was also used. The results for this analysis are presented in table 3.8.

The error standard deviation values were calculated assuming that an ideal filter and differentiator were used. Therefore the true error standard deviations were probably higher. These error estimates are used in section 4:5.1 to perform a sensitivity analysis of the computed resultant intersegmental moment.

3:5.5 LIMB KINEMATICS

To illustrate how the procedures described in this chapter may be used this section examines the change in the carrying angle during elbow flexion. The subject was instructed to keep the forearm and hand in a neutral position, that is with the hand mid-way between full pronation and full supination. The subject then flexed the elbow joint. The variation in carrying angle was considered as a function of elbow flexion angle, see figure 3.12.

The range for elbow flexion of 0 to 145 degrees is similar to values from the literature (see section 3:2.3), as is the range for the carrying angle -7 to 17 degrees. The carrying angle was measured approximately on the subject using a goniometer (Atha Flexitractor) when the elbow was fully extended and fully flexed. These measurements compared well with the extremes of the range of movement reported here as measured from the film.

To see if the subject permitted any longitudinal rotation of the forearm during the movement, the amount of longitudinal rotation was plotted against flexion angle, see figure 3.13. The graph shows that the subject did permit longitudinal rotation during the examined movement. The member reference frame used for this analysis assumed that the radius did not move in relation to the ulna, and this is a possible source of error in these angular measures. There was no way of quantifying the effect of this on the computed state variables; the following discussion assumes that its influence was small.

TABLE 3.8 - An analysis of the anticipated minimum standard deviation of the noise affecting state variables, calculated using equations of Lanshammer (1980).

	STANDARD DEVIATION OF NOISE	SIGNAL BANDWIDTH	STANDARD DEVIATION OF NOISE FOR DERIVATIVE		
			0	1	2
POSITION	m	Hz	m	$m.s^{-1}$	$m.s^{-2}$
X	0.0016	6.3	0.000402	0.009178	0.281414
Y	0.0050	6.3	0.001255	0.028681	0.879420
Z	0.0019	4.7	0.000412	0.007023	0.160647
ANGLES*	rad	Hz	rad	$rad.s^{-1}$	$rad.s^{-2}$
F/E	0.0075	3.0	0.001299	0.014137	0.206414
AB/AD	0.0112	4.0	0.002240	0.032503	0.632765
S/P	0.0134	2.6	0.002161	0.020379	0.257877

(N.B. * - the angles refer to rotations about the F/E flexion-extension axis, AB/AD abduction-adduction axis, and S/P supination-pronation axis.)

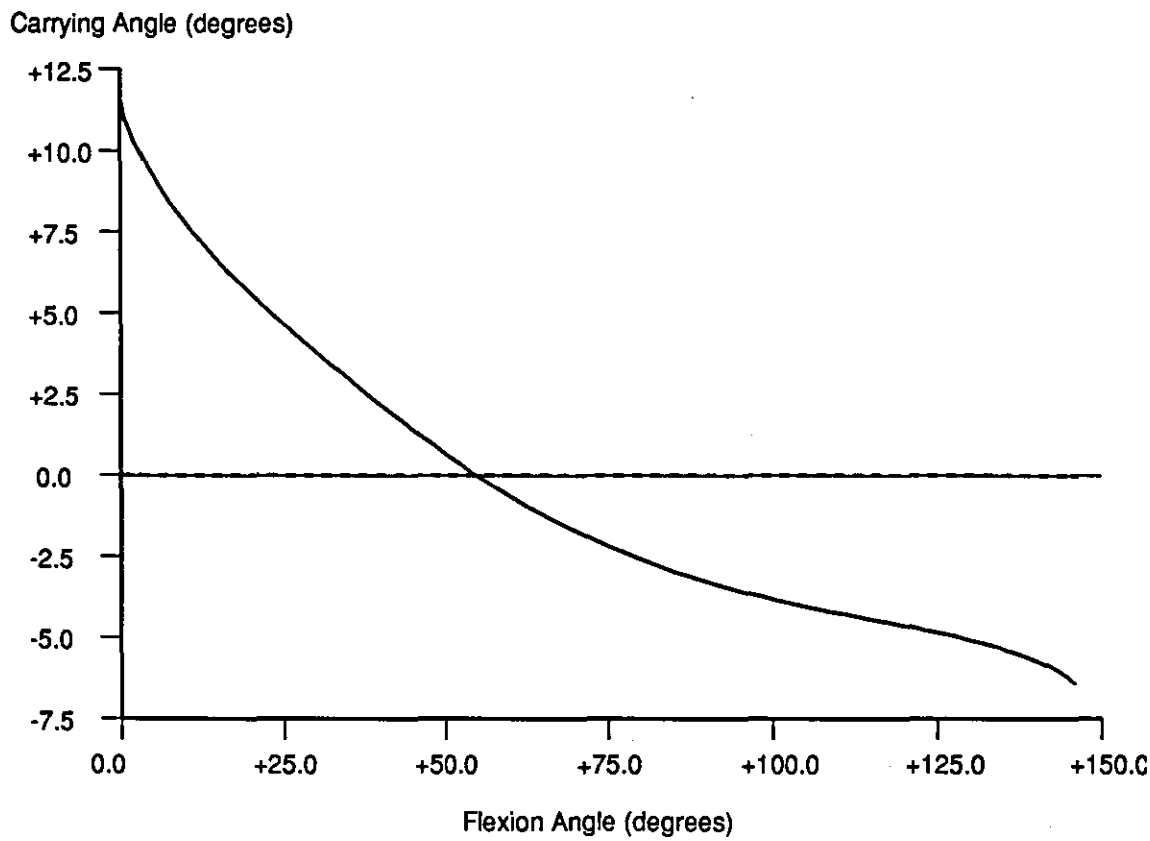

FIGURE 3.12 - The variation in carrying angle with amount of elbow flexion.

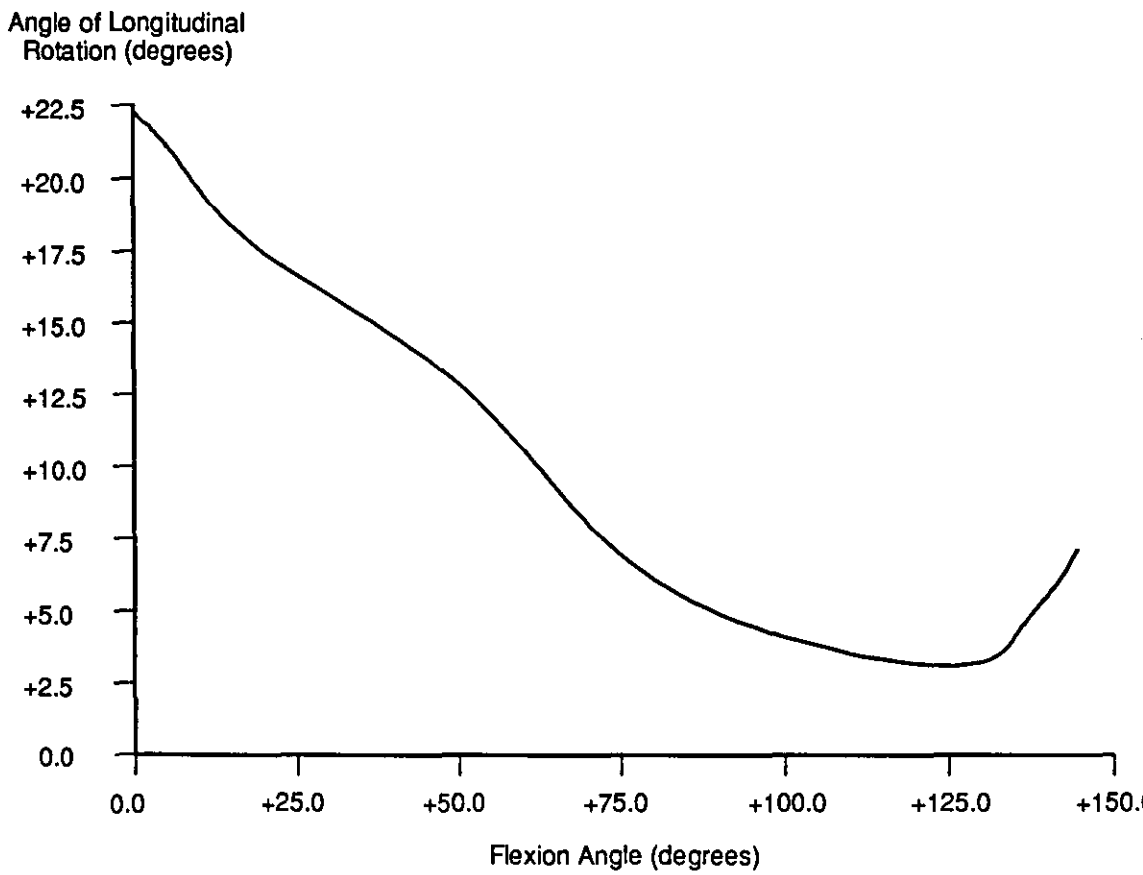

FIGURE 3.13 - The variation in longitudinal rotation of the forearm with amount of elbow flexion.

Chao and Morrey (1978) examining dry bone specimens found that, during a simulated flexion, the forearm rotated about its longitudinal axis when the arm was in any one of three initial positions. In light of their findings some longitudinal rotation should be expected. In this study this rotation was greater in range than reported by Chao and Morrey (1978), this additional rotation could be due to two factors. Either the subject differs structurally from those in the study of Chao and Morrey (1978), or the subject executed the movement with additional longitudinal rotation of their own volition. The shape of the curve in figure 3.13 is very similar to that of Chao and Morrey (1978). The fact that the subject exhibited longitudinal rotation during the movement does not affect the reported change of carrying angle with flexion as Chao and Morrey (1978) showed that carrying angle was independent whether the forearm was in a supinated or pronated position during flexion.

The non-rigidity of the distal member reference frame for these analyses makes it difficult to precisely define the motion of the bones of the forearm. Another reference frame was used for the analyses of the dumbell curls in which the rigidity assumption is not invalidated by longitudinal rotation of the forearm.

3:5.6 SUMMARY

The preceding sections have analysed and quantified the errors associated with the measurement processes. In the next chapter kinematic information is used to compute the resultant intersegmental moments at the elbow joint during a dumbell curl, and the errors associated with this kinematic information are used to estimate the accuracy of these moments.

CHAPTER IV

MUSCLE MOMENT DETERMINATION

INTRODUCTION

Inverse dynamics permits the estimation of the resultant joint forces and moments. These forces and moments are the result of forces due to the muscle, ligament forces, and forces due to articular surface contact. By making certain assumptions it is possible to estimate the net moments caused by the muscles crossing a given joint. This chapter is concerned with calculating the muscle moments acting about a joint. The kinematic variables required for this process were derived using the procedures described in chapter III. To determine the resultant joint moments and forces, the inertial properties of the distal rigid body must be known. Therefore this chapter contains details of the computation of the inertial properties of the subject's forearm and hand, and of the dumbell which the subject grasped. A sensitivity analysis was performed to estimate the accuracy of the resultant joint moments, the results of which are reported in this chapter.

4:1 REVIEW OF ANTHROPOMETRIC TECHNIQUES

To determine the forces and moments acting about a joint due to the movements of a rigid body articulating about that joint it is necessary to know the mass, location of the centre of mass, and moments of inertia of the rigid body about three orthogonal axes. In studies of human movement the segments of the human body are idealised as rigid bodies. The inertial properties of body segments can be obtained using various techniques which are reviewed in the following sections.

This review is divided into three sections reflecting the major initiatives in the determination of body segment inertial parameters. This information can be derived from cadaver data, measurements on live subjects, or the geometric modelling of body segments. These divisions are notional as there are many overlaps, for example density data from cadaver studies are often incorporated into geometric models. In each section a selection of techniques is reviewed.

4:1.1 CADAVER STUDIES

Dempster (1955) dissected eight male cadavers. From measures taken on these cadavers he presented figures for estimating segment mass as a fraction of total body mass, and centre of mass location as a fraction of segment length. Barter (1957) combined the data of Dempster (1955) with the data from three male cadavers dissected by Braune and Fischer (1889), and one cadaver dissected by Fischer (1906). Using only one independent variable (body mass) he produced regression equations for estimating segment mass.

Dempster (1955) used a compound pendulum to derive the transverse moments of inertia of cadaver body segments about joint axes. Plagenhoef (1971) used the data of Dempster to calculate the mean radius of gyration values for each segment.

Clauser, McConville, and Young (1969) dissected 14 male cadavers and produced regression equations for estimating segment mass and centre of mass location for 14 body segments. They used up to three dimensions in these equations including segment length, depth, breadth, and circumference, in addition to subject mass. The locations of the centres of mass of the segments were presented in their report as percentages of segment length. Segment lengths were measured using appropriate bony landmarks. Hinrichs (1990) re-examined their data and presented centre of mass locations based on segment length measured from joint centres.

Chandler, Clauser, McConville, Reynolds, and Young (1975) dissected six cadavers, and calculated the three principal moments of inertia for 14 segments. Hinrichs (1985) used these data to produce regression equations to calculate segment moments of inertia, based on the lengths and perimeters of the segments. The author recommended that these equations should not be applied to limbs with perimeter and length values outside the range of the subjects in the original study of Chandler et al. (1975).

Of the many cadaver studies attempting to estimate body segment parameters, most include segment mass and centre of mass location but few estimate moments of inertia of the segments or the whole body. Due to the relative paucity of moment of inertia data some authors have recommended the scaling of the moment of inertia values of a cadaver or group of cadavers so that they can be used for a living subject. Hay (1974) suggested that if the data of Dempster (1955) were used, the subject for whom the parameters were required should be matched in terms of anthropometric measurements to one of the cadavers, and that cadaver's moment of inertia values used. Wilson and Hay (1974) scaled cadaver moment of inertia values for living subjects using variations in segment mass and length. Dapena (1978) used a similar procedure but used subject height in place of segment length. Presumably this substitution was based on the assumption that segment lengths are directly proportional to subject height. Forwood, Neal, and Wilson (1985) examined these scaling techniques using moment of inertia values about the transverse axis from Chandler et al. (1975) as the criterion. The techniques compared were: matching the subject to a selected cadaver; scaling of moment of inertia data using subject height and subject mass; and scaling moment of inertia data using subject segment length and subject mass. Statistical analysis of the results, with the limitation of the sample size of only five (one set of data from one of the cadavers of Chandler et al. (1975) was not used), showed that scaling data using subject height and mass produced the most accurate results. In addition to these experimental results it should also be noted that such a scaling procedure would probably not be appropriate for moment of inertia about the longitudinal axis as the distribution of mass in this plane is not strongly related to subject mass.

Cadaver studies have a number of common problems. It is difficult to make inter-study comparisons because different investigators have used different definitions of segments, and different dissection techniques. The age and former health of the cadavers makes extrapolation to a live population dubious. The samples are small, and generally not typical of the general population. The measurements taken from cadavers may not reflect those of a live population, due to changes in the inertial properties of the segments, caused by changes in the density of tissues resulting from degeneration, loss of fluids, changes in the distribution of fluids within the segments, and because some cadavers are embalmed or placed in a

preserving medium prior to dissection.

4:1.2 EXPERIMENTAL DETERMINATION

It is possible to determine body segment inertial parameters experimentally on live subjects. The simplest method is to obtain segmental volume using an immersion technique (e.g. Katch, Weltman, and Gold, 1974; Drillis, Contini, and Bluestein, 1964). These techniques are harder to apply to proximal segments, but can be satisfactorily applied to the hand and forearm. Given segment density, segment mass can be computed.

If the volume of a segment is estimated using an immersion technique then centre of mass can be found by locating the point of mid-volume. This technique was used by Drillis et al. (1964). Clauser et al. (1969) using cadaver segments of known centre of mass showed that this technique tended to estimate the centre of mass proximal to its true location. This has implications for geometric modelling of limbs, where if uniform density is assumed, the centre of mass is assumed to be mid-volume. Experimental difficulties in measuring the total segment volume and mid-volume may account in part for the results of Clauser et al. (1969). The variation in density along a segment would also tend to displace the centre of mass away from the mid-volume point.

Bernstein (1967) used a reaction board to compute the mass and centre of mass of the limbs on 152 subjects. It is not possible using this technique to compute both segment mass and centre of mass simultaneously; one parameter must be known to compute the other. Another problem arises as the distribution of mass within the segment may vary as the limb is moved.

Drillis et al. (1964) computed moment of inertia values by taking plaster casts of body segments. The compound pendulum technique was then used to assess the moments of inertia of the plaster casts. Corrections were made to allow for the differences in the densities of the cast and body segment. Uniform density was assumed throughout the plaster casts and the segments.

Fenn, Brody, and Petrilli (1931) proposed a quick-release technique for determining the moment of inertia of proximal segments. Bouisset and Pertuzon (1968) employed this technique for determining the moment of inertia of the forearm and hand. The quick release technique is based on the measurement of linear force and acceleration when the limb has been released from exerting a static moment. Moment and angular acceleration were computed from the linear force and acceleration values, and the moment of inertia evaluated as the quotient of these two variables. Cavanagh and Gregor (1974) examined the variations in estimated moments of inertia for the shank and foot about the knee joint axis, when different moments were exerted by the subjects and when the position of force application was varied. The authors showed that by changing these two variables the estimated moments of inertia varied, consequently they questioned the reliability of this technique.

Hatze (1975) used a suspension method for estimating the passive visco-elastic moments of a joint, the location of the centre of mass, and the moment of inertia of a segment. The limb was oscillated when

suspended from a spring based mechanism. The time period and the change in amplitude of the oscillations permitted calculation of the parameters. The mass of the limb was required to compute the location of the centre of mass. This technique and the quick release technique are most applicable to distal segments and for calculating transverse moments of inertia.

Dainis (1980) expressed the location of the centre of mass of a system of linked rigid segments as a polynomial function of time during free-flight. Records of the positions of the end points of the segments served as inputs for the polynomial, the coefficients of which could then be evaluated using a linear least-squares technique. It was then possible to derive the centre of mass location of the whole system, and then the mass and centre of mass locations of the segments. Results were obtained in two-dimensions for three different systems: three linked rods; a three segment representation of a body during a gymnastic vault; and a six link representation of a body performing a tucked somersault. Errors in the prediction of the acceleration of the whole body centre of mass served as an estimate of accuracy of the derived parameters. The predicted centres of mass locations for some segments were outside the segments. The accelerations of the centres of mass of the systems were less than 0.1 $m.s^{-2}$ away from their true values, whereas using the data of Dempster (1955) produced errors of up to 1.2 $m.s^{-2}$.

Vaughan, Andrews, and Hay (1981) performed a two-dimensional analysis of three different movements all including a single footed contact with the ground, and two of which included a flight phase. A non-linear objective function was formulated which minimised the difference between the terminal segment ground reaction force as measured directly by a force plate and as calculated from a combination of segment anthropometry and kinematics. The mass, centre of mass locations, and moments of inertia for 14 segments were all calculated. Comparisons were made with values derived from the data of Dempster (1955), Clauser et al. (1969), and Chandler et al. (1975). The activities examined were a long jump take off, a running stride, and kicking. There was a large variation in predicted parameters for the same subject for the different activities.

The studies of Dainis (1980) and Vaughan et al. (1981) both have common assumptions which may account for their inaccuracies. They assumed the mechanical model adopted was valid, that the segments were rigid, and the movements studied could be represented in two-dimensions. Deriving accurate kinematic data is also problematic. It is particularly difficult when second derivative values are calculated from noisy displacement data. Dainis (1980) made his measurements on bodies in free-flight. This is more likely to produce more accurate kinematics than the measures taken during the impact situations studied by Vaughan et al. (1981).

It is possible to measure the inertial properties of segments using a variety of imaging techniques. Brooks and Jacobs (1975) used gamma mass scanning to measure mass distribution in animal segments and found a maximum error of 4.6 percent in calculating the moments of inertia of three lambs legs. The measurements were derived from the principle that when a gamma radiation beam passes through a substance the strength of the beam diminishes in relation to the density of the substance. Zatsiorsky and Seluyanov (1983, 1985) were the first (and only researchers to date) to apply this technique to a large

number of male subjects (n=100). Their sample population included large athletic specimens. In their 1983 paper multiple linear regression equations for estimating segment inertial properties were presented using subject height and mass as the independent variables. New multiple regression equations for estimating the segment inertial properties were presented in their 1985 paper, where segment length and different circumferences were used as the independent variables.

Huang and Wu (1976) developed a technique which allowed the calculation of tissue densities in a segment in vivo using computerized tomography (CT). Rodrigue and Gagnon (1983) used CT scans to compute the densities of the forearms from 10 cadavers (20 forearms in total). Comparison of the density values with those obtained from hydrostatic weighing showed that the CT scan overestimated density by a mean value of 2.1 percent. Ackland, Henson, and Bailey (1988) used CT scans to examine the variation in density along the longitudinal axis of the leg, and found that the density data of Dempster (1955) overestimated shank density for both a cadaver specimen and a live subject.

Magnetic resonance imaging (MRI) unlike gamma mass scanning and CT scans does not expose the body to radiation. Martin, Mungiole, Marzke, and Longhill (1989) used MRI to calculate the inertial parameters of eight baboon cadaver arm segments. Images were taken at 0.015 m intervals along the limbs and then manually digitized. Criterion values were obtain by hydrostatic weighing, direct weighing, a reaction board, and a compound pendulum. The mean percentage differences and standard deviations were: volume 6.3 ± 5.0; density 0.0 ± 3.1; mass 6.7 ± 2.8; centre of mass location -2.4 ± 8.2; and transverse moment of inertia 4.4 ± 3.0. The standard deviations for these estimates were very high which indicates that this technique was not very precise. The same research group performed a study on live subjects using MRI (Mungiole and Martin, 1990). Their paper is discussed in section 4:1.4. Of note here is the reported higher density values for the shank of 12 adult males, compared with values reported in Dempster (1955), Clauser et al. (1968), and Chandler et al. (1975).

4:1.3 GEOMETRIC MODELS

Body segments are generally of irregular shape, but for the purposes of modelling, body segments have been represented by geometric solids. These solids can be described mathematically, permitting derivation of segmental inertial parameters. The dimensions of these shapes are obtained by taking anthropometric measurements on the experimental subject (e.g. segment length and circumference). Amar (1920) was one of the first researchers to use this approach when he computed the moments of inertia of the limbs by modelling them as truncated cones, and the trunk as a cylinder. Whitsett (1963) developed a 14 segment model of the human body. The shapes used were ellipsoids, elliptical cylinders, truncated cones, spheres, and rectangular parallelepipeds. The segment masses were determined from the regression equations of Barter (1957) and centre of mass locations were determined from Dempster (1955). Moments of inertia were computed from equations relating to the geometric solid, for these calculations density was assumed uniform longitudinally along a segment. Hanavan (1964) modelled the whole body as 15 segments. Segment density was computed as the quotient of the mass of the segment computed from Barter (1957) and the volume of the geometric solid modelling the segment.

Jensen (1976) used a photogrammetric technique based on an original suggestion by Weinbach (1938). The body was divided into 0.02 m thick elliptical discs from which segmental inertial parameters were estimated for the 16 segments into which the body had been divided. Jensen applied his model, and that of Hanavan (1964), to an 11 year old male swimmer and found large differences between the models. In 1978 a further analysis of three boys was undertaken. Body mass estimates using Jensen's model had a less than two percent error, compared with direct measurement. Density values were obtained from Dempster (1955) and density was assumed uniform longitudinally along each segment.

Gagnon and Rodrigue (1979) showed that the forearm model of Hanavan (1964) underestimated segment volume by an average of 15 percent when applied to 29 male college students. When the limb was modelled as five truncated cones in series, segmental volume was under estimated by five percent.

Hatze (1980), presented a 17 segment model for which 242 anthropometric measures had to be made directly on the subject. Each body segment was divided into a number of geometric solids. The variations in density values along the longitudinal axis of a segment were taken from measurements made by Demspter (1955) on one subject. Account was also taken of variations in density due to fat, utilizing the data from "a special sub-cutaneous fat indicator". The geometric solids employed did not assume that all the segments were symmetrical. Model predictions were made on four subjects, and the model values were compared with values determined experimentally. Transverse moment of inertia values were computed using the suspension method of Hatze (1975). The parameters calculated from the model were reported to give accuracy better than three percent with a maximum error of five percent.

The model of Hatze is the most sophisticated and complete model of the human body yet undertaken. It suffers as all models do because it cannot be completely validated. Its accuracy must be assessed in relation to experimentally determined segmental inertial parameters and the efforts of the modeller to consider as many pertinent factors as possible. In Hatze's case this has resulted in a complex model.

Hall and Depauw (1982) developed an 18 link model composed of geometric solids. The centre of mass of the whole body as computed by the model was compared with that measured by a reaction board. For 40 subjects of varying age, the mean error in whole body centre of mass location was 1.6 percent.

4:1.4 DISCUSSION

Little work has been done on comparing the various approaches. Sprigings, Burko, Watson, and Laverty (1987) compared the model of Hatze (1980) with the ratio data of Demspter (1955) and the regression equations of Clauser et al. (1969) for the determination of the centre of mass. Ten male subjects were filmed performing a tucked jump. The acceleration of the centre of mass was used as the criterion. The model of Hatze gave the acceleration values closest to that due to gravity. Mungiole and Martin (1990) compared criterion data derived from MRI to assess a number of commonly used techniques for deriving inertial properties of the lower leg of 12 athletic adult males. The same research group (Martin et al., 1989) examined the MRI technique using the arms of baboon cadavers. In this earlier study the standard deviations of the errors for the MRI technique compared with direct measurement of parameters were high

(see section 4:1.2 for more details). They claimed that these errors were due to a problem with the preparation of the specimens; they anticipated that these errors were smaller in the later study. Mungiole et al. (1990) reported that for the determination of lower leg inertial parameters the different models all gave similar estimates of the centre of mass location. The mass and transverse moment of inertia values showed a greater spread in estimates for the different techniques. It was not possible to draw any further conclusions as the MRI data were not considered accurate enough to be a criterion.

A study was therefore undertaken to further evaluate a number of techniques for deriving body segment inertial parameters. The moments of inertia values were used as the criterion, as their values are influenced by all the other parameters.

4:2 INVESTIGATION OF ANTHROPOMETRIC METHODS

The purpose of this section is to evaluate a number of models for the determination of the moments of inertia of the upper limb. As this study was concerned with elbow flexion the inertial parameters of the forearm and hand were all that were required; the upper arm is included for completeness.

4:2.1 METHODOLOGY

To assess the anthropometric techniques under investigation it was necessary to have a suitable criterion with which to compare the computed values.

Anthropometric data derived from cadavers are accurate but scarce. The study by Chandler et al. (1975) derived the centre of mass, segment mass, and moment of inertia about three axes for each of 14 segments on six male subjects. These moment of inertia data for the upper limb were used as the criterion in the present study. In addition to these body segment inertial parameters Chandler et al. (1975) provided other measurements which facilitated the application of a number of anthropometric techniques. The moments of inertia were defined about three orthogonal axes through the centre of mass of each segment, see figure 4.1. Data for the right and left limbs were averaged, following the procedure of Hinrichs (1985). The moment of inertia data for two mutually perpendicular axes orthogonal to the longitudinal axis of each limb were also averaged to give one transverse moment of inertia. In the study by Chandler et al. (1975) the hands were measured in "...various relaxed positions..." (page 63). Therefore it was not possible to accurately compare computed moment of inertia values for this segment.

To aid analysis the techniques assessed in this study were divided into three groups: 1a, simple statistical models; 1b, complex statistical techniques; and 2, geometric models. The differences between calculated and true values were computed and used to determine the mean absolute percentage error.

$$ME = \frac{100}{n} \sum_{i=1}^{n} \frac{|I_T - I_b|}{I_T} \qquad [4.1]$$

Where:-

ME - is the mean absolute percentage error

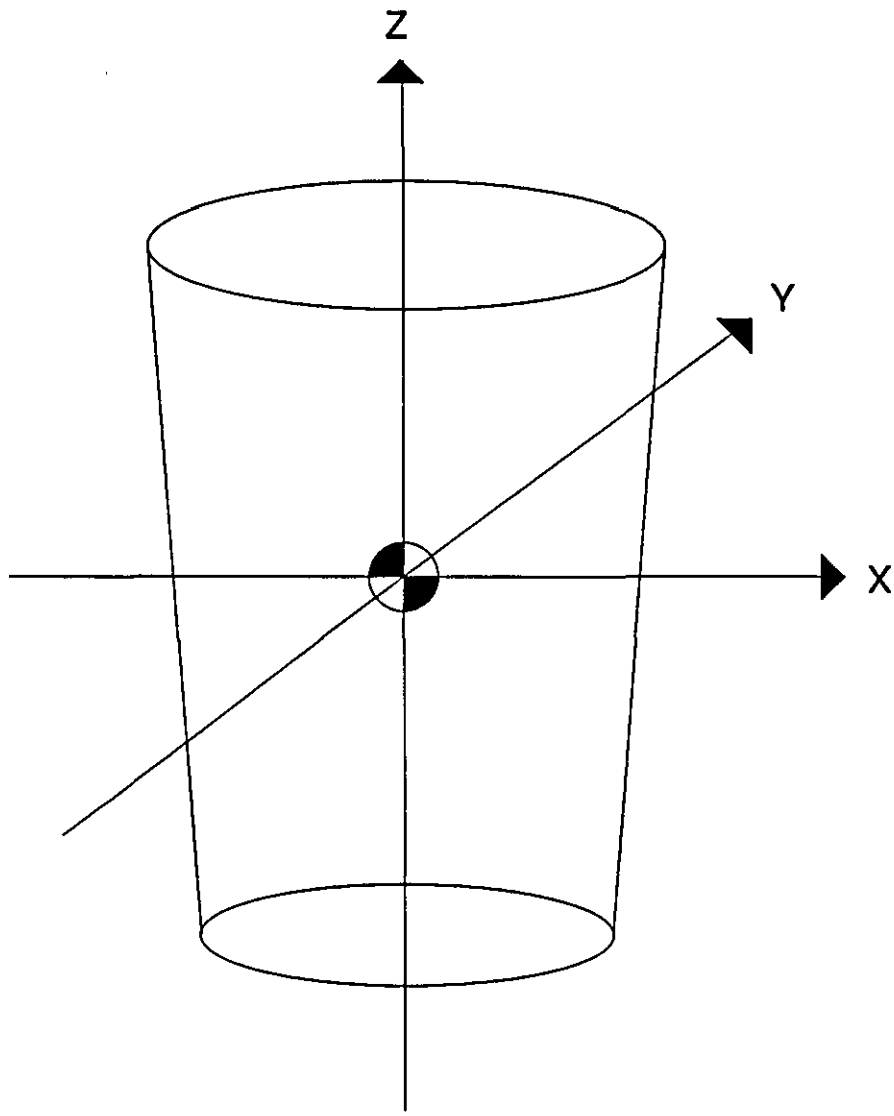

FIGURE 4.1 - A body segment represented by a truncated cone, with the principal axes passing through the centre of mass of the segment.

n - is the number of values

I_{tr} - is the true moment of inertia value

and I_e is the estimated moment of inertia value.

GROUP 1a : Simple Statistical Techniques

The moment of inertia values about the transverse axes through each segment centre of mass for eight male cadavers were reported by Dempster (1955). These data were used to examine the accuracy of scaling moment of inertia data. A study by Forwood et al. (1985) suggested that from a variety of scaling techniques investigated the most successful procedure employed the group mean moment of inertia for each segment and scaled it for each subject using subject height and mass (Dapena, 1978). This procedure was adopted for the data of Dempster (1955) in the present study. Therefore the mean data of Dempster (1955) were scaled to provide estimates of the moments of inertia of the individual cadavers in the study of Chandler et al. (1975).

The segment moments of inertia for the subjects in the study of Chandler et al. (1975) were estimated using the formulae:-

$$I_p = I_s * C \qquad [4.2]$$

Where:-

I_p - is the predicted segment moment of inertia

I_s - is the the mean segment moment of inertia of the sample group

and C is the subject specific scale factor.

$$C = \frac{(H_s * M_s)}{(H_m * M_m)} \qquad [4.3]$$

Where:-

H_s - is subject height

M_s - is subject mass

H_m - is the mean height of the subjects

and M_m is the mean mass of the subjects.

GROUP 1b : Complex Statistical Techniques

Three different complex statistical models were assessed, each involving a set of equations which related the segment moment of inertia values to one or more easily measurable parameters. The first set of equations was that of Zatsiorsky and Seluyanov (1983) who related subject height and mass to segment moment of inertia. Their moment of inertia data were derived from gamma scanning measurements on 100 healthy subjects. These equations produced moment of inertia values for two transverse axes which were averaged to give one transverse moment of inertia value. There was insufficient information in the report of Chandler et al. (1975) to implement the equations of Zatsiorsky and Seluyanov (1985).

The second set of equations assessed was that of Hinrichs (1985) who presented a set of linear regression equations derived from the data of Chandler et al. (1975). The results reported for the regression equations of Hinrichs were the best results obtained from all the different regression equations presented in that report.

The regression equations of Hinrichs (1985) do not reflect how the moment of inertia values of a segment were affected by the dimensions of the limbs e.g. length and circumference. Therefore a third set of equations was formulated which attempted to relate these pertinent physical dimensions to segment moment of inertia. The volume and mass values for the segments can be attained by representing them as geometric shapes. If a segment is modelled as a cylinder the following equations may be stated:-

$$\text{Volume} = V = \pi . r^2 . L \qquad [4.4]$$

$$\text{Mass} = m = V.\rho \qquad [4.5]$$

Where:-
r - is the radius of the cylinder
L - is the length of the cylinder
and ρ is the density of the cylinder.

The moment of inertia for the cylinder is calculated using:-

$$I = \frac{m.r^2}{2} \qquad [4.6]$$

$$I = \frac{m.\left(L^2 + 3.r^2 \right)}{12} \qquad [4.7]$$

Where:-
I_l - is the longitudinal moment of inertia
and I_t is the transverse moment of inertia.

Using the relationship between the circumference of a circle and its radius it is possible to represent these equations in the form of the following non-linear equations:-

$$I = K1 . C^4 . L \qquad [4.8]$$

$$I = K2 . C^2 . L^3 + I . \frac{1}{2} \qquad [4.9]$$

Where:-
C - is the circumference of the cylinder
and K1 and K2 are constants.

Using a linear regression technique, the constants were determined. These constants are presented in table 4.1. The circumferences were defined as follows:-
The hand - the mean of hand and wrist perimeter values.
The forearm - the mean of wrist, maximum forearm, and elbow perimeter values.
The upper arm - the mean of the elbow, maximum upper arm, and axillary perimeter values.

A cylinder is a simple geometric shape which offers an approximation to the shape of the limbs under investigation, and has moment of inertia equations that are easily put into the form of non-linear equations. This approach was taken by Morlock and Yeadon (1986) who produced non-linear equations for estimating the moments of inertia of the thigh also using the data of Chandler et al. (1975). While this study was being undertaken Yeadon and Morlock (1989) produced a more complete treatment of the use of non-linear equations for the prediction of moment of inertia.

GROUP 2 : Geometric Models
The upper arm and forearm were modelled both as one truncated cone, and two truncated cones in series. There were insufficient measures in the report of Chandler at al. (1975) to extend the modelling to more than two truncated cones. Such an approach is common in the literature e.g. Apkarian, Naumann, and Cairns (1989) modelled limb segments as single truncated cones, and Yeadon (1984) used two truncated cones in series to model the upper arm and forearm. In the present study the dimensions provided in Chandler et al. (1975) were used to model the hand as both a single elliptical disc and a truncated cone. The equations used to compute the inertial properties of these geometric solids are presented in Appendix C.

Various density data were used as inputs for the geometric models, see table 4.2. Rodrigue and Gagnon (1983) reported density values at 16 equidistant locations along the longitudinal axis of the forearm of a "typical subject". The three available circumferences on the forearm were used and via linear interpolation the circumferences determined when the forearm was further divided into 16 truncated cones. The variable density data were then used in the model of the forearm.

4:2.2 RESULTS AND DISCUSSION

Table 4.3 presents the results for the data scaling. The results for the scaling of the data of Dempster (1955) were not very accurate, even though the procedure used was found to give the most accurate results in the study of Forwood et al. (1985). In this later study the mean data of Chandler et al. (1975) were scaled back onto the individual subjects in the study using various scaling techniques. In the present study a more rigorous assessment was performed as the data which were scaled were those of Dempster (1955) which were scaled onto the individual subjects of Chandler et al. (1975).

The results for the complex statistical techniques are presented in table 4.4. The results from the model of Zatsiorsky and Seluyanov (1983) were very poor. One possible explanation for this may be the different division of limbs into separate segments. The designation of segment boundaries is often "fuzzy", and varies between researchers. The details presented by Zatsiorsky and Seluyanov (1983) provided

TABLE 4.1 - The constants of the non-linear equations.

	K1	K2
UPPER ARM	0.9601	6.2178
FOREARM	0.9185	5.4034
HAND	1.2774	8.0112

(N.B - circumference and length measurements in metres, moment of inertia in $kg.m^2$)

TABLE 4.2 - The densities of the segments of the upper limb, as reported in major studies ($kg.m^{-3} \times 10^3$).

STUDY	UPPER ARM	FOREARM	HAND
DEMPSTER	1.07	1.13	1.16
CLAUSER*	1.056	1.098	1.109
CHANDLER	1.080	1.052	1.004

(N.B. - * these values are not reported in this study but are calculated from mean volume and mass values.)

TABLE 4.3 - The mean absolute percentage error in predicting the moments of inertia of the segments of the upper limb, using scaling of data.

	MEAN ABSOLUTE PERCENTAGE ERROR		
	UPPER ARM	FOREARM	HAND
TECHNIQUE	I_x	I_x	I_x
Scaling of data of Dempster (1955)	10.3	19.1	19.1

insufficient information to facilitate a detailed analysis of their segment boundary definitions. Using the same data as in their 1983 study, Zatsiorsky and Seluyanov (1985) developed multiple linear regression equations to describe body segment inertial parameters. Their study is to be commended for its sample size (n=100), and the fact that measurements were made on a live, athletic population, as opposed to cadavers resulting from geriatric or chronically ill subjects. These aspects may also account for some of the inaccuracies found in the present study, as cadaver data was used as the input into their regression equations.

The results for the remaining two sets of regression equations are flattering as the equations were derived from the data upon which they were subsequently tested. The regression equations of Hinrichs (1985) produced better results than the non-linear equations. In an attempt to estimate the effect of trying these techniques on new data, both sets of regression equations were re-formulated for the forearm only, but leaving out the data of subject number three. The linear regression equations related moment of inertia to maximum forearm circumference. These equations then had to estimate the moment of inertia values for subject number three. The results of this analysis are shown in table 4.5. Subject number three was the largest of all the subjects, having the largest longitudinal moment of inertia, and the second largest transverse moment of inertia. This result illustrates the weakness in the linear regression fit when data outside the original data range are considered. The non-linear equations approximate more closely the relationship between body dimensions and moment of inertia therefore in this analysis better results were obtained outside the original data range using these equations.

The results for the various geometric models are presented in table 4.6. The geometric models of the forearm and upper arm showed increased accuracy when more sections were used in the models. The accuracy in the volume estimation places a limit on the accuracy of the moment of inertia predictions. The accuracy of the volume estimations are presented in table 4.7. Examination of equations 4.5 and 4.6 for the cylinder and the equations in Appendix C suggests that with greater accuracy in volume estimation more accurate moment of inertia estimates could be obtained. If sufficient measurements had been available it would have been possible to model the limbs using more truncated cones (or other appropriate shapes), which should result in greater accuracy in volume estimation. Such an approach has been taken in the work of Jensen (1978) and Hatze (1980).

The geometric models showed sensitivity to the density estimates used. Of the three sets of density data reported in table 4.2 that of Dempster (1955) were the highest. The mean forearm density reported by Rodrigue and Gagnon (1983) of 1.06×10^{-3} kg.m^{-3} (n=12) was also less than that reported by Dempster (1955). It was only possible to consider variable density for the forearm segment. These data were obtained using CT scanning on one subject only (Rodrigue and Gagnon, 1983). These data did not result in an increase in accuracy of the moment of inertia estimation. There could be an error here resulting from extrapolating data from one subject.

TABLE 4.4 - The mean absolute percentage error in predicting the moments of inertia of the segments of the upper limb, using statistical techniques.

	MEAN ABSOLUTE PERCENTAGE ERROR					
	UPPER ARM		FOREARM		HAND	
TECHNIQUE	I_t	I_l	I_t	I_l	I_t	I_l
Zatsiorsky and Seluyanov (1983)	25.4	50.9	16.0	23.4	50.9	153.2
Hinrichs (1985)	0.9	1.9	6.3	9.1	7.6	19.5
Non-linear equations	6.1	6.2	4.3	19.8	9.4	28.0

TABLE 4.5 - The longitudinal and transverse moments of inertia of one cadaver forearm, using equations calculated from a reduced data set.

	I_l	%DIFF	I_t	%DIFF
REAL VALUE	15.0	-	83.0	-
LINEAR REG.	18.3	22.0 %	106.1	27.8 %
NON-LIN EQN.	12.8	14.7 %	75.1	9.5 %

(N.B. - in this table units for moments of inertia were $kg.m^2 \times 10^4$.)

TABLE 4.6 - The mean absolute percentage error in predicting the moments of inertia of the segments of the upper limb, using different geometric models with various density values.

	MEAN ABSOLUTE PERCENTAGE ERROR					
	UPPER ARM		FOREARM		HAND	
MODEL	I_t	I_l	I_t	I_l	I_t	I_l
1 TRUNCATED CONE						
Dempster Density	12.2	8.5	14.8	24.3	7.5	25.9
Clauser Density	11.2	7.0	11.6	22.9	9.8	26.4
Chandler Density	7.3	4.6	8.2	20.4	12.1	23.9
2 TRUNCATED CONES						
Dempster Density	11.7	7.7	13.1	20.7	-	-
Clauser Density	7.2	4.6	9.9	18.5	-	-
Chandler Density	7.2	4.3	5.3	14.9	-	-
Variable Density	-	-	9.6	15.8	-	-
1 ELLIPTICAL DISC						
Dempster Density	-	-	-	-	7.7	28.1
Clauser Density	-	-	-	-	10.6	24.5
Chandler Density	-	-	-	-	11.8	22.3

(N.B. - in the table "-" refers to values which were not possible to calculate due to insufficient information in the report of Chandler et al. (1975).)

TABLE 4.7 - The mean absolute percentage error between the volume of the body segments and their estimated values.

	MEAN ABSOLUTE PERCENTAGE ERROR		
MODEL	UPPER ARM	FOREARM	HAND
1 TRUNCATED CONE	7.2	12.2	5.4
2 TRUNCATED CONES	6.7	7.4	-
1 ELLIPTICAL DISC	-	-	7.6

4:2.3 SUMMARY

On the data investigated the regression equations of Hinrichs (1985) gave the best results. It was shown that these regression equations do not perform well outside of their sample range whilst the non-linear equations showed improved accuracy for extrapolation outside of the sample range. Problems can also arise due to variations between studies in the precise definitions of segments. The geometric modelling techniques gave acceptable accuracy. An increased number of truncated cones making up the model could have resulted in better volume estimation, and consequently potentially better moment of inertia estimation. There would appear to be no limitation to the sample range with these techniques, and researchers are free to define segment boundaries which are most suitable for their study. There is a need for further examination of the ways of determining accurate body segment inertia parameters, with imaging techniques (gamma mass scanning, CT, and MRI) perhaps providing the most promising avenue for research in the clarification of this important area.

4:3 SUBJECT SPECIFIC ANTHROPOMETRY

In light of the investigation in the previous section the inertial properties of the forearm and hand were determined using a geometric modelling approach.

4:3.1 GEOMETRIC MODELLING

This section discusses three issues relating to geometric modelling of segments: choice of geometric solids; the assumption that each segment is a rigid body; and the assumption of uniform density.

Table 4.8 gives details of some of the different solids used to represent the hand and forearm segments. The differences in the models of the hand are due to it being modelled in either a closed (gripping) or flat position. The most complex model is that of Hatze (1980) where the hand is modelled as a prism to which a hollow half-cylinder and an arched rectangular cuboid (thumb) are attached. The model of Hatze (1980) does not assume that the segment is symmetrical. In 1982 Hall and Depauw modelled the hand as a triangular section of a right-angled parallelepiped. The hand was modelled in an open flat position. This solid meant that the centre of mass location was fixed at one third of the segment length from the wrist. Yeadon (1984) also modelled the hand in an open position as a cone. The centre of mass was fixed at one quarter of the segment length from the wrist joint. The hand in this study was gripping a dumbell, so a model was adopted of the hand in this position. It consisted of a truncated cone to represent the heel/ base of the hand and a hollow cylinder representing the fingers grasping the dumbell.

The forearm has been modelled as a variety of shapes, see table 4.8. The models of Hatze (1980) and Jensen (1978) both assume that the forearm has different moments of inertia about its two transverse axes. In their study of six cadavers Chandler et al. (1975) found that for the forearm segment the moments of inertia through the two transverse axes were very similar, see table 4.9. This supports the assumption that this segment can be considered to be symmetrical about its long axis. The model adopted here for the forearm was a series of truncated cones, therefore the two transverse axes will have the same moment of inertia value. As the accuracy of volume estimation has an influence on the other derived parameters, a model consisting of more solids will give a better estimate of volume. Therefore the

TABLE 4.8 - Geometric solids used to represent the forearm and hand segments.

AUTHOR	FOREARM	HAND
Whitsett (1963)	truncated cone	sphere*
Hanavan (1964)	truncated cone	sphere*
Jensen (1976)	series of elliptical discs	series of elliptical disc
Hatze (1980)	ten elliptical discs	a prism, hollow half-cylinder and an archedrectangular cuboid*
Hall and Depauw (1982)	truncated cone	triangular section of right-angled parallelepipeds.
Yeadon (1984)	two truncated cones	cone

(N.B. - * Hand - modelled in grip position)

TABLE 4.9 - The moments of inertia about the two transverse axes through the forearm of the cadavers of Chandler et al. (1975) (Units $kg.m^2 \times 10^4$).

SUBJECT	RIGHT		LEFT	
NUMBER	Ixx	Iyy	Ixx	Iyy
1	54	52	67	62
2	99	94	80	81
3	94	90	75	73
4	45	45	49	49
5	59	55	54	52
6	50	51	64	61

(N.B.- Ixx and Iyy were the moments of inertia about two transverse axes passing through the centre of mass, as defined by Chandler et al. (1975).)

forearm was modelled as a series of truncated cones. The truncated cones were each 0.02 m high except the final cone which was shorter to allow for segment length not being a precise multiple of 0.02 m.

In using a geometric solid to model a segment it is assumed that the segment is rigid, but this does not strictly apply because the mass does not remain stationary, and because segment boundaries are not fixed. When the forearm rotates about its longitudinal axis it does not move as a rigid body. The distal part of the segment rotates more than the proximal, causing a relative redistribution of the mass of the segment between the two transverse axes. There is no currently adopted technique for accounting for this variation during longitudinal rotation of the forearm. In this study the forearm was modelled in the neutral position.

As mentioned in section 4:1.2 the precise definition of segment boundaries is a problem. These boundaries should be clearly defined for the purposes of modelling, but in reality are "fuzzy". Although geometric modelling does not circumvent this problem it does permit the researcher to define the boundaries as deemed appropriate for the particular study.

Related to the assumption that the model segments are rigid is the assumption that the density throughout the segment is constant. If constant segment density is assumed in geometric modelling, the centre of mass is assumed to coincide with the centre of volume. Using cadaver segments Clauser et al. (1969) showed that this assumption led to systematic error when using an immersion technique to estimate centre of mass. This discrepancy could be part explained by methodological problems in finding the mid-volume point. The difference could also be due to variations in segment density, and therefore mass distribution along the longitudinal axis of the segment.

Only Hatze (1979b,1980) has incorporated variable density values into an anthropometric model. Hatze (1979b,1980) used the variable density data of Dempster (1955) from his dissection of one cadaver. Rodrigue and Gagnon (1983) have shown that for one subject the density of the forearm varies along the longitudinal axis of the segment. A study by Ackland et al. (1988) examined density distribution in the leg using CT scanning. Using one leg from a cadaver specimen and a live subject's leg they showed that the mean density data of Dempster (1955) overestimated the density of both limbs. The pattern of variation in density along the longitudinal axes of the cadaver limb and live subject's limb were the same, although the cadaver's density values were lower. Ackland et al. (1988) also examined the influence of using variable density values rather than a constant density value as inputs to a model of the lower leg consisting of five elliptical discs. Their results indicated that the constant density assumption
"...when modelling the human body was shown to produce minor errors in the estimation of inertial properties of the leg segment." (page 154)
It has not yet been shown whether this result is applicable to other segments.

In this study the task was to choose the most appropriate density data. There are still insufficient variable density data to justify incorporating these into the present model. As the study of Clauser et al. (1969) had the largest sample size and carefully controlled experimental protocol these density values were used.

Recent studies have shown that it is possible to obtain variable density information from CT scanning (e.g. Rodrigue and Gagnon, 1983; Ackland et al., 1988). A larger variable density data base may soon be available and consequently improve the accuracy of moment of inertia predictions using geometric models.

4:3.2 SUBJECT ANTHROPOMETRIC DETAILS

The forearm, hand, and dumbell were all modelled using geometric solids. A diagram of the model is presented in figure 4.2.

The forearm was modelled as a series of truncated cones. The level of the elbow flexion-extension axis was marked on the subject using a marker pen. The forearm was then divided longitudinally into sections of 0.02 m, with marks made on the skin at each of these divisions. The perimeters of these sections were obtained using a measuring tape. The forearm consisted of 13 truncated cones.

The hand was modelled whilst gripping the dumbell. The hand was modelled in two parts: a truncated cone on top of which was a hollow cylinder. The truncated cone represented the section of the hand from the flexion-extension axis of the wrist to the first metaphalangeal joint of the thumb. The appropriate perimeter measures were taken. The length of the hollow cylinder was the width of the four knuckles measured when the hand was gripping the dumbell. The inner radius of the cylinder was the radius of the dumbell handle. The perimeter was measured at both ends of the hand whilst gripping the dumbell, and the mean of these two values was used as the outer radius.

It was also necessary to know the inertial characteristics of the dumbells. They were modelled as a series of three cylinders. It was possible to measure accurately the radii of the cylinders and so derive the volume of the dumbells. The mass could be measured directly, and as the dumbell was perfectly symmetrical about all three axes the centre of mass location was easily calculated. By assuming that the dumbells were of uniform density it was possible to determine the remaining inertial parameters. As the dumbells were made of a single material and were not hollow, the assumption of uniform density was valid. The inertial parameters for the dumbells were therefore considered to be accurate.

The inertial properties of the forearm, hand, and dumbells are presented in table 4.10. The subject at the time of data capture was 1.68 m tall, with a mass of 65.10 kg, and 25 years of age.

4:3.3 ACCURACY OF INERTIAL MEASURES

It was not possible to directly assess the accuracy of inertial parameters of the forearm and hand used to compute limb kinetics, estimated using the geometric models. This section investigates the accuracy of these measures by perturbating the forearm and hand inertial values used to compute the inertial parameters of the whole system (forearm, hand, and dumbell).

As there were no criterion values for inertial properties of the subject's forearm and hand it was not possible to directly assess the model accuracy. However the relative influence of these parameters on the

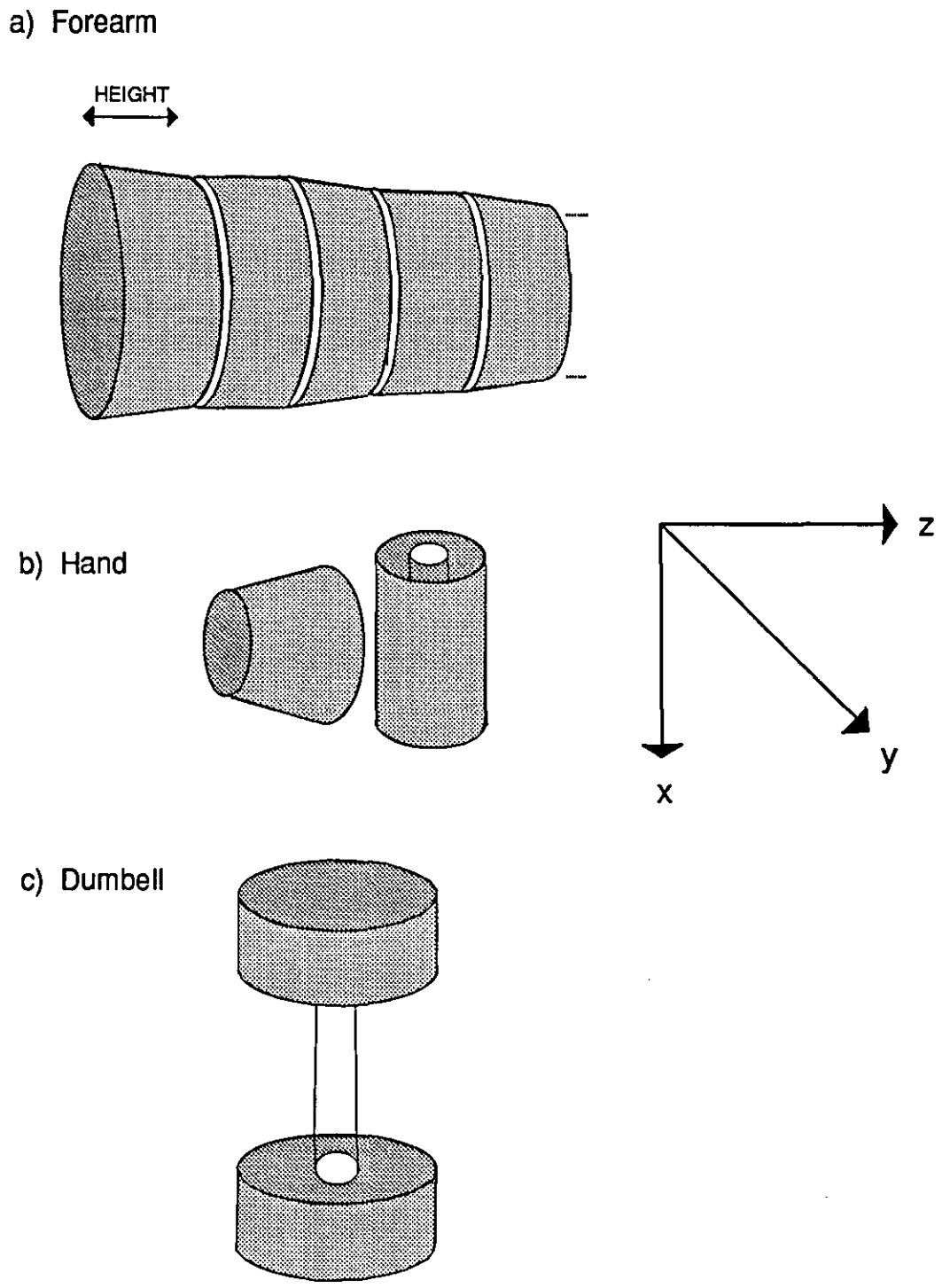

FIGURE 4.2 - A diagram showing configuration of the geometric solids used to model the forearm, hand, and dumbell for determination of inertial properties.

TABLE 4.10 - The inertial properties of the forearm, hand, and dumbells.

INERTIAL PROPERTY	FOREARM	HAND	15 kg DUMBELL	17.5 kg DUMBELL
MASS (kg)	0.998	0.411	15.100	17.37
CENTRE OF MASS (m)*	0.1059	0.0599	0.000	0.000
I_X (kg.m^2)	0.0052	0.0005	0.04067	0.04704
I_Y (kg.m^2)	0.0052	0.0006	0.13929	0.17355
I_Z (kg.m^2)	0.0006	0.0003	0.13929	0.17355

(N.B - * for the subject the centre of mass location is the distance from the proximal joint centre to the centre of mass along the longitudinal axis only, as the segment was assumed symmetrical about the other axes.)

inertial properties of the whole system could be examined. It can be assumed that the mass, centre of mass location, and moments of inertia of the dumbells are accurate. These values for the two dumbells are much larger than the values for the hand and forearm, see table 4.10. As the forearm, hand, and dumbell were all considered to be one rigid body the influence of inaccuracies in the estimation of the inertial parameters of the forearm and hand on the whole system were examined. The following analysis is for the 15 kg dumbell only.

The only direct check on the accuracy of the anthropometric measures was direct measurement of the volume of the forearm and hand. The volume of displaced water when the forearm and hand were immersed was measured as 1.299 litres. This compares favourably with the value of 1.297 litres calculated with the geometric model, a difference of 0.15 percent. This is better than the accuracy in volume estimation that was reported by Gagnon and Rodrigue (1979), for the forearm only, which was modelled as five truncated cones in series. Reference to tables 4.6 and 4.7 shows that the more accurate the volume estimation the more accurate the estimated moment of inertia values were. The volume estimation here is much better than the accuracy of volume estimations reported in table 4.7. Ackland et al. (1988) claimed that accurate volume estimation was more important than accurate density values for predicting lower limb moments of inertia.

To examine the effect of the accuracy of density estimates, different density values were used as inputs to the model of the forearm and hand. This information was combined with the details of the dumbell to compute the inertial parameters of the whole system. The percentage differences were evaluated between the whole system inertial parameters as originally calculated using the density values of Clauser et al. (1969) and the whole system inertial parameters computed using other density values. These results are reported in table 4.11. The effect of different density values on the mass and location of the centre of mass of the whole system differed by less that one percent in all cases examined. The largest difference was for the moment of inertia for the X axis where the error reached 2.67 percent. This occurred when the density values were five percent different from the selected values. With the other cadaver density data sets the maximum difference in any of the computed parameters was less than 2.5 percent.

The influence of constant density values has been assessed, but it is also possible to use variable density values in geometric models (Hatze 1979b, 1980). If volume is well estimated and an appropriate mean density value is used, mass will be estimated with good accuracy. But variable densities in the truncated cones making up the segments could have an effect on the centre of mass location and the moments of inertia of the segments. Using the same procedure as in section 4:2.1 the forearm was further divided into 16 sections so the variable density values of Rodrigue and Gagnon (1983) could be used as inputs to the model of the forearm. As this paper had no density values for the hand it was not possible to perform a full analysis of the effect of this variable density data on the whole system. The effect of these variable density values on the inertial properties of the forearm was small, giving a percentage differences of -2.42 percent for mass, -1.25 percent for centre of mass location, -0.35 percent for transverse moment of inertia, and -2.19 percent for longitudinal moment of inertia. The effect of an error in any one of the parameters is

TABLE 4.11 - The effect of different density values for the forearm and hand on the inertial parameters of the whole system, expressed as the percentage difference between the inertial parameters calculated using the density values of Clauser et al. (1969).

	PERCENTAGE DIFFERENCE				
DENSITY DATA	MASS	C. OF MASS	I_x	I_y	I_z
Clauser et al. (1969) increased by 5 %	0.43	-0.20	2.67	1.31	3.37
Clauser et al. (1969) decreased by 5 %	0.43	0.20	-2.69	-1.32	-0.03
Dempster (1955)	0.29	-0.12	1.57	0.77	0.02
Chandler et al. (1975)	-0.49	0.18	-2.28	-1.12	-0.04

analysed next. It is shown that if these errors were assumed to apply for both the forearm and hand these percentage differences are small enough that they would have little effect on the inertial properties of the whole system.

To assess the influence of inaccuracy in any one of the parameters, each of the parameters computed using the density data of Clauser et al. (1969) was changed by five and 10 percent, and its influence on the whole system examined. These changes are artificial because it is unlikely that any one parameter would change without another also changing. The results for this analysis are shown in table 4.12. The mass of the whole system was not very sensitive to changes in the mass of the forearm and hand. The effect of this parameter was greatest on the transverse moments of inertia of the whole system. The accuracy of mass estimation is dependent on the accuracy of the volume and density values. It has been established that volume has been well estimated by the model, and the accuracy of the density estimates has already been discussed.

Centre of mass location depends on how well the changes in volume of the forearm have been estimated (if density is assumed constant). Mungiole and Martin (1990) showed that a variety of techniques produced estimates for the location of the centre of mass within 2.5 percent of one another. It would appear that this parameter is well predicted by a variety of techniques. As volume has been accurately modelled, if the assumption of constant density is valid the centre of mass location can be regarded as fairly accurate. The change in centre of mass location when using variable density for the forearm was shown to be small. If centre of mass location had been poorly located it would have resulted in large errors in the moment of inertia values about the transverse axes.

The total system moment of inertia values were not strongly influenced by the variations in the moment of inertia values of the forearm and hand. Moment of inertia values of the whole system were more dependent on the location of the centre of mass than on the forearm and hand moment of inertia values.

4:3.4 SUMMARY

Although it was not possible to directly assess the accuracy of the anthropometric measures used in the present study, an indirect estimation was performed. The volume estimation produced by the geometric model was accurate and compared favourably with figures from the literature. The use of different density values produced an error of less than three percent in any one of the parameters. If any one of the derived parameters was varied by five percent its effect on the whole system was also found to have less than four percent difference on the whole system. The whole system seemed most sensitive to the estimation of the location of the centre of mass. This parameter was dependent on accuracy of volume estimation and the assumption of constant density. The effect of the available variable density values on this parameter was shown to be small.

Although not evaluated, the influence of inaccuracies in the inertial parameter values for the forearm and hand on the whole system for the trial with the 17.5 kg dumbell were anticipated to be further reduced as the dumbell's inertial properties would have had increased influence.

TABLE 4.12 - The effect of change in any one of the parameter values on the inertial parameters of the whole system, expressed as the percentage difference between the inertial parameters of the whole system calculated using the density values of Clauser et al. (1969), and the perturbated values.

	PERCENTAGE DIFFERENCE				
VARIED PARAMETER	MASS	CENTRE OF MASS	I_X	I_Y	I_Z
MASS 5%	0.427	-0.202	1.707	0.834	0.000
MASS 10 %	0.853	-0.403	3.399	1.660	0.000
CENTRE OF MASS 5%	0.000	0.223	-3.672	-1.794	0.000
CENTRE OF MASS 10%	0.000	0.447	-7.155	-3.495	0.000
MOMENT OF I_X and I_Y 5%	0.000	0.000	0.969	0.475	0.034
MOMENT OF I_Z 10%	0.000	0.000	1.938	0.951	0.067

4:4 MUSCLE MOMENT DETERMINATION

The purpose of this section is to detail the procedures used to determine the muscle moments about the elbow joint during arm flexion.

Resultant joint moments can be calculated for an activity given the appropriate kinematic data and the external forces (zero for a body end point free in space). These moments are caused by the active muscular tension, and by the passive deformations of any tissues which may cross or surround the joint. All of these contributions must be accounted for if a resultant joint moment is to be called the muscle moment.

4:4.1 ASSUMPTIONS ABOUT RIGID BODY SYSTEM

This section will discuss the assumptions inherent in a rigid body analysis of human movement.

The assumption of rigidity implies that there is no motion of the segment relative to its own member reference frame. In the general case this assumption is false as the muscles, organs, blood, and other bodily fluids move relative to the member reference frame. Denoth (1986) in a theoretical analysis of the impact of a segment onto a hard surface showed that this "wobbling mass" was a significant variable contributing to the ground reaction forces. It is still difficult to measure these effects and until they can be quantified the rigid body model is the best approximation.

In the rigid body model adopted for kinematic and kinetic analysis of human movement there are often restrictions placed on joint motion. The maximum number of degrees of freedom a joint can have is six. In most two-dimensional studies the joints are assumed to have only one degree of freedom, for example the elbow joint in the study of Yeo (1976). The current model considers the joint to have three degrees of freedom, rotational only. The assumption here is that the joint structure does not allow any translational movement. This assumption is common to other researchers examining the elbow (e.g. An, Morrey, and Chao, 1985; Youm, Dryer, Thambyrajah, Flatt, and Sprague, 1979). The joint is also considered to be frictionless, although some joint friction may be included in models of joint passive visco-elasticity (see section 5:2.5).

In the computation of the joint moment the point of force application at the joint is required. The point is assumed to be the joint centre, but in human movement the joint centre or axis is non-stationary (e.g. Youm et al., 1979). The joint centre, or correctly for three-dimensional studies the joint axis, is assumed to be fixed at a position ascribed before the processing of the data. As discussed in section 3:1.5 the accuracy of the kinematic data in this study did not permit the in vivo calculation of the instantaneous helical axes. If the true joint centre or axis was computed for each sample interval and used to compute the resultant joint moment this could result in a change of resultant moments. If it is not possible to compute the joint centre or axis for each sample interval, the ascribed joint centre or axis should be positioned in relation to its reported location in the literature. Such an approach was taken in this study. Implicit in this modelling assumption is that there is a single bony contact point, although this would rarely be the case in human joints.

The problem of lack of rigidity also has an influence on the inertial properties of the rigid body. This was discussed in section 4:3.1.

Finally one assumption specific to the present model is that the forearm and hand were considered to be one rigid link. This assumption is invalidated if there is any movement at the wrist. The subject was instructed to allow no movement at the wrist and trials were disregarded if the subject reported this to happening.

4:4.2 CALCULATION OF RESULTANT JOINT MOMENT

Inverse dynamics allows the estimation of the intersegmental resultant forces and moments. These forces and moments are the result of muscle forces, ligament forces, and forces due to articular surface contact. The following relationships can be stated:-

$$F_J = \sum_{i=1}^{NM} (F_{Mi}) + \sum_{j=1}^{NL} (F_{Lj}) + \sum_{k=1}^{NC} (F_{Ck}) \qquad [4.10]$$

Where:-

F_J - is the intersegmental resultant force with reference to some predefined joint centre J

F_{Mi} - is the muscle force of the i^{th} muscle

F_{Lj} - is the ligament force of the j^{th} ligament

F_{Ck} - is the force at the k^{th} articular contact point

and NM, NL, and NC are the number of muscles, ligaments, and articular contact points respectively.

$$M_J = \sum_{i=1}^{NM} (r_{Mi} \times F_{Mi}) + \sum_{j=1}^{NL} (r_{Lj} \times F_{Lj}) + \sum_{k=1}^{NC} (r_{Ck} \times F_{Ck}) \qquad [4.11]$$

Where:-

M_J - is the intersegmental resultant moment at the joint centre J

and r_{Mi}, r_{Lj}, and r_{Ck} are the vectors from the joint centre to the line of action of the muscle, ligament, and articular contact point respectively.

(x - refers to the cross-product.)

There are a number of common assumptions incorporated into the rigid body model used to determine joint kinetics. The articular contact force is assumed to act through a single point only, which is the pre-selected joint centre. This makes the moment arm zero and makes its contribution to the resultant intersegmental moment zero. It is also assumed that ligament forces can be ignored, therefore the resultant intersegmental moment is assumed to be caused entirely by the muscles. As a consequence of these simplifications the resultant intersegmental moment is often called the muscle moment.

All of the preceding assumptions were made in this study with the following modification. In section 5:2.5

the joint passive visco-elasticity (JPV) was modelled. JPV is a composite term taking into account the passive moments caused by any structures crossing the joint. If the resultant joint moment is calculated and the moments caused by joint passive visco-elasticity subtracted, some of the contribution to the moment from the ligaments and joint friction will have been accounted for. This procedure was adopted in this study to calculate the muscle moments about the elbow joint.

The net effect of all the forces acting on the segment can be expressed using Newtons second axiom:-

$$m.a = F_I = F_P + F_D + F_g \qquad [4.12]$$

Where:-

m - is the mass of rigid body

a - acceleration of centre of mass of rigid body

F_I - is the inertial force

F_D - is the distal reaction force

F_P - is the proximal reaction force

and F_g is the force due to gravity acting on the segment.

The forearm, hand, and dumbell were considered to be one segment. As they were freely moving in space throughout all analysed movements there was no distal reaction force or moment.

The inertial forces were calculated as the product of the acceleration of the centre of mass in the inertial reference frame and the mass of the segment. The acceleration of the centre of mass was computed using the quintic generalised cross-validated spline described in section 3:4.5. The mass of the segment was computed from the anthropometric model. The gravitational force is the product of the mass of the segment and g (the acceleration due to gravity). F_I and F_g were computed in the inertial reference frame and then transformed into the forearm reference frame.

$$F_I = [T].m.\begin{bmatrix} X_{ACM} \\ Y_{ACM} \\ Z_{ACM} \end{bmatrix} \qquad [4.13]$$

$$F_g = [T].m\begin{bmatrix} 0 \\ 0 \\ -9.81 \end{bmatrix} \qquad [4.14]$$

Where:-

[T] - transformation matrix from inertial reference frame to member reference frame

m - is the mass of the rigid body

and X_{ACM}, Y_{ACM}, Z_{ACM} are the accelerations of the centre of mass.

The proximal force was calculated by substitution of the appropriate values in equation 4.12.

The effect of all the moments acting on the joint is given by:-

$$M_{CM} = M_D + M_P + r1.F_P + r2.F_D \quad [4.15]$$

Where:-

M_{CM} - is the moment about the centre of mass of the segment

M_P - is proximal joint moment

M_D - is the distal joint moment

and r1, r2 are the moment arms of the force vector about the centre of mass.

As the axes of the member reference frame are coincident with the principal axis of the segment the moment of force about the centre of mass can be computed using Euler's equations:-

$$M_{CMX} = I_X\dot{\omega}_X + (I_Z - I_Y).\omega_Z\omega_Y \quad [4.16a]$$

$$M_{CMY} = I_Y\dot{\omega}_Y + (I_X - I_Z).\omega_X\omega_Z \quad [4.16b]$$

$$M_{CMZ} = I_Z\dot{\omega}_Z + (I_Y - I_X).\omega_Y\omega_X \quad [4.16c]$$

Where:-

M_{CGX}, M_{CGY}, and M_{CGZ} - are the moments about the centre of mass along the axes X,Y, and Z

I_X, I_Y, I_Z - are the moments of inertia about the axes of the member reference frame

ω_X, ω_Y, ω_Z - are the angular velocities

$\dot{\omega}_X$, $\dot{\omega}_Y$, and $\dot{\omega}_Z$ are the angular accelerations.

The details of the calculations of the angular velocities and angular accelerations are given in section 3:1.4.

The resultant joint moment can then be calculated for the three axes by substitution of computed values in equation 4.15. Once these have been calculated the moments due to the joint passive visco-elasticity can be subtracted and the muscle moment acting about the joint calculated. A positive moment about the flexion-extension axis was assumed to be a flexion moment, and a negative moment about the supination-pronation axis a moment causing supination. The moments about the y axis (abduction-adduction axis) were small compared to those about the other axes, therefore they were not considered further.

4:5 EXPERIMENTAL RESULTS

This section analyses the resultant joint moments recorded for the activities studied.

4:5.1 ASSESSMENT OF ACCURACY

There was no criterion data available with which to assess to the accuracy of the estimated moments, but estimates have been made of the accuracy of the state variables and parameters used to compute these moments. Using this information it was possible to make an estimate of the errors associated with the

calculation of the resultant joint moments during the studied activities. This analysis is for trial #3 only, but the general trends reported also apply for the other trials.

The accuracy of the inertial parameters were estimated in section 4:3.3. To investigate the effect of inaccuracies in the different inertial parameter values on the estimated resultant joint moments the inertial properties of the distal system were varied by amounts comparable with their relative accuracies. This was done separately for each of the parameters and for all of them together. The changes in the estimated resultant joint moments were evaluated by computing the mean difference between the moment values calculated using the non-perturbated and the perturbated values. The standard deviation of this difference was also computed. The mass of the system and the location of the centre of mass were changed by one percent, the moments of inertia about the X and Y axes by five percent, and the moment of inertia about the Z axis by three percent. The results for this analysis are presented in table 4.13.

Both the resultant joint moments about the flexion and supination axes were fairly insensitive to inaccuracies in the inertial parameters of the distal segment. The maximum difference for the resultant moment about the flexion-extension axis was less than 1.0 N.m, and less than 0.08 N.m for the supination-pronation axis.

The effects of the accuracy of the kinematic variables used to compute the resultant joint moments were assessed. In section 3:5.4 estimates were made of the standard deviation of the noise contaminating the kinematic variables describing the position and attitude and their derivatives. The errors in the linear and angular displacement values were ignored due to their small magnitude. For each of the remaining kinematic variables used to compute the resultant joint moments one or two standard deviations of the noise was added to, or subtracted from these variables. The resultant joint moments were then calculated and the mean difference found between these and the moments computed using the non-perturbated kinematic variables. This was performed for all of the perturbated kinematic variables separately and for all of them together. To complete this analysis the effects of inaccuracies in both the inertial parameters and kinematic variables were assessed. This was done by perturbating all the inertial parameters by the amounts used previously and all the kinematic variables by one and two standard deviations. The results for this analysis are presented in table 4.14.

Comparison of tables 4.13 and 4.14 shows that the resultant joint moments were more sensitive to errors in the kinematic variables than to errors in the inertial parameters. The mean differences were small for the resultant joint moments about both the flexion-extension and supination-pronation axes. For the resultant joint moment about the flexion-extension axis the standard deviations were larger than the mean values, indicating the sensitivity of these measures to the kinematic variables. The maximum absolute difference for the one standard deviation case was 4.78 N.m, and for the two standard deviation case was 9.55 N.m. These differences occurred early during the movement.

TABLE 4.13 - The variation in the resultant joint moment when different inertial values were used for the distal rigid body (forearm, hand, and dumbell).

PARAMETER AND PERCENTAGE CHANGE	FLEXION MOMENT (N.m)		SUPINATION MOMENT (N.m)	
	MEAN DIFFERENCE	STANDARD DEVIATION	MEAN DIFFERENCE	STANDARD DEVIATION
Mass +1 %	.26	.154	-.02	.043
Mass -1 %	-.26	.154	.02	.043
Centre of mass +1 %	.32	.154	-.02	.013
Centre of mass -1 %	-.32	.154	.02	.013
Moments of inertia X and Y axes +5 %	.01	.008	.00	.014
Moments of inertia X and Y axes -5 %	-.01	.008	.00	.014
Moment of inertia Z axis +3 %	.00	.005	.00	.030
Moment of inertia Z axis - 3 %	-.00	.005	.00	.030
Mass +1 %, centre of mass +1 %, Moments of inertia X and Y +5 %, Z +3 %	.59	.309	-.04	.054
Mass +1 %, centre of Mass +1 %, Moments of inertia X and Y +5 %, Z +3 %	-.58	.306	.04	.054

TABLE 4.14 - The variation in the resultant joint moment when perturbated kinematic data and inertial parameters were used for the distal rigid body.

	FLEXION MOMENT (N.m)		SUPINATION MOMENT (N.m)	
AMOUNT ADDED TO KINEMATIC VARIABLES	MEAN DIFFERENCE	STANDARD DEVIATION	MEAN DIFFERENCE	STANDARD DEVIATION
Plus one standard deviation	-.37	3.722	-.23	.174
Minus one standard deviation	.37	3.722	.23	.174
Plus two standard deviations	-.75	7.444	-.46	.348
Minus two standard deviations	.75	7.444	0.46	.348
Plus one standard deviation and inertia values*	-.95	3.793	-.19	.187
Minus one standard deviation and inertia values*	-.21	3.522	.26	.175
Plus two standard deviation and inertia values*	-.58	.306	.04	.054
Minus two standard deviation and inertia values*	.15	7.163	.49	.343

(N.B - * the inertial parameters of the distal segment were varied as follows: mass of the system by ±1 %, the location of the centre of mass by ±1 %, the moments of inertia about the X and Y axes ±5 %, and the moment of inertia about the Z axis by ±3 %)

The resultant joint moments about the supination-pronation axis were much smaller than those about the flexion-extension axis. The standard deviations for the resultant joint moment were much smaller than the mean value for the supination-pronation axis, indicating that these moments were less sensitive to errors in the kinematic variables than the moments about the flexion-extension axis. The maximum absolute differences were 0.53 N.m for the one standard deviation case, and 1.07 N.m for the two standard deviation case.

When inaccuracies in the kinematics were combined with the anticipated inaccuracies in the inertial parameters, there were small changes in the resultant joint moments. These results serve to confirm that these moments are more sensitive to the anticipated errors in the kinematic variables than to the inaccuracies in the inertial parameters.

The joint centre of the system was selected with reference to studies of joint kinematics in the literature, see section 3:2.3. If the joint centre had been incorrectly located this could have resulted in an error in the estimated resultant joint moments. The location of the joint centre was therefore varied by 0.01 m from its pre-selected position sequentially for all three axes on the distal member reference frame. This variation of 0.01 m was greater than the errors anticipated from the three-dimensional measurement system, and so reflects the combined effects of errors in the measurement system and variations in the location of the joint centre. These variations in the location of the joint centre would be caused by incorrect initial positioning of the joint centre or by movement of the joint centre during the course of the movement away from its assumed fixed location. Small variations in the location of the joint centre and the instantaneous helical axis have been reported in the literature for the elbow joint during flexion and supination (e.g. Youm et al., 1979; Chao and Morrey, 1978). For completeness these different joint centre locations were also combined with anticipated errors in the kinematic variables and inertial parameters. The results of this analysis are presented in table 4.15.

The differences in estimated moments due to incorrect location of the joint centre were small. The maximum absolute differences were 1.44 N.m for the flexion-extension axis, and 2.53 N.m for the supination-pronation axis. When combined with anticipated errors in the inertial parameters there were small differences in the moments. When errors in the location of the joint centre were combined with errors in the kinematic variables, the differences were increased compared with the cases when only the joint centre location was changed. When the joint centre location and inertial parameters were changed the differences were comparable with the differences for the case when only the kinematic variables were changed. This demonstrates that the moments estimated in this study were most sensitive to inaccuracies in the kinematic variables. Increased differences may have arisen if the joint centre location had been varied by different amounts throughout the movement.

4:5.2 COMPARISON OF TRIALS

The resultant joint moments were calculated for three of the trials: a single dumbell curl with the maximum load the subject could curl (17.5 kg), trial #2; the first repetition of five consecutive curls with 15 kg, trial #3; and a single dumbell curl with a 15 kg dumbell at maximum speed, trial #4. The resultant joint moments

TABLE 4.15 - The variation in the resultant joint moment when joint centre location was varied; in addition perturbated kinematic data and inertial parameters were used for the distal rigid body.

	FLEXION MOMENT (N.m)		SUPINATION MOMENT (N.m)	
CHANGE IN JOINT CENTRE LOCATION*	MEAN DIFFERENCE	STANDARD DEVIATION	MEAN DIFFERENCE	STANDARD DEVIATION
Moved +0.01 m along X axis	.00	.000	-.41	1.045
Moved -0.01m along X axis	.00	.000	.24	.950
Moved +0.01 m along Y axis	.04	.055	.04	.889
Moved -0.01m along Y axis	-.02	.043	-.12	.915
Moved +0.01 m along Z axis	-.82	.484	.00	.000
Moved -0.01m along Z axis	.82	.484	.00	.000
Moved +0.01 m along X,Y, and Z axes	-.78	.440	-.41	1.340
Moved -0.01m along X,Y, and Z axes	.81	.457	.07	1.274
Moved +0.01 m along X,Y, and Z axes, plus inertial values	-.20	.146	-.46	1.369
Moved -0.01 m along X,Y, and Z axes, minus inertial values	.81	.457	.27	1.326
Moved +0.01 m along X,Y, and Z axes, and plus one s.d. of kinematic errors	-1.14	3.780	-.71	1.520
Moved +0.01 m along X,Y, and Z axes, and minus one s.d. of kinematic errors	.59	3.788	.07	1.274
Moved +0.01 m along X,Y, and Z axes, plus positive kinematic and inertial values errors	-.57	3.698	-.77	1.548
Moved +0.01 m along X,Y,and Z axes, plus negative kinematic and inertial values errors	.59	3.788	.27	.1326

(N.B. - * movements in joint centre were made along the member reference frame for the distal segment.)

were used as inputs to the models described in the next two chapters. These moments are shown in figures 4.3 and 4.4. A brief description of the moments follows.

The flexion moments were all non-zero at the start of the activity. This was because the subject had to support the dumbell. Analysis of the orientation of the forearm also shows that the arm was partially flexed before the curl actually started. All sequences were analysed until the subject started to lower the dumbell again, therefore the final part of each curve passes through zero and becomes an extension moment. The zero moment occurs at the point of maximum flexion during the curl. The absolute maximum flexion moment was 46.24 N.m, 48.24 N.m, and 44.78 N.m for the fast curl, the maximum curl, and the first repetition of five curls respectively. The maximum curl may not have been truly the maximum because the dumbells were available in increments of 2.5 kg only. The subject was not capable of 20 kg but may have been able to curl some intermediate weight. The fast repetition, trial #4, was only just faster than the first repetition of five with the same weight, trial #3.

The supination moments from all of these trials showed a rapid change after around a quarter of a second. This change can be explained because it is around this time that the dumbell moves clear of the body. If too large an amount of supination occurred before this time the path of the dumbell would be obstructed by the body, unless the arm is abducted from the body which did not happen in any of these trials. Once the dumbell had moved clear of the body there was a rapid supination of the forearm which explains the rapid change in the supination moment. If the dumbell was held in a fully supinated position throughout the curl, during the top range of the movement the path of the dumbell would again be obstructed by the body, which explains why before full flexion there was a pronatory moment as the dumbell was rotated in order to allow full flexion.

4:5.3 SUMMARY

The preceding sections reported the results of a sensitivity analysis of the resultant joint moments at the elbow joint during dumbell curls. These moments were most sensitive to the kinematic variables used to compute them, and were least sensitive to errors in the joint centre location and inertial parameters of the forearm and hand. These moments are used in the next two chapters to examine the individual muscle forces during these dumbell curls.

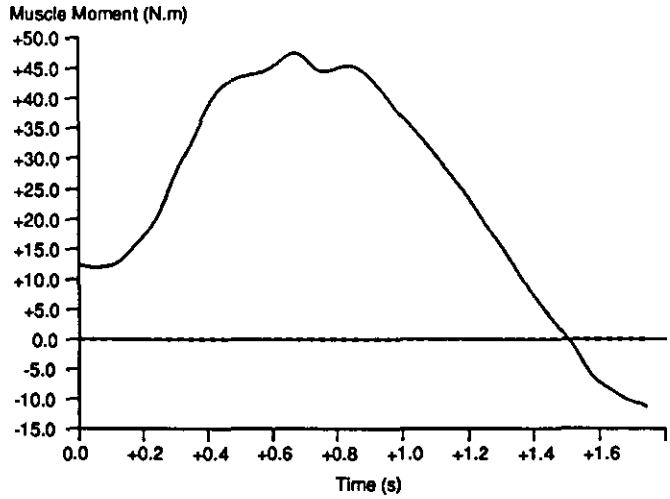

FIGURE 4.3a - The muscle moment for trial #2 (maximum repetition).

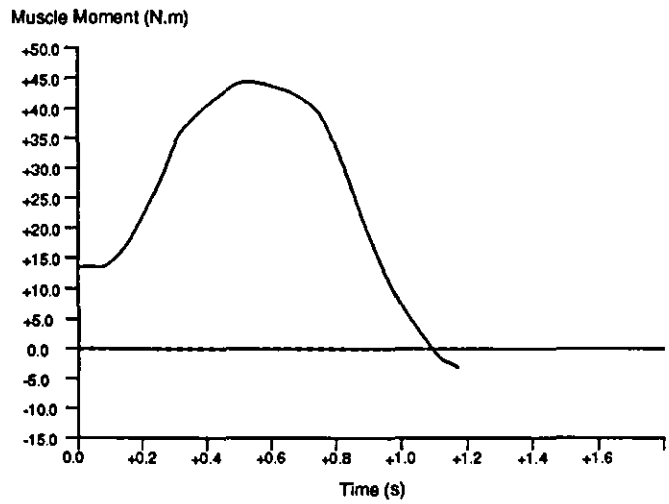

FIGURE 4.3b - The muscle moment for trial #3 (first of five repetitions).

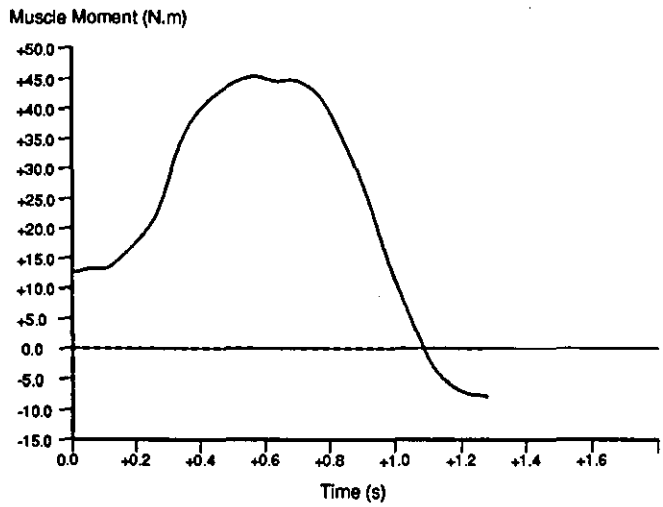

FIGURE 4.3c - The muscle moment for trial #4 (fast repetition).

(N.B. - For all these trials a positive moment indicates flexion, a negative one extension.)

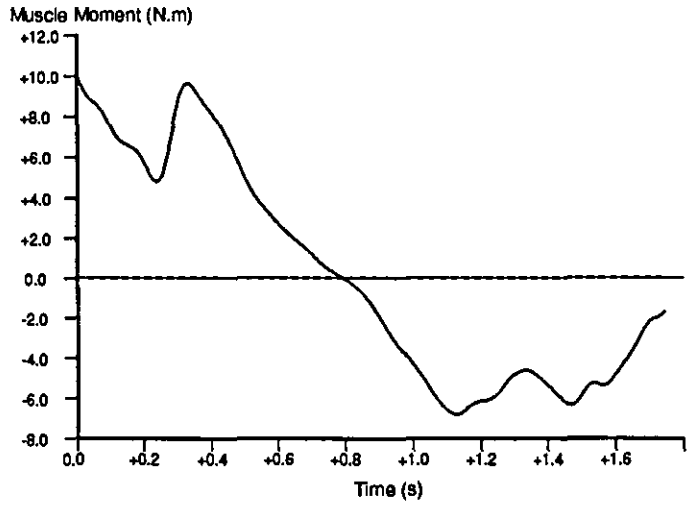

FIGURE 4.4a - The muscle moment for trial #2 (maximum repetition).

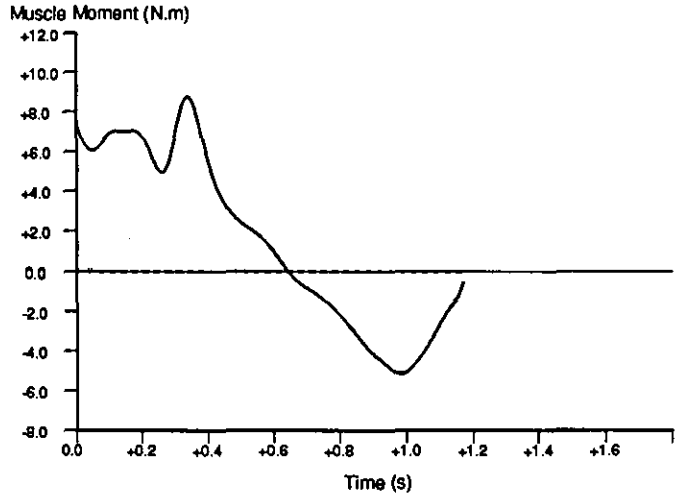

FIGURE 4.4b - The muscle moment for trial #3 (first of five repetitions).

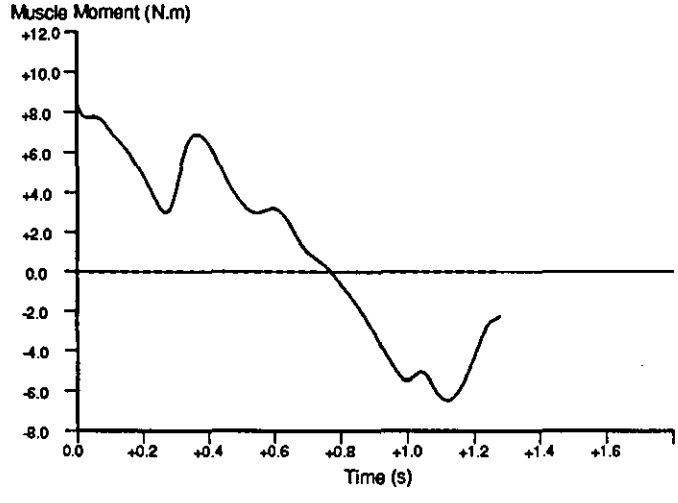

FIGURE 4.4c - The muscle moment for trial #4 (fast repetition).

(N.B. - For all these trials a positive moment indicates supination, a negative one pronation.)

CHAPTER V

MODELLING THE MUSCLES

INTRODUCTION

The purpose of this chapter is to present the model used to represent the muscles causing elbow flexion. The chapter is divided into six parts each dealing with some aspect of muscle modelling. The property to be modelled is first reviewed then modelling approaches are discussed before a model is adopted. The procedures for the determination and validation of the model parameters are also detailed.

5:1 MUSCLE ARCHITECTURE

The following sections give details of muscle architecture. For the model of muscle developed in this study, the relevant aspects of muscle architecture were considered to be: the positions of the origins and insertions, the lines of action, the moment arms, and the angles of pennation of the muscles. Muscle lengths and moment arms are required as inputs for the optimization procedures discussed in Chapter VI; the methodologies used to compute these state variables are given in the following sections.

5:1.1 THE MUSCLES

The three muscles included in the model are the biceps, brachialis, and brachioradialis. Although there are other muscles crossing the elbow joint that may contribute to flexion of the elbow joint and rotation of the forearm, these muscles were ignored. This simplification has previously been made by other researchers (e.g. Wilkie, 1950; Yeo, 1976; Crowninshield and Brand, 1981; and An, Kaufman, and Chao, 1989). This assumption is supported by the research of An, Hui, Morrey, Linscheid, and Chao (1981). They examined four cadavers and measured the muscle moment arms at a variety of joint configurations. They also calculated the cross-sectional area of the muscles crossing the elbow joint. The product of the moment arm of the muscle and its cross-sectional area was used as an indicator of each muscle's contribution to joint moment. The results of their analysis showed that the biceps, brachialis, and brachioradialis were the major flexors of the elbow joint. Figure 5.1 is a diagram of the origins and insertions of the three muscles, and includes the approximate lines of action of the muscles.

The biceps has two heads which join together as they approach the elbow. The long head originates from the supra-glenoid tubercle of the scapula, and runs along the bicipital groove of the humerus. The short head originates from the coracoid process of the scapula. The long head lies on the lateral side of the short head. The distal tendon of the biceps inserts onto the posterior edge of the radial tuberosity. Although the biceps commonly has two heads, Amis (1978) in his analysis of four cadavers found a third head present in one of the cadavers. The physiological cross-sectional area of this muscle was only 10 percent of the total physiological cross-sectional area of the whole bicep. Greig, Anson, and Budinger (1952) found 28 out of 130 limbs investigated had a third head.

The brachialis lies beneath the biceps, and has a broad origin on the lower two thirds of the anterior surface of the humerus. The muscle passes over the anterior surface of the elbow joint. It converges and

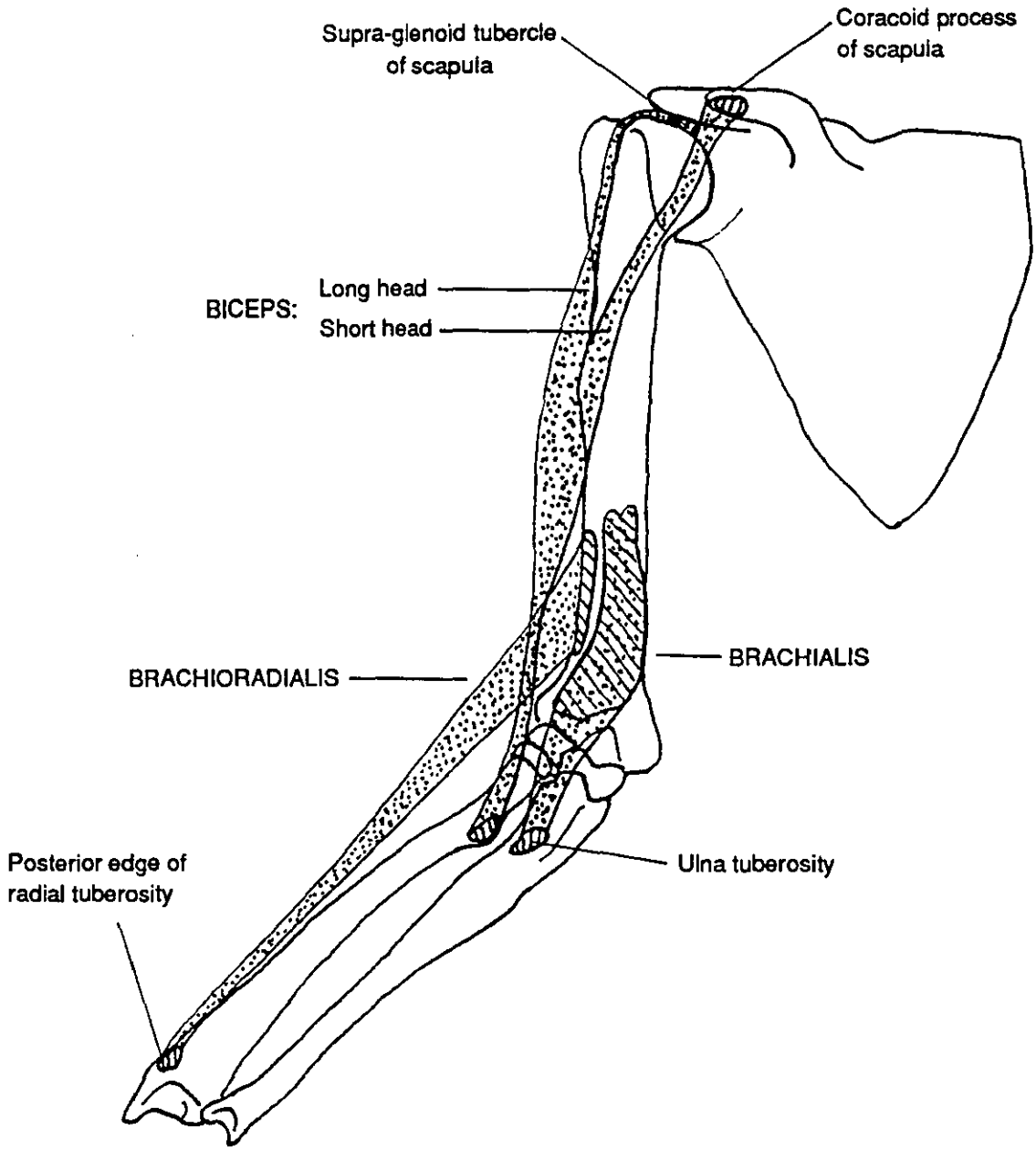

FIGURE 5.1 - Medial view of right arm, showing origins, insertions, and approximate lines of action of the biceps, brachialis, and brachioradialis.

inserts onto the ulnar tuberosity and coronoid process.

The brachioradialis has its origin on the proximal two thirds of the lateral supracondylar ridge. After passing over the capitulum it passes on the lateral surface of the radius to insert onto the radius distally near the styloid process.

The positions of the origins and insertions of the muscles of interest on the subject were determined using osteometric scaling.

5:1.2 OSTEOMETRIC SCALING

Osteometric scaling is the extrapolation from dry bone specimen landmarks to another specimen, normally a live subject. The locations of the origins and insertions of muscles and ligaments are often inaccessible on a live subject. This information can be obtained from the results of cadaver dissection. Direct application of these data to a live subject is inappropriate as demonstrated by the analysis of Lew and Lewis (1977) on human femurs and tibias. Therefore some form of scaling is appropriate as the physical dimensions of the bones of the cadaver and the subject are likely to be different. Osteometric scaling attempts to circumvent these problems.

The following procedures have been adopted for using cadaver data for a live subject:-

1. No scaling - some researchers have adopted data from cadavers or dry bone specimens with no scaling allowance for the differences in geometry between subjects e.g. Amis, Prochazka, Short, Trend and Ward (1987).
2. Uniform scaling - where all the dimensions of the bone are scaled in the same proportions e.g. Crowninshield and Pope (1975).
3. Homogeneous Scaling - scaling along prescribed principal axes, these being placed along the critical dimensions of the bone of interest. For example Morrison (1970) used this procedure for the tibia and femur: the axes were defined relative to the important dimensions of the tibia and femur (e.g. condylar width and depth, bone length). Lew and Lewis (1977) scaled along principal axes, as did Sommer, Miller, and Pijanowski (1982). Homogeneous scaling is at best only an approximation to the variations in the shapes of bones, between specimens and subjects.
4. Non-homogeneous scaling - scaling is performed along arbitrary axes, as opposed to the predefined axes used to define the bone. Lewis, Lew, and Zimmerman (1980) suggested a scaling method involving non-homogeneous scaling based on finite-element principles.

The homogeneous transformation technique of Lew and Lewis (1977) incorporates a uniform stretch of differing amounts along three mutually orthogonal axes. The transformation matrix is derived from the three-dimensional coordinates of four landmarks on both a dry bone specimen, and the same four landmarks on the subject. They compared their technique with the scaling technique of Morrison (1970), and with no scaling, on human tibias and femurs. Their technique and the scaling procedure of Morrison (1970) were more accurate than no scaling. They used this technique to estimate in vivo ligament lengths in the human knee (Lew and Lewis, 1978). There is no account taken in their technique of the errors in

the measured positions of landmarks on either the specimen or subject.

The non-homogeneous scaling technique of Lewis et al. (1980) is based on finite element principles, where either four landmarks are modelled as a tetrahedron, or eight landmarks as a hexahedron. Only the eight noded hexahedron permits non-homogeneous scaling. In an analysis of two human femurs the non-homogeneous scaling was more accurate than the homogeneous scaling. Unfortunately in the analysis of human subjects it is very hard to locate eight bony landmarks so that a non-homogeneous transformation can be undertaken, this reduces the general applicability of this technique. As with the homogeneous scaling of Lew and Lewis (1977) there was no attempt in their technique to account for errors in locating the bony landmarks.

The homogeneous scaling technique of Sommer et al. (1982) incorporates a mirror transformation which allows a right hand specimen to be scaled to the left hand side of a subject. As the measured locations of points on both the specimen and subject will contain some errors, a linear least squares technique is employed to reduce the effect of these errors.

These osteometric scaling techniques are of use when examining the kinematics of muscle, but there is a general lack of data. There are two major sources for the lower limb. Brand, Crowninshield, Wittstock, Pedersen, Clark, and van Krieken (1982) provided data of the averaged scaled locations of the origins and insertions of 47 muscles from the dissection of three cadavers (six lower limbs). White, Yack, and Winter (1989) also provided data suitable for osteometric scaling for 40 muscles of the lower limb. To date no such data are available for the upper limb.

5:1.3 PROCEDURE FOR DETERMINING ORIGINS AND INSERTIONS

In this study it was not possible to identify enough bony landmarks on the subject to permit use of the non-homogeneous scaling technique of Lewis et al. (1980), therefore a homogeneous scaling technique was used. As the homogeneous scaling technique of Sommer et al. (1982) uses a least squares formulation to account for errors in the locations of the identified landmarks, this technique was used. The transformation matrix incorporates:-

1. A three-dimensional rigid body translation.
2. A three-dimensional rigid body rotation.
3. Some form of size adjustment.

The first two transformations result in alignment and orientation of the specimen limb onto the subjects, whilst the scaling either stretches or compresses the relevant dimensions. The product of this transformation matrix and the location of the points measured on the specimen gives the estimated position of these points on the subject.

To determine the positions of the origins and insertions, measurements were made of a dry bone specimen approximately matched for size with the experimental subject. The measurements were taken using the same experimental protocol as described for the static data capture which was able to locate points with a RMS error of 2.3 mm, which compares favourably with the RMS error reported by White et al.

(1989) of 2 mm for a three-dimensional anthropometer. On the dry bone specimen a humeral and a forearm reference frame were defined, using four bony landmarks for each reference frame. Humeral and forearm reference frames were defined on the subject with reference to the same four bony landmarks. The centroid of the muscles' origins and insertions were marked on the specimen. For the biceps both heads were considered to originate from the top of the bicipital groove. Using the technique of Sommer et al. (1982) transformation matrices were formed relating the humeral reference frame of the specimen to the humeral reference frame of the subject, and forearm reference frame of the specimen to the forearm reference frame of the subject. The positions of the origins and insertions on the specimen were multiplied by the appropriate transformation matrix which scaled and mapped them onto the subject. The locations of the origins and insertions of the muscles were now known on the subject.

There are a number of errors associated with such measurements. There will be errors in the location of these points as a direct consequence of errors in the measuring device, and difficulties in locating the points. The latter may be particularly difficult on the subject where the landmark is covered by skin, especially as it may be necessary to use landmarks which are covered by muscle and other tissues. Finally errors may arise from the assumption that geometric differences between specimens can be accounted for by homogeneous scaling, although Lew and Lewis (1978) have shown that these errors may not be too great. To assess the errors in locating the points on the skeleton in this study, all points on the skeleton were digitized twice, on two separate days. The RMS difference between the two digitizations gave an indication of the precision of the location of origins and insertions. The mean RMS difference for all three axes was 3.5 mm. As the system could only locate points with a RMS difference of 2.3 mm this was accepted as reasonable precision.

5:1.4 LINES OF ACTION

There are two common approaches for modelling the line of action of muscles. These are the straight line model and the centroid line model. With the straight line modelling approach an approximate origin and insertion are identified on the appropriate body segments between which a straight line is considered to be the line of action of the muscle. Therefore any force as a consequence of the modelled muscle is along the line of this model.

Researchers may use various assumptions for their particular problem. Muscles with broad attachments (e.g. brachioradialis in Yeo, 1976) are simplified to one central point. Dostal and Andrews (1981) in their model of hip musculature "re-attached" muscles as was appropriate for their study e.g. the bicep femoris which inserts on to the head of the fibula and lateral head of tibia, was considered attached to the femoral condyles. Such a "re-attachment" is only performed once the effects of the line of action of the muscle have been considered.

In the centroid line model the line of action of the muscle is considered to be the line defined by the locus of the centre of the transverse cross-section of the muscle. It was originally proposed by Jensen and Davy (1975). This technique allows for the curvature of the muscle's line of action. Therefore the force transmitted by the muscle is at a tangent to the curve joining the centroids of the consecutive cross-

sections. Jensen and Davy (1975) compared moment arms calculated using the centroid model with those calculated with a straight line model. For the muscles crossing the hip they found that moment arms differed from one to 12 percent between the two representations of the muscles' lines of action.

One of the major drawbacks of the centroid line model is that it requires a lot of data collection and processing to derive the required information. At present this information is only available for a few muscles, as a consequence of cadaver studies (e.g. Jensen and Metcalf, 1975). The technique requires sectioning of the muscles, therefore the centroid path for one muscle can only be calculated for one joint configuration per specimen, although some researchers have estimated the centroid by taking appropriate measures around the outside of the muscle under examination (e.g. Amis, Dowson, and Wright, 1979). It is also questionable how applicable such information is to different subjects as between subject variations in muscle cross sectional area may change the centroid line of the muscle. If the muscle is not fusiform the cross-section may be oblique to the fibre length and the centroid will not be the same as the line of action of the muscle. When the muscle is under tension in vivo the centroid line model may not represent a muscle in such a state as well as the straight line model. If the muscle's line of action is moved due to the motion of the joint or other muscles, a straight line model could be adjusted to allow for changes more easily than the centroid model. With increased availability of imaging techniques many of the drawbacks of the centroid line model may be obviated.

5:1.5 PROCEDURE FOR DETERMINING MUSCLE LENGTH

There is not enough information currently available in the literature to use a centroid line model of the muscles in this study, nor was it feasible to generate such data. Therefore a straight line model was used. From the osteometric scaling the positions of the origins and insertions of the muscles were known.

During the activity, given three non-collinear landmarks on the upper arm and three on the forearm the corresponding reference frames could be calculated using the technique described in section 3:1.3. To compute the Cardan angles (section 3:1.4) it was necessary to compute the orientation matrix which transformed points from the humeral reference frame to the forearm reference frame. Origins of the muscles were defined in the humeral reference frame, and the insertions were defined in the forearm reference frame. As the locations of the insertions were known in the forearm reference frame, it was necessary to transform these points onto the humeral reference frame, so all points were known in the same reference frame. This transformation was performed using the transpose of the matrix used for computing the Cardan angles. A line could then be defined between the origin and insertion of the muscle, the length of this line giving the length of the muscle at that moment.

The true origin of the biceps is on the scapula. This means that it is possible that movement of the shoulder will influence the length of this muscle. During the activity studied the humerus did not move significantly. Therefore changes in length of the biceps due to movement of the shoulder joint were minimised, and so ignored in the calculation of the length of this muscle.

5:1.6 MUSCLE MOMENT ARMS

Moment arm data can be derived from a number of sources:-

1. Direct measures - where the measures are taken from the experimental subject for example using X-rays (e.g. Smidt, 1973), or another imaging technique.

2. Cadaver measures - where moment arms are measured on cadavers. These techniques either employ the centroid method for estimating the line of action of the muscle (e.g. An et al., 1981), or the straight line model (e.g. Edgerton, Roy, and Apor, 1986) .

3. Geometric models - where the moment arm of the muscle is described using a geometric relationship between joint angle and the moment arm of the muscle (e.g. Wilkie, 1950).

4. Dry bone models - measurements are made on a dry bone specimen, and then extrapolated to an experimental subject. Dostal and Andrews (1981) measured the moment arms of muscles using "string" running between the origins and insertions of a dry bone specimen. Alternatively the origins and insertions of the muscles are identified on a dry bone specimen and extrapolated to an experimental subject, and the moment arms are estimated by assuming that the muscles run in a straight lines from their origins to their insertions (e.g. Pierrynowski and Morrison, 1985b).

Crowninshield and Brand (1981) obtained moment arm information for the three major elbow flexors using X-rays. This information was not generally applicable as it was for one joint configuration only.

Amis et al. (1979) calculated the moment arms of the muscles crossing the elbow joint about a flexion-extension axis for one embalmed cadaver. The centroid technique of Jensen and Davy (1975) was used but rather than taking a cross-section this was estimated by taking the appropriate measures around the outside of the muscle under examination. Joining the centroids gave the line of action of each muscle, which were then used to calculate the moment arms of the muscles. This technique permitted one cadaver limb to be used for more than one joint configuration. In this analysis the moment arms of the biceps, brachialis, and brachioradialis remained constant up to 35 degrees of flexion, after which angle they changed with increasing angle of flexion.

An et al. (1981) examined four cadavers to determine the moment arms of the muscles crossing the elbow joint about a flexion-extension axis, and a supination-pronation axis. They used the centroid method of Jensen and Davy (1975). Their results were compared with other studies and they concluded that the direct measurement of moment arms on cadavers and use of the centroid method gave comparable results. Their results showed that longitudinal rotation of the forearm changes the moment arm of the muscles about the flexion-extension axis when the angle of flexion remains constant.

Cadaver based studies have to assume that measurements made on the cadaver reflect what happens in a live subject. This assumption may be invalid. If the muscle is active its path may be changed due to tension in the muscles, movement of other muscles, or joint movement. In cadaver studies it is difficult to allow for these eventualities.

Both Wilkie (1950) and van Zuylen, van Velzen, and Denier van der Gon (1988) have presented models

which permit the calculation of the moment arms of the elbow flexors. The upper arm and forearm were modelled as straight lines with their intersection at the elbow joint centre. The angle between these two lines is the amount of flexion at the elbow joint. To determine the muscle moment arms the distances of the origins and insertions from the elbow joint centre are required. Assuming that muscles work in straight lines muscle moment arms can be calculated using the Cosine Rule, at any elbow joint angle. Van Zuylen et al. (1988) presented a similar model to Wilkie but the muscles were not assumed to attach directly onto the upper arm and forearm axes. They presented data for the biceps, brachialis, and brachioradialis. Only the brachioradialis did not attach directly onto either axis. To compare the two models the data from van Zuylen et al. (1988) for the brachioradialis were used as inputs to both models. Both models assume that the forearm does not rotate about its longitudinal axis during flexion. A graph of the results is shown in figure 5.2. The graph shows that the refinement of van Zuylen et al. (1988) makes very little difference to the moment arm values when compared with the model of Wilkie (1950).

Examination of the graph shows that both models predict a moment arm of zero for a fully extended arm; the results of cadaver studies show that this is not the case (Amis et al., 1979; An et al., 1981). The models of Wilkie (1950), and van Zuylen et al. (1988), and the data of Braune and Fischer (1889) suggest that as a result of flexion the moment arm of the brachioradialis follows a parabolic path, whereas the data of Amis et al. (1979) suggests that it is linear. This difference may be because Amis et al. (1979) used the centroid method for determining the line of action of the muscles, whereas in the other cases a straight line model was used.

Brand et al. (1982) examined the influence of incorrect location of the origins and insertions of muscles on the moment arms of 47 muscles of the lower limb. The true locations of the origins and insertions were perturbated by ±10 mm separately in the three coordinate directions. They reported that the errors in the moment arm estimations after these perturbations were "generally less that 10 percent".

In vivo moment arms have been measured using a variety of techniques. Smidt (1973) used X-ray analysis to measure the moment arms of muscles crossing the knee. He calculated the centre of rotation of the knee joint using a graphical technique. Nemeth and Ohlsen (1985) used computer-aided tomography (CT) to calculate the moment arms for the hip flexors and extensors. Rugg, Gregor, Mandelbaum, and Chiu (1990) used magnetic resonance imaging (MRI) to compute the moment arms of the triceps surae and the tibialis anterior about the ankle joint They also compared the moment arm calculations when the centre of rotation was either assumed fixed centre or moving; the moving centre of rotation was calculated using the technique of Reuleaux (1875). The moment arm of the triceps surae tendon was found to be an average of 3.1 percent greater using a fixed centre of rotation than it was using the moving centre of rotation. The difference for the tibialis anterior was 2.5 percent. These in vivo studies also have the advantage that the muscles can be under tension when the measurements are taken.

5:1.7 PROCEDURE FOR DETERMINING MOMENT ARMS

To determine the length of the muscle it was necessary to define a line representing the line of action of

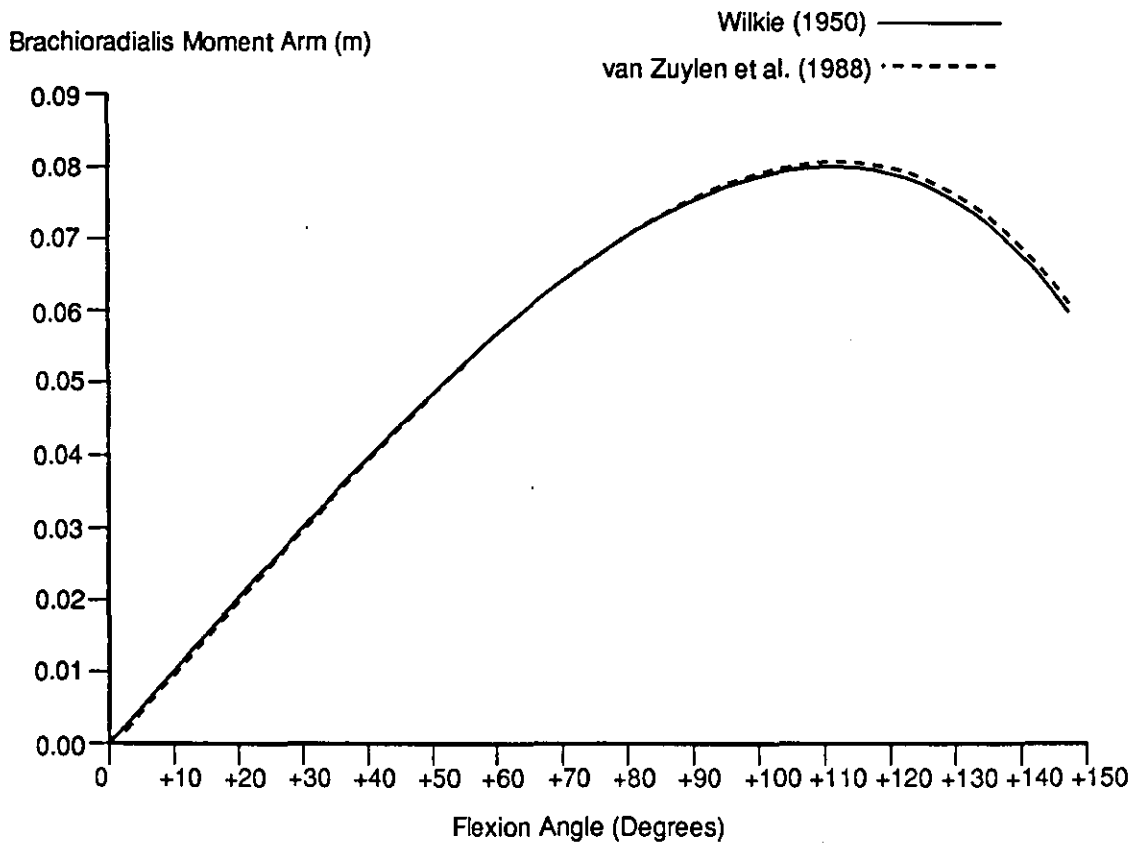

FIGURE 5.2 - The moment arm of the brachioradialis using the models of Wilkie (1950), and van Zuylen et al. (1988).

the muscle. The moment arm is the shortest distance from the muscle line of action to the centre of rotation of the joint. The procedure for calculating the lines of action of the muscles was given in section 5:1.5, given this information three-dimensional geometry gave the moment arms of the muscles. The joint centre was assumed fixed. Amis (1978) and An et al. (1981) showed that at zero degrees flexion the moment arms of the biceps, brachialis, and brachioradialis were not zero. To account for these variations when the straight line actually passed through the trochlea, a constant value was assigned to the flexion moment arm up to 35 degrees of flexion. This data was derived from the earlier scaling of the data and was assumed to be half of the breadth of the trochlea.

5:1.8 MUSCLE PENNATION

To examine the effect of muscle pennation researchers have modelled the pennated muscle using simple geometry. In modelling pennated muscle it is assumed that muscle volume during contraction remains constant, and the thickness of the muscle remains constant. Authors using these assumptions include Alexander (1968), Woittiez, Huijing, Boom, and Rozendal (1984), Pierrynowski and Morrison (1985b), and Otten (1988). There is limited evidence to support the assumption of constant volume. Baskin and Paolini (1967) examined the volume changes in the frog gastrocnemius and found that there was only a 0.03 percent change in volume as a result of a twitch. Figure 5.3 is a schematic diagram of pennated muscle. For this model if volume remains constant then thickness must remain constant (i.e. - the distance between the planes of the insertion remains constant). A model of pennated muscle architecture is now developed and this assumption examined:-

$$T = L_F . \mathrm{Sin}(\theta) \qquad [5.1]$$

Where:-

T - is the thickness of the muscle

L_F - is the length of the muscle fibres

and θ is the angle of pennation.

$$\text{Volume} = V = T.L_{TS}.W \qquad [5.2]$$

Where:-

L_{TS} - is the length of the tendon sheet (see figure 5.3)

and W is the width of the muscle.

At rest:-

$$V_R = T_R.L_{TS}.W = L_{FR}.\mathrm{Sin}(\theta_r).L_{TS}.W \qquad [5.3]$$

Where:-

T_R - is the thickness of the muscle at rest

L_{FR} - is the length of the muscle fibres at rest

and θ_r is the angle of pennation at rest.

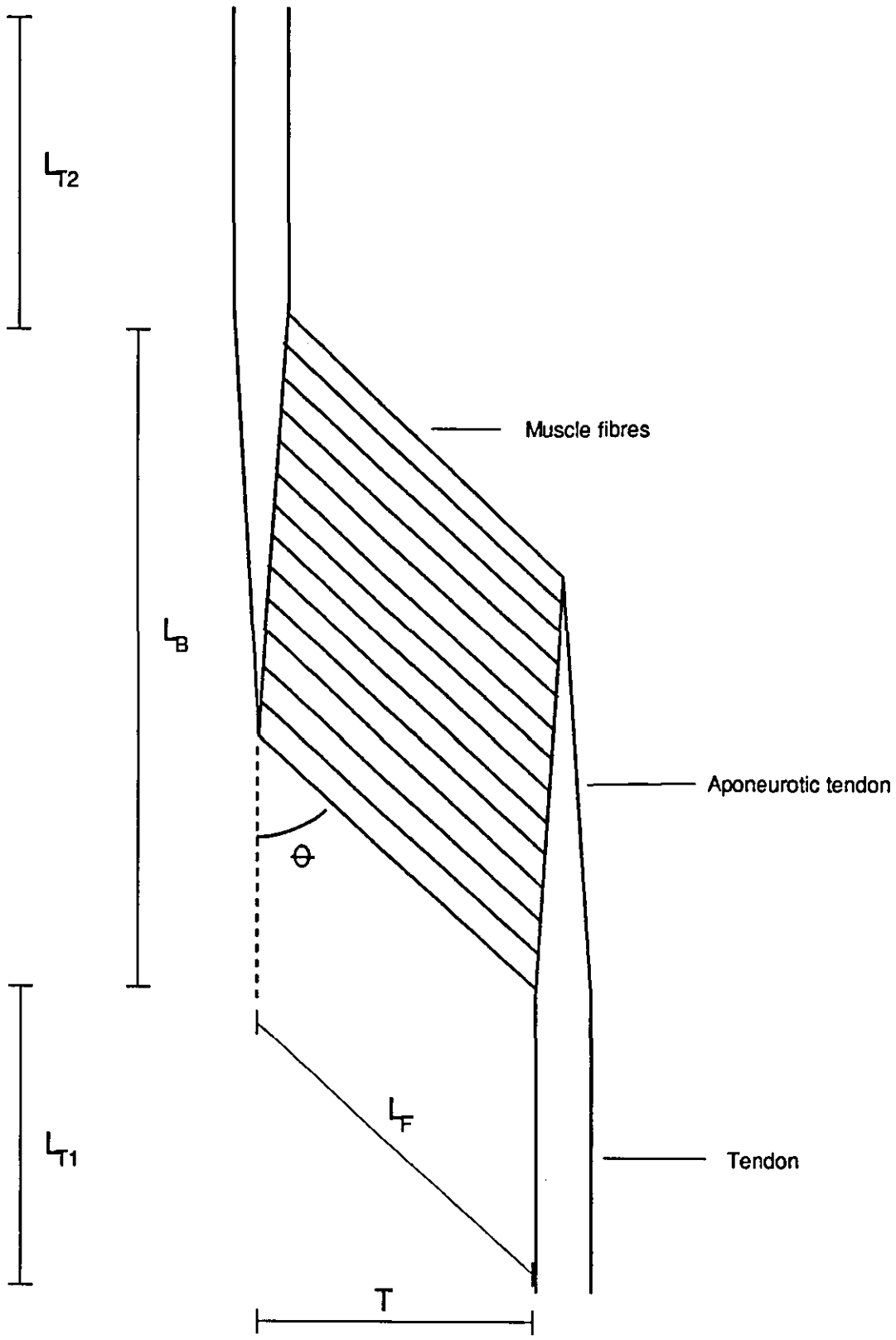

FIGURE 5.3 - Diagram of a pennate muscle, where θ is the angle of pennation. (See text for explanation of other abbreviations.)

During a contraction:-

$$V = T.L_{TS}.W \qquad [5.4]$$
$$= L_F.Sin(\theta).L_{TS}.W$$

The assumption is that the volume remains constant therefore:-

$$V = V_R \qquad [5.5]$$

Which implies:-

$$L_{FR}.Sin(\theta_r).L_{TS}.W = L_F.Sin(\theta).L_{TS}.W \qquad [5.6]$$

Dividing by $L_{TS}.W$ gives:-

$$L_{FR}.Sin(\theta_r) = L_F.Sin(\theta) \qquad [5.7]$$

Which shows that if volume is assumed to remain constant so must muscle thickness.

Using a model based on the assumptions it is simple to make adjustments to allow for the force in the tendon being different from the muscle force. For parallel fibred muscles:-

$$F_T = F_M \qquad [5.8]$$

Where:-

F_T - is the force in the tendon

and F_M is the force produced by the muscle fibres.

For pennated muscles:-

$$F_T = F_M.\ Cos(\theta) \qquad [5.9]$$

The short head of the biceps is the only pennated muscle in the model of the flexors causing forearm flexion (see section 5:4.1.3). At rest with an angle of pennation of 3.3 degrees, the influence of muscle pennation is not significant ($\cos(3.3) = 0.998$), but as the muscle contracts the angle of pennation will increase and its influence may be more significant. The effect of a change in angle of pennation can be investigated using the following calculations:-

At rest:-

$$L_{TA} = L_{BR} - [\ Cos(\theta_r)\ .\ L_{FR}\ ] \qquad [5.10]$$

Where:-

L_{BR} is the length of the belly of the muscle at rest.

If as the muscle contracts the length of the muscle belly (L_B) is known then:-

$$L_B = L_{TA} + [\,\mathrm{Cos}(\theta).L_F\,] \qquad [5.11]$$

$$L_B - L_{TA} = \mathrm{Cos}(\theta).L_F = T.\,\mathrm{Cos}(\theta).(\mathrm{Sin}(\theta))^{-1} \qquad [5.12]$$

$$\mathrm{Cos}(\theta).(\mathrm{Sin}(\theta))^{-1} = (\,\mathrm{Tan}(\theta)\,)^{-1} \qquad [5.13]$$

Therefore:-

$$\mathrm{Tan}(\theta) = \frac{T}{(L_B - L_{TA})} \qquad [5.14]$$

Using mean data of the four cadavers analysed in Amis (1978):-

θ_r = 3.3 degrees

L_{FR} = 164.8 mm

T = 9.5 mm

The length of the muscle belly at rest is not known but substitution of equation 8 into equation 12 after suitable re-arrangement gives:-

$$\frac{T}{\mathrm{Tan}(\theta)} - (\,\mathrm{Cos}(\theta_r)\,.\,L_{FR}\,) = L_B - L_{BR} \qquad [5.15]$$

The right hand side remains unknown, but if the angle of pennation is assumed to increase to eight degrees, then the change in length of the belly of the short head of the biceps would be 96.9 mm. Although the length of the belly of the muscle was unknown in this example, if it is assumed to be around 180 mm, this represents a 50 percent reduction in the length of the belly which is beyond the expected maximum reduction resulting from full elbow flexion. Therefore as cos(8) = 0.990, it is still reasonable to ignore the influence of muscle pennation on the length of the muscle fibres in the short head of the biceps.

The tendinous sheet will stretch as a result of the force from the fibres, causing the fibres to curve to maintain constant volume. Otten (1988) modelled the stretching of the tendinous sheets and consequential curving of the fibres. He found that these two factors had no influence on the force-length curve of the muscle tendon complex.

5:1.9 SUMMARY

In the preceding sections the bones and muscles which are modelled have been described. The techniques used to determine the lengths and moment arms of the muscles causing elbow flexion have been presented. The influence of pennation of muscle fibres has been examined, and its influence on the present model assessed and shown to be negligible.

5:2 MUSCLE MECHANICS

The purpose of this section is to detail the mechanical properties of skeletal muscle. In this context muscle is considered to include the tendon and the muscle fibres. These properties are reviewed, then modelling approaches discussed, before a model is adopted for this work.

5:2.1 MUSCLE MODELS

There are two types of muscle model: those which are mechanical analogues of muscle, which are phenomenological in nature, and those which model events at a microscopic level such as the kinetic model of Huxley (1957).

Most mechanical models consist of a series elastic component (SEC), a contractile component, and sometimes a parallel elastic component (PEC). Hill (1938) presented one of the earliest models which consisted of an elastic component in series with a contractile component, with an elastic component parallel to these components, see figure 5.4c. There are two possible arrangements for the three component model; these are shown in figure 5.4. The work of Jewell and Wilkie (1958) showed that both of these model types (figure 5.4b, and 5,4c) describe the mechanical behaviour of muscle well. Others have used the simpler two component model of muscle (e.g. Bobbert, Huijing, and van Ingen Schenau, 1986). The sites of the SEC, PEC, and contractile component will be discussed in later sections. A Hill type mechanical model was used in this study.

In 1957 Huxley suggested a kinetic model of muscle which attempted to predict the mechanics and energetics of muscle by considering the chemical interactions of the actin, and myosin cross-bridges. The model was based on the acceptance of the sliding-filament theory of muscular contraction (Pollack, 1983). The model assumed that the cross-bridges could exist in two biochemical states, either attached or detached. There have been many revised models based on this original model. Huxley and Simmons (1971b) extended the 1957 model to account for tension transients when the cross-bridges remain attached, by considering changes in the cross-bridge structure while the bridges are being formed. Hill, Eisenberg, Chen, and Podolsky (1975) presented a detailed mathematical model which combined the details of Huxley's 1957 model with the 1971 revisions. Their treatment demonstrated that Huxley's 1957 model was incomplete thermodynamically as it did not take account of the relationship between the bonding rates of the cross-bridges, the stiffness of the cross-bridges, and the energy associated with certain biochemical states. Their formulation of this two-state model took account of the thermodynamic deficiencies of Huxley's model; it was called the "self-consistent two-state model". Eisenberg, Hill, and Chen (1980) extended this model to allow for four cross-bridge states, two attached, and two detached. The detached states were considered to occur the moment just after detachment, and just before re-attachment. The attached states corresponded to the states in the model of Huxley and Simmons (1971b).

These models do not include the properties of tendon, or allow for the passive visco-elasticity of the muscle. Such models provide a theoretical framework for considering the actual mechanisms underlying muscle action and have explained many of the observed phenomena of muscle action (Huxley, 1980).

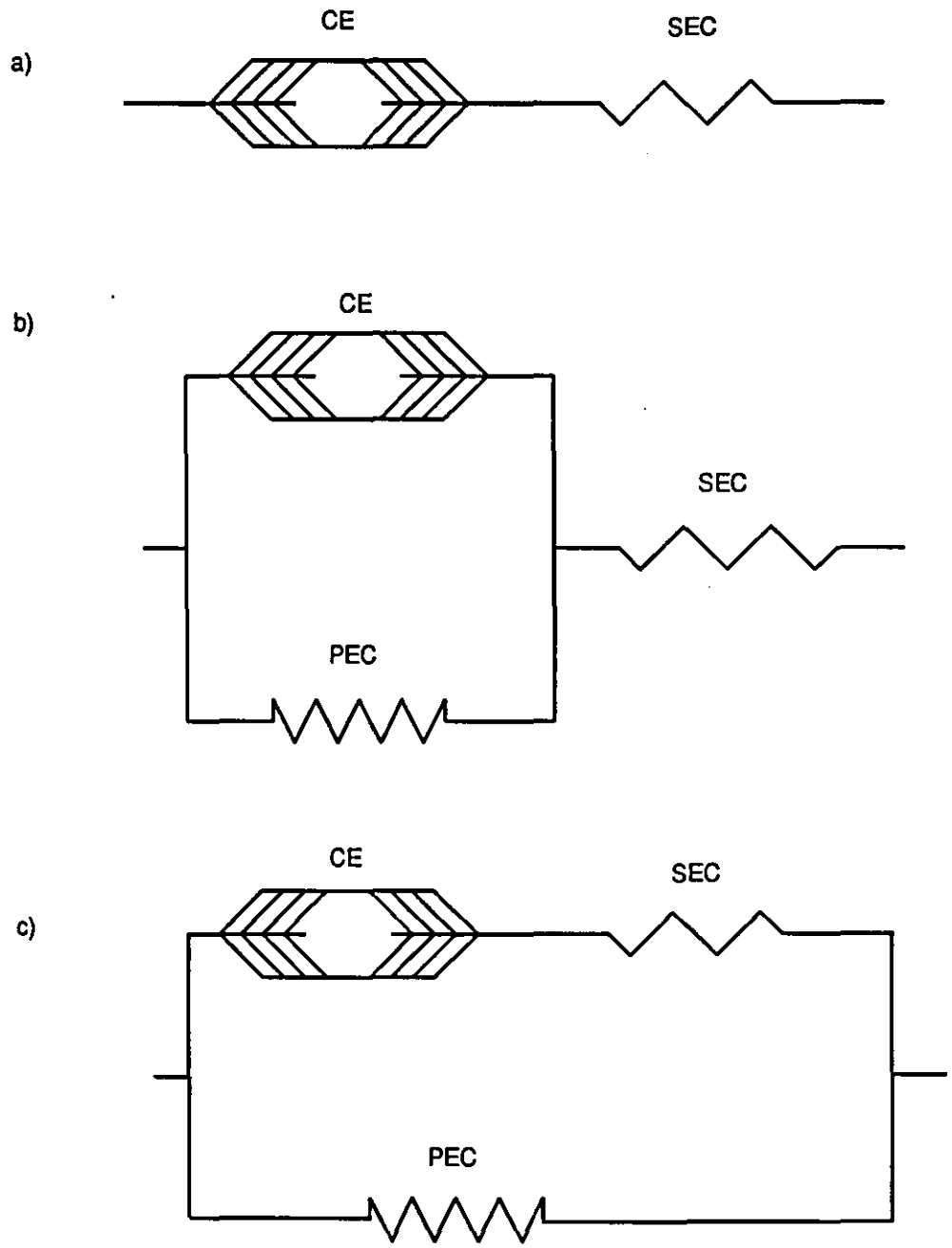

FIGURE 5.4 - Two and three element mechanical analogue models of muscle.

They have not yet been regularly incorporated into biomechanical studies of human movement. Zahalak (1981, 1986) has performed work in this area, working with a simplified version of Huxley's 1957 model. The model is represented by four first order differential equations, resulting in a model that is more complex than the Hill type models often used, but significantly simpler than the Huxley model. Predictions made using the model were compared with data obtained from studies on cat soleus. The model was able to predict accurately the force produced by a muscle yielding to a constant velocity stretch, and the decrease below the isometric level of muscle force production after small amplitude sinusoidal stretches (Zahalak, 1986). Hill's model fails to take account of these phenomena. Ma and Zahalak (1987) extended the earlier muscle model of Zahalak (1981, 1986) to incorporate the thermodynamic changes of Hill et al. (1975), developing what he referred to as a self-consistent distribution-moment model of muscle. These modifications of the earlier model resulted in a simpler formulation, and demonstrated increased accuracy in the predictions of the energetics of muscle particularly for slow stretches, during which it has been shown experimentally that heat production is lower than during an isometric muscle action (Abbott and Aubert, 1951).

5:2.2 FORCE-LENGTH RELATIONSHIP

The contractile component of muscle has two properties: the force-length relationship, and the force-velocity relationship. The former is dealt with in this section and the latter in the next.

The force produced by the contractile component is due to the interaction of the actin and myosin filaments which make up the sarcomere of the muscle. There are a number of theories which attempt to explain how the force is generated. The most popular of these is the cross-bridge theory (Pollack, 1983). This theory claims that force is generated as cross-bridges extend from the thick filaments (myosin) to attach to the thin filaments (actin), the cross-bridges then undergo a chemical and structural transition which cause a tensile force. This cycle continues as the cross-bridges detach and re-attach. The force produced is dependent upon the degree of the overlap between the actin and myosin filaments (Gordon, Huxley, and Julian, 1966), if the muscle is maximally active. As the muscle lengthens, the area of overlap between the thick and thin filaments decreases and therefore the number of possible cross-bridges is reduced thus reducing the maximal tension. At short muscle lengths there is a fall in the force produced. This is attributed to the extensive overlap of the filaments interfering with the formation of the cross-bridges. The results of Gordon et al. (1966) were for amphibian muscle, the same relationship between filamentary overlap and muscle tension was demonstrated for human muscle by Stevens, Dickinson, and Jones (1980). Muhl (1982) has shown that the length-force curve of whole muscle has a larger ascending limb than descending limb.

There are various mathematical models used to represent the force-length relationship of muscle. Although the relationship between muscle fibre length and force is non-linear, it has been modelled as a linear function e.g. Bahill (1981), and Pedotti, Krishnan, and Stark (1978). Bahler (1968), Woittiez, Huijing, Boom, and Rozendal (1984), and van Ingen Schenau, Bobbert, Ettema, de Graaf, and Huijing (1988) modelled this relationship using a polynomial and assumed the relationship was parabolic. Hatze (1981b) used a Gaussian function, which assumed that this relationship was asymmetrical. Otten (1987)

extending his study of 1985 presented a model which also assumed the relationship was asymmetrical. The equation presented by Otten (1987) was similar to that of Hatze (1981b) but took more account of the asymmetries of the force-length relationship.

Hof and van den Berg (1981) and Winters and Stark (1985) combined the force-length and joint angle muscle moment arm relationships, giving a joint moment-angle relationship. Such a relationship is hard to formulate, as although a muscle's moment arm may be constant for a given joint angle, the muscle fibre length is not. Both of these relationships are subject specific, and are complex functions of joint angle. The combination of these functions makes it difficult to partition their relative contribution to joint moments.

Pierrynowski and Morrison (1985a,b) used the force-length model of Hatze (1981b) (their equation 8, Hatze (1981b) equation 3.33). The adoption of this model by Pierrynowski and Morrison (1985b) was incorrect. Instead of using the optimal length of the muscle they used the maximum length of the muscle as one of the equation parameters: the latter is much easier to estimate than the former, but they are not interchangeable. Furthermore this model was advanced by Hatze (1981b) as the model of the force-length relationship of an isolated fibre; the force-length relationship of a whole muscle is different as the optimum length of the fibres making up this muscle will show a Gaussian distribution. Bagust, Knott, and Lewis (1973) have shown that the variance in the optimal length of muscle fibres can be very large in cat fast twitch muscle fibres. Stephens, Reinking, and Stuart (1978) found a standard deviation in the motor unit of cat medial gastrocnemius of 3 mm in the optimal length of fibres which had a mean length of 18 mm. The rat gastrocnemius muscle fibres were shown to have a variation in optimal length of approximately 20 percent (Holewijn, Plantinga, Woittiez, and Huijing, 1983). Therefore Hatze (1981b) presented a different model for the force-length relationship of whole muscle.

The model of the force-length relationship used in this study is that of Hatze (1981b):-

$$F_l = F_{lO} \cdot \exp\left[-\left(\frac{Q - 1}{SK}\right)^2\right] \qquad [5.16]$$

$$Q = \frac{L_F}{L_{FO}} \qquad [5.17]$$

Where:-

F_l - is the maximum isometric tension used at a given muscle fibre length

F_{lO} - is the maximum isometric force produced at the optimum length of the muscle fibres

L_F - is the length of the muscle fibres

L_{FO} - is the length at which the muscle fibres exert their maximum tension (optimum length)

and SK is a constant specific for each muscle where SK>0.28.

This model was selected for a number of reasons. It takes into account the non-linear and asymmetrical force-length relationship of muscle. It is not as complete as the model of Otten (1987) but requires the determination of fewer parameters. This model also takes into account the statistical variations in the optimum length of the muscle fibres. The parameter SK reflects the spread of the length-tension curve. It assumes that the muscle fibres are all of the same resting length. With specific reference to the muscles

causing elbow flexion, Kaufman, An, and Chao (1989) claimed that on close examination the lengths of the individual muscle fibres making up a muscle were all similar.

5:2.3 FORCE-VELOCITY RELATIONSHIP

The accepted convention in studies of muscle is for muscle shortening to be designated a positive velocity (concentric muscle action), and muscle lengthening a negative velocity (eccentric muscle action). The force-velocity relationship is non-linear. Taking an isometric contraction as the starting point, as the muscle fibre velocity increases the muscle force decreases. During an eccentric muscle action as muscle fibre velocity decreases the muscle force increases. This description of the force-velocity relationship assumes that the muscle remains at the same length for all velocities. If there was a change in muscle length the maximum isometric force would change and therefore the capability for force production at different muscle velocities at that length would change.

The force-velocity relationship can be explained by cross-bridge theory. If the muscle is shortening the actin binding sites will be moving past the myosin cross-bridges. The amount of time in which the cross-bridges can bind is limited, as the velocity of contraction increases the time for the formation of cross-bridges decreases. Therefore as velocity increases there is a decrease in the number of active cross-bridges that exert a force. For negative velocities the increasing force with decreasing velocity is attributed to stretching of the cross-bridges (Huxley, 1957), resulting in higher force generation per cross-bridge even though the number of cross-bridges formed is reduced.

A number of mathematical models have been used to represent the force-velocity relationship of muscle. Fenn and Marsh (1935) and Aubert (1956) both used exponential functions, each requiring two constants. Van Ingen Schenau et al. (1988) used a polynomial requiring three constants. In this study the model of the force-velocity relationship of Hill (1938) was adopted. This relationship was chosen because so many studies have fitted Hill's equation to their data that it is relatively easy to obtain the parameters required for the model. The equation described by Hill (1938) was:-

$$F_V = a.\frac{(V_{max} - V_F)}{b + V_F} = \frac{b.(F_I + a)}{b + V_F} - a \qquad [5.18]$$

Where:-

F_V. is the maximum possible force at a given muscle fibre velocity

a,b - are constants

V_{MAX} - is the maximum speed of shortening of the fibres

V_F - is the current speed of shortening of the fibres

and F_I is the maximum isometric tension used at a given muscle fibre length.

Hill (1970) demonstrated that his model of the force-velocity relationship is appropriate even when the properties of the muscle fibres making up the muscle vary.

This equation has dominated the literature, with most studies on isolated muscle fitting force-velocity data

to this function. However there are some shortcomings of the model. The equation does not apply to eccentric muscle action. Also it may not also apply for very fast extensions of muscle when the force-velocity relationship may be discontinuous (Sugi, 1972). The force-velocity relationship of muscle has been shown to be affected by pre-stretching of the muscles (e.g. Cavagna and Citterio, 1974; Edman, Elzinga, and Noble, 1978). The activities examined in this study were selected so that the anticipated force-velocity behaviour of the muscles would be within the limitations imposed by Hill's equation.

Some of the key features of the equation are:-
1. It reflects the maximum speed of the muscle fibres as:-

$$b = a.\ V_{MAX}/F_I \qquad [5.19]$$

2. At V_{MAX}, F_V must be zero.
3. The greater the curvature of the force-velocity curve the lower the ratio a/F_I.
4. The values of the constants vary with temperature.
5. As the value of F_I is length specific as soon as the length of the muscle is changed F_I must be a re-calculated.
6. The constants 'a' and 'b' are normally considered numerically in relation to maximum isometric force and maximum velocity respectively.

5:2.4 MUSCLE PARALLEL VISCO-ELASTICITY

Passive visco-elasticity has been considered in two ways, first by muscle physiologists who have tried to identify the sites and quantify the passive visco-elasticity of isolated muscle (e.g. Hill,1938; Jewell and Wilkie, 1958), and by biomechanicians who have looked at the passive visco-elasticity about joints (e.g. Engin, 1979; Yoon and Mansour, 1982). To avoid confusion the former shall be called muscle passive visco-elasticity (MPV), and the latter joint passive visco-elasticity (JPV). MPV is reviewed in this section, and JPV in the next.

MPV can be seen in isolated muscle when it is receiving no neural stimulation: as the muscle lengthens the tension developed is due entirely to those elements lying parallel to the contractile element of the muscle. These elements have been grouped together and called the PEC. A muscle develops no tension in the PEC until the muscle is at a length greater than its resting length, before this the PEC are "slack". Work on isolated muscle is normally concerned with a range of lengths which do not involve MPV.

Banus and Zetlin (1938) completed some of the earliest work on MPV and identified the site of parallel visco-elasticity as the connective tissue surrounding the muscle, the fasciae. The fasciae are the sarcolemma surrounding the individual muscle fibres, and the outer connective tissue - endomysia, and perimysia. Street and Ramsey (1965) examined isolated frog muscle fibres and showed there was visco-elasticity in the sarcolemma of the fibres. Carlson and Wilkie (1974) claimed that the tension-length curve for the PEC is directly dependent on the amount of connective tissue in the muscle. These tissues causing parallel visco-elasticity all move in fluid, which causes a damping element associated with the

parallel visco-elasticity (Alexander and Johnson, 1965).

Jewell and Wilkie (1958) produced a stress-strain curve for the PEC of frog skeletal muscle. This curve was very similar to those produced by Yamada (1970) for human muscle. Both curves were exponential. By examining the stress-strain relationship for resting muscle and its fasciae, Yamada (1970) determined that the major site for the PEC was the fasciae. Although MPV has primarily been identified in sites lying in parallel with the contractile element, when the muscle is at rest there may be some residual cross-bridges which could account for some MPV, (Ebashi and Endo, 1968; Hill, 1968).

The MPV is not always included in models of muscle in vivo. In their study of locomotion, Pierrynowski and Morrison (1985a,b) decided that based on the available evidence the moments due to the MPV were small enough to ignore in the model they used to estimate muscle forces. In the muscle model used to examine human jumping, Bobbert et al. (1986) also ignored MPV. In contrast to these studies Hatze (1976) incorporated both types of visco-elasticity (joint and muscle) into his model of muscle, although MPV was only considered for biarticular muscles, as it was felt that MPV for the mono-articular muscles was incorporated into the model of joint passive visco-elasticity. In later work this distinction between the MPV for mono-articular and biarticular muscles was not made (Hatze, 1981b).

Analysis of flexion and supination of the elbow by Chapman (1975), and Chapman, Caldwell, and Selbie (1984), determined that the PEC of muscle made no significant contribution to the joint muscle moment throughout nearly all of the range of elbow flexion and supination. In light of these findings MPV was not directly included in the present model. Even though the MPV has been ignored in the model of muscle developed here, much of the MPV is incorporated in the model of joint passive-visco-elasticity (section 5:2.5). Therefore MPV is included, at least in part, as a lumped term for all the muscles crossing the elbow joint. Although some of the contribution of MPV to the joint moment will be included in the joint passive visco-elasticity, this would not be the case for biarticular muscles, as it may require movement of both joints to stretch the muscle enough to bring any contribution from MPV into action. The biceps crosses three joints, and the influence of one of these joints, the shoulder joint, on the length of the biceps has been ignored (see section 5:1.5).

5:2.5 JOINT PASSIVE VISCO-ELASTICITY

Joint passive visco-elasticity (JPV) can be quantified by the forced movement of a passive limb through a prescribed range of movement whilst measuring the resistive moments (e.g. Engin, 1979). Others have used techniques based around the passive movement of a limb at a constant velocity about a joint (e.g. Hayes and Hatze, 1977). There has been to date no comparison of the different techniques employed to measure JPV. The JPV of various joints has been assessed, for example Yoon and Mansour (1982) determined it for the hip, whilst Siegler, Moskowitz, and Freedman (1984) determined JPV for the ankle, and Engin and Chen (1986) for the shoulder complex.

Johns and Wright (1962) examined the JPV of the wrist of a cat. Structures considered to contribute to the passive moment about the joint were sequentially severed and the passive moment re-assessed. By

following this procedure the contributions of different structures to the JPV were assessed. Their analysis showed that in the mid-range of movement the joint capsule contributed 47 percent of the passive moment, the muscles 41 percent, the tendons 10 percent, and the skin two percent. Towards the extremes of joint motion the tendons had a greater effect. Therefore JPV is the net moment about a joint caused by all the passive structures crossing or surrounding the joint.

Broadly there are two sources of JPV, one resulting from the muscles crossing the joint, and the other due to the structure of the joint. The muscles as described in section 5:2.4 have a muscle specific passive visco-elasticity, therefore the JPV will reflect the sum of this muscle passive visco-elasticity for all the muscles crossing the joint. MPV is dependent on the length of the muscles, so varies with joint angle and muscle force. For some multi-articular muscles the movement of one joint may not stretch the muscle sufficiently for it to lengthen beyond its resting length and so they will not contribute to the JPV.

Structures other than the muscles contribute to the JPV. Ligaments may cause a moment at some joint angles, particularly towards the end of the range of joint motion where the ligaments are responsible for maintaining joint integrity. There may also be a contribution from the friction at the joint. JPV is generally measured under conditions of low joint loading, with little or no active muscle tension, where the contribution from joint friction would be expected to be small. When the joint load is increased friction may also increase, and with it JPV.

Engin (1979) examined the passive moments about the elbow joint on three subjects. The JPV was measured for pronation and supination about the radius-ulna axis of the elbow, and for elbow flexion. For pronation and supination within the voluntary range of motion (which permitted 75 degrees of pronation and 85 degrees of supination), the highest resulting passive moments were between 2 N.m and -2 N.m for all the subjects.

Hayes and Hatze (1977) also examined JPV at the elbow joint about the flexion-extension axis only. Their data for the elbow joint had a constant value in the mid-range of 1.4 N.m, 1.0 N.m, and 1.4 N.m for their three subjects for both flexion and extension. At the extremes of joint motion the value for the JPV increased to around 10 N.m for full extension and -10 N.m for full flexion. The value for full extension and the mid-range compare well with the data of Engin (1979), but for full flexion Engin reported a value of -20 N.m. The data of Engin was collected by the forced movement of a limb and the flexion values were actually beyond the normal voluntary range of motion. The JPV value from the data of Engin (1979), for the maximum degree of elbow flexion reported by Hayes and Hatze (1977), was approximately -10 N.m which compares well with the data reported by Hayes and Hatze (1977).

In an extension to his earlier work Engin examined the JPV of the elbow joint beyond the normal full elbow extension (Engin and Chen, 1987). These data are of particular use in the examination of how the human body responds to trauma, where the elbow may be extended beyond its normal range. The data provides JPV values for the region 20 degrees beyond normal full extension. In the context of the present study such data were not required.

A model was developed which relates the angle of elbow flexion to the moment caused by the JPV about the elbow joint centre. The function was fitted to the data of Engin (1979). The major assumption of this model is that JPV is similar for different subjects. The data from three subjects reported by Engin (1979) were all very similar. These data also showed good correspondence with that of a further three subjects in the study of Hayes and Hatze (1977), so this assumption is justified with reference to the limited evidence. The function used was:-

$$M_p(\alpha) = C1.\exp(C2.\alpha) + C3.\exp(C4.\alpha) + C5 \qquad [5.20]$$

Where:-

$M_p(\alpha)$ - is the passive moment at joint flexion angle α

and C1, C2, C3, C4 and C5 - are constants.

The values of these constants are 12.49, -5.73, -0.02, 2.58, and 0.04 respectively, when joint flexion angle is measured in radians.

The graph of this function is shown in figure 5.5. The shape of this curve is typical of the curves presented for the JPV of the elbow joint (Engin, 1979; Hayes and Hatze, 1977). As the results of Engin (1979) only produced small passive moments about the supination-pronation axis these moments were ignored and consequently not modelled. As the model is only related to joint angle and not angular velocity there is no viscous component included in the model. This model takes no account of the changes in JPV which may occur when the muscles are more active, or when the joint is subjected to a higher load. Although JPV includes some influence from MPV, this relationship is only approximate as MPV depends on muscle length which is a function not only of joint angle but also of muscle force.

5:2.6 TENDON ELASTICITY

When activated a muscle develops tension in the muscle fibres. This tension is transferred to the skeleton via the elastic structures in series with the fibres. There are two sites of series elasticity: in the tendon, and in the muscle fibres themselves. This section will review tendon elasticity and the next muscle fibre elasticity.

Tendons are composed mostly of the protein collagen. Harkness (1961) examined the achilles tendon of man, and found it to be composed of 86 percent collagen. When viewed under a light microscope tendons have a crimped wave like appearance. Dale and Baer (1974) showed that this crimping (actually in the collagen) unfolds during the initial loading of the tendon. The initial part of the stress-strain curve for tendon is due to the unfolding of the collagen. Tendon is not uniform along its whole length. The insertion onto the bone is a gradual transition from tendon to fibro-cartilage. The tendon is also anchored onto the bone by fibres from the periosteum of the bone (Cooper and Misol, 1970). At the other end there is a gradual transition from tendon to muscle.

A number of researchers have determined the stress-strain relationship for tendon. Bennet, Ker, Dimery, and Alexander (1986) working with mammalian tendon found that it had a breaking strain of 0.08. They also found that the stress-strain curve of tendons has a hysteresis, which means there is a difference in the modulus of elasticity depending on whether the tendon is being loaded or unloaded.

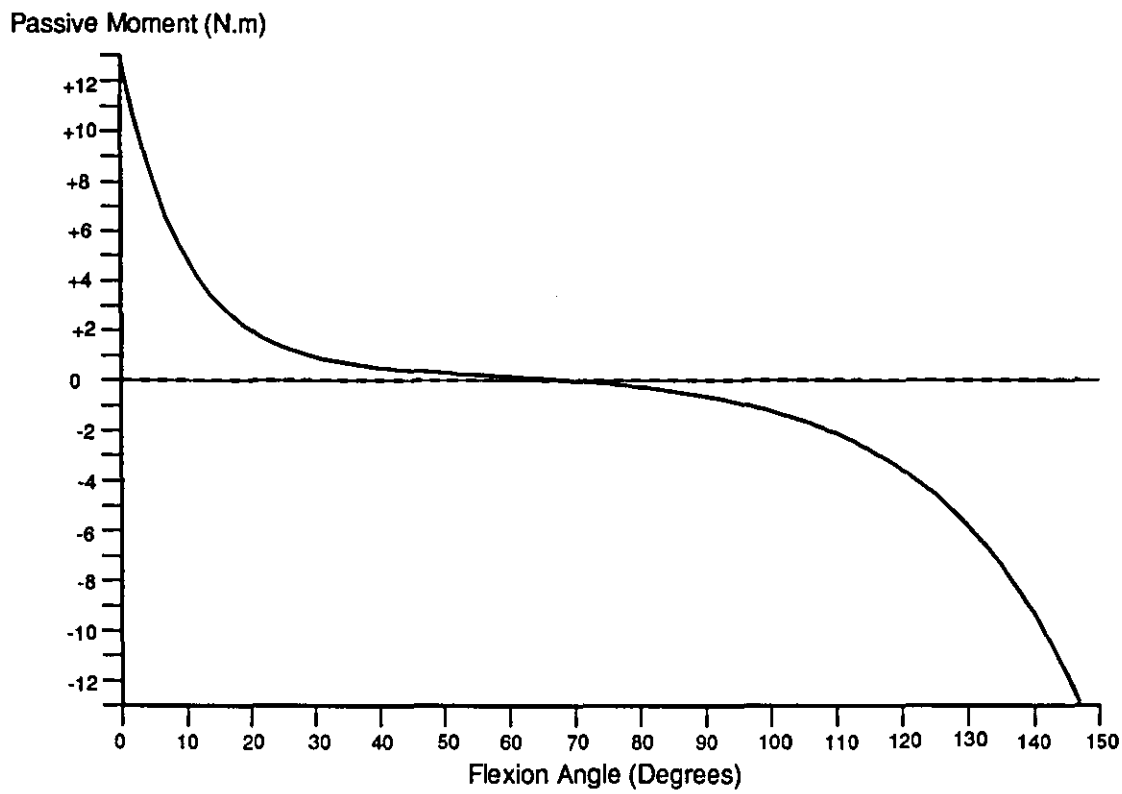

FIGURE 5.5 - The passive visco-elastic moment of the elbow joint as a function of the joint flexion angle, estimated using equation 5.20.

The precise role of tendon in animal movement is unknown. Ker, Dimery, Bibby, Kester, and Alexander (1987) examined the storage of energy in running, and identified the achilles tendon as a major site of energy storage. Others have suggested that it is not the ability of tendon to store energy but its compliance, which allows the muscle to have one velocity whilst its components have different velocities, which determines its role in movement. Bobbert et al. (1986) in the examination of plantar flexion during jumping, showed that without the compliance of tendon the high shortening velocity of the triceps surae, and high joint moment produced by this muscle group would not be possible. Similar results were shown for level walking in man by Hof, Geelen, and van den Berg (1983) and for wallabies hopping by Morgan, Proske, and Warren (1978). During hopping when the wallaby gastrocnemius muscle was developing near maximum tension there was eight times as much movement in the tendon as in the muscle (Morgan et al., 1978). The wallaby gastrocnemius tendons are long to accommodate this, and the animals become more efficient with increasing speeds of hopping as this mechanism plays an increasing role.

A number of models have been suggested to model tendon elasticity: Hatze (1981b) presented an exponential function; Bahler (1967) used a polynomial series; Pierrynowski and Morrison (1985a,b) and Ker, Dimery, and Alexander (1986) used Hooke's law. A model of tendon elasticity based on Hooke's law was used in this study. The model used in this study was:-

$$L_T = L_{TR} \cdot \left[1.0 + \frac{F_M}{A_T E}\right] \qquad [5.21]$$

Where:-

L_T - is the length of the tendon

L_{TR} - is the resting length of the tendon

F_M - is the force exerted by the muscle on the tendon

A_T - is the cross-sectional area of the tendon

and E is Young's modulus of elasticity for tendon.

Although Bennet et al. (1986) showed that there was hysteresis in the stress-strain curve of tendon no model has yet included this. Its effect can be considered small enough to be insignificant for the purposes of the analysis undertaken here.

5:2.7 MUSCLE FIBRE ELASTICITY

When muscle, with the tendon removed, is released from an isometric contraction and allowed to shorten against a load less than the previous isometric load, the shortening has two phases; a fast phase followed by a slow phase. The fast phase is attributed to the release of the energy stored in the elastic components of the muscle fibres. As the contractile machinery is slower to react than the SEC the second phase is attributed to the contractile component of the fibres. Such analysis, which shows the existence of muscle elasticity, has been undertaken by a number of researchers e.g. Hill (1950), and Bahler (1968).

Huxley and Simmons (1971a) in a theoretical analysis of isolated frog muscle suggested that the site of the elasticity was the cross-bridges. They hypothesised that the specific site may be within the myosin filaments. This proposal was further supported by the work of Morgan (1977), on the soleus of

anaesthetised cats. As well as having an elastic component, muscle fibres have a viscous component. Woledge (1961) quantified the damping component for the frog sartorius muscle, whilst Bahler (1967) quantified it for the rat gracilus anticus muscle. This damping component is so small compared with the elastic component, that Ford, Huxley, and Simmons (1977) reported that muscle fibre elasticity seemed to be almost completely free of damping.

Jewell and Wilkie (1958) examined the elasticity of muscle at different lengths and maximum stimulation. Their results indicated that muscle elasticity was not dependent on muscle length. Huxley and Simmons (1971a) showed that muscle elasticity was dependent on the number of cross-bridges formed. Morgan (1977) found muscle elasticity to be a linear function of force. This confirmed the findings of Huxley and Simmons (1971a) that muscle elasticity is proportional to the number of cross-bridges formed. Ford, Huxley, and Simmons (1981) working with the frog tibialis anterior showed that muscle elasticity was directly proportional to the number of active cross-bridges. At maximum overlap they estimated that 80-90 percent of the compliance was due to cross-bridge elasticity.

Stienen, Blangé, and Schnerr (1978) working with frog sartorius claimed a maximal stretch of 11-15 nm per half sarcomere. Bagshaw (1982) reports a resting length of the sarcomere of frog sartorius of 2.5 μm (range in contraction of 2.0-3.6 μm). Combining these two sets of data suggests a maximum stretch from resting length of 0.88 to 1.2 percent. These results indicate that the muscle fibres will maximally stretch around 1 percent. As the muscle fibres do not make up all of the muscle length the effect of muscle fibre stretch on muscle length would be smaller.

In the muscles modelled in this study the length of the muscle belly was not large enough for muscle elasticity to be a more dominant form of SEC elasticity than tendon elasticity. As muscle elasticity is dependent on the number of cross-bridges formed, during sub-maximal activity the amount of stretch would be a complex function of muscle fibre length and the active state. In the procedures used in the next chapter to estimate muscle forces during sub-maximal activity it would be difficult to estimate the amount of stretch in the muscle fibres. Therefore muscle elasticity was not included in the model of muscle; this makes the modelling procedures used in the next chapter more tractable.

5:2.7 SUMMARY

The elements of a model to represent mechanical properties of muscle have been presented. The model incorporates three components. Each muscle has a contractile component in series with an elastic component. There is a PEC representing the joint passive visco-elasticity, which is parallel to all of the muscles. The elasticity of the muscle fibres has been ignored. The parameters for each of the models have been identified, their determination is detailed in section 5:4.

5:3 ACTIVE STATE DYNAMICS

Muscles are capable of exerting different force levels concomitant with the activity being undertaken. The active state is a measure of how active the muscle is. It is the purpose of the following sections to describe how the active state of muscle is varied: active state dynamics. To understand active state

dynamics it is necessary to describe the function of motor units, and their relationship with muscle fibre types. The way in which muscle force is modulated, and the role of calcium in this process are also discussed.

5:3.1 MOTOR UNITS

In human skeletal muscle one motoneuron will innervate a number of muscle fibres via its axonal branches. All the fibres innervated by a motoneuron constitute a motor unit. When the motoneuron fires, all the fibres in that motor unit will be active simultaneously. The muscle fibres making up a motor unit are not constrained to be adjacent. Muscles vary in the number of motor units they contain, the size of these motor units, and the number of fibres making up the motor units. For the larger muscles in man the number of motor units per muscle can vary from around 100 to over 1000 (Henneman and Mendell, 1981). Buchthal and Schmalbruch (1980) collected and re-examined data from the literature and presented the following details for the biceps, and brachioradialis.

TABLE 5.1 - The properties of the motor units of the biceps and brachioradialis.

	BICEPS	BRACHIORADIALIS
Number of motor units in muscle	774	330
Number of muscle fibres in muscle	580000	130000
Mean number of fibres per motor unit	750	390

No information was reported for the brachialis.

5:3.2 MOTOR UNITS AND MUSCLE FIBRE TYPES

Muscle fibres can be divided into two major groups: fast twitch and slow twitch. The work of Brooke and Kaiser (1970) has provided a nomenclature for these fibre types which relates to their histochemical and biochemical profiles. Type I fibres have a long contraction time (slow twitch), compared with the type II fibres, and are well adapted for aerobic glycolysis. All type II fibres have short contraction times (fast twitch), this fibre type has two subdivisions. The type IIa fibres have a high capacity for anaerobic metabolism but also have a capacity for aerobic metabolism e.g. relatively high levels of succinic dehydrogenase-tetrazolium, nicotinamide dinucleotide-tetrazolium reductase (necessary co-enzymes in the Krebs cycle), and myoglobin compared with the type IIb fibres. Type IIb fibres also have a high capacity for anaerobic glycolysis but have little capacity for aerobic metabolism.

The properties of the muscle fibres are determined by the motoneurons that innervate the fibres. Cross-innervation studies have demonstrated this dependence (e.g. Buller, Eccles, and Eccles, 1960; Yellin, 1967). Yellin (1967) re-innervated the soleus of the cat which is composed predominantly of type I fibres, with a nerve from muscle with a heterogeneous fibre type distribution. As a consequence of the re-innervation the soleus eventually contained an increased proportion of type II fibres.

Burke, Levine, Tsairis, and Zajac (1973) provided a nomenclature for motor unit types which correlates strongly with the fibre type classification of Brooke and Kaiser (1970). Burke et al. (1973) used the following classification system: FF fast twitch and fatiguable; FR fast twitch fatigue resistant; and S slow twitch. Table 5.2 demonstrates the relationship between fibre types and motor units classified in these ways.

As there is a very close correlation between muscle fibre types and motor unit types, it is possible to imply the properties of one from data gathered from the other.

5:3.3 MUSCLE RECRUITMENT

In some of the earliest work examining the modulation of muscle force, Adrian and Bronk (1929) identified two mechanisms that could increase the force of a voluntary contraction: either more motor units could be recruited; or the rate of discharge of the already active motor units could be increased. The latter mechanism is known as rate coding. This section reviews recruitment, the next reviews rate coding.

Research has indicated that in the majority of cases recruitment takes place in a fixed order; motor units are recruited in increasing order of their motoneuron size. This order is known as either the "Henneman size principle" (Henneman, Somjen, and Carpenter, 1965), or the "size principle". The S motor units have the smaller motoneurons, and the FF and FR the larger. The smaller the motoneuron the lower the input resistance, and therefore the lower the excitation threshold; therefore smaller motor units are recruited first. Milner-Brown, Stein, and Yemm (1973a) found a correlation of greater than 0.8 between the size of the motoneuron and the order in which the motor units were recruited. Freund, Budingen, and Dietz (1975) reported that the total force at which motor units were recruited was a direct function of their axonal conduction velocities, for human forearm muscles. The axonal conduction velocity is in turn a direct function of the diameter of the motor axon, showing the inter-relationship of motor unit properties.

Desmedt and Godaux (1977) accepted the size principle for normal movements, and investigated how it applied for fast and ballistic movements. They measured the activity of single motor units in the tibialis anterior in man using indwelling electrode electromyography (EMG). Their measurements supported the concept of the orderly recruitment of motor units moving from S to FR and FF units. In fast movements the FT units were firing sooner than in "normal" activity but the ST units were not silent. Most of the studies which confirm the size principle have been on muscles during isometric or ramp contractions. Grimby (1984) has shown that the principle also applies during human locomotion. He examined the tibialis anterior during walking of increasing speed and during slow running.

If all motor units produced the same tension when tetanically stimulated, the relationship between percentage of motor units recruited and the percentage of maximum force developed would be linear. In practice, as more motor units are recruited, the increase in the proportion of the muscles maximum tension developed is logarithmic (Burke, 1980). Milner-Brown et al. (1973a) examined the contractile properties of 145 motor units from the first dorsal interosseous muscles of three males. They found that the maximum twitch tension in the units varied from 0.1 to 10 g (sic). They showed that there was an approximately

TABLE 5.2 - The inter-relationship of muscle fibre type and motor unit types, and the major properties of each. (The information to produce this table was obtained from Burke and Edgerton, 1975.)

FIBRE TYPE:	IIb	IIa	I
MOTOR UNIT TYPE:	FF	FR	S
AXONAL CONDUCTION VELOCITY	***	***	*
CAPILLARY SUPPLY	*	**/***	***
FIBRE DIAMETER	***	***	*
CONTRACTILE TIME	*	*/**	***
ENDURANCE TIME	*	**/***	***
RELATIVE CONCENTRATIONS OF:-			
OXIDATIVE ENZYMES	*	**/***	***
GLYCOLYTIC ENZYMES	***	***	*
GLYCOGEN	***	**	*
MYOGLOBIN	*	***	***

Where *** = HIGH ** = MEDIUM * = LOW.

logarithmic relationship between the number of motor units recruited and the twitch tension. The same relationship had earlier been demonstrated with the motor units of the cat gastrocnemius (Wuerker, McPhedran, and Henneman, 1965). In the former study the "weaker" units had longer contraction times. It was these slower contracting units which were recruited first.

In summary the size principle states that motor units are recruited in the following order:-

S - FR - FF

or in terms of fibre type:-

Type I - Type IIb - Type IIa

Stephens and Usherwood (1977) have suggested that although the size principle holds, the clear division of motor unit types may not exist and that some low force units may be fast twitch, and some high force units may have long twitch times.

5:3.4 RATE CODING

Variation in motor unit excitation frequency causes different levels of force output (Burke, 1967), this is called rate coding. The lowest firing rate for a motor unit is its force recruitment threshold. The maximum firing rate for a motor unit causes the motor unit to produce its maximum force. The lowest firing rate for a motor unit is 6-8 Hz, whilst the maximum firing rates range from 10 Hz to 60 Hz (Freund, 1983, Burke, 1981). Smaller muscles responsible for fine controlled movements tend to have higher maximum firing rates compared with larger muscles responsible for gross movements.

In fast ramp and ballistic contractions the motor units initially fire at rates greater than that required to produce maximum force in the specific motor units. For example Grimby, Hannerz, and Hedman (1981) examining the short toe extensors of man found an initial firing rate of 100 Hz, whereas a rate of only 50 Hz was required to produce maximum force. These higher firing rates did not produce a greater muscle tension, but did increase the rate of force development.

5:3.5 RATE CODING VERSUS RECRUITMENT

When modelling muscle activation dynamics it is important to know the relative contributions of these two mechanisms: rate coding and recruitment. Using EMG techniques some researchers have measured the activity of individual motor units. Using EMG it is possible to determine the voluntary force level at which a motor unit is recruited. The force at which a motor unit is recruited is expressed as a percentage of the maximum voluntary contractile force (MVCF) of that muscle. Such analyses are limited to muscles which are easily accessible.

Milner-Brown, Stein, and Yemm (1973b) examining the first dorsal interosseous (a small hand muscle) found that up to 33 percent of MVCF the increased force was due to the recruitment of more fibres rather than from increased force output from the already recruited fibres. They claimed
"Increased rate proved to be responsible for the coarser adjustments that are made at higher force levels."

(page 384, Milner-Brown et al.,1973b)
In the extensor digitorum communis of the middle finger, motor units were recruited up to 70 percent of MVCF, (Monster and Chan, 1977). In both the biceps and the deltoid, motor units were recruited up to 80-90 percent of MVCF (Kukulka and Clamann, 1981; de Luca, Le Fever, McCue, and Xenakis, 1982). Denier van der Gon, Ter Haar Romeny, and van Zuylen (1985) showed that in the biceps during a slow ramp contraction the firing rate of the motor units generally remained constant. This suggests that in this type of contraction the biceps increments its force using recruitment rather than rate coding. At lower forces recruitment was the mechanism responsible for increasing force output rather than rate coding.

The work of Milner-Brown and colleagues (1973a,b) demonstrates the general principle that small motor units tend to have recruitment as the major mechanism for muscle tension modulation, whereas larger motor units tend to use rate coding as the major mechanism. De Luca et al. (1982) gave the following explanation for this mechanism. Small motor units tend to be responsible for fine movements and as they are small, recruitment would permit smooth transitions in force levels. The larger motor units can still produce relatively smooth contractions using rate coding, but recruitment permits the rapid development of large forces.

5:3.6 EFFECTS OF DIFFERENT MOVEMENT PATTERNS

There is evidence to suggest that different motor units are preferentially recruited in the same muscle for different movements. Denny-Brown (1949) showed that in the flexor profundus digitorum the motor units recruited to initiate wrist flexion were different from those used for gripping. Person (1958) examining the rectus femoris, a biarticular muscle, showed that the order in which some motor units were recruited was reversed when the muscle was engaged in either hip flexion or knee extension. Examining the gastrocnemius, Wagman, Pierce, and Burges (1965) suggested that the pattern of activation of the motor units depends on: joint position, the position of the limb in space, and the task being undertaken.

Examining motor unit recruitment in the long head of the biceps, Ter Haar Romeny, van der Gon, and Gielen (1982) showed that up to 50 percent of the MVCF, some motor units were only recruited for flexion, whilst others were recruited only for supination. They also showed that the recruitment threshold seemed to depend on the task, therefore units with a high threshold for flexion have that threshold lowered if flexion and supination are performed simultaneously. Research performed by the same group, Ter Haar Romeny, van der Gon, and Gielen (1984), suggested that the movement specific recruitment thresholds were related to the location of the motor unit in the long head of the biceps brachii. Those motor units recruited for all activities were located centrally and medially, whilst laterally located motor units were preferentially recruited for flexion, and the medially located ones for supination.

Freund (1983) has suggested that there may be advantages in movement selective recruitment. Firstly, having units for a similar task all in the same place may allow them to be recruited by a localised reflex response. Secondly the location of the motor unit may allow the motor units to be more efficient at executing that task. Another advantage maybe that in repetitive activity a slight change in movement pattern may use another set of motor units therefore changing the site of fatigue and allowing the formerly

recruited units to recover.

In summary, the force output of a muscle depends on a number of factors:-
1. Which motor units are recruited. (This may in part be movement dependent.)
2. The rate of discharge of the motoneuron attached to the motor unit (rate coding).
3. The mechanical properties of the muscle fibre/motor unit.
4. The biochemical properties of the muscle fibre/motor unit.

The chemical messenger which causes a fibre to exert a force is calcium. The details of calcium activity are given in the next section.

5:3.7 CALCIUM ACTIVITY

In resting muscle the interaction between the actin and myosin is inhibited by the troponin-tropomyosin, which prevents the hydrolysis of the adenosine triphosphate (ATP) and therefore the release of energy necessary for interaction of the actin and myosin. Excitation causes the release of calcium ions into the sarcoplasm from the terminal cisternae of the sarcoplasmic reticulum. The calcium diffuses across the sarcomere to bind to the troponin, decreasing the inhibitory effect of the troponin-tropomyosin (Civan and Podolsky, 1966). The resulting hydrolysis of ATP provides the energy for the formation of cross-bridges. The amount of calcium therefore determines the amount of activation. Relaxation is the reverse process, the removal of the calcium ions, where the uptake by the sarcoplasmic reticulum is aided by the buffers in the myoplasm.

As the degree of activation of the muscle is dependent on the concentration of calcium ions, the rate of change of concentration in the sarcoplasmic reticulum gives an indication of the change in activation of the muscle. Aequorin is a protein which gives off light when it binds with a calcium ion, and has been used in many studies to demonstrate the relationship between muscle activation and calcium ion concentration (e.g. Ridgway and Gordon, 1975; Rudel and Taylor, 1973; Allen, Blinks, and Pendergast, 1977).

Julian (1971) attempted to quantify the relationship between the concentration of calcium and the percentage of maximum force a muscle was exerting. Examining the semitendinosus of frog he found a non-linear relationship between calcium ion concentration and the percentage of maximum force the muscle was exerting. These results were questioned because of the high potassium chloride concentrations in the bathing solution, (Edman, 1979). Julian and Moss (1981) have repeated much of the methodology of Julian (1971) with careful control of the ionic strength of the bathing solutions and found similar results for variations in force with calcium ion concentration. A similar curve showing the same relationship between calcium ion concentration and percentage of maximum muscle force, was produced for the rabbit psoas muscle by Kawai (1982).

Podolsky and Teichholz (1970) showed that for muscle forces greater than 20 percent of maximum, calcium ion concentration had no effect on muscle velocity. They suggested that calcium ion concentration controls the number of cross-bridges which may be formed but not the kinetics of the cross-

bridges. Julian and Moss (1981) and Julian, Rome, Stephenson, and Striz (1986) suggested that the velocity of contraction of the muscle fibres is also controlled by the concentration of calcium ions but for the full range of muscle forces. Edman (1979) and Thames, Teichholz, and Podolsky (1974) have suggested that this mechanism only applies up to around one third of a muscle's maximum force.

There have been a number of models of the dynamics of calcium activity. Taylor (1969) described calcium dynamics by a set of third order differential equations where the output force was a linear function of the concentration of calcium ions. This relationship has since been shown not to be the case for non-static muscle actions (e.g. Julian, 1971). The model of Gillis, Thomason, Le Fevre and Kretsinger (1982) included parvalbumin, which is a soluble calcium binding protein. The model was described by five first order non-linear differential equations. Their model showed that parvalbumin had little effect on the time course of calcium ion concentration during stimulation, but had a significant effect on removal of calcium ions during relaxation.

5:3.8 ACTIVE STATE

The active state of a muscle was originally defined by Hill (1938) as relating to the immediate ability of a muscle to exert a force as a result of stimulation. This active state declined gradually once the stimulus was removed. In 1949b Hill redefined active state as the tension which could be developed after stimulation without lengthening or shortening. This definition has a number of deficiencies, particularly because it takes no account of the influence of the SEC, and the force-velocity relationship of the muscle fibres, and because the active state is assumed to be achieved immediately upon stimulation. Hill (1965) said with reference to his own work,

'...in the end one begins to wonder whether the term has any exact meaning! The facts are certainly not as simple as they seemed at first, but that is the usual history of research.' (page 68)

Sandow, Taylor, and Preiser (1965) introduced the concept that the active state should be related to the number of calcium ions bound to the troponin. The definition of active state is one that has growing prevalence in the literature, and which is used in this study is:-

'...we define the active state q to be the relative amount of Ca bound to troponin.' (page 139, Ebashi and Endo, 1968).

Therefore when q=0 there are no calcium ions bound to the troponin, or at least it is at its resting level, so the muscle is inactive. When q=1 the troponin is saturated with calcium ions, so the muscle is maximally active. Therefore for a given length and velocity the force developed by a contractile element is a function of q.

It has been suggested by Rack and Westbury (1969) that there is a relationship between the length of the muscle fibres and the active state. This means that the active state caused by a certain concentration of calcium ions is dependent on the length of the fibre. These results have not been generally accepted, for example Julian, Moss, and Sollins (1978) questioned the findings because of the way in which the whole muscle was innervated, which they claimed did not guarantee that all the fibres were activated.

5:3.9 MODELS OF ACTIVATION

This section is concerned with the models which have been used to represent activation dynamics.

Wani and Guha (1975) presented a model in which the force output of a muscle was dependent on the number of motor units recruited and the frequency at which those motor units were stimulated. Each motor unit was ascribed a different maximum tension threshold force which increased through the motor unit population with order of recruitment. As size increased there was a decrease in contraction time. They assumed that the force output of a motor unit increased linearly with increasing frequency of stimulation, although this relationship is in fact non-linear (Milner-Brown et al.,1973b). In their model, rate coding becomes the dominant factor for increasing muscle tension as more motor units are recruited. This corresponds well with the literature, but the model is constrained so that there is rate coding in the smaller motor units, which is not necessarily the case (Burke, 1980). This model does not consider calcium activity.

Zheng, Hemami, and Stokes (1984) presented a model for a single motor unit. They presented an equation which relates muscle force to stimulation frequency, thereby eliminating the need to define a relationship between calcium activity and muscle force.

Winters and Stark (1985) divided neuromuscular excitement into two parts: electromechanical coupling dynamics and neural excitation. Electromechanical coupling dynamics was represented by a time constant which effectively puts a delay into their model to allow for events such as neural conduction, passage through the neuromuscular junction, and the time for the muscle to conduct the impulse. The time constants were dependent on the muscle fibre type being considered. Neural excitation was determined from EMG, with muscle force being a direct linear function of activation.

In a series of publications Hatze presented details of a model for activation dynamics (Hatze, 1977a; Hatze, 1977b; Hatze and Buys, 1977). The definition of Ebashi and Endo (1968) was adopted for the active state. Therefore the model developed was based around the dynamics of calcium. In Hatze's model the muscle is divided into motor units which are of increasing size, permitting the model to follow Henneman's size principle. Although Hatze and Buys (1977) divided the muscle into motor units of different sizes they did not allow for a decrease in contraction time with increasing size, which is a typical phenomena of motor units (eg. Milner-Brown et al., 1973b).

Hatze (1977a,b) determined the active state using a second order differential equation which incorporated a length dependent function. This length dependence was derived from the results of Rack and Westbury (1969) who showed that in the cat soleus the stimulus rate produces an 'S' shaped curve in relation to relative tension. They also showed that the stimulus rate required to produce tension varied with the length of the muscle. At short lengths a high stimulation frequency was required to produce a response, whereas near the optimum length of the muscle fibres a lower rate was required. This length dependent activation is not a generally accepted phenomena (see section 5:3.7). The relationship between the active state and muscle force was described by a first order differential equation.

Davy and Audu (1987) used a simplified version of the Hatze model to study muscle activity during locomotion. Muscles were not divided into motor units but recruitment of the muscle was considered as a fraction of the whole muscle activated. Their formulation is inconsistent because some equations appearing in the main body of the text are re-formulated in the appendix to the paper with different constants.

5:3.10 MODEL OF ACTIVATION DYNAMICS

In the next chapter details are given of a model to estimate the individual muscle forces of a number of muscles contributing to a moment about a joint. This model requires, given the previous active state of the muscle, the maximum and minimum active states which can be expected at the next instant in time, as a consequence of either an increase in stimulation (where possible) or the maximum possible reduction in stimulation. To do this two parts of the activation process are considered: effect of stimulation on the active state, and the relationship between calcium concentration and muscle force. In this section the model of activation dynamics used in this study is presented.

It was decided to assume that the muscle force of the elbow flexors is controlled by recruitment (Kukulka and Clamann, 1981; De Luca, et al., 1982; Denier van der Gon, et al., 1985) rather than rate coding. It was therefore not necessary to model the individual motor units, but it was assumed that at any moment a certain proportion of the whole muscle was active. This may not be so when the muscle is fatigued but such conditions were not examined in this study.

Pierrynowski and Morrison (1985b) presented equations that allowed the next level of active state of a muscle to be determined given the previous state and allowing for either maximum stimulation or no stimulation. The equations were:-

For full stimulation $$q(t) = q(t-\Delta t) + [\, 1 - \exp(-\Delta t/TC) \,] \,.\, [1 - q(t-\Delta t) \,] \qquad [5.22]$$

and for full relaxation $$q(t) = q(t-\Delta t) - [\, 1 - \exp(-\Delta t/TC) \,] \,.\, q(t-\Delta t) \qquad [5.23]$$

Where:-
$q(t)$ - is the active state at time t
Δt - is the sample interval
and TC are time constants
These constants were 0.034 for fast fibres, and 0.073 for slow fibres for full relaxation, and 0.003 for full stimulation, for both fibre types.

The different constants ascribed for the two muscle fibre types are appropriate, as Wells (1965) when examining rat muscle showed that there was a much quicker decay in active state in a muscle of heterogeneous fibre composition than in one of predominantly type I fibres. The curves resulting from the equations 5.22 and 5.23 are very similar to those produced by Miledi, Parker, and Scalow (1977) and Melzer, Rios, and Scneider (1986). Figure 5.6 shows the effect of stimulation on the active state using this

model.

The isometric force a muscle can exert is a linear function of the active state; the following relationship can be stated:-

$$F_f = q(t) \,.\, F_l \qquad [5.24]$$

Where:-
F_f is the maximum isometric force the muscle can exert at the current active state.

But for dynamic muscle actions the relationship is more complex. The data of Julian (1971) demonstrates that the ratio a/F_l is dependent on the active state of the muscle. Hatze and Buys (1977) fitted an exponential function to the data of Julian (1971). The results of Julian and Moss (1981) also show such a relationship. Therefore:-

$$a/F_f = a/F_l \,.q(t)^{-0.28} \qquad [5.25]$$

Where:-
a/F_f - is the ratio scaled as a consequence of active state q
and a/F_l is the ratio when the q =1.

Therefore once the active state is known it is possible to calculate the force output of the muscle using the relationships in equations 5.24 and 5.25. The graph in figure 5.7 illustrates this relationship.

5:3.11 SUMMARY

This section has reviewed the mechanisms by which muscle force is modulated. The relationship between motor unit type and muscle fibre type has been examined. A model of muscle activation was adopted which assumes that the force output of a muscle is determined by recruitment. The model is based on the principle of active-state. The model ignores the influence of fatigue on the activation and force output of muscle.

5:4 DETERMINATION OF MUSCLE MODEL PARAMETERS

For the muscle model described in earlier sections various parameters are required for each muscle. These parameters are L_{FR}, L_{FO}, L_{TR}, F_{IO}, SK, V_{MAX}, 'a', 'b', A_T, and E. It is the purpose of the following sections to give the details of how these parameters were obtained. For the purposes of this study a number of different lengths were defined for each muscle: these are represented diagrammatically in figure 5.8.

5:4.1 LITERATURE SOURCES

This section reviews the sources of parameter values that were derived from the literature.

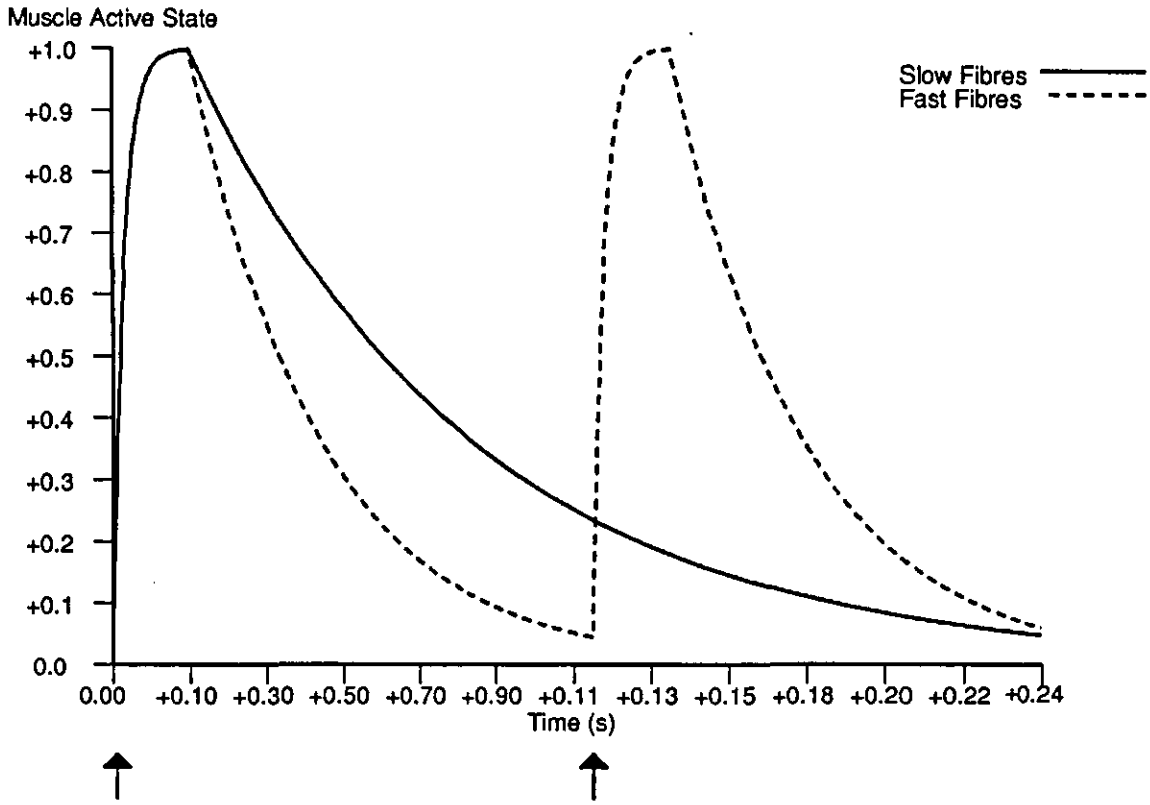

FIGURE 5.6 - The variation in muscle fibre active state with stimulation.

(NB - Arrows mark full stimulation of the muscle fibres for a period of 0.02 s; the second stimulation was for the fast fibres only.)

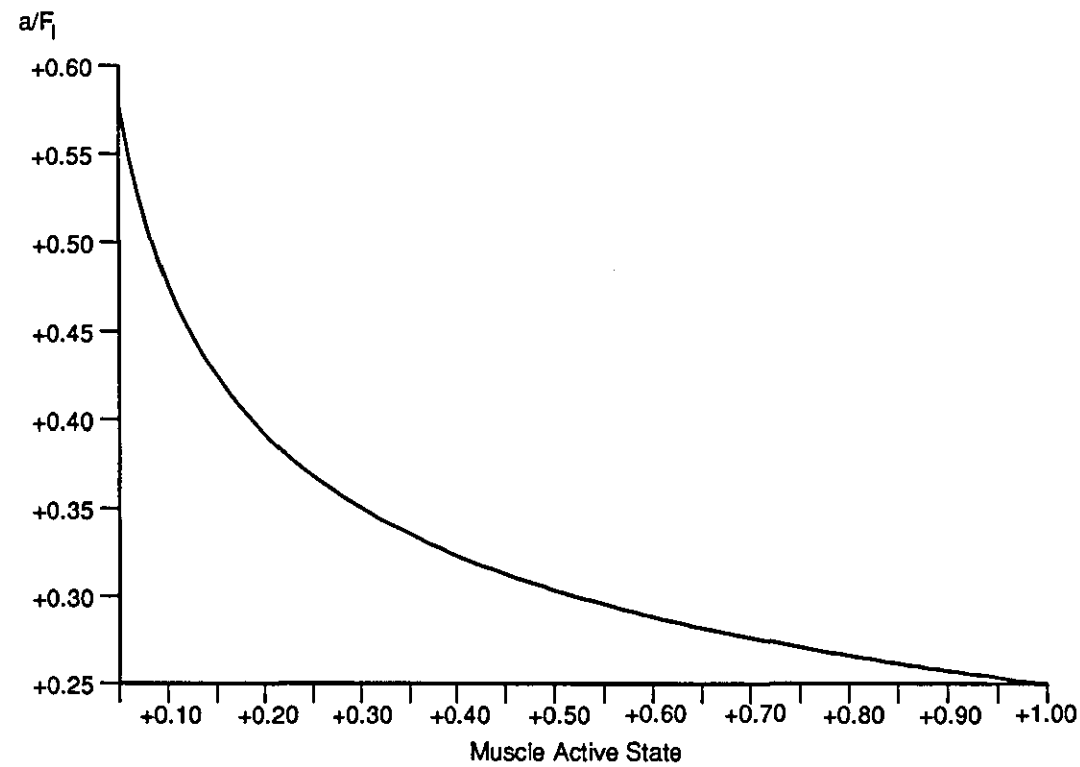

FIGURE 5.7 - The effect of the active state on Hill's constant 'a'.

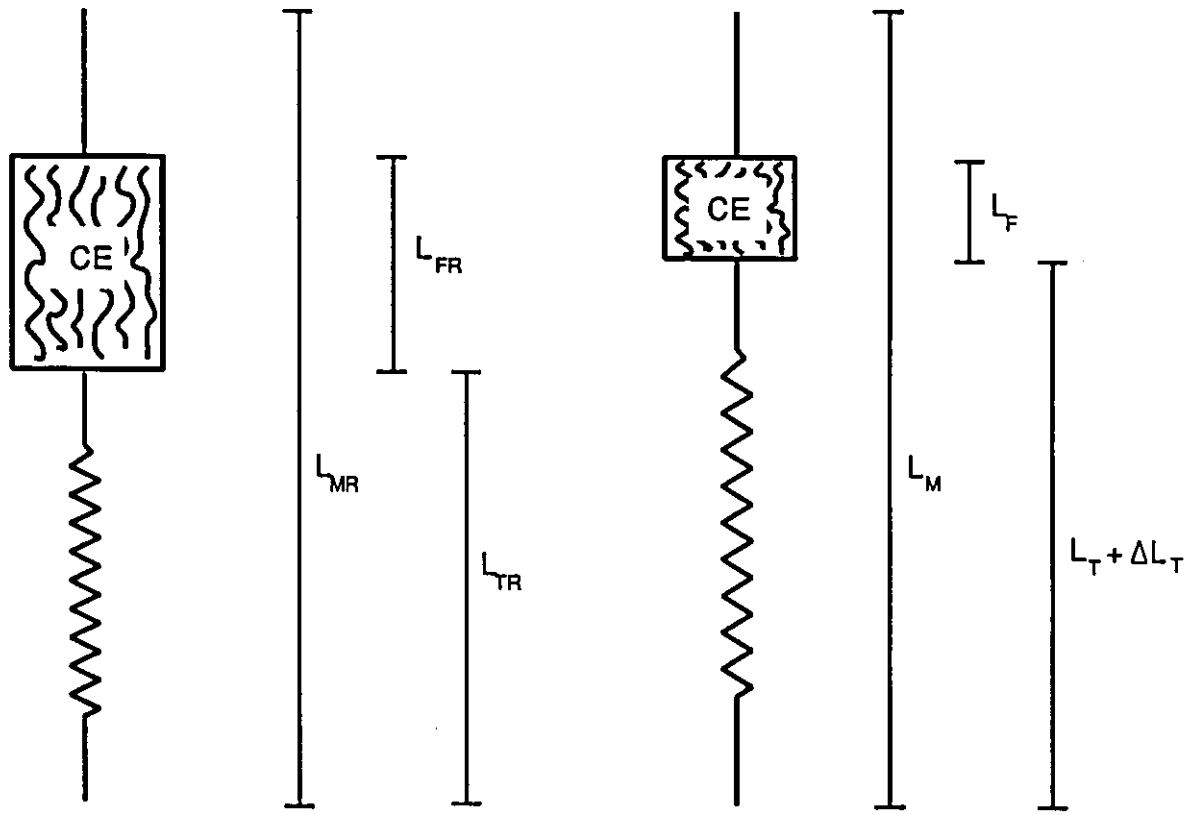

FIGURE 5.8 - The dimensions of a muscle at rest and during a concentric muscle action.

5:4.1.1 TENDON FIBRE LENGTH RATIO

Close (1965) gave the ratio of 0.35-0.40 for muscle fibre length to resting muscle-tendon complex length. Van Zuylen et al. (1988) calculated the fraction of muscle resting length which was muscle fibre for the major elbow flexors. These were: biceps 55 percent; brachialis 70 percent; and brachioradialis 65 percent. A similar ratio for the biceps was found by Amis et al. (1987) from the dissection of one cadaver. Friederich and Brand (1990) examined this ratio of muscle fibre length to muscle length in the lower limbs of two cadavers. They claimed

"The ratios of muscle length to muscle fiber length show considerable variability between muscles, but remarkable consistency in a given muscle in various specimens." (page 93)

Without any contradictory evidence it has been assumed that this consistency also applies to the upper limb.

5:4.1.2 TENDON ELASTICITY

There are a number of techniques that purport to measure series elasticity in vivo (e.g. Goubel, Bouisset, and Lestienne, 1971; Cnockaert, Petuzon, Goubel, and Lestienne, 1978). There are a number of problems with such techniques. A major problem is that it is very difficult to isolate the SEC of the different muscle groups, so values are for the net effect of all muscles crossing a joint. For modelling individual muscles such data are of little use. Therefore values for the elasticity of the tendon were adopted from the literature. Accurate data are required, the source of which must be considered. Blanton and Biggs (1970) compared the tensile strength of tendons from different sources. Their major findings were:-

1. Embalming enhanced the tensile strength.
2. The was no significant difference between superior and inferior limbs.
3. Extensors had greater tensile strength than flexors (in adults only).
4. Foetal tendon tensile strength was less than adult tendon tensile strength.

Bendict, Walker and Harris (1968) also demonstrated that the tensile strength of extensor muscle tendons was 20 percent greater than that of the tendons associated with flexors. Their tendon samples were all taken from the lower limb.

From equation 5.21, the model of tendon elasticity, the following relationship can be stated:-

$$\Delta L_T = \frac{L_{TR} \cdot F_M}{E \cdot A_T} \qquad [5.26]$$

Where:-

ΔL_T - is the change in length of the tendon

L_{TR} - is the resting length of the tendon

F_M - is the force exerted by the muscle on the tendon

A_T - is the cross-sectional area of the tendon

and E is Young's modulus of elasticity for tendon.

Of the variables used in this model the resting length of the tendon is known, and the muscle force will be determined, but the cross-sectional area of the tendon and the Young's modulus of elasticity remain

unknown.

The data of Ker et al. (1986) for tendon gave a value for Young's modulus of elasticity outside of the "toe region" of 1500 MPa, and reported tendon rupturing at a strain of 0.08. At maximum muscle isometric stress the strain in tendon has been shown to be 0.04 (Bobbert, Brand, de Hann, Huijing, van Ingen Schenau, Rijnsburger, and Woittiez, 1986; Morgan et al., 1978). As the tendon model used is linear there is enough information to determine the remaining parameters.

If the muscle is not pennated:-

$$F_T = F_M \qquad \text{[5.8 re-stated]}$$

then:-

$$0.04 = \frac{L_T - L_{TR}}{L_{TR}} = \frac{F_{IO}}{A_T E} \qquad \text{[5.27]}$$

If F_{IO} is known then it is possible to calculate a constant K:-

$$K = A_T.E \qquad \text{[5.28]}$$

F_{IO} is calculated using the procedure described in section 5:4.2. It is not necessary to separate the cross-sectional area of the tendon from the modulus of elasticity for the tendon.

The two assumptions in this model are that the stress-strain relationship of tendon is linear, and that the relationship between the maximum isometric force of a muscle and the extension of that muscle's tendon at that force, is constant for different muscles. The first assumption is valid outside of the "toe region" of the stress-strain curve (Ker et al., 1986). There is some indirect evidence supporting the second assumption.

The stress that a muscle can develop is greater when a muscle yields to a force than it is during either an isometric or concentric muscle action, the strain in the tendon is consequently greater. As the model parameters were determined assuming a tendon strain of 0.04 during a maximum isometric action, and as tendon ruptures at much higher strains (e.g. 0.08, Ker et al., 1986), there is still ample tendon stretch available for safety during an eccentric muscle action. Elliot and Crawford (1965) examined the tendons of adult rabbits. Their study reported that the ratio of maximum tetanic tension of a muscle to its tendon thickness was constant. This implies that for their sample the tendon properties were directly correlated with the muscle they were attached to. Such an assumption for the elbow flexors may be justified in light of the study of An, Hui, Morrey, Linscheid, and Chao (1981) who claimed that
"...an interesting and potentially useful observation has been noticed during this study. The physiological cross-section of a muscle was found to be closely correlated to its tendon cross-sectional area." (page 667).

5:4.1.3 MUSCLE PENNATION

From the dissection of four cadavers by Amis (1978) the angles of pennation of the elbow flexors were calculated. The long head of the biceps showed no pennation, the short head at its resting length had a mean angle of pennation of 3.3 degrees. Both the brachialis and brachioradialis were parallel fibred. The influence of muscle pennation on the force output of muscle fibres was examined in section 5:1.6.

5:4.1.4 MUSCLE FIBRE TYPES

Although there is a lot of data on the muscle fibre type distribution in the lower limbs, there is less data on the upper arm. One of the few studies to determine the muscle fibre type distribution for the upper limb was that of Johnson, Polgar, Weightman, and Appleton (1973). They took two muscle samples from each of six cadavers; one superficially and one from deep in the muscle belly. For muscles with more than one head "in several instances" they took samples from all the heads, but this was not the case for the biceps, and no samples were taken from the brachialis. The mean percentage of type II fibres was 53.6 for the biceps, and 60.2 for the brachioradialis. Nygaard, Houston, Suzuki, Jorgensen, and Saltin (1983) took one biopsy sample from each of four subjects from the biceps, they reported that the biceps contained a mean value of 58 percent type II fibres. MacDougall, Sale, Alway, and Sutton (1984) took one biopsy sample from 25 male subjects and found that the biceps consisted of 61 percent (± 5.1 percent) type II fibres.

There is a lack of reliable information on muscle fibre type distribution although such information is necessary for muscle modelling. Though biopsy studies provide useful information, their accuracy is questionable. Blomstran and Ekblom (1982) in a methodological examination of the estimation of muscle fibre distribution using the muscle biopsy technique, have shown that at least two samples are required to reduce the variability of the muscle fibre type distribution estimation. Lexell, Henriksson-Larsen, and Sjostrom (1983) and Johnson et al. (1973) have shown that there is regionalization in the distribution of muscle fibre types, so that one fibre type predominates towards the centre of the limb. These limitations mean that accurate biopsy data is difficult to obtain.

For the model the following values for the type II fibres were adopted: biceps 53.6 percent, brachialis 50 percent, and the brachioradialis 60.2 percent. The value for the brachialis was assigned arbitrarily, the other values were based on the data of Johnson et al. (1973). The appropriateness of these values is assessed via a sensitivity analysis in section 5:5.2.

5:4.1.5 FORCE-LENGTH MODEL PARAMETERS

The parameters required for the force-length relationship were estimated using the procedure described in section 5:4.2. Initial estimates of these parameters were required, the estimation of these parameters is discussed in this section. The parameters to be estimated are: the optimum length of the muscle fibres (L_{FO}), the maximum isometric force of the muscles (F_{IO}), and the shape parameter SK.

The resting lengths of the muscle were measured in vivo using the procedures described in section 5:1.5, the portion of these lengths which were muscle fibre were estimated using the ratio data of van Zuylen et al. (1988), see section 5:4.4.1. Close (1972) estimated that the resting length of the muscle fibres was

120 percent of their optimal length. An et al. (1989) examined the muscles causing elbow flexion and estimated the optimal lengths of the muscles. This information is not generally applicable because individuals' muscle lengths are unique. However, the authors more usefully reported that the flexion angles at which these optimal lengths occurred were 75, 78, and 80 degrees for the biceps, brachialis, and brachioradialis respectively. These figures correlate well with the data of Edgerton, Roy and Apor (1986) who examined 14 subjects performing maximum isokinetic elbow flexions at a number of different velocities. They found that the maximum moment occurred at a mean joint angle of 80 degrees. The lengths of the three elbow flexors were computed at 78 degrees of flexion, and initial estimates made of the optimum lengths of the muscle fibres assuming that the tendon in series with each of the muscles was inelastic.

Table 5.3 present the details of four studies which computed the cross-sectional areas of the muscles causing elbow flexion. It was possible to express the mean cross-sectional areas of the muscles as relative ratios. Specifically the following ratios were calculated:-

2.9	:	3.7	:	1.0
(BICEPS	:	BRACHIALIS	:	BRACHIORADIALIS)

Assuming during a maximum isometric elbow flexion, that 78 degrees of elbow flexion is the angle at which all three muscles are closest to their optimal lengths, the muscles will all be exerting near their maximum tension. The muscle moment about the joint would therefore be approximately:-

$$MM = \sum_{i=1}^{NM} r_i \,.\, SM.\ CSA_i \qquad [5.29]$$

Where:-

MM - is the muscle moment about the joint

NM - is the number of muscles (3 in this case)

r_i - is the moment arm of the i^{th} muscle

SM - is the specific tension of muscle

and CSA_i is the cross-sectional area of the i^{th} muscle.

As the approximate cross-sectional areas of the muscles are known and have been expressed in terms of the CSA of one of the muscles, equation 5.29 can be expanded and with the appropriate substitution the following equation results:-

$$MM = SM.CSA_3\left(2.9\ r_1 + 3.7\ r_2 + r_3\right) \qquad [5.30]$$

There is considerable debate in the literature as to the specific tension of muscle, e.g. Powell, Roy, Kanim, Bello, and Edgerton (1984), Ariano, Armstrong, and Edgerton (1972), and Witzmann, Kim, and Fitts (1983) have all suggested that fast and slow twitch muscle fibres have different specific tensions, whereas Hellander and Thulin (1962), Sexton and Gerston (1967), and Close (1972) have argued that they are the same. Spector, Gardiner, Zernicke, Roy, and Edgerton (1980) have proposed that this

TABLE 5.3 - Summary of the cross-sectional areas (CSA) of the major elbow flexors.

STUDY	NUMBER OF CADAVERS	BICEPS CSA (cm^2)	BRACHIALIS CSA (cm^2)	BRACHIORADIALIS CSA (cm^2)
Braune and and Fischer (1989)	4	9.0	12.4	3.0
Amis (1978)	4	5.7	5.6	1.7
An et al. (1980)	4	4.6	7.0	1.5
Edgerton et al. (1986)	4	3.8	4.7	1.8
Group Mean	16	5.8	7.4	2.0

difference occurs only when the slow twitch fibres are found in a muscle of predominantly fast twitch muscle fibres. These studies have estimated specific tension from collections of fibres. There are a number of methodological problems with such an analysis. It is not possible to guarantee that all the fibres are activated. If the muscle has any degree of pennation, the force the fibres develop will be different from that measured at the tendon. Therefore specific tension values from single fibre preparations are preferable to those from whole muscle or many fibred preparations. Lannergren and Westerblad (1987), and Stephenson and Williams (1981) from the results of the analysis of single fibre preparations reported a specific tension of muscle of 350 kPa.

As the difference between the specific tension of fast and slow twitch fibres has not been conclusively established their maximum specific tensions were assumed equal. This means that the specific tension of muscle does not need to be explicitly known to solve equation 5.30. Solution of this equation and use of the ratio information derived earlier gives estimates of the maximum isometric tensions of each of the three elbow flexors.

The shape parameter SK in the model of Hatze (1981b) has to be greater than or equal to 0.28, with no upper limit specified. SK was arbitrarily assigned an initial value of 0.50.

5:4.1.6 HILL'S CONSTANTS

Hill's constants are normally expressed as ratios of the maximum isometric force and the maximum contraction velocity of a muscle. In an extensive review of the properties of muscles, Close (1972) reported the normal range for the a/F_t ratios as 0.25-0.30 for fast twitch muscle fibres, and 0.15-0.17 for slow twitch muscle fibres, in mammalian muscles.

Herzog (1987a) used an optimization approach to find the values of 'a' and 'b' for his model of four leg extensor muscles executing a leg extension. Using Hill's model 'a' and 'b' were adjusted until the results of the model were as close as possible to the observed output of the leg extensors under various isokinetic conditions. No account was made for possible different fibre types in the leg extensors.

The procedure of Herzog (1987a) is attractive but has certain restrictions. Isokinetic contractions do not occur naturally. Even if the joint angle changes at a constant velocity this does not guarantee constant velocity in the leg extensor muscle fibres, but this constant velocity was assumed in the study of Herzog (1987a). With changing joint angle the moment arms of the muscles also change and this has a potential effect on the velocity of the muscle. Even if muscle velocity remains constant this does not mean that muscle fibre velocity is constant. Muscle velocity is the sum of tendon velocity and muscle fibre velocity, but these two values are not necessarily equal at any instant in time (e.g. Bobbert et al., 1986), with the former being dependent on muscle force, which as has been established is a non-linear function of muscle fibre length and velocity. At the higher velocities there may be no involvement of the slow fibres which will not be able to contract actively at such velocities. In this case adjustment of 'a' and 'b' will be for the fast fibres, whilst at lower velocities where both fibre types are involved, adjustment of 'a' and 'b' will be for a combination of fast and slow fibres. The optimization algorithm attempted to adjust 'a' and 'b' across

a wide range of velocities. A superior approach would have been to estimate 'a' and 'b' for the fast muscle fibres at the high isokinetic velocities. This would have given an estimate of the distribution of muscle fibre types and the constants 'a' and 'b' for the fast fibres. Slower isokinetic velocities could have been used to calculate the constants for the slow fibres, given that the contribution from the fast fibres would already have been known.

The values of the constants 'a' and 'b' are dependent on the maximum isometric force (F_I) of the muscle and the maximal contractile velocity (V_{MAX}). The maximum isometric force and maximal contractile velocity are very sensitive to variations in temperature, therefore so are 'a' and 'b'. Ranatunga (1983,1984) examined the effect of a ten degree change in temperature on the shortening velocity of rat muscle. (Q10 is the Temperature Coefficient - the measure of the increase in the rate of a process produced by raising the temperature by 10 degrees Celsius). Changing the temperature from 25 to 35 degrees Celsius had a Q10 value for fast fibres of 1.8, and 2.0 for slow fibres. Edman (1979) working with isolated frog muscle found a Q10 of 2.7 for velocity of shortening, and 1.2 for maximum tetanic force for starting temperatures from 2 to 10 degrees Celsius.

Considering the limitations of the procedure of Herzog (1987a) and the lack of other well established procedure, the values of 'a' and 'b' were taken from the literature. In light of the preceding review it was required that the muscle from which the parameters had been determined should be human skeletal muscle, examined at a temperature of 37 degrees, and that fast and slow fibres should be differentiated. A study that meets these criteria is that of Faulkner, Clafin, and McCully (1986). The ratio of a/F_I was computed, fitting the data to Hill's equation by minimising the sum of squared errors in the velocity dimension. For type II fibres the value was 0.25 and for the type I fibres 0.15. The maximum isometric force was computed using the procedure detailed in section 5:4.2, and the maximum shortening velocity was computed using the procedure given in the following section. Given these two values 'a' and 'b' were obtained from:-

$$a.V_{MAX} = b.F_I \qquad [5.31]$$

5:4.1.7 MAXIMUM VELOCITY OF MUSCLE

The maximum velocities of the muscle fibres are required for input into Hill's equation. The maximum velocity of shortening is often expressed in terms of the number of resting fibre lengths per second ($fl.s^{-1}$). Faulkner et al. (1986) examining bundles of human muscle fibres found that type II fibres had a maximum velocity of shortening of 6 $fl.s^{-1}$, and type I fibres 2 $fl.s^{-1}$. The ratio of these velocities corresponds well with animal studies. Close (1964) examined the predominantly slow twitch soleus and the predominantly fast twitch extensor digitorum longus of female Wistar rats. The speed of shortening of the extensor digitorum longus was three times faster than the soleus. The values of Faulkner et al. (1986) were used in this study.

5:4.1.8 SUMMARY

The preceding sections have detailed the sources of the parameters used in the muscle model. For those parameters determined experimentally the initial values required in the estimation procedure have been

presented. Many of these parameters are at best only approximations; their influence on the model will be assessed by a sensitivity analysis in section 5:5.2.

5:4.2 EXPERIMENTAL DETERMINATION

The previous section has provided information on most of the muscle parameters. The following parameters were determined experimentally: L_{FO}, F_{IO}, and SK. This section describes the procedure used to estimate these parameters.

The resultant joint moment was determined for maximum isometric contractions of the elbow flexors at different degrees of elbow flexion. The subject's upper body and upper arm were fixed while the degree of elbow flexion varied. The subject pulled on a handle using the elbow flexors only. The handle was attached to the force plate (Kistler 9281B12) by an inelastic steel cable. The force of the pull on the handle was measured by the force plate, which was connected to an analogue to digital converter interfaced to an Acorn BBC computer. The force was sampled at 100 Hz for a sample period of 10 seconds, and the maximum force calculated, this was assumed to reflect the force at the hand grasping the handle. Rest was allowed between each of twelve trials which were performed in a random order to reduce and distribute the effect of fatigue. Trials were rejected if the maximum force recorded via the force plate was not maintained for three seconds; if the subject considered the trial to be non-maximal; or if the subject reported wrist movement. The position and orientation of the upper arm, forearm, and hand were determined using the procedures described for the static data capture. The resultant joint moment was calculated assuming the reaction forces at the hand were in static equilibrium with the joint reaction forces. Using the assumptions discussed in section 4:4.2 the resultant joint moment was considered to be the net muscle moment about the elbow joint.

From the position and orientation of the upper arm and forearm, and using the procedures described in sections 5:1.5 and 5:1.7, the lengths and moment arms of the modelled muscles were determined for each of the trials. The net muscle moments, muscle lengths, and moment arms were all known for the 12 different joint angles. The following relationship can be stated:-

$$T_{model} = \sum_{i=1}^{NM} r_f \cdot F_{IOi} \cdot \exp\left[-\left(\frac{Q_i - 1}{SK_i}\right)^2\right] \qquad [5.32]$$

Where T_{model} is the muscle moment determined from the muscle model
The remaining variables have been described elsewhere, the addition of the i subscript provides a reference to a specific muscle.

If estimates are made of the muscle parameters the accuracy of these muscle parameters can be assessed by evaluating the difference between the muscle model predicted moment and the measured moments, over a number of trials at different joint angles. This can be stated as:-

$$U = \sum_{j=1}^{NT} \left(T_{real_j} - T_{model_j}\right)^2 \qquad [5.33]$$

Where:-
U - is the sum of the square of the difference between the experimentally measured moments and the muscle model calculated moments
NT - is the number of experimentally determined moments
T_{realj} - is the experimentally determined moment for trial j
and T_{modelj} is the moment estimated by the muscle model for trial j.

Equation 5.33 is suitable to use as an objective function in an optimization routine, where the task would be to minimise U by systematically varying the nine unknown muscle parameters. More details of the optimization procedure used are given in section Appendix D. For the optimization routine initial estimates of the parameters were required and constraints were placed reflecting the expected maximum and minimum values of the parameters.

The optimum length of the fibres was constrained to be less than the resting length of the muscle fibres and greater than half of this length. The initial estimate of the optimum length was set at the length of the muscles at 78 degrees of flexion, minus the resting length of each muscle's tendon (see section 5:4.1.5). The maximum isometric force of the muscles was estimated using the procedure described in section 5:4.1.5. The upper and lower limits were set at twice and half of these initial estimates respectively. The value of SK was constrained by the model used, see section 5:2.2, and its initial value was set to 0.50.

Equation 5.32 requires the length of the muscle fibres for each trial. For the first run of the optimization routine it was assumed that the tendon in series with each of the muscles was inelastic, therefore:-

$$L_F = L_M - L_{TR} \qquad [5.34]$$

After the first run the new estimates of the muscle parameters were used to estimate the muscle fibre lengths for each of the trials. The following relationship was used:-

$$L_F = L_M - L_T \qquad [5.35]$$

The force the muscle fibres could exert was calculated using the new parameter that was set assuming the tendon was at its resting length. Once a force had been computed the length of the tendon (L_T) was calculated using equation 5.21. A new estimate of the length of the muscle fibres was therefore obtained, so the muscle force was again estimated using this new muscle fibre length. Before each new run of the optimization routine, the computation procedure to estimate the muscle fibre lengths was repeated until the change in tendon length was insignificant (<0.0001 m). Using the revised set of muscle parameters and muscle fibre lengths, equation 5.33 was again minimised, giving new estimates of the parameters. This whole procedure was repeated until U could not be minimised further. The parameters determined using this procedure are presented in table 5.4.

TABLE 5.4 - The muscle parameters determined for the force-length model of the elbow flexors.

PARAMETER	BICEPS	BRACHIALIS	BRACHIORADIALIS
L_{MR} (m)	0.301	0.126	0.280
L_{FR} (m)	0.166	0.088	0.182
L_{TR} (m)	0.135	0.038	0.098
L_{FO} (m)	0.142	0.085	0.143
SK	0.280	0.280	0.378
F_{IO} (N)	600.6	1000.9	262.2

(N.B. - the remaining muscle model parameters can all be determined from these values.)

It was difficult to assess the accuracy of these muscle parameters. The final value of U in equation 5.33 was 1.11. The tightness of the fit of the parameters to the test data was good considering that the experimentally determined moment values can be considered to contain errors. These parameters are valid in that they gave a good fit to the experimentally determined muscle moments. But it is possible that there were other parameter combinations which may have produced a minimum. To test whether the result was a minimum, a second optimization routine was used on the same problem to see if it arrived at the same solution (see Appendix D for details of this routine). The same results were produced from both algorithms indicating that this was a minimum solution.

The solution space was limited by the constraints placed on the variables. Therefore the solution is part dependent on the validity of the constraints placed on the model parameters. The constraint placed on SK was dependent on the model used to represent the force-length relationship. The upper constraints on the optimal lengths were only that they should be less than the resting length of the muscle fibres, which is reasonable because it is unlikely that the optimal lengths of the muscle fibres would be greater than their resting lengths. If the optimal length of the muscle fibres was greater than or equal to the resting length of the muscle fibres the muscle would not be able to exert its maximum tension in vivo. The lower constraint was arbitrarily assigned to speed up the convergence of the algorithm by limiting the solution space. Validation of this assumption was obtained when the algorithm was re-run with the lower constraint being that the optimal muscle fibre length be equal to or greater than zero, and the same parameters were determined.

The final constraint was placed on the maximum isometric force of each of the three muscles. The constraint on this parameter was based on cross-sectional area data from the literature (section 5:4.1.5). The initial estimates were based on this information, see section 5:4.1.5. The maximum values were set at twice these initial values, and the minimum at half these initial values. These constraints were used to reduce the solution space and to stop the optimization routine selecting one muscle only to produce all the joint moments. The resulting ratio of the muscle forces was approximately 2.3 : 1.0 : 3.8 (biceps, brachioradialis, brachialis). These ratios are similar to those indicated in table 5.3 for the cross-sectional areas of the muscles.

The force-length relationships of the three elbow flexors are presented in figure 5.9, using the parameters determined in this section.

5:5 MODEL VALIDATION

In the preceding sections the parameters for the muscle model have been presented. To validate the model of the force-length relationship an independent test is required, as the tightness of the fit of the model to the experimental data in not an independent assessment. The parameters for the force-length model were also used to determine the parameters for the force-velocity model. Therefore a validation of the muscle model under dynamic conditions is required, which would effectively assess both the force-length model, and force-velocity model simultaneously. To accomplish a validation of the model a simulation of movement was undertaken, using the muscle model. By comparing the results from the

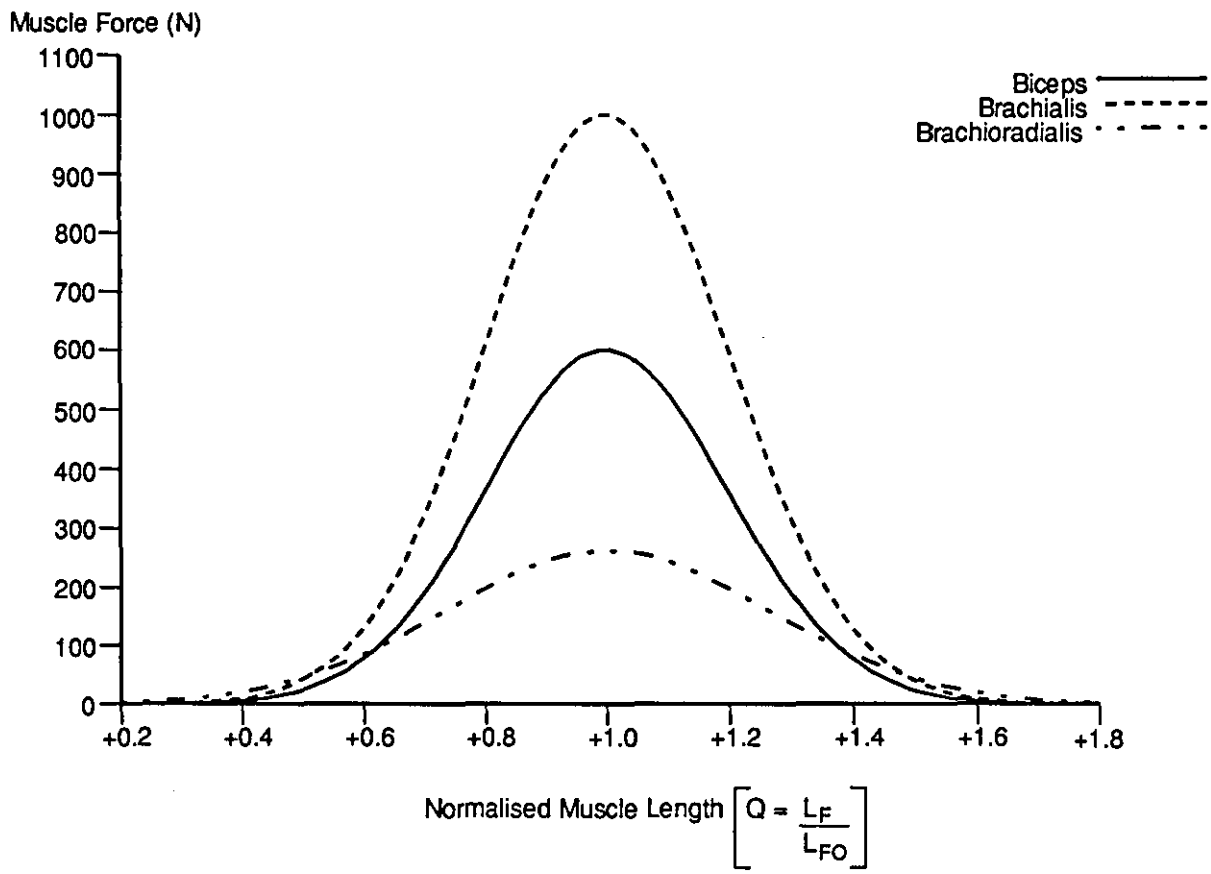

FIGURE 5.9 - The force-length relationship for the elbow flexors.

simulation with the actual performance, an assessment of the validity of the model could be made. The following sections present the details of the simulation and the results.

5:5.1 SIMULATION PROCEDURE

Trial #4 was a dumbell curl at maximum speed. It was therefore assumed that during part of this movement the three elbow flexors in the model were being maximally stimulated simultaneously. As the activity started with the dumbell still and no movement of the upper arm, during the initial phase of the curl the muscles are assumed to have been at non-maximal stimulation but to have rapidly reached a maximum once the movement started. As the initial degree of activation in each of the muscles remains unknown, it is only valid to assume maximum activation during the middle phase of the activity. After the middle phase the subject must slow the dumbell down to avoid personal damage at the extreme of joint flexion. A simulation routine was developed which permitted the estimation of the muscle moments during this middle phase of the dumbell curl, assuming maximum activation. By comparing the results from the simulation with the muscle moments computed using inverse dynamics, it was possible to assess the accuracy of the parameters used for the muscle model.

The force in the tendon is equal to the force in the muscle fibres, if the fibres are not pennated. As the model used for the stress-strain relationship of tendon is linear, the stiffness of the tendon is constant for all lengths of the tendon, and is given by:-

$$K = \frac{dF_T}{dL_T} = \frac{dF_M}{dL_T} \qquad [5.36]$$

Where K is the stiffness of the tendon

The rate of change of the muscle force is the product of tendon stiffness and the rate of change in length of the tendon. The following relationship can be stated:-

$$\frac{dF_M}{dt} = \frac{dF_T}{dt} = \frac{dF_T}{dL_T} \cdot \frac{dL_T}{dt} \qquad [5.37]$$

The rate of change in tendon length is equal to the difference between muscle velocity and muscle fibre velocity:-

$$\frac{dL_T}{dt} = V_m - V_F \qquad [5.38]$$

Re-arrangement of equation 5.18 allows muscle fibre velocity to be calculated from muscle force:-

$$V_F = \frac{b(F_1 - a)}{(F_m + a)} - b \qquad [5.39]$$

Substitution of equation 5.38 into equation 5.37 gives the following:-

$$\frac{dF_M}{dt} = K\left(V_M - V_F\right) \qquad [5.40]$$

The ordinary differential equation in equation 5.40 was solved using a variable step-size fifth order Runge-Kutta technique (Press, Flannery, Teukolsky, and Vetterling, 1986). The length of the muscle was computed for each sample interval using the procedures described in section 5:1.5. Differentiating the length of the muscle with respect to time using the spline routine described in section 3:4.5 gave the velocity of the muscle (V_M). The velocity of the muscle fibres (V_F) was calculated using equation 5.39. To reduce the size of the integration step the data was interpolated over a new time base ($\Delta t = 0.0001$). At each sample interval once the muscle force had been computed the new length of the muscle fibres was computed, by integrating muscle fibre velocity. This new muscle fibre length was used to compute the maximum isometric force (F_l) for input into equation 5.39, and this value of maximum isometric force was used for the next integration step. The initial values for the muscle forces were set for the integration assuming that each of the muscles was exerting a maximal isometric action.

This procedure was repeated for each of the muscles in the model. Once the muscle forces had been computed, this information was combined with the muscle moment arm information to estimate the muscle model moment:-

$$T_{model} = \sum_{i=1}^{NM} r_i \cdot F_{Mi} \qquad [5.41]$$

Where:-

T_{model} - is the muscle moment estimated by the muscle model

NM - is the number of muscles

r_i - is the moment arm of the i^{th} muscle

and F_{Mi} is the force exerted by the i^{th} muscle.

5:5.2 RESULTS

To assess the accuracy of the model the moments computed using it were compared with the moments computed using inverse dynamics. Because the model assumed maximal activation throughout the movement, and this was only assumed to occur in the middle section of the actual movement, comparison between the two data sets was only performed for the middle section of the data, commencing after 30 percent of the activity and stopping after 80 percent. Figure 5.10 shows the moment predicted using the model and that produced using inverse dynamics.

The sensitivity of the model to the parameters was assessed by varying certain parameters in the model and seeing the change in the model predicted moments compared with those produced by inverse dynamics. The results of this analysis are presented in table 5.5. If all the muscle fibres were considered to be type I fibres, the difference between the muscle model produced moment and that produced by inverse dynamics was greater than with the original parameter set. If all the fibres were considered to be type II fibres the decrease in accuracy was not as great as when the fibres were considered to be all type I fibres. When the fibre type distribution for each of the muscles was assumed to be 50 percent for each of the two fibre types there was an increase in accuracy of the muscle model to inverse dynamics fit. This either indicates that this ratio was closer to the actual fibre type distribution of the subject than the ratio originally chosen, or that changing this parameter in the model accounted for some unknown deficiency in

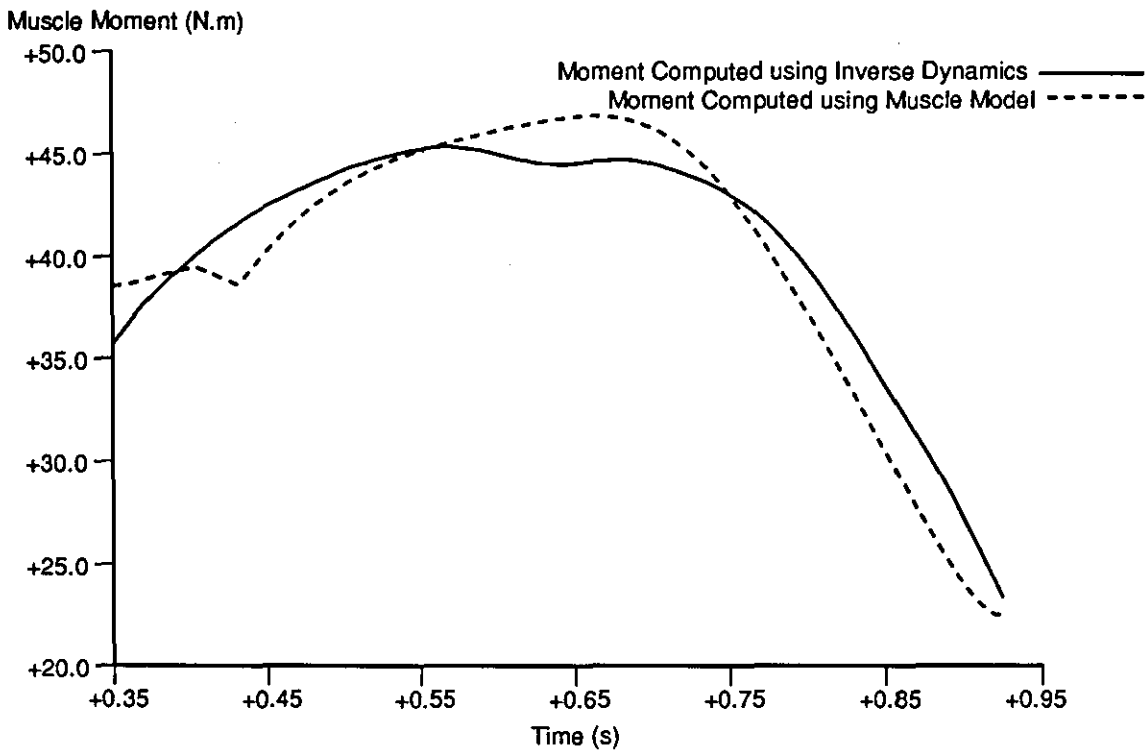

FIGURE 5.10 - The muscle moment for a dumbell curl (trial #4) predicted using a muscle model, and that predicted using inverse dynamics.

TABLE 5.5 - The difference between the muscle moment at the elbow joint during flexion, computed using a muscle model and inverse dynamics, when the parameter values for the muscle model were varied.

CHANGE IN MODEL PARAMETER	MEAN DIFFERENCE (N)	STANDARD DEVIATION	% ROOT MEAN SQUARED DIFFERENCE
Original parameter set	1.37	2.22	6.59
All fibres considered type I	16.80	5.07	44.37
All fibres considered type II	-5.94	3.87	17.91
50% type I, and 50% type II fibres	0.37	2.15	5.50
Tendon strain 0.08 at F_{IO}	-3.39	3.49	12.28
Tendon inelastic	0.83	3.70	9.55
Pedotti parameter set	0.12	3.54	8.93
Muscle moment arms increased by 5%	-0.49	2.38	6.12
Muscle moment arms decreased by 5%	3.23	2.15	9.81
Muscle moment arms increased by 10%	-2.36	2.59	8.85
Muscle moment arms decreased by 10%	5.10	2.16	14.00

one or more of the other parameters in the model.

Tendon elasticity was changed to assess the sensitivity of the model to this parameter. In the muscle model of Bobbert et al. (1986) the tendon was assumed to exhibit a strain of 0.08 when the muscle exerted its maximal isometric force, therefore in the present model this value was substituted for the value of 0.04 in equation 5.27. The muscle model predicted muscle moment compared much less favourably with the inverse dynamics predicted moment when tendon had this degree of elasticity. The performance of the model was investigated when the tendon was assumed inelastic. In this case the tendon remained at its resting length, and muscle fibre velocity was equal to muscle velocity. The model fit was more accurate for this parameter change than the other parameter change for the tendon model, but was not as accurate as with the original parameter set.

Pedotti, Krishnan, and Stark (1978) included a muscle model in their examination of the muscle forces during human walking. For this model they assumed a/F_l was equal to 0.30 for all the muscle fibres making up the muscle, this is higher than the value used here. They also assumed that the maximum velocity of the muscles was 2.5 $fl.s^{-1}$ (resting fibre lengths per second). These parameter values were substituted into the model. The mean error was very small with these values but the standard deviation of the difference was much larger, as was the %RMS difference, than with the original parameter set.

To determine the moment caused by each muscle about the joint it is necessary to calculate their moment arms. The final analysis looks at the sensitivity of the model to changes in this variable. For each sample interval the moment arm was either increased or decreased by five or 10 percent. These changes generally resulted in an increase in the difference between the two data sets. In the case where the moment arms were increased by five percent there was a small decrease in the difference between the two data sets, which could be explained by some error in the moment arm information or because the changes in this variable accounted for a deficiency in one or more of the other parameters. The moment arms were calculated assuming that the muscles acted in straight lines, whereas the line of action of the muscles and therefore their moment arms could be altered by a number of factors, see section 5:1.4. There may have been errors in the location of the origins and insertions of the muscles. Therefore the precise source of any errors in the moment arm information is hard to identify. The change in the accuracy due to increasing the moment arm by five percent did not provide a large increase in model accuracy compared with the original parameter set.

The preceding analysis constitutes a limited sensitivity analysis on some of the parameters and one of the variables in the muscle model. This analysis has indicated that the original parameter set produced estimations of the muscle moments in close agreement with the muscle moments as determined by inverse dynamics. The muscle fibre type distributions were the parameters in the original parameter set based on the least information. When these parameters were changed so the muscles all had equal proportions of type I and II fibres, the muscle model showed closer agreement with the muscle moments computed using inverse dynamics. Therefore for all subsequent analyses the fibre type distribution was changed to 50 percent type I and type II fibres for all the muscles.

This sensitivity analysis was limited as the parameters have only been changed for all muscles simultaneously, and for a limited number of parameter value changes. This was necessitated because the muscle force estimation procedure was very slow, taking over 30 minutes of CPU time per muscle for the trial investigated. However the analysis performed here has shown that the model gives reasonable accuracy in predicting muscle moments during maximal activity. The muscle model and parameters are therefore presumed to have a degree of validity, although they were examined here for a maximal activity, and in the next chapter they are used to examine sub-maximal activity.

5:5.3 MODEL ASSUMPTIONS

There were a number of assumptions in the muscle model developed in this chapter. This section identifies those assumptions which are pertinent to the simulation procedure just described. The model assumed that only three muscles were responsible for elbow flexion, and these muscles were assumed to be maximally active. There were a number of variables used as inputs to the model: moment arms, muscle lengths, and muscle velocities. The accuracies of all of these variables are dependent on the accuracy with which the estimations of the origins and insertions of the muscles were calculated, and on the assumption of a straight line of action between origin and insertion. To obtain the velocity of the muscle it was necessary to differentiate the muscle length with respect to time. Such differentiation is a source of error as discussed in section 3:4.8. Finally the model had to assume that tendon elasticity was constant, and that by comparison muscle fibre elasticity was insignificant.

5:5.4 SUMMARY

The earlier sections of this chapter presented a muscle model, these later sections have been concerned with the validation of this model and its parameters. The model parameters, although many are estimates, demonstrated a reasonable accuracy in predicting muscle forces during maximal activity.

5:6 MUSCLE ENERGETICS

The energy necessary for the interaction of the contractile proteins comes directly from adenosine triphosphate (ATP). ATP is a high energy compound which when broken down to adenosine diphosphate and a phosphate group produces energy. There are four potential sources of ATP: that stored in the muscle; from the breakdown of phosphocreatine; and from aerobic, and anaerobic glycolysis. The contractile proteins utilize this energy to do work, a by product of which is heat. It is the purpose of this section to review the sources of heat and work in active muscle, and to present expressions which estimate the rate of energy consumption. These expressions will be used in the next chapter to formulate an objective function used to estimate muscle forces.

There are three components associated with heat production in a muscle.

1. Resting heat - which provides the base line, and is constant.
2. Initial heat - produced when a muscle is active.
3. Recovery heat - liberated after contraction, as the muscle recovers.

By studying the liberation of these heats, which have been assumed to mirror the energetics occurring in

the muscle, greater understanding has been achieved of the energetics of a muscular contraction. The initial heat varies depending on whether the muscle is acting isometrically, concentrically, or eccentrically. This review will focus on the initial heat.

5:6.1 SOURCES OF ENERGY CONSUMPTION

Mommaerts (1969) showed that the rate of energy consumption as a result of a muscular contraction was the sum of five components:-

$$E = AHR + MMHR + MSHR + MWR + DHR \qquad [5.42]$$

Where:-

E - is the rate of energy consumption of an active muscle

AHR - is the activation heat rate

MMHR - is the muscle maintenance heat rate

MSHR - is the muscle shortening heat rate

MWR - is the mechanical work rate of muscle

and DHR is the rate of energy dissipation in the passive structures.

Stein, Oguztoreli, and Capaday (1986) formulated a similar expression but included a term for the rate of energy expended at rest. This rate was not included in the above expression as only the heat required above resting level for a muscular contraction was considered.

Gibbs (1978) was concerned about the division of the heat produced by muscle into various components "The adoption of such a format does not imply a belief that the basis for such a subdivision is interpretable at a molecular level. It seems that at best these equations are phenomenological and may obscure rather than enhance thermodynamic understanding of how muscle functions." (page 185).
As endeavours are made to further understand muscle function, these divisions are still made and are justified as they account for all of the heat released during a muscular contraction.

The final term in equation 5.42 is due to the rate of energy dissipation in the muscles due to the viscous component of muscle. The contribution to E from DHR is small compared with the other sources (Hatze and Buys, 1977) and so is ignored in the model developed here, and therefore it is not further discussed in this review.

5:6.2 MECHANICAL WORK

Work is done when a force moves an object through a distance, therefore the mechanical work rate of a muscle is the product of the muscle force and its contraction velocity. The expression for the work rate of muscle is:-

$$MWR = F_M.V_F \qquad [5.43]$$

Where:-

F_M - is the force exerted by the muscle fibres

and V_F is the velocity of contraction of the muscle fibres

5:6.3 ACTIVATION HEAT

Hill (1949a) defined the activation heat as a

"... 'triggered' reaction setting the muscle in a state in which it can shorten to do work." (page 210)

The knowledge of the mechanisms causing this heat have evolved since the definition was suggested. The process of activation involves the release of calcium ions, the binding of these ions to the troponin, and the other reactions associated with initiating the cross-bridge cycle. Woledge (1971) related the activation heat rate to the release and uptake of the calcium ions by the sarcoplasmic reticulum. Activation heat was defined by Homsher, Mommaerts, Ricchiuti, and Wallner (1972) as

"...the thermal accompaniment of the liberation of calcium into the sarcoplasm, its movements to and from the myofibrillar binding sites and its return to its storage site by an ATP dependent transport system in the sarcoplasmic reticulum." (page 602).

This is the only portion of the heat production not associated with the consequences of the interaction of actin and myosin. Woledge (1971) gave the following equation for quantifying activation heat rate:-

$$AHR = H_a.\exp(-a.t) \qquad [5.44]$$

Where:-

AHR - is the heat rate due to activation

H_a - is the activation heat rate constant

a - is a constant

and t is time.

To study this heat the muscles are stretched before stimulation so that cross-bridges cannot form between the actin and myosin filaments, therefore no tension develops and the heat liberated is entirely due to the activation heat. Homsher et al. (1972) used such a protocol when studying the activation heat in frog semitendinosus muscles and found that activation heat accounted for 20-25 percent of the total heat of an isometric contraction at optimal length. Similar results were presented by Smith (1972). Kean, Homsher, Sarian-Garibian, and Zenplenyi (1976) during a five second stimulus of muscle, found that 50 percent of the activation heat was accounted for by ATP splitting. The remaining heat was assumed to come from the activation process involving calcium, for example the release of the calcium, and the binding of the calcium to the troponin, and to the parvalbumin. Fraser (1972) used infra-red to measure the temperature of amphibian skeletal muscle, and suggested that the binding of the calcium to the troponin-tropomyosin contributed to the activation heat.

5:6.4 MAINTENANCE HEAT

Maintenance heat is the heat required to maintain a force. It is therefore dependent on the amount of tension in the muscle.

Aubert (1956) modelled the heat production during an isometric contraction, excluding the activation heat, with the following expression:-

$$MMHR = Hl.\exp(-Lt) + Hb \qquad [5.45]$$

Where:-
MMHR - is the maintenance heat rate
Hl - is the labile heat rate
L - is a labile heat constant
t - is time
and Hb is the stable heat rate.

The rate of labile heat production becomes stable during the first five seconds at zero degrees Celsius in frog muscle. The claim of Woledge (1971) that labile heat is associated with activation is confirmed, as the amount of heat is independent of length and tension in the muscle. Woledge also claimed that stable heat is due to actin and myosin interaction. Abbott and Howarth (1973) confirmed that 75-80 percent of the stable heat is due to the actin and myosin reaction, whilst the remainder is dependent on activation.

Early work by Hill (1938) examined the rate of energy consumption in maximally active muscle, and identified all the sources of heat that Mommaerts (1969) identified except for the rate of dissipation of heat in the passive structures. Hill (1938) presented the following equations for the rate of energy expenditure for a fully active muscle:-

$$e = h + F_M.V_F \qquad [5.46]$$

Where:-
e - is the rate of energy consumption
and h is rate of heat production

The activation and shortening heat were shown to be the sum of:-

$$h = hm + MSHR \qquad [5.47]$$

Where:-
hm - is the maintenance and activation heat

Hill (1964b) re-examined this work and showed that the maintenance and activation heat were approximately equal to the product of the force velocity coefficients 'a' and 'b'.

$$AHR + MMHR = hm = a.b = (a/F_l).(a/F_l).F_l.V_{MAX} \qquad [5.48]$$

Woledge (1971) examined the use of the product 'a' and 'b' as the maintenance heat. Heat measurements have only been made on the muscles of a few species of animals. He found this assumption to be supported by experimental evidence from frog (Hill, 1938) and tortoise muscle (Woledge, 1968), but not for muscle from chicken (Cranfield, 1971). This assumption has not been validated for human muscle, although similar energetic modelling based around this assumption has been undertaken (e.g. Hatze and Buys,1977; Davy and Audu, 1987).

5:6.5 SHORTENING HEAT

To discuss the shortening heat it is necessary to describe the Fenn Effect. Fenn (1923,1924) found that the total energy liberated during a contraction (the sum of the heat released and the work performed) increased if the muscle was allowed to shorten and therefore to do work. Prior to this it had been believed that a set amount of energy was available as a consequence of stimulation, and that this energy would appear as heat and work, with the precise ratio depending on the conditions under which the muscle operated (e.g. load, length change). This result showed that the events associated with a muscle action are dependent on chemical changes, and that these changes are regulated by the load on the muscle and the amount of shortening. The measures made in these early studies of Fenn were erroneous due to a calibration error (Hill and Woledge, 1962), but the principle presented is still upheld.

The shortening heat rate is the heat produced by the muscle as it shortens. It is proportional to the degree of activation and the velocity of shortening

As muscle fibres shorten the muscle liberates heat. Curtin and Woledge (1978) attributed this heat to the increased rate of cross-bridge cycling, which leads to an increased rate of ATP splitting.

Hill (1938) claimed that the shortening heat rate for a fully active muscle is:-

$$MSHR = a.V_F \qquad [5.49]$$

Where:-

a - is the constant from Hill's force-velocity equation

and V_F is the absolute velocity of shortening .

Hill (1964a) showed after more sensitive measurements of isolated muscle that the coefficient 'a' was not, as he had originally believed, the coefficient of the shortening heat. The term alpha was introduced Where:-

$$\alpha = 0.18\ F_l + 0.16\ F \qquad [5.50]$$

Therefore the rate of heat production becomes:-

$$h = hm + V_F.(0.18\ F_l + 0.16\ F) \qquad [5.51]$$

or

$$h = hm + V_F.\alpha \qquad [5.52]$$

Woledge (1968) suggested that the ratio a/F_l is related to the thermodynamic efficiency of muscle. Wendt and Gibbs (1973) examining rat muscle claimed that slow twitch muscle fibres are more efficient than fast twitch muscles, at sustaining a contraction. This 1973 study seems to verify the claim of Woledge, as results from various sources (e.g. Wells, 1975, Close, 1972, and Faulkner et al., 1986) report the type II fibres having a higher a/F_l ratio than type I fibres.

Homsher and Kean (1978) found that the shortening heat is influenced by the degree of filamentary overlap. This relates to equation 5.51 as according to the work of Gordon et al. (1966) the F_l will vary with the degree of filamentary overlap.

5:6.6 HEAT OF ECCENTRIC MUSCLE ACTION

So far the discussion has only dealt with concentric muscle actions; in this section the heat production during an eccentric muscle action will be briefly discussed. Abbott, Aubert, and Hill (1951) and Abbott and Aubert (1951) showed that as muscles were subjected to a slow stretch the rate of heat production increased, but the proportion of heat output to work done decreased compared with equivalent concentric studies. Hill and Howarth (1959) showed that by stretching an active muscle much faster than in the study of Abbott et al. (1951) it was possible to reduce the heat given out by the muscle, and in certain conditions it was possible to reduce this heat to zero. Chemical measurements on stretched muscles have shown that there is less ATP usage during these contractions than during an isometric contraction (Curtin and Davies, 1975). Gillis and Marechal (1974) studied the incorporation of radio-active labelled phosphorus into ATP of rabbit muscle, and examined eccentric muscle action. The amount of the phosphorus incorporated was very small during stretches, which suggested that the re-synthesis of ATP was of less importance during these stretches.

The present study does not attempt to model the energetics of eccentric muscle actions. This has been undertaken by Fitzhugh (1977) who by making assumptions about that the maximum force of an eccentric muscle action and by setting the constants in Hill's equation as direct ratios to this value, provided equations to estimate the heat production during eccentric muscle action.

5:6.7 SUMMARY

The energetics of muscular contractions were discussed in this section. Given the information presented in this section it is possible to formulate a model which gives the rate of energy consumption associated with a muscular contraction. The model used equations 5.43, 5.48, and 5.51.

CHAPTER VI

ESTIMATING MUSCLE FORCES

INTRODUCTION

The purpose of this chapter is to detail the procedures used to estimate the individual forces in the muscles causing elbow flexion. The problem of estimating muscle forces is discussed in the first section. There have been a number of techniques used to estimate muscle forces and these are reviewed in the next sections. Procedures for determining muscle forces using static optimization procedures are discussed. The following sections present a comparison of a number of techniques. The final section presents a new procedure for the estimation of individual muscle forces.

6:1 THE PROBLEM OF ESTIMATING MUSCLE FORCES

In section 4:4.2 it was shown that given appropriate kinematic and kinetic information and by making certain assumptions, it is possible to compute the moments caused by the muscles. These muscle moments represent the net effect of all the muscles acting about a joint. The system producing these moments and forces is generally redundant, therefore finding the individual contribution of each muscle to a joint moment is an indeterminant problem. To illustrate the problem an example is given.

The upper limb is modelled as a two segment, planar, frictionless, articulated linkage. The forearm and hand are considered one segment, the upper arm the other; these two segments articulate about a pin joint. Joint flexion is assumed to be caused by three muscles: the biceps, brachialis, and brachioradialis. The moment about the y axis is:-

$$MM_Y = \sum_{i=1}^{NM} R_i \cdot F_{Mi} \qquad [6.1]$$

Where:

MM_Y - is the muscle moment about the Y axis, which is coincident with the flexion axis of the elbow

NM - is the number of muscles

R_i - is the moment arm of the i^{th} muscle

and F_{Mi} is the muscle force of the i^{th} muscle.

Using the subject specific muscle data gathered in the last Chapter, the muscle moment arms were computed for the elbow joint flexed to a joint angle of 90 degrees. Although not strictly the case the muscles were assumed to be able to exert a maximum isometric force at this joint angle equal to the force they could exert at their optimal lengths. This information is presented in table 6.1. If a muscle moment of 10 N.m is acting about the Y axis it can be deduced from equation 6.1 that any one of the three muscles in the model could produce this moment. The graph in figure 6.1 represents the solutions available to this problem. It can be seen that there are an infinite number of solutions available in the solution plane for this problem. This analysis assumes that there was no co-contraction of the antagonists at the elbow joint.

TABLE 6.1 - The maximum muscle force, and the moment arm for a two-dimensional example of isometric elbow flexion.

MUSCLE	MOMENT ARM	MAXIMUM FORCE	MAXIMUM MOMENT
BICEPS	0.036 m	600.6 N	21.6 N.m
BRACHIALIS	0.021 m	1000.9 N	21.0 N.m
BRACHIORADIALIS	0.054 m	262.2 N	13.9 N.m

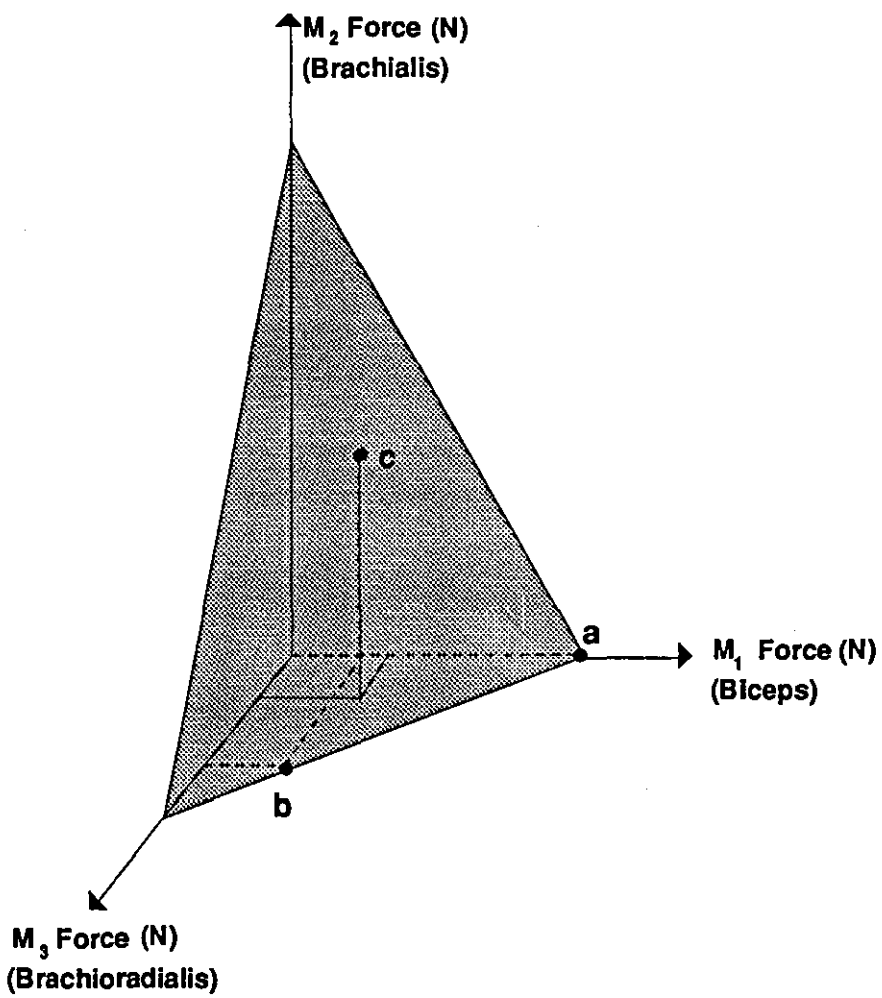

FIGURE 6.1 - Diagram showing the possible solutions for the three elbow flexors producing a joint torque of 10 N.m. The solution plane is shaded. Point **a** represents a solution using one muscle only, point **b** uses two muscles, and point **c** uses all three muscles to satisfy the moment.

In essence it can be stated that it is not possible to compute the muscle forces causing a movement using kinematic and kinetic information only, if the number of muscles is larger than the number of degrees of freedom at the joint. Therefore to estimate the individual muscle forces it is necessary to gather more information so that the solution becomes determinant. This is normally done by placing restrictions on the physiological system, for example the maximum force that any one of the muscles can exert.

6:2 REVIEW OF METHODS: ESTIMATING MUSCLE FORCES

There are a number of ways of estimating individual muscles forces; for ease of reviewing these are divided into five categories.

6:2.1 DIRECT MEASUREMENT OF MUSCLE FORCES

A strain gauge of some kind fitted to the tendon has been used to measure the sum of the forces produced by the motor units in the muscle attached to the tendon. Such an approach has been taken in a number of animal studies. Walmsley, Hodgson, and Burke (1978) measured the force produced by the medial gastrocnemius and soleus of the cat during locomotion. Van den Bogert, Hartmann, Schamhardt, and Sauren (1988) determined the force in the digital flexor of a horse using a liquid metal strain gauge (Riemersa and Lammertink, 1988). As such techniques are highly invasive there have been few studies using these techniques in man. Komi, Salonen, Jarvinen, and Kokko (1987) have measured the force in the Achilles tendon of man during locomotion.

There are a number of drawbacks in the direct measurement of muscle forces. Hahs and Stiles (1989) have shown that buckle transducers attached to muscles may not only measure the muscle force but also the other forces acting on the limb. As the techniques used are highly invasive, measured muscle forces may not be representative of what actually occurs in the muscle during normal activity. To measure the force in a muscle it must be accessible, restricting which muscles can be examined. As a consequence of this restriction not all the muscles crossing a joint can necessarily have their muscle forces measured.

In the future direct measurement of muscle force in man may become technically more viable, at which time such measures could be used to validate other non-invasive methods used to estimate muscle forces.

6:2.2 ESTIMATING MUSCLE FORCES FROM ELECTROMYOGRAPHY

Electromyography (EMG) is used to study the electrical activity produced by a muscle. The measurements of Lippold (1952) suggested that the mean rectified integrated EMG is linearly proportional to the muscle contractile force for isometric contractions. This relationship has subsequently been supported by other researchers (e.g. Komi, 1973; Hagberg, 1979). By taking into account the force-length and force-velocity relationship of muscle, it has been argued (Hof and van den Berg, 1981a) that this linear relationship holds for dynamic contractions. This linear relationship between force and rectified integrated EMG for isometric actions has been questioned by some researchers, for example Simons and Zuniga (1970), and Rau and Vredenbreght (1973). The latter researchers claimed that this relationship is quadratic. Hof and van den Berg (1977) suggested that the failure of researchers to find a linear

relationship was due to them only analysing one of the muscles causing the measured joint moment. In their analysis of plantar flexion when the weighted sum of the integrated EMG of the triceps surae and tibialis anterior were considered, a linear relationship was found between the EMG signal and muscle forces, but when each muscle was considered individually such a clear relationship was not found. The problem with such techniques is that there are many methodological problems associated with the use of EMG which may explain these difference (Bigland-Ritchie, 1981).

The model developed by Hof and van den Berg (1981a-d) predicted individual muscle activity by assuming that the relationship between integrated EMG and muscle activity is linear. Their model included a model of muscle which incorporated a contractile component demonstrating a linear force-length and a non-linear force-velocity relationship, as well as a SEC and PEC. After the experimental determination of muscle parameters the model was evaluated by comparing plantar flexion moments predicted by the model with values determined from a kinetic analysis of the movements. Hof and van den Berg (1981b) reported RMS errors in predicting plantar flexion moments from 4 N.m to 19 N.m, for eight subjects whose peak moments were between 80 and 180 N.m. Comparison of the computed moments with those estimated by the EMG driven muscle model for slow concentric muscle actions produced peak errors of 50 N.m (Hof and van den Berg, 1981c). In a later analysis of stepping and walking by Hof, Pronk, and van Best (1983), the muscle moments computed via a kinetic analysis were compared with those predicted by the EMG model. Although not explicitly reported, analysis of their figure 1 suggests that for the five subjects peak differences were all in excess of 40 N.m.

Olney and Winter (1985) presented a model which considered the activity of the ankle dorsiflexors and plantarflexors, and the knee extensors and flexors during walking. Four different models were evaluated by comparing the muscle moments computed by the EMG model with those produced after an inverse dynamics analysis of the activity. The most complex model gave the most accurate results. The muscle model employed was quite simple, with force-length and force-velocity both modelled using linear relationships. The RMS error for this model in predicting ankle moments for four subjects during walking was 8.1 N.m. An interesting observation about these two EMG driven muscle models (Hof and van den Berg, 1981a-d; Olney and Winter, 1985) is the difference in the way in which the EMG signals were processed. Hof and van den Berg (1981a-d) used a band-pass filter on their EMG signal (30-600 Hz) whereas Olney and Winter (1985) used a low-pass filter, with the highest cut-off frequency for the EMG signal from any one of the muscles being 2.8 Hz.

There are many methodological problems associated with obtaining a reliable and quantifiable EMG signal (Hof, 1984; Bigland-Ritchie, 1981). Both of the techniques reviewed required extensive calibration. These techniques are invasive and not all the muscles of interest may be accessible if surface electrodes are to be used.

6:2.3 DYNAMIC OPTIMIZATION

The basic methodology in dynamic optimization is that the human body segment dynamics are modelled (e.g. Marshall, Jensen, and Wood, 1985; Pandy and Berme, 1988), using such a model the joint moments

have to be found which cause the body segments to move so that some performance criterion is maximised. The joint moment generators are complex muscle models in the more sophisticated models, in which case the optimization procedure has to find the activation of the muscles necessary to produce the body motion which will maximise some performance criterion. Although this methodology intends to examine the control mechanisms of human movement, if the simulated movement compares well kinematically and kinetically with the measurements on an experimental subject, the muscle activity can be inferred from the simulation. Such studies can also be called optimal control problems.

Hatze (1976) examined a task where a subject had to kick a target as quickly as possible. A weight was attached to the foot to make this kicking motion slow. The performance criterion was to minimise the time to perform the action. A two segment model was used, with five muscles. The muscle model included a SEC, PEC, and a contractile component which had a non-linear force-length, and force-velocity relationship. A model of the activation dynamics was also included. The simulated movement showed close correspondence with the actual performance. In later work Hatze (1981c) used a 17 segment, 46 muscle model to perform a two-dimensional analysis of long jumping. The performance criterion was to achieve maximum horizontal distance. The more complex muscle model of Hatze (1978) was used for these simulations. The ground reaction forces predicted using the optimal solution compared well with those measured using a force plate. Hatze (1983) claimed that the differences between an optimal simulation of a long jump and the actual performance of an athlete indicated potential for improved technical execution of the skill.

Zajac, Wicke, and Levine (1984) examined jumping caused by plantar flexion only. Both maximal vertical and horizontal jumps were examined. The performance criterion was to maximize horizontal or vertical displacement of the centre of mass of the body. Three different muscle models were evaluated, the most complex included a SEC, and a contractile component with force-length and force-velocity relationships. The force-velocity relationship was assumed to be linear, and the moment arm of the triceps surae at the ankle was assumed to remain constant. Given initial starting conditions the activation of the triceps surae had to be calculated which would satisfy the performance criterion. Kinematic data were also presented for one experimental subject performing a maximum vertical jump, this showed reasonable temporal correspondence with the model predictions. A later study by the same research group modelled more body segments and used a more sophisticated muscle model. Pandy, Zajac, Sim, and Levine (1990) presented a four segment eight muscle model of the human body jumping, with the performance criterion being that the centre of mass of the body should obtain maximum vertical displacement. The kinematics and kinetics of the model of jumping were compared with measurements made on eight subjects performing maximum vertical jumps, Pandy and Zajac (1991). The mean kinematics and kinetics of the subjects jumping showed good temporal correspondence with those derived from the model.

For maximum effort jumping studies (Hatze, 1981c; Zajac et al., 1984) a performance criterion is easily established; maximal vertical or horizontal distance. In other movements such a criterion is not easily identified, particularly for everyday activities. Therefore these techniques are not generally applicable.

Marshall, Wood, and Jennings (1989) simulated the two-dimensional segmental kinematics of the single stance phase of walking. Using the start of the stance phase as the initial condition, the movement was simulated with the performance criterion being constrained so that the body should end in the same final position as was achieved in the actual movement. Seven different objective functions were investigated with their appropriateness being assessed by comparing how well the simulated movements compared with the actual movements. The three objective functions which gave the best results were minimising the sum of the joint moments, minimising the segmental angular jerks, and minimising the sum of the segmental mechanical energies. This model did not include muscle. For comparison purposes the kinematics of the body were considered in three groups: head and trunk; the support leg; and the free leg. Their results highlight the problem in finding a general performance objective for an everyday activity such as walking, as none of the criterion provided the best results for all three groups. The authors hypothesised that a different performance criterion may be operating for each body part.

6:2.4 CONTROL MODELS

In these techniques the way in which the system is controlled is assumed to be known. There is no optimization of some criteria. The simplest control model is to assume that the muscles satisfy the muscle moment in some fixed ratio of individual forces. Bankov and Jorgensen (1969) assumed that the muscles causing elbow flexion exerted forces in a ratio similar to the masses of the muscles. This resulted in:-

$$\text{BICEPS FORCE} = \text{BRACHIALIS FORCE} = 2 * \text{BRACHIORADIALIS FORCE} \qquad [6.2]$$

Using a similar model, Simpson (1975) assumed that the three major elbow flexors produced forces in proportion to their cross-sectional areas, therefore:-

$$\text{BICEPS FORCE} = 2 * \text{BRACHIALIS FORCE} = 2 * \text{BRACHIORADIALIS FORCE} \qquad [6.3]$$

Such a procedure was also used by Amis, Dowson, and Wright (1980). The ratios in equation 6.3 are somewhat different from the ratios of the cross-sectional areas discussed in section 5:4.1.5.

These criteria have some physiological basis, as the force a muscle can exert is proportional to both its mass, and its cross-sectional area. None of these criteria takes into account the force-length or force-velocity relationships of the muscles.

Pierrynowski and Morrison (1985a,b) examined the muscle forces in walking. The muscle model used incorporated a SEC for both the muscle fibres and tendons, and a contractile component exhibiting non-linear force-length and force-velocity relationships. Muscle length and velocity were obtained from the three-dimensional kinematics of the movement, and this information was combined with information concerning the previous activity of the muscles, to compute the length and velocity of the muscle fibres and tendons. Using the muscle model and a model of activation, the maximum and minimum force each muscle could produce at each sample interval was calculated. A control model then selected the muscles to satisfy the resultant joint moments, which took into account the muscle fibre type distribution.

By assuming that muscle activation in the triceps surae was maximal throughout a vertical jump, Bobbert, Huijing, and van Ingen Schenau (1986) estimated the forces produced by these muscles. A Hill type model of muscle was used, (Hill, 1938). The muscle lengths were obtained from kinematic data of the movement of the limbs. Solution of a first order differential equation gave the muscle forces. To evaluate the accuracy of the model the muscle moment was estimated from a kinetic analysis of the movement and compared with the muscle moment estimated from the sum of the products of the muscle forces and their moment arms. The results for this comparison were presented graphically and showed good agreement except at the beginning of the movement, where the muscle would be least likely to be maximally active. Such an analysis is not generally applicable because it cannot routinely be assumed that muscles are maximally active.

A control model similar to that of Bobbert et al. (1986) was used in section 5:5.2 to validate the muscle model used in this study.

6:2.5 STATIC OPTIMIZATION

This group of techniques uses the mathematical technique of static optimization to estimate muscle forces. The problems are formulated in the following way:-

Objective Function

$$\text{Minimise } U(X_1, X_2, \ldots\ldots, X_n) \qquad [6.4]$$

Subject to

Equality constraints

$$\Psi_k(X_1, X_2, \ldots\ldots, X_n) = 0 \qquad k = 1, e \qquad [6.5]$$

Inequality constraints

$$\Phi_l(X_1, X_2, \ldots\ldots, X_n) > 0 \qquad l = 1, f \qquad [6.6]$$

Where:-

n - is the number of independent variables

X_i - are the independent variables

e - is the number of equality constraints

and f is the number of inequality constraints.

The objective function, U, indicates the way in which the muscles are considered to be recruited to produce the joint moment. Seireg and Arvikar (1973) were the first to use such a technique, their objective function minimised the sum of the muscle forces. The equality constraint was that the sum of the products of the muscle forces and their moment arms should equal the muscle moment. This constraint has been relaxed by some researchers to allow for the inaccuracies in the model used to compute the muscle moment (e.g. Patriarco, Mann, Simon, and Mansour, 1981). Inequality constraints are sometimes imposed, for example the muscle forces are limited to values below those indicated by the product of the cross-sectional areas of the muscles and the maximum muscle stress (e.g. Koolstra, van Euden, Weijs, and Naeije, 1988).

The objective functions are either linear or non-linear with different solution procedures required for these different formulations. To obtain the muscle forces over the course of a limb's movement, the static optimization must be used for each sampled interval. These techniques are reviewed in more detail in section 6:3.

6:2.6 SUMMARY

There are a number of different techniques available to estimate muscle forces. Direct measures are highly invasive, but may be of use for validating other techniques. EMG based models are invasive and require extensive calibration, and some of the assumptions upon which the models are based have been questioned. Dynamic optimization is used in part to analyse motor control, but the results can also give muscle activity. The major disadvantage of these techniques is their lack of general applicability, as it is difficult to formulate a performance criterion. They can be easily validated by comparing the simulated movement with the actual movement. Control models do not optimize a function but present a possible way in which the neuro-muscular system may be working. The simplest of these models provide only crude approximations, the more complex are based on physiological principles so theoretically may give better estimates. Static optimization assumes that when muscles are recruited they are recruited in such a way that some function relating to the muscle forces is minimised, for example the sum of the all the muscles stresses. These procedures are difficult to validate.

6.3 STATIC OPTIMIZATION

The following sections review some of the linear and non-linear optimization approaches for estimating muscle forces. In this review it is taken that the objective function is minimised, and that even if no other equality constraints are applied the sum of the products of the muscle forces and their moment arms must equal the muscle moment, and muscle forces must be equal to or greater than zero. General problems with optimization procedures are also discussed, and the problem of model validation is considered.

6:3.1 LINEAR OPTIMIZATION

Linear optimization is sometimes referred to as linear programming. The algorithm most commonly used to solve linear optimization problems is the Simplex developed by Dantzig (1963). Seireg and Arvikar (1973) used a number of linear objective functions to examine the quasi-static activities of leaning forward from the hip and squatting. Their study was two-dimensional with the body being modelled as five segments, with the lines of action of the muscles being modelled as straight lines. The locations of the origins and insertions were estimated from measurements taken from an anatomy text and scaled to the experimental subject in some unspecified way. Seven objective functions were examined by Seireg and Arvikar (1973); they claimed that the best correspondence of predicted muscle activity to that indicated by EMG signals, was obtained when using an objective function which minimised the sum of the muscle forces plus four times the sum of the resultant moments produced at all the joints in the lower extremity. Seireg and Arvikar (1975) applied this objective function to the examination of walking. The predicted muscle forces showed good temporal correspondence with EMG data. The accuracy of this objective function is questionable. Examination of their results shows that few muscles were active simultaneously. Also muscles with relatively small physiological cross-sectional areas, as reported by Friederich and Brand

(1990), were reported as developing large forces, for example the tibialis anterior had a reported force of 2100 N.

Calderale and Scelfo (1987) used a similar objective function to Seireg and Arvikar but used a different weighting scheme for the joint moments. Rather than employ the same weighting for all joints, the weighting differed for the four joints considered (4000 for hip and ankle, 400 for the knee, and four for the patella). No justification was given for selecting these weightings. Maximum stress levels were also imposed on the muscles. EMG measurements taken from five muscles during locomotion showed that the activity of the muscles had good temporal matching with the muscle activity indicated by EMG signals.

McLaughlin and Miller (1980) examined the forces in the muscles of the wrist during a tennis backhand stroke. They formulated an objective function based on the work of Seireg and Arvikar (1973, 1975) which minimised the weighted sums of the muscle stresses, joint moments, and joint reaction forces. The muscle stresses were constrained to some non-stated value. The weighting factors resulted in the sum of the reaction forces being removed from the criterion, as the weighting for this was zero.

MacConaill (1967) claimed that muscular action, under certain conditions, is governed by a principle of minimal action

"Principle of Minimal Total Muscular Force states that 'no more total muscular force is used than is both necessary and sufficient for the task to be performed, whether this be one of supporting some weight or carrying out a movement, the resistance to which may vary from zero upwards.'" (page 413).

Penrod, Davy, and Singh (1974) proposed an objective function which minimised the sum of the muscle forces, which they claimed was equivalent to minimizing the muscular effort. They claimed that this function

"....is intuitively appealing and may represent an accurate picture for a normal, healthy system familiar with the loads it sustains." (page 128)

They suggested that it may be appropriate to place constraints on the maximum muscle forces, but did not impose any such constraints.

Yeo (1976) examined static elbow flexion, using the objective function of minimisation of the sum of the muscle forces. The EMG studies of Basmajian and Latif (1957), and Pauly, Rushing, and Scheving (1967), showed the three major elbow flexors were all active during elbow flexion. The objective function resulted in the muscles being recruited in decreasing order of size of their respective moment arms. If no constraint was placed on the force the individual muscles could exert, then the moment was entirely provided by the brachioradialis which had the largest moment arm in the model.

Barbenel (1983) examined mastication and biting in a model consisting of four muscles. Using the objective function of minimization of the sum of muscle forces, he found only one muscle was predicted to be active yet EMG data indicated that this was not the case.

Hardt (1978) used a four link model of walking, with 31 muscles modelled as straight lines. Two linear

objective functions were compared. The first function was the minimisation of muscle forces as proposed by Penrod et al. (1974). The muscle activities predicted using this function showed poor correspondence with muscle activity indicated by EMG signals. The second function was a linear model which attempted to minimise the instantaneous energy requirements of the active muscles. The model consisted of: mechanical work rate, which was considered constant for eccentric muscle actions, and to be the product of muscle velocity and muscle force if a muscle was shortening; and maintenance heat rate which was assumed constant for concentric muscle actions and zero for eccentric muscle actions. Muscle energetics was discussed in section 5:6, a brief critique of Hardt's model follows.

The first component in the model corresponds to mechanical work rate, but here Hardt (1978) used muscle velocity rather than muscle fibre velocity to compute this term. As the rate of shortening of the muscle fibres often differs from that of the muscle (e.g. Bobbert et al., 1986) this term will generally provide an over estimate of energy requirements. The use of a constant value for mechanical work rate during eccentric muscle actions is not strictly correct, as the energy during an eccentric muscle action varies with the force and velocity of contraction (e.g. Woledge, 1971). The final component, maintenance heat rate, was represented by a constant value, but is actually a function of muscle fibre length (e.g. Hill, 1964b). It also varies for eccentric muscle actions (Hill and Howarth, 1959). The model ignores shortening heat and activation heat which both make significant contributions to the energy consumption of a muscle (Oguztoreli and Stein, 1983). This objective function showed good correspondence between muscle activity and muscle activity indicated by EMG signals. The objective function preferentially selected lengthening muscles because they were the least expensive in energetic terms. It also favoured muscles with shorter moment arms as these muscles had the lower velocities. Low velocities were also less costly energetically according to the model of Hardt (1978).

Patriarco et al. (1981) performed a three-dimensional analysis of walking. They used two systems simultaneously to obtain kinematic data which was used to give an error estimate for the muscle moments. This information was then used to relax the normal equality constraint that the sum of the products of the muscle forces and their moment arms have to equal the resultant joint moment. Two objective functions were compared: the minimisation of the sum of the muscle forces, and an adaptation of the model of Hardt (1978). In addition two constraints were applied: the maximum forces in the muscles were constrained to be less than the maximum force as estimated using the muscle model of Pedotti, Krishnan, and Stark (1978); and similar muscles were forced to share the load in proportion to their cross-sectional area. The second objective function produced results which showed good correspondence with EMG data.

Crowninshield (1978) proposed an objective function which required the minimisation of the sum of the muscle stresses, with the addition of the constraints that the muscle stresses should be above zero and less than a value associated with the maximum muscle stress. A two-dimensional analysis of static and isokinetic elbow flexion was performed, with the lines of action of the three major flexors modelled as straight lines. This objective function selected those muscles with the largest product of muscle moment arm and physiological cross-sectional area. In this study when no limit was placed on muscle stress the biceps was used exclusively, as it had the largest product of moment arm and physiological cross-

sectional area. When the maximum stress for each of the muscles was constrained to less than 60 $N.cm^{-2}$ the biceps was used exclusively until it reached this stress level, then the brachioradialis was used until it reached the same stress level, and finally the brachialis was recruited. When the maximum stress was set to 40 $N.cm^{-2}$ there was continuous synergism in all three muscle for the activities investigated. The muscle activity predicted by this objective function and the last constraint (40 $N.cm^{-2}$) were temporally well correlated with EMG data.

Crowninshield, Johnston, Andrews, and Brand (1978) used the same objective function to analyse muscle force during walking. The study was performed in three-dimensions and included 30 muscles modelled as straight lines. For two subjects EMG data were collected at the same time as the kinematic and kinetic data. Muscle activity corresponded well with muscle activity indicated by EMG signals.

An, Kwak, Chao, and Morrey (1984) compared the results of five different objective functions used to compute the forces in seven muscles considered to cause elbow flexion, and supination. The objective functions included the minimisation of: the sum of the muscle forces; the sum of the muscle stresses; the sum of the square of the muscle forces; and the sum of the square of the muscle stresses. The last two objective functions were non-linear. A new objective function was also formulated: the minimisation of the maximum muscle stress experienced by the most stressed muscle, with the addition of an inequality constraint limiting the upper stress of the individual muscles. The two linear objective functions reported activity in one muscle only. The non-linear functions and the new function predicted that all the muscles were active. A further analysis was undertaken where the new objective function was evaluated when the muscles had to provide a moment for supination as well as for flexion. In this case the activity of the muscles compared well with EMG data from the literature.

Koolstra et al. (1988) performed a three-dimensional analysis of the human masticatory system during static biting. The model consisted of 16 muscles whose activities were selected by minimising the relative activity of the most active muscle. The relative activity was defined as the force in the muscle divided by its maximum possible force. The maximum force a muscle could develop was calculated from the product of the muscle's physiological cross-sectional area and the maximum stress associated with muscle. Their objective function is essentially the same as that of An et al. (1984) as:-

$$U_a = \sigma_i \qquad U_b = F_{Ri} \qquad \text{[6.7] and [6.8]}$$

$$\sigma_i = F_{Mi} / CSA_i \qquad F_{Ri} = F_{Mi} / (CSA_i \,.\, MMS) \qquad \text{[6.9] and [6.10]}$$

Where:-

U_a - is the objective function of An et al. (1984)

U_b - is the objective function of Koolstra et al. (1988)

σ_i - is the stress in the i^{th} muscle

F_{Mi} - is the force in the i^{th} muscle

F_{Ri} - is the relative muscle force in the i^{th} muscle

CSA_i - is the cross-sectional area of the i^{th} muscle

and MMS is the maximum muscle stress associated with muscle.

As MMS is constant, the two objective functions give the same results, as long as there is no pennation in one or more of the muscles.

Bean, Chaffin, and Schultz (1988) presented a technique where the muscle forces were predicted after having to fulfil two objective functions sequentially: the double linear programming method. The first objective function was the minimisation of the sum of the muscle stresses, and the second was the minimisation of the sum of the muscle forces. Both objective functions had the same constraints in that the muscle stresses could not be greater than some predefined value. They compared their approach of double linear programming with solutions from other objective functions; the others gave unrealistic muscle forces. Their model was a three-dimensional model of lateral bending of the back and contained 10 muscles. The phasing of the recruitment of the muscles in the model, predicted using the double linear programming approach, was temporally similar to EMG data. In their analysis they showed that the sequential application of the linear programming procedure with the different objective functions gave very similar results to the double linear programming method, but took more computation time.

All of the techniques described in this section rely on the Simplex algorithm to solve their specific optimization problem. The Simplex algorithm is described in Appendix D. The nature of the solution requires that the number of non-zero variables is less than the total number of constraints plus one. For example in a two-dimensional study if the only constraint is that the muscle moment should be satisfied by the predicted muscle forces, only one muscle will be predicted to be active. This presents a major limitation for linear objective functions, and means that constraints are necessary if load is to be shared between more than one muscle.

6:3.2 NON-LINEAR OPTIMIZATION

The first non-linear objective function was suggested by Pedotti et al. (1978). They performed a two-dimensional examination of walking, with an 11 muscle model. Four objective functions were compared: sum of the muscle forces; sum of the muscle forces squared; sum of the relative muscle forces; and the sum of the relative muscle forces squared. Relative muscle force was determined by dividing the muscle force by the maximum muscle force at the current length and velocity for each of the muscles. To account for the length and velocity of the muscles the force-length relationship was modelled as being linear, and the force-velocity relationship was modelled using the equation of Hill (1938). Pedotti et al. (1978) failed to take account of the tendon in series with the muscle fibres, and rather than use muscle fibre length and velocity as inputs to their equations for the force-length and force-velocity relationship they used muscle length. As discussed previously the velocity of the muscle may not be the same as the velocity of the muscle fibres. There was also no account taken of the muscles in the model which showed significant degrees of pennation. Even so this model was one of the first to take account of the properties of muscles. All the objective functions were constrained so the predicted muscle forces were below their respective maximum levels as computed using the force-length and force-velocity relationships. EMG data were collected on two subjects, and used to indicate when muscles were active. Using this as the

criterion, the fourth objective function (the sum of the relative muscle forces squared) was judged to give the best estimation of individual muscle activity. There was no physiological justification offered for this objective function.

Herzog (1986) used a similar objective function to Pedotti et al. (1978) but used a more sophisticated model to predict the maximum muscle force at any given muscle fibre length and velocity. To validate the model isokinetic knee extensions were examined, with four muscles assumed to produce the knee joint muscle moment. A muscle model was used to estimate what the actual muscle forces were at various instances during different velocity maximum isokinetic actions. The resultant joint moment predictions using the muscle model were within 12 percent of the values from the isokinetic dynamometer. These muscle force predictions from the muscle model were used to evaluate three objective functions. The three objective functions assessed all had different ways of computing the denominator (the maximum muscle force) in the objective function. In the first case maximum muscle force was based solely on the physiological cross-sectional area of the muscles. In the second case muscle size, maximum muscle stress, and muscle fibre type distribution were all used in the model to predict the maximum muscle force. The third objective function used a model which also incorporated the physiological cross-sectional area, the pennation, length, and velocity of the muscle. The first two objective functions were not as accurate as the third.

A similar analysis of the more successful objective function was performed by Herzog (1987b,c) where he showed his objective function to be more accurate than that of Dul, Johnson, Shiavi, and Townsend (1984b), and Crowninshield and Brand (1981). Even though his objective function was superior to the other two, the muscle force predictions from his objective function were ± 200 N from the muscle model predictions in some of the cases examined. This objective function incorporated more information about the contractile conditions of the muscle than any other study to date, for which it should be commended. However, the model still managed to predict muscle forces which were greater than those which the muscles could achieve at their current contractile conditions. Herzog (1987c) claimed that this objective function was dependent on the contractile conditions of the muscles and kept the metabolic cost of the movement low.

Crowninshield and Brand (1981) proposed a new objective function, which was the minimisation of the sum of the cube of the muscle stresses. As endurance time is a non-linear function of muscle stress, it was claimed that this function effectively maximised endurance time. This objective function was first demonstrated for static elbow flexion, where all three flexors in the model were predicted to be active. The function was then applied to some three-dimensional data of walking. Muscle activity for this analysis showed good correspondence with EMG data. This model was recommended for prolonged repetitive activities.

Pedersen, Brand, Cheng, and Arora (1987) examined four objective functions for estimating muscle forces during walking. Results were compared with EMG signals taken from 10 muscles on the experimental subjects, and EMG information for a further 20 muscles was obtained from the literature. They evaluated

the objective functions using a figure of merit which indicated the degree of correspondence between the period of muscle activity indicated by the EMG, and that predicted by the objective functions. They suggested that EMG signals should not be used quantitatively for validation, but only qualitatively. The objective functions were: minimisation of the sum of muscle forces; minimisation of the sum of muscle stresses; minimisation of the sum of muscle forces cubed; and minimisation of the sum of muscle stresses cubed. Although the sum of the muscle forces is a linear objective function it was minimised using a non-linear algorithm. The two non-linear objective functions were also examined with the relaxation of the equality constraint that the sum of the product of the muscle forces and their moment arms had to equal the muscle moment, so that these muscle moment estimations had to lie within boundaries reflecting the accuracy of each joint's muscle moment. The linear objective function only predicted a limited number of muscles active. The sum of the muscle stresses cubed and the sum of muscle forces cubed, gave the highest results for the figure of merit. The relaxation of the net muscle moment values in the equality constraint did not result in a large change in the muscle forces for the non-linear objective functions, but did result in a reduced hip joint contact force.

Denoth (1988) performed a closer examination of the objective function of Crowninshield and Brand (1981). Using the static elbow flexion data of Crowninshield and Brand (1981) it was demonstrated that their objective function did not maximise endurance time, which was longer if all the muscles exerted equal stress. A model was presented of the leg which consisted of three muscles. There were moments at both the ankle and the knee. One of the muscles was biarticular and could contribute to moments at both joints. The analysis showed that the stress in the biarticular muscle was in direct ratio with the order to which the stress was raised. The study of Crowninshield and Brand (1981) claimed good correspondence of predicted activity with EMG data, although Denoth (1988) questioned the use of EMG data for the validation of objective functions.

Pedersen and Brand (1989) compared hip joint contact forces predicted using the optimization procedure of Crowninshield and Brand (1981) with the direct measurement from a radio-telemetered hip prosthesis (Davy, Kotzar, Brown, Heipe, Goldberg, Berilla, and Burstein, 1988). Their model assumed that the hip contact force passed through the hip joint centre, and the ligaments at the hip made no contribution to the hip moment. A number of muscles in the model crossed both the hip and knee joint, three different constraints were placed on these muscles: they could only contribute to the flexion-extension component at the hip; they could only contribute to the flexion-extension and varus-valgus components at the hip; and finally they could contribute to all moments. The model predicted hip forces which were much greater than those measured in vivo. The model which allowed the biarticular muscles to contribute only to the flexion-extension moment, gave the most accurate results. No information was presented to demonstrate any temporal matching of the data. In their study the cross-sectional areas of the muscles were estimated for the subject from cadaver data; Brand, Pedersen, and Friederich (1986) had already demonstrated the sensitivity of this objective function to errors in these data. As well as assumptions involved in the kinematic and kinetic data gathering, it may be that after total hip arthroplasty the subject was using a new strategy for recruiting muscles, rather than the strategy which the objective function was intended to model.

Dul, Townsend, Shiavi, and Johnson (1984b) examined 13 different objective functions and associated constraints, using a theoretical model of isometric knee flexion. The objective functions were all concerned with the minimisation of the sum of either the muscle forces, or the muscle stresses, with these values to the power of one, two, or three. Constraints were also imposed, which limited either maximum muscle force or maximum muscle stress. Also a degree of load sharing between the muscles was enforced by imposing that the forces or stresses in certain pairs of muscles were in fixed ratios. The findings of this study confirmed that linear objective functions tend to recruit muscles in a set order, and that non-linear functions show muscle synergism over a range of loads. The paper concluded that a method is needed to validate non-linear objective functions.

Dul et al. (1984a) proposed an original objective function. The function was selected so that the load sharing between the muscles was such that the absolute time for which the activity could be performed was maximised. A function was developed which, given the muscle fibre type distribution and the maximum force the muscle could develop, gave the endurance time of a muscle when exerting a given force. The objective function selected the muscles so that the endurance time of the muscle with the shortest endurance time was maximised. The objective function was selected because of the assumption that for everyday learned activities, muscle are recruited so muscular fatigue is minimised. This function was used to examine the theoretical model of knee flexion of Dul et al. (1984b). All three functions predicted all the muscles to be simultaneously active. The objective functions of Pedotti et al. (1978) and Crowninshield and Brand (1981) recruited the muscles in a linear order related to the moment arms of the muscles.

Walmsley et al. (1978) took direct measures of muscle forces in cats. Dul et al. (1984a) compared these forces with the forces predicted using a number of different objective functions. The muscle force predictions using the objective function of Dul et al. (1984a) were similar to the measured forces. A number of other objective functions were evaluated on the same data, and the linear objective functions were found to be very poor at predicting muscle activity, no constraints were placed on these functions. Of the other non-linear objective functions the best results were found by minimising the sum of the muscle forces squared. The other objective functions evaluated were the sum of the muscle stresses squared and cubed, and the sum of the relative muscle forces squared and cubed. Although the authors called this the minimum fatigue criteria, it does not account for changes in recruitment patterns when one of the muscles is at the end of its endurance limit or approaching this limit. The objective function of Pedotti et al. (1978) was assessed, but not strictly, as the maximum muscle force term used by Dul et al. (1984a) was based on the product of the physiological cross-sectional area and the maximum muscle stress. Pedotti et al. (1978) evaluated the maximum muscle force for each sample interval, and took into account variations in the maximum muscle force due to the force-length and force-velocity relationships.

A further analysis of objective functions takes place in section 6:4.

6:3.3 DISCUSSION

This section is concerned with general principles of static optimization. The basic premise of estimating

muscle force using static optimization is that it is possible to formulate an objective function and appropriate constraints which reflect how the body actually recruits the muscles concerned.

The human body is capable of a wide range of activities, and it is unlikely that the body recruits muscle using the same protocol for sprinting 100 metres as it would for running a marathon. If such criteria do exist there are perhaps different functions for different types of activity. Also it could not be expected that the same criterion would apply to unlearned activities.

The objective functions formulated are generally concerned with minimisation of muscle force or muscle stress. There is no physiological evidence to suggest that the human body recruits muscle in such a way as to minimise either of these factors. The study of Hardt (1978) attempted to model the energy consumption concerned with muscular actions. To test these formulations some valid criterion is required.

Many of the objective functions do not have a proven physiological basis. The force output of a muscle is a complex function of the length, velocity, and degree of activation of its fibres. By taking account of the previous or current states of the muscles, some knowledge of the mechanics of muscle could be incorporated into the model used to estimate muscle forces. However, most models do not attempt to do this. In the objective functions of Pedotti et al. (1978) and Herzog (1986) some of the properties of muscle were considered. Factors such as fatigue and storage of elastic energy are even more complex phenomena which occur in human muscles but which have not yet been considered in static optimization studies of muscle forces.

6:3.4 VALIDATION

The primary method used to validate both linear and non-linear optimization formulations has been the use of EMG signals. These signals are used to indicate when the muscles are active and this information is then compared with the activity of the muscles as predicted by the optimization procedure. Most of the non-linear objective functions predict load sharing between all of the modelled muscles, and have generally been validated using this criterion. Such information does not give a true indication of the relative or absolute activity of the muscles.

Muscle models of varying degrees of sophistication have been used to examine the validity of optimization formulations. For example, by using a muscle model to compute the maximum force that a muscle can exert, optimization criteria have been invalidated if muscle force estimates have been higher than these physiologically based maxima. It could be argued that such information should be included in the optimization model as an inequality constraint. Herzog (1986) evaluated optimization formulations by predicting muscle forces using a muscle model which assumed the muscles were maximally active. The muscle forces predicted using different objective functions were then compared with the muscle model forces. Such a validation is primarily only as good as the estimates of the muscle forces made by the muscle model, and is only applicable for maximal and near maximal conditions, which do not frequently occur in the everyday activities which many of these objective functions were formulated to investigate (e.g. walking). If the activity is maximal or near maximal, and there is no co-contraction of antagonists, an

optimization procedure is not required to estimate muscle forces: a muscle model such as that described in section 5:5.1 can be used. Herzog (1986) used such a method to arrive at his criterion values. This approach of course assumes that the muscle model used is valid.

Dul et al. (1984a) used data of muscle forces measured in vivo in cats to evaluate their objective function. Their validation was only partial as they had to estimate many of the parameters for their model without much knowledge of the experimental animals. Pedersen and Brand (1989) attempted a validation of the objective function of Crowninshield and Brand (1981) using hip contact force data measured in vivo. The number of studies where muscle forces or joint contact forces have been measured are small. If such data are used from the literature, model parameter estimation is more difficult than if the researcher measures the muscle forces in vivo and tests the objective function. Such sources of data are generally highly invasive.

Most of these methods are at best only partial validations and are better viewed as methods to invalidate optimization formulations. No optimization technique can be classified as having been truly validated but a number can be said to have been invalidated. The next section will further examine the "invalidation" of optimization formulations.

6:4 COMPARISON OF OBJECTIVE FUNCTIONS

It is the purpose of the following sections to examine a number of optimization formulations: objective functions and constraints. Their validity will be examined by considering the EMG signal from the muscles, and basic muscle properties.

6:4.1 METHODOLOGY

A number of objective functions were examined under three different conditions: isometric muscle action; sub-maximal concentric muscle action; and maximal concentric muscle action. Three different constraints were also used in combination with the objective functions.

The objective functions were divided into three sets. The first was only concerned with the minimisation of the sum of muscle forces, this was done with the forces being raised to different powers. The second set examined objective functions which minimise some function of the sum of muscle stresses. The final set was concerned with the minimisation of the sum of the relative muscle forces. The basic formulation can therefore be stated as:-

$$\text{Minimise} \qquad U = \sum_{i=1}^{NM} g(F_{Mi}) \qquad [6.11]$$

Subject to

$$MM = \sum_{i=1}^{NM} R_i \cdot F_M \qquad [6.12]$$

Where:-

NM - is the number of muscles in the model

$g(F_{Mi})$ - is some function of the force of the i^{th} muscle
F_{Mi} - is the force exerted by the i^{th} muscle
MM - is the muscle moment
and R_i is the moment arm of the i^{th} muscle.

Both linear and non-linear objective functions were examined, for which different solution procedures were required. The linear objective functions were solved using the Simplex algorithm based on the FORTRAN code presented by Siddall (1982). The non-linear objective functions were solved analytically using Lagrangian multipliers. All these techniques are described in Appendix D. Three different constraints were used with these objective functions. The constraints placed on each muscle were:-
Constraint 1 - limiting muscle force so it was less than or equal to the maximum isometric force possible by the muscle (this occurs at the muscle fibres optimal length),
Constraint 2 - limiting the maximal muscle force by accounting for the current length of the muscle using the force-length model of muscle described in 5:2.2,
Constraint 3 - limiting the maximum force that the muscle can exert by taking into account the force-velocity model of muscle described in section 5:2.3. This constraint was not appropriate for condition A which was an isometric muscle action.

As discussed in section 6:3.4 there are three basic methods used to try and validate objective functions. They are comparison of the muscle forces or activity as predicted by the objective function with: muscle activity indicated by EMG data, muscle forces predicted by a muscle model, and muscle forces as measured in vivo. The conditions examined here were concerned with the first two methods, there were no data available with which to implement the third method.

The objective functions were examined under three conditions. These conditions were formulated using data described in the earlier chapters. The three conditions were:-

Condition A
The subject had their elbow flexed to 130 degrees, and during an isometric muscle action produced a joint flexion moment of 20 N.m; this was 76 percent of the maximum moment that the subject could exert at this joint angle. Basmajian and Latif (1957) examined EMG signals from the three major elbow flexors in 20 subjects using indwelling electrodes. They reported that with and without load during elbow flexion the three flexors modelled here were all active simultaneously, irrespective of whether the activity was dynamic or static. Pauly et al. (1967) examined the EMG activity of 18 subjects using indwelling electrodes, and reported that during flexion all the flexors were active simultaneously. In condition A although the forces exerted by the muscles were not known, from these EMG studies it can be inferred that the objective functions should predict all of the muscles to be active simultaneously. The forces predicted should also be below physiological maxima.

Condition B
The second condition was to predict muscle forces during elbow flexion when the muscle fibre velocities

were known. The conditions were the same as in condition A, but this time the muscle fibres had known velocities. Again the muscle forces were not known but the objective function should predict all the muscles to be active simultaneously, and predict force levels which should be equal to or below the maxima that the muscles should be able to exert as indicated by the force-length and force-velocity relationships.

Condition C

The final case investigated was based on the data gathered in section 5:5.2, the simulation of the maximal dumbell curl. Herzog (1987b,c) used muscle forces estimated using a muscle model to evaluate his objective function. The simulation model presented in section 5:5.1 allowed the prediction of the individual muscle forces during this maximal activity. One instant during the dumbell curl (trial #4) was chosen and the muscle forces predicted using the muscle model from that instant were used as the criterion. The data from this same instant were used as inputs for the objective functions and muscle model.

For each of the conditions various parameters and variables were required as inputs to either the muscle model or the objective function. The muscle parameters were the same as those described in section 5:4.2. The variables required were the moment arms, lengths, and velocities of the muscles and their fibres, and the net muscle moment. For condition A these were obtained from the static data capture at a joint angle of 130 degrees. For condition B these were obtained from trial #3, again at a joint angle of 130 degrees, and muscle fibre velocity was assumed equal to muscle velocity. For condition C the variables were obtained from trial #4 and the simulation procedure described in section 5:5.1. For condition C the muscle fibre velocity was obtained from the simulation procedure. As muscle velocity is sometimes used rather than muscle fibre velocity as the input to models (e.g. Pedotti et al., 1978; Hardt, 1978), this value was also used to evaluate the potential error when using muscle velocity rather than muscle fibre velocity as the input to the models of the force-velocity relationship.

It is assumed that for the three conditions examined the three modelled muscles were solely responsible for producing the moment about the joint.

6.4.2 OBJECTIVE FUNCTIONS

The objective functions were divided into three sets.

Set I - the objective functions evaluated in this set were all concerned with the minimisation of some function of the muscle forces. Specifically the objective functions were:-

$$U1 = \sum_{i=1}^{NM} F_{Mi} \qquad U2 = \sum_{i=1}^{NM} \left(F_{Mi}\right)^2 \qquad U3 = \sum_{i=1}^{NM} \left(F_{Mi}\right)^3$$

$$U4 = \sum_{i=1}^{NM} \left(F_{Mi}\right)^{10} \qquad U5 = \sum_{i=1}^{NM} \left(F_{Mi}\right)^{100}$$

Where:-

NM- is the number of muscles

and F_{Mi} is the force exerted by the i^{th} muscle.

Set II - the objective functions evaluated in this set were all concerned with the minimisation of the sum of some function of the individual muscle stresses. The cross-sectional areas of the muscles were not known but the maximum isometric muscle forces were known. From the discussion in 5:4.1.5, the specific tension of muscle is known so it was possible to calculate the muscle cross-sectional areas. The objective functions were:-

$$U6 = \sum_{i=1}^{NM} \sigma_i \qquad U7 = \sum_{i=1}^{NM} (\sigma_i)^2 \qquad U8 = \sum_{i=1}^{NM} (\sigma_i)^3$$

$$U9 = \sum_{i=1}^{NM} (\sigma_i)^{10} \qquad U10 = \sum_{i=1}^{NM} (\sigma_i)^{100} \qquad U11 = \sigma$$

Where:-

NM- is the number of muscles

σ_i - is the stress in the i^{th} muscle

$$\sigma_i = \frac{F_{Mi}}{CSA_i}$$

F_{Mi} - is the force exerted by the i^{th} muscle

CSA_i - is the cross sectional area of the i^{th} muscle

and σ is the stress experienced by the most stressed muscle.

Objective function U11 was the function recommended by An et al. (1984), and requires the minimization of the maximum muscle stress experienced by the most stressed muscle. In this case the muscle forces are therefore distributed as a function of their cross-sectional areas, which is the same as one of the control models described in section 6:2.4.

Set III - the objective functions in this set were concerned with the minimisation of the sum of the relative muscle forces. Relative muscle force is defined as the fraction of muscle force which the muscle is producing divided by the maximum muscle force the muscle could produce under the current physiological conditions. The objective functions evaluated in the previous set were all concerned with the minimisation of some function of the muscle stress. The objective functions in this set can be considered to use muscle stress, but they update it to allow for the current physiological state of the muscle. This has been done by using maximum muscle force rather than muscle cross-sectional area as a denominator for the equations. When a muscle is exerting its maximum isometric force at optimal length, the objective functions are identical, as in this case muscle force is equal to the product of muscle cross-sectional area and the specific tension of muscle, with the latter being constant. As soon as the muscle fibres move away from this length or have a velocity, this relationship does not apply. Therefore for these objective functions the denominator is based on muscle properties. Such objective functions have been formulated by Pedotti et al. (1978), and Herzog (1987b,c). The objective functions were:-

$$U12 = \sum_{i=1}^{NM} \frac{F_{Mi}}{F_{MMi}} \qquad U13 = \sum_{i=1}^{NM} \left[\frac{F_{Mi}}{F_{MMi}}\right]^2 \qquad U14 = \sum_{i=1}^{NM} \left[\frac{F_{Mi}}{F_{MMi}}\right]^3$$

$$U15 = \sum_{i=1}^{NM} \left[\frac{F_{Mi}}{F_{MMi}}\right]^{10} \qquad U16 = \sum_{i=1}^{NM} \left[\frac{F_{Mi}}{F_{MMi}}\right]^{100}$$

Where:-

NM - is the number of muscles

F_{Mi} - is the force exerted by the i^{th} muscle

and F_{MMi} is the maximum possible force, under current physiological conditions, of the i^{th} muscle.

F_{MMi} was calculated by each of three methods; these methods were designated a, b, and c. In method a F_{MMi} was calculated based on the force-length relationship of the muscles. In method b F_{MMi} was calculated by considering the force-length and force-velocity relationships of the muscles, in this case using muscle fibre velocity. In method c F_{MMi} was also calculated by taking into account the force-length and force-velocity relationships of the muscle, but in this case muscle velocity was used rather than muscle fibre velocity.

6:4.3 RESULTS AND DISCUSSION

The results for the three conditions are presented in Appendix E in tables E.1, E.2, and E.3, (because there were criterion values for condition C the percentage difference between the predicted and criterion values are also presented in table E.3). Any reference to accuracy refers to condition C only. The term physiological maximum muscle force is used in this and following sections; it refers to the maximum force a muscle can produce given the current length and velocity of its muscle fibres.

Four linear objective functions were examined, U1, U6, U11, and U12, but the following discussion in this paragraph does not refer to objective function U11. As discussed in Appendix D, the number of active muscles predicted by a linear objective function depends on the number of constraints imposed, therefore without the imposition of equality constraints none of these objective functions predicted all the muscles to be simultaneously active under any of the conditions. For objective function U1, the muscle with the largest moment arm was selected in preference to the other muscles. This selection was particularly inappropriate because in the present study the muscle with the largest moment arm in all three conditions was the brachioradialis, which also had the lowest possible maximum force. When the muscle forces were constrained, the brachioradialis was always estimated to be maximally active. For condition A where the subject was exerting 76 percent of the maximum joint moment, it would seem to be unlikely that one muscle would be maximally active. For objective functions U6 and U12 the muscle with the largest product of the muscle moment arm and the denominator in each of the objective functions was preferentially selected over the other muscles. These objective functions therefore chose the muscle which could make the largest contribution to the joint moment; in both cases this was the biceps. When the muscle forces were not constrained, the biceps was predicted to produce all of the joint moment. The

procedures by which these objective functions recruited muscles were not based on any established physiological principles.

Objective function U11 selected the muscles in relation to their cross-sectional areas. At its optimal length the maximum isometric force a muscle can exert is a linear function of its cross-sectional area, under which conditions this objective function would theoretically be realistic. All three muscles would not obtain their optimal lengths simultaneously, and away from these lengths the isometric maximal forces are complex non-linear functions of each muscle's cross-sectional area. In conditions A and B the muscle fibre lengths were significantly different from their optimal lengths so that the maximal forces they could exert were different from their maximum isometric forces. The force that the brachioradialis could exert in relation to its maximum force was the most diminished, due to its particular force-length relationship, consequently this muscle was always predicted to be producing a force greater than or equal to its maximum force. For conditions B and C the brachioradialis had the highest velocity so again it was predicted to have a muscle force greater than or equal to the maximum possible force, depending on whether constraints were imposed or not. This objective function does have a physiological basis as the muscle forces are indirectly distributed in relation to the maximum force a muscle can exert, but such a condition is most valid when all of the muscles are closest to their optimum lengths during isometric muscle actions. Away from such conditions due to the force-length and force-velocity relationships, the forces the muscle can exert are more complex functions of the properties of the muscles.

Non-linear problems sometimes converge to a local rather than a global minimum. The advantage of linear objective functions is that they are guaranteed to converge to a global minimum (Arora, 1989). Of the linear objective functions examined here (U1, U6, U11, and U12) only U11 predicted all three muscle to be simultaneously active without the imposition of additional constraints. When constraints were added the muscle which had been preferentially selected under the no constraint condition automatically had a muscle force value equal to the imposed constraint.

All of the objective functions in set I estimated muscle forces which were in excess of the physiological maximum when no constraints were placed on the muscle forces. This was also the case when the muscle forces were constrained to be less than the maximum isometric force possible by the muscles. Ignoring U1 the other objective functions in this set predicted all the muscles to be active simultaneously, but in most of the cases one or two of the muscles were predicted to be maximally active whilst the third muscle was often predicted to be producing less than half of its physiological maximum force. It seems unlikely that the body would recruit muscles in such a way because the maximally active muscle would not be able to sustain that level of activation for prolonged periods, whereas if the muscle moment was satisfied by all three muscles working at sub-maximal levels the activity could be maintained for longer periods. For conditions B and C when the muscle forces were constrained to be equal to or less than the muscle forces predicted by the force-velocity relationship (constraint 3), the muscle forces were constrained to such an extent that the objective function made little difference to the predicted force levels. The non-linear objective functions in set I were solved analytically using the procedure described in Appendix D. Analysis of equation D.8 shows how the load is shared between the two muscles, i and j,

with this group of objective functions:-

$$\frac{F_{Mi}}{F_{Mj}} = \left[\frac{R_i}{R_j}\right]^{\left(\frac{1}{p-1}\right)} \qquad [6.13]$$

Where p is the power to which the muscle force has been raised in the objective function.

It can be seen that in this set of objective functions, the way the load is shared between pairs of muscles is a function of the moment arms of the muscles and p, but takes no account of physiological properties of the muscles. This equation also indicates that as the value of p increases, the influence of the muscle moment arms on the ratio of load sharing between the muscles decreases, and for larger values of p the right-hand side of the equation tends towards one. Therefore for large values of p the muscles all have equal or similar forces; the tendency for this to occur is illustrated by objective function U5 where p was equal to 100.

Some of the objective functions in set II have been used by researchers, for example Crowninshield (1978), and Crowninshield et al. (1978) used objective function U6, and Crowninshield and Brand (1981) used objective function U8. For the non-linear formulations the objective functions all predicted the muscles to be simultaneously active, but for condition A for all of the objective functions one or two of the muscles were predicted to be producing muscle forces which were either equal to or greater than the maximum force the muscle could exert under the physiological conditions. The solutions for these objective functions, and those in set III, were obtained using the analytical solution presented in Appendix D, a re-arrangement of equation D.8 illustrates how the difference in force varies between two muscles i and j:-

$$\frac{F_{Mi}}{F_{Mj}} = \left[\frac{R_i}{R_j}\right]^{\left(\frac{1}{p-1}\right)} \cdot \left[\frac{A_i}{A_j}\right]^{\left(\frac{p}{p-1}\right)} \qquad [6.14]$$

Where A_i is either the cross-sectional area of muscle i or the maximum muscle force, depending on whether an objective function from set II or III is being solved.

It can be seen that the way in which the moment is accommodated by the solution of the objective function is not dependent on load, but is a function of the moment arm and the cross-sectional area of the muscles. For example for objective function U7 the degree of load sharing between the muscles is solely dependent on the product of the muscle moment arms and cross-sectional areas. Although these mechanical considerations must be important, there is no allowance made here for the physiological properties of the muscles, other than their maximum isometric force. Allowance can be made for the properties of the muscles in the constraints but the objective functions will predict the muscle forces in the ratios described in equation 6.14 up to the constraint level.

Further analysis of equation 6.14 shows that as the value of p increases, the value resulting from the division of one moment arm value by another, all raised to the power of 1/(p-1), tends to one, and so has

no influence. As the value of p increases, the result of p/(p-1) tends to one, meaning that for large values of p the muscle forces are shared between the two muscles in direct proportion to their cross-sectional areas. This was the case for U10 with no constraints where p=100, and so results for all conditions using this objective function were very similar to the results for U11 which distributed the muscle forces in proportion to their cross-sectional areas.

The objective functions in set III are based on those suggested by Pedotti et al. (1978) and Herzog (1987b,c). For condition A all of these objective functions predicted muscle forces which were equal to or greater than the physiological maxima; as this was a sub-maximal activity such estimates are unrealistic. Except for the linear objective function U12 all these objective functions predicted all the muscles to be active simultaneously for all conditions.

Objective function U13b was equivalent to the function used by Herzog (1987b,c), who did not impose any constraints on his muscle force values. Herzog (1987b,c) used a muscle model to produce maximum muscle force estimates for the denominator in his objective function. It would seem to be a logical extension to use these to constrain muscle forces. For all conditions examined here, without constraints, this objective function predicted muscle forces in excess of physiological maxima.

Under the dynamic conditions when only the force-length relationship was used (U13a-U16a), this group of techniques was not very accurate. For all of these non-linear objective functions, for condition A the brachioradialis was estimated to produce muscle forces greater than or equal to its physiological maximum. The most accurate results were obtained when the relative muscle forces were calculated from the force-length and force-velocity relationships, using muscle fibre velocity as input to the force-velocity relationship (U13b-U16b). Placing constraints on this group of objective functions made little difference to the accuracy of the results. As p increased so did the accuracy of the muscle force prediction using the non-linear objective functions in set III. This can be explained by analysing equation 6.14. It has already been established that as p increases the ratio of muscle forces depends on the ratio of the cross-sectional areas in equation 6.14. For this class of objective functions the muscle cross-sectional areas are replaced by the maximum muscle force under current physiological conditions. For objective function U16b, which gave the most accurate results for condition C, this meant that the objective function made all the muscles have the same relative force. Such a procedure is attractive because it ensures load sharing between the muscles, and for sub-maximal activity one muscle is not preferentially selected to be maximally active.

For condition C the results were more accurate when using muscle velocity rather than muscle fibre velocity, for all the objective functions except U13b-U16b. Consideration must be given to implementing these objective functions in this way, thus avoiding the complexity of having to compute muscle fibre velocity.

This discussion has focussed on the results from the three conditions all of which were performed at high intensities (75 to 100 percent of maximum). This level of intensity occurs frequently in many sporting activities but not so frequently in everyday activities. These results must be regarded in this light, although

some of the trends reported clearly apply across the full range of intensities because of the nature of the mathematical formulation used to obtain the muscle force estimates.

6:4.5 CONCLUSION

For the linear objective functions U1, U5, and U12 there was no sharing of the load unless additional constraints were placed on the solution plane. These objective functions preferentially selected a single muscle: when the sum of the muscle forces was minimised (U1), the muscle with the largest moment arm was selected; when the sum of the muscle stresses was minimised (U5), the muscle with the largest product of cross-sectional area and moment arm was selected; and when the sum of the relative muscle forces was minimised (U12), the muscle with the largest product of maximum muscle force and moment arm was selected. Even when constraints were imposed, the other muscles only became active once the preferred muscle was maximally active. The results of this analysis invalidate the "Principle of Minimal Total Muscular Force" (MacConaill, 1967), for the cases examined here.

The non-linear objective functions estimated load sharing between the muscles for all conditions examined. Without the addition of constraints muscle forces in excess of the physiological maximum were estimated, except U16b condition B. Analysis of the analytical solutions to these non-linear objective functions shows that the solution to these functions does not depend on load but on the muscle moment arm, and the denominator in the objective function (if there is one), see equations 6.13 and 6.14.

In the two dynamic conditions the muscle forces were more realistic when the third constraint was added. This constraint was particularly appropriate because condition B was near maximal activity and condition C was maximal activity. In the latter case the muscle forces were equal to the constraint conditions so the objective functions became redundant. These results do indicate that the imposition of constraints is required if the estimated muscle forces are going to have any degree of validity. To impose these additional constraints there are a number of requirements: a model of the muscles causing the activity, parameters for the model, and the input variables for the model. To date very few of the optimization studies have incorporated a muscle model where model parameters have been obtained from the experimental subject, Herzog (1987b,c) being a notable exception. If such a model is employed, it is relatively simple to impose constraints based on the force-length relationship of muscle, but the force-velocity relationship is harder to apply. To use the force-velocity relationship the muscle fibre velocity is required. As can been seen from the analysis for condition C, if muscle velocity is used instead of muscle fibre velocity, different maximum values are obtained. In this case the maximum forces the muscles could exert were so constrained that it was not possible for them to satisfy the equality constraint, that is the sum of the products of the maximum muscle forces and moment arms was less than the muscle moment at the joint. A possible solution to this would be to use muscle velocity to obtain an estimate for constraint values, as it is much easier to estimate in vivo than muscle fibre velocity. These constraints could then be relaxed by some amount allowing for the fact that muscle fibre velocity may be lower than the muscle velocity.

No one objective function was clearly superior. The accuracy of the results increased when constraints

were placed on the solutions, which were based on established properties of muscle, i.e. force-length, and force-velocity relationships.

It may be concluded that objective functions with a greater physiological basis are required. If this is not attempted, physiological constraints should be placed on the muscle forces estimated using other objective functions. There is also a need for a means of validating such procedures: measurement of the individual human muscle forces in vivo for all the muscles crossing a joint, for a range of activities, would provide a valuable contribution to this area of research.

6:5 A NEW OBJECTIVE FUNCTION

The purpose of the following sections is to present a new objective function designed to estimate individual muscle forces in vivo. The objective function is tested under the same conditions used to evaluate the other objective functions and is then used to compute the muscle forces during two of the dumbell curls, trials #2, and #3.

6:5.1 RATIONALE

The most successful objective functions examined in the previous sections focussed on functions of muscle stress or relative muscle force. In engineering applications minimising the sum of the stresses in the component parts of a system is a justifiable approach. Human muscles are capable, in vivo, of tolerating stresses greater than the maximum that they can exert themselves (Yamada, 1970), therefore minimising the sum of the muscle stresses only has limited physiological justification. It has been shown in a limited number of studies that the human body moves to minimise the energy requirements necessary to produce the movement. Cotes and Meade (1960) examining horizontal treadmill walking showed that the stride frequency selected by the walkers required the least energy expenditure, compared with walking at stride frequencies less than or greater than the selected frequency. In a similar study examining running, Cavanagh and Williams (1982) have shown that when running at a constant speed a group of subjects selected a stride length which minimised the energy cost for running at that speed, with changes in stride length resulting in an increased energetic cost to run at the same speed. McMahon, Valiant, and Frederick (1987) presented evidence to suggest that the preferred style of running also requires the lowest energy cost. Similar phenomena have been reported in swimming salmon (Brett, 1965). Based on this concept it is hypothesised that the human body recruits muscles to produce a joint moment in such a way that the total energetic cost to the muscles causing the movement is a minimum. The next section presents the formulation of an objective function designed to select muscles to satisfy a joint moment which attempts to minimise the energetic cost of producing that movement, whilst taking into account other physiological properties of the muscles.

6:5.2 FORMULATION

The objective function was designed to minimise the energetic cost of satisfying the moment.
The objective function was:-

$$U = \sum_{i=1}^{NM} (E_i)^2 \qquad [6.15]$$

Where:-

NM - is the number of muscles

and E_i is the rate of energy consumption by the i^{th} muscle.

This non-linear objective function was selected because of the limitations of the solutions to linear objective functions discussed in Appendix D.

Objective functions are normally constrained so that the product of the muscle forces and their respective moment arms were equal to the muscle moment. In this case this constraint was relaxed to allow for the inaccuracy of the muscle moment estimations, therefore using the results reported in section 4:5.1 the following constraints were enforced:-

$$MM - TOL \leq \sum_{i=1}^{NM} R_i . F_i \qquad [6.16]$$

$$MM + TOL \geq \sum_{i=1}^{NM} R_i . F_i \qquad [6.17]$$

Where:-

MM - is the muscle moment

TOL - is the tolerance selected to reflect the accuracy with which the muscle moment has been estimated

R_i - is the moment arm of the i^{th} muscle

and F_i is the force exerted by the i^{th} muscle.

The tolerance levels (TOL) were set at 1 N.m, although the estimated errors in the joint moments were greater than this (see section 5:4.1), particularly for errors in the kinematic data. Given a broader range of tolerances, muscle moments were only predicted for the lower tolerance band, equation 6.16, because generally this required lower muscle forces and therefore had a lower energetic cost. With the tolerance limits used this did not occur.

The rate of energy consumption by an active muscle was described in Chapter V, and represented by equations 5.43, 5.48, and 5.51. Therefore the rate of energy consumption of a muscle is:-

$$E_i = F_i V_{Fi} + a_i b_i + V_{Fi} (0.18 F_{li} + 0.16 F_i) \qquad [6.18]$$

Where:-

V_{Fi} - is the velocity of the muscle fibres of the i^{th} muscle

a_i and b_i - are the constants from Hill's equation, see equation 5.18

and F_{li} is the maximum isometric force of the i^{th} muscle at the current length of its muscle fibres.

The force output of each muscle is determined by the length and velocity of the muscle fibres, and the active state of the muscles. Therefore from equation 6.18, the rate of energy consumption of an active

muscle is also determined by the length and velocity of the muscle fibres and the active state of the muscle. Control of the muscles by the nervous system is not instantaneous, a muscle is not turned on and off in an instant (bang-bang control) rather it takes time for force to develop, and time for it to reduce. Therefore a model of active state was used to allow for the nervous control of movement, this model used equations 5.22 and 5.23. Given the current active state of the muscles these equations gave the maximum and minimum active states that could be attained by the next time interval assuming either full stimulation or no stimulation respectively. Therefore the active states of the muscles were constrained so that the active states chosen to produce the muscle force to satisfy equations 6.15, 6.16, and 6.17 were between the minimum and maximum active state values:-

$$Q_i > Qmin_i \qquad [6.19]$$

$$Q_i < Qmax_i \qquad [6.20]$$

Where:-

Q_i - is the active state of the i^{th} muscle

$Qmin_i$ - is the minimum active state the i^{th} muscle can attain

and $Qmax_i$ is the maximum active state the i^{th} muscle can attain.

Equations 5.22 and 5.23 automatically constrain the maximum active state to greater than zero and less than or equal to one. Based on these equations the shortest time in which the active state can change is 0.003 seconds. Therefore data was interpolated over a new time base ($\Delta t = 0.005$), to allow for a finer adjustment of the active state. Interpolation was performed using the spline procedures described in Chapter III.

The whole procedure for calculating the muscle forces is presented in the form of a flow diagram in figure 6.2. The equations used for each stage in the process are written in the appropriate box in the flow chart. The initial conditions were computed by assuming that the velocity of the muscle fibres was equal to the velocity of the muscle. The initial maximum isometric force was computed by assuming that at the current muscle lengths each muscle was exerting a maximum isometric force, using the iterative procedure described in section 5:4.2. For this first instant the activation levels were not bounded. The velocities of the muscle fibres were determined by computing the velocity of the tendon using first order backwards central difference equations (Miller and Nelson, 1973). The difference between tendon velocity and the muscle velocity gave the velocity of the muscle fibres. The optimization algorithm used to find the activation levels and therefore the muscle forces, was based on the direct search method of Hooke and Jeeves (1961), it is described in Appendix D.

In summary the muscle forces were computed by considering the objective function (6.15), subject to the constraints (6.16, 6.17, 6.19, and 6.20). The active state was selected to find a minimum solution to equation 6.15 and to satisfy equations 6.16 and 6.17 whilst keeping active state values within boundaries dictated by the previous activity of the muscle and the limitations placed on the maximum rate at which the active state can either rise or fall. The procedure had to be repeated for each sample interval, with new constraints for the muscle moment, muscle moment arms, and minimum and maximum active states for

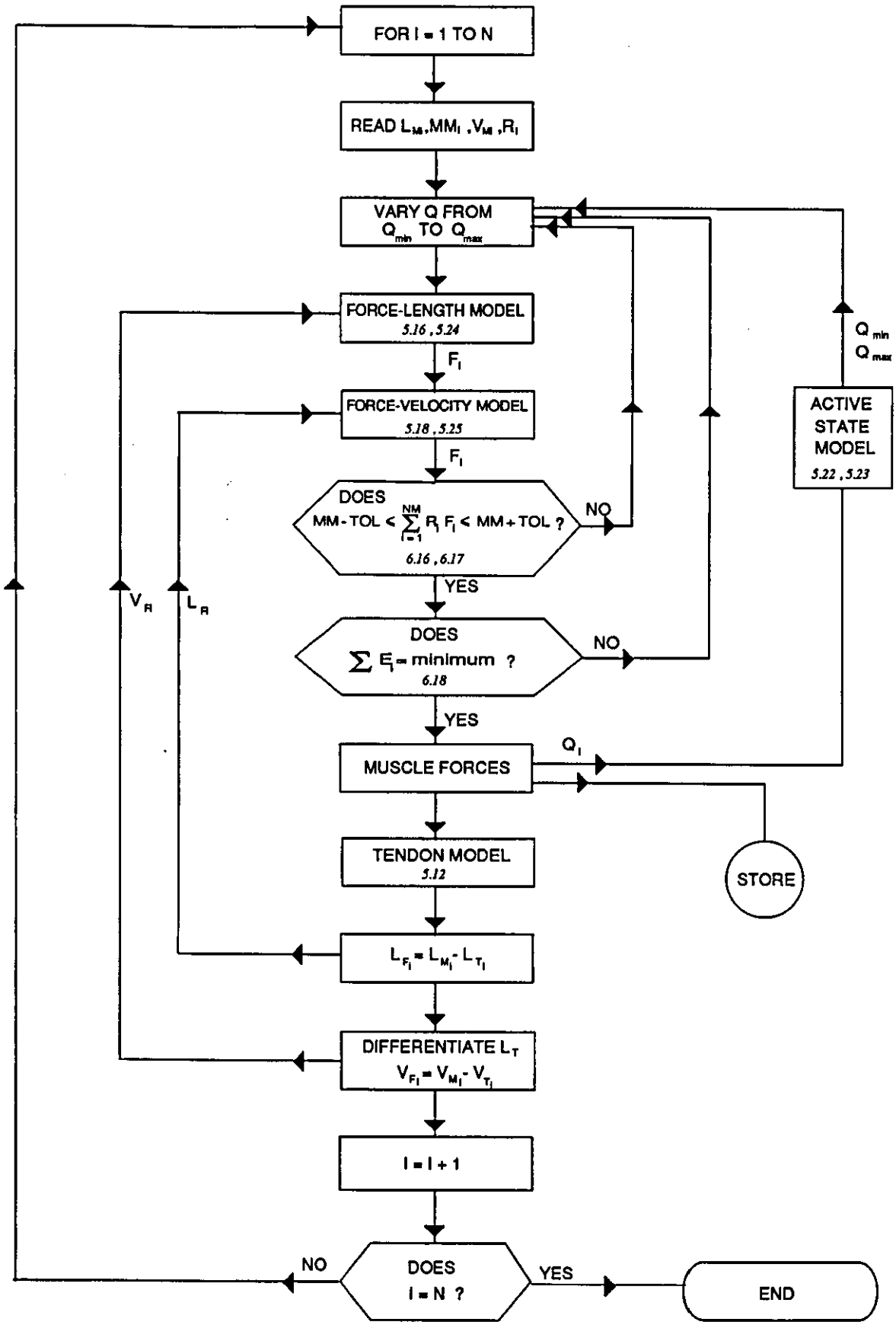

FIGURE 6.2 - A flow diagram illustrating the procedure for estimating the muscle forces, using the new objective function. The figures in the boxes refer to the equations which are the embodiment of the model used to compute the variables.

each muscle.

6:5.3 RESULTS

To test the objective function it was used to compute the muscle forces for the three conditions described in section 6.4.1. The results for this analysis are presented in table 6.5. For condition A all three muscle were estimated to be producing non-maximal forces, for condition B there was also load sharing between the muscles. For condition C the optimization formulation predicted all three muscles to be maximally active simultaneously.

TABLE 6.2 - The muscle forces estimated using the new objective function, for the three conditions.

CONDITION	BICEPS FORCE (N)	BRACHIALIS FORCE (N)	BRACHIORADIALIS FORCE (N)
A	457.5	672.1	32.5
B	480.4	536.5	68.1
C	438.9	995.6	103.7

To complete this analysis, the objective function and associated constraints described in the previous section were used to estimate the muscle forces for two of the trials. The muscle forces were estimated for trials #2, and #3. To show the effect of the objective function the muscle forces were also computed for each instant assuming that the muscles were maximally active, these are plotted on the same graph. The graphs showing the estimated and maximal muscle forces are shown for the two trials in figures 6.3 and 6.4.

Trial #2 was performed with the heaviest dumbell the subject could curl. In section 4:5.2 it was discussed how this may not have been the true maximum of the subject and the muscle force estimations reflect this. Trial #3 was the first of 5 repetition of a dumbell curl with 15 kg, the objective function estimated that the muscles were generally not exerting a maximal force throughout the movement. As the subject had to perform a further four repetitions after this analysed effort this pattern of recruitment has some justification.

6:5.4 DISCUSSION

The ability of the model presented, to estimate muscle forces in vivo has not been proven by direct experimental evidence. This criticism can also be made of the other objective function based models used to estimate muscle force in human movement. The results of the model for the three conditions presented in section 6.4.2 were all physiologically realistic, so it is validated from that point of view. The objective function was formulated based on the assumption that muscles are recruited in such a way that the rate of energy expenditure is minimised. No direct experimental evidence was found to support this theory, and it is not claimed that this is how the body recruits muscle, however a possible mechanism is presented. Such a mechanism may well come into play in a "fright, flight, or fight response", where presumably there are two possible "strategies": the minimization of metabolic energy expenditure, or the maximization of the

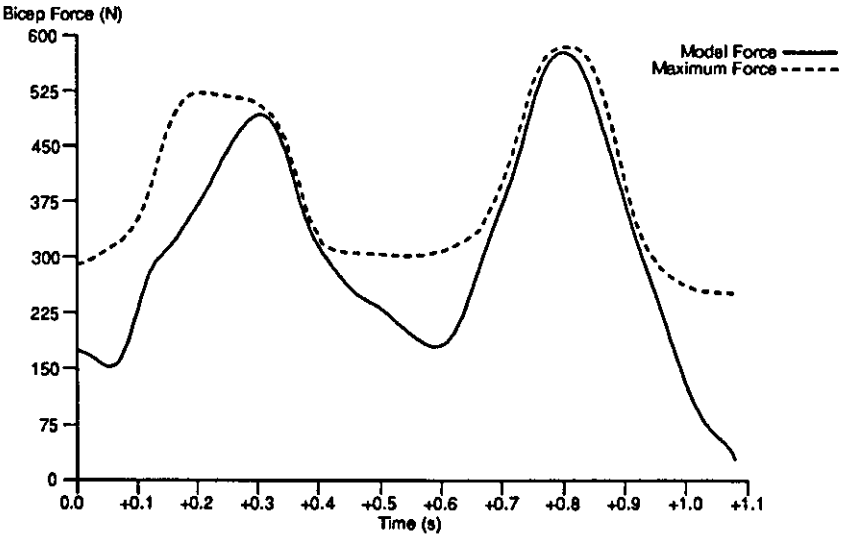

FIGURE 6.3a - The estimated force exerted by the bicep for trial #2.

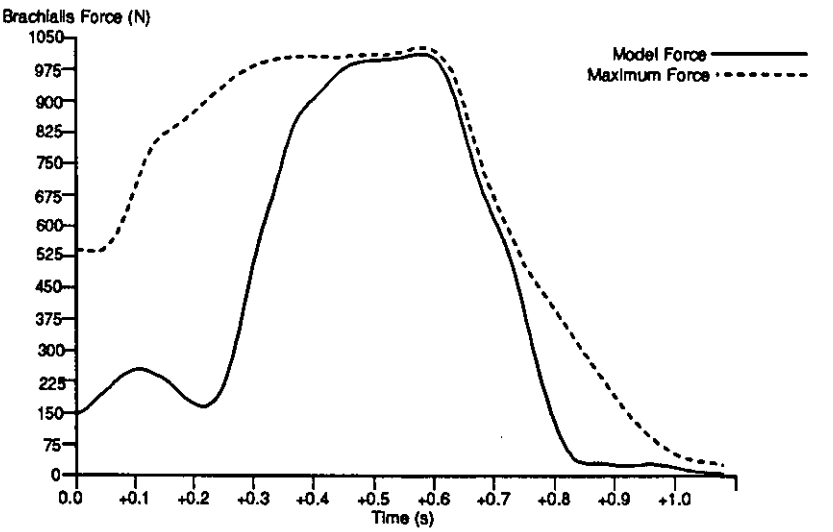

FIGURE 6.3b - The estimated force exerted by the brachialis for trial #2.

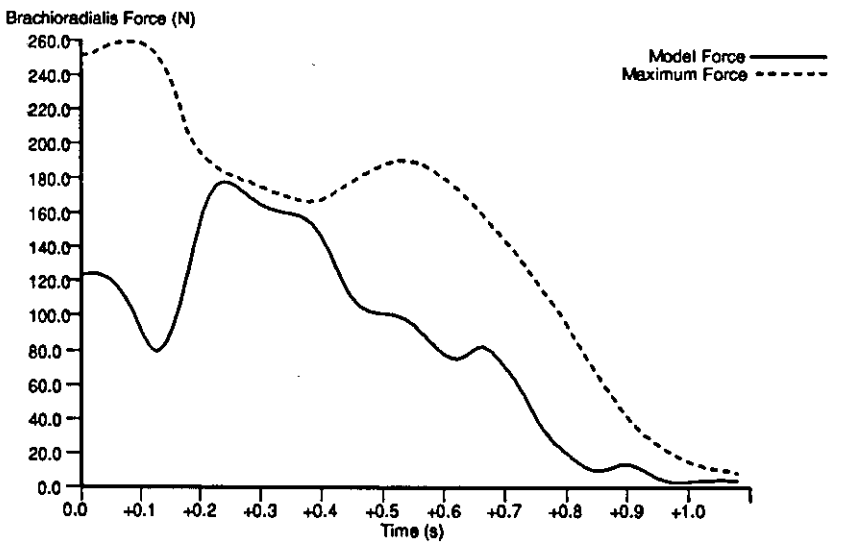

FIGURE 6.3c - The estimated force exerted by the brachioradialis for trial #2.

FIGURE 6.3 - The muscle forces for trial #2, estimated using the new objective function. The dotted line shows the maximum forces the muscles could have exerted given maximum activation.

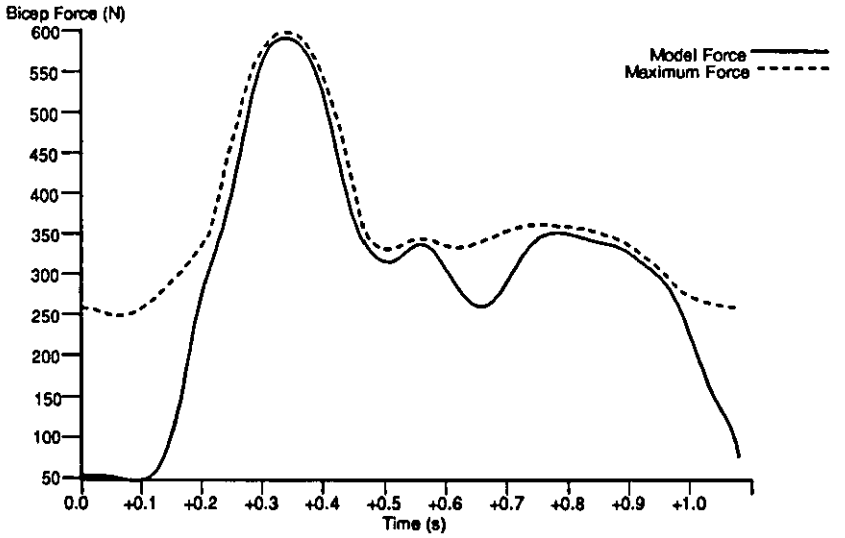

FIGURE 6.4a - The estimated force exerted by the bicep for trial #3.

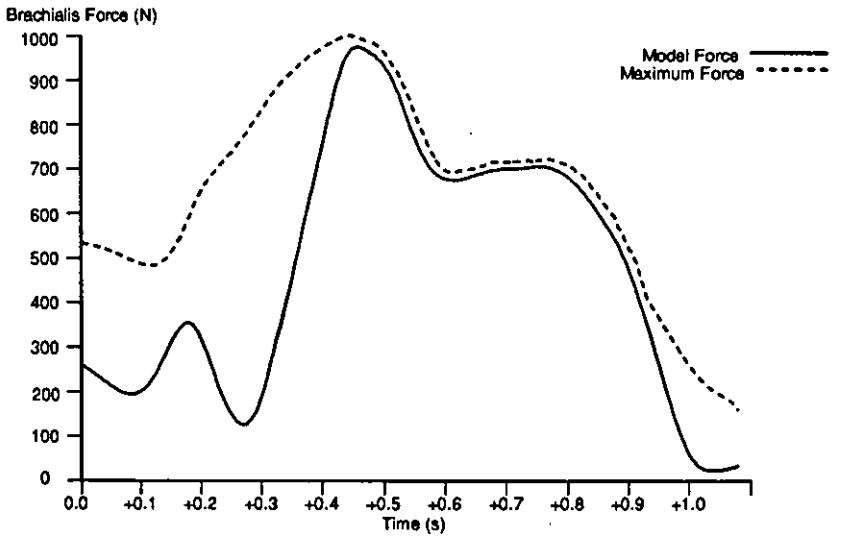

FIGURE 6.4b - The estimated force exerted by the brachialis for trial #3.

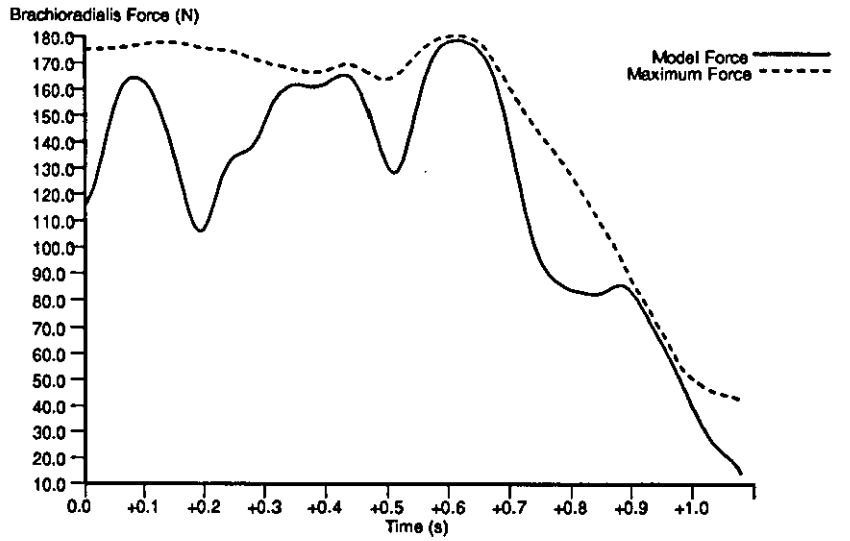

FIGURE 6.4c - The estimated force exerted by the brachioradialis for trial #3.

FIGURE 6.4 - The muscle forces for trial #3, estimated using the new objective function. The dotted line shows the maximum forces the muscles could have exerted given maximum activation.

muscle power. Whether such a "strategy" is in use in the situations studied here is as yet unknown.

Hardt (1978) presented an objective function designed to minimise the energy cost of producing a muscle moment, the shortcomings of which were discussed in section 6:3.1. The model presented in section 6:5.2 attempts to include more pertinent details of the physiological system which is being modelled. Most of the objective functions reviewed in sections 6:3.1 and 6:3.2 included little if any of the mechanical or physiological properties of the muscles in their optimization formulations.

The objective function used is physiologically based, although it is not supported by direct experimental evidence. The model includes nervous control of muscles, allowing for the previous activity of the muscles. The forces exerted by the muscles were automatically within physiological maximum limits because the force-length and force-velocity relationships were included in the model. The tendons which lie in series with the muscle fibres of each muscle have also been included in the model, because the elastic properties of these tendons can influence the force-length and force-velocity properties of the whole muscle.

6:5.5 SUMMARY

As discussed previously, it is difficult to thoroughly validate a model designed to estimate muscle forces during sub-maximal activity. The model presented here has not been validated fully although it has estimated muscle activity in accordance with EMG signals and the physiological properties of muscles. The model is not presented as an answer to the problem of estimating individual muscle forces in vivo, but to show how more physiological information can be incorporated into static optimization schemes used to estimate individual muscle forces.

CHAPTER VII

DISCUSSION AND SUMMARY

INTRODUCTION

The purpose of this Chapter is to summarise the analyses undertaken in each of the chapters, and discuss their significance and implications for further research.

7:1 CINE-PHOTOGRAMMETRIC PROCEDURES

Human movement generally occurs in three spatial dimensions. Although others have examined elbow flexion in two dimensions only (e.g. Hay, Andrews, and Vaughan, 1983), such a simplification was not made in this study. In fact as shown by An, Hui, Morrey, Linschied, and Chao (1981) the moment arms of the elbow flexors are dependent on the three-dimensional orientation of the forearm, therefore to obtain accurate moment arm information it was necessary to study the movements in three dimensions. It was the purpose of Chapter II to review some of the photogrammetric techniques used in biomechanics to obtain the position of points in space using three-dimensional cine-photogrammetry, and to detail the technique used in the present study.

The technique used to obtain this three-dimensional information was the direct linear transformation (DLT) (Abdel-Aziz and Karara, 1971). Its primary advantages were that it permitted non-metric cameras to be used, positioning of the cameras was arbitrary and did not need to be measured. The major disadvantage was the requirement of a three-dimensional distribution of control points throughout the space in which the activity was to take place. To obtain these control points a calibration structure was used. Due to the dimensions of the space in which the activity to be studied took place, the size, manufacture, and stability of the calibration structure did not present a problem.

The assumption of measuring the accuracy of the DLT using the reconstruction of the control points used to perform calibration, was examined. Such an assessment procedure does not provide an independent measure of accuracy, and cannot be considered a real test of the accuracy of a technique as the control points were used to calibrate the system initially. Reconstruction of control points reflects the accuracy of the mathematical techniques employed and any unaccounted for aspects of the photogrammetric process (including noise); it does not necessarily reflect the accuracy of the technique in locating unknown points in space. The results of this analysis indicated that with the DLT to get a true estimation of accuracy, an alternative assessment criteria to that of reconstruction of the control points used for calibration, is required. In this study a second set of control points was used to evaluate the accuracy of the DLT photogrammetric technique.

The control points required for the DLT are normally mounted on a calibration structure which is placed in the space of interest before the activity, filmed, and removed. The shape and size of the calibration structure is dependent on the activity to be studied, but there have been different methods used to distribute the control points in the space of interest. To assess the influence of control point distribution,

different control point configurations were investigated. This analysis indicated that the so called "Christmas tree" control point configuration (van Gheluwe, 1978) was the least accurate of the all the configurations investigated. These results also indicated that it is more important to surround the space in which the activity is to take place than to have control points inside the space. Other control point configurations may exist which could result in superior reconstruction accuracy.

The reduction in reconstruction accuracy if the activity took place outside of the calibrated space was quantified. These figures were not relevant in this study as all of the activities studied took place in the calibrated space. A further and more detailed examination of these errors would be of value, particularly if the DLT was going to be used in the field where only a small calibration object may be viable.

Hatze (1988) presented a modified version of the DLT for which he reported a greater accuracy in the location of points in space than the normal DLT. Miller, Shapiro, and McLaughlin (1980) discuss a similar procedure to Hatze (1988) which they claimed resulted in no increase in accuracy compared with the conventional solution. The accuracy figures reported by Hatze (1988) must be questioned because he assessed the accuracy of his technique by reconstructing the positions of control points used for calibration. There is also some question as to whether his implementation of the conventional DLT was optimal in a least squares sense, see section 2:1.5. Ignoring these criticisms the modified DLT technique of Hatze warrants further investigation in the future due to the significant increases in accuracy which he reports compared with the conventional DLT.

There are methods used in photogrammetry where the positions of the control points are only considered as approximations and are adjusted along with parameter estimation (e.g. Kenefick, Gyer, and Harp, 1972; Brown, 1978). This approach automatically adjusts for errors in the locations of the control points. In fact Brown (1968, 1978) found using such an approach that a three-dimensional distribution of control points was not required, but that multiple views of a two-dimensional distribution of control points is sufficient to perform calibration which will subsequently permit the location of points in a three-dimensional reference frame. Such methods have not been commonly employed in biomechanics, yet they offer the potential for increased reconstruction accuracy and eliminate the requirement of a three-dimensional distribution of control points. Woltring (1978, 1980) used a modified version of this type of approach.

An issue related to the cine-photogrammetric process is the location of points which have been obscured during the recording process. Obscured markers are often estimated during digitizing, or given a value as a result of interpolation using adjacent values. An analysis of this problem to determine the best procedures to locate these points, or to permit an estimation of the errors introduced when using such a procedure, would provide useful insight into the problems arising due to these errors. This problem is particularly relevant for opto-electronic techniques when analysis is attempted on-line, or when the system tries to automatically track markers during data processing.

Although Chapter II focussed on the procedures for cine-photogrammetry, many of the procedures examined could also be applied in opto-electronic measurement techniques, which have increasing use in

the study of human movement (e.g. WATSMART, SELSPOT).

7:2 LIMB KINEMATICS

Chapter III was concerned with the procedures used to determine the kinematics of the movements studied. The location of a rigid body in three-dimensional space is specified by the position and attitude (orientation) of that body. The techniques used to determine the position and attitude of a rigid body were divided into three groups: direct, unweighted least-squares, and iterative cine-photogrammetric. There has not to date been a direct comparison of techniques representing each of these groups; such a comparison would be valuable. An unweighted least-squares technique was used in this study.

To determine the attitude and position of a rigid body requires knowledge of the positions of at least three non-collinear markers on the rigid body. The points from which the position and attitude of a rigid body are determined in human movement analysis are generally marked or placed on the skin of the subject, in which case the markers are likely to move. This movement will be due to movement of the underlying skin. In this study the influence of marker movement on inter-marker distances was examined, but this only gave a partial indication of the amount of marker movement. The problem of determining the kinematics of the bone(s) making up a segment was described by Chao and Morrey (1978) who said "Accurate reconstruction of skeletal axes based on cinematographic data is extremely difficult because of the relative motion existing between the skin and the bone, and the obscureness of the prominent bony landmarks from the X-ray projection views. Imposition of soft tissue constitutes another source of error in both of these methods. The best one can hope for is to produce the gross motion of the segments but not the actual rotations occurring at the skeletal structure." (page 57)
The estimated movements of the bones in the forearm using the techniques discussed in this study were similar to the data of Chao and Morrey (1978) but is was not possible to quantify any further how accurately the movements of these bones had been measured. Lafortune and Hennig (1991) affixed markers directly to the skeleton using cortical pins, a study comparing skin based marker attitude and position estimates with those based on markers affixed directly to the skeleton would be valuable as such an approach would allow an assessment of how well the skin based markers permit the description of the movement of the underlying bones. These cortical pins may well be subject to vibrations which could hinder the measurement process. A correction procedure presented by van den Bogert, van Weeren, and Schamhardt (1990) for skin movement in horses may also have an application in human movement studies; a preliminary study would be to fully quantify these skin movements in human movement. Finally if these problems are circumvented another problem arises, that is the precise definition of member reference frames, which have a functional significance to the bone(s) of the segment. With the continued development of imaging techniques (e.g. computerized tomography, magnetic resonance imaging) it may lead to better description of member reference frames and allow their relationship to the movements of the bones they are used to describe to become better defined.

The definition of joint angles depends on how the appropriate member reference frames have been defined, therefore the way in which joint angles are defined varies between researchers, making it difficult to compare studies. Some researchers have used helical axes to describe joint motion (e.g. van Dijk,

Huiskes, and Selvik, 1979; Youm and Yoon, 1978; Siegler, Chen, and Schneck, 1988). The use of helical axes to describe joint motion has an advantage because their determination is not dependent on the way in which reference frames are defined. Using the formulae presented by Woltring, Huiskes, de Lange, and Veldpaus (1985) it was shown that the data produced in this study were not accurate enough to allow the instantaneous helical axes to be defined. It was concluded that in the present study the accuracy in locating the markers was too low to make instantaneous helical axis estimations feasible. As the reconstruction technique used had high accuracy levels compared with other techniques, these results suggest that unless improved reconstruction accuracy is available it is not possible to compute the instantaneous helical axes for gross body movements in vivo using cine-photogrammetric techniques. Even if the reconstruction accuracy was improved, it might still be necessary to model skin based marker movements so the instantaneous helical axes could be estimated.

Due to the nature of the recording process the data in this study were contaminated with noise, therefore it was necessary to smooth these data to reduce the high frequency components of the signal which were identified as noise. In addition to this smoothing of the raw data, accurate derivative data were required. Smoothing of noisy data prior to differentiation improves the accuracy of the estimated derivatives as does the appropriate selection of a differentiation technique. Therefore a number of techniques were investigated in order to select techniques (or a technique, as sometimes one technique will suffice for both smoothing and differentiation) to use in this study. These techniques were assessed using data generated from mathematical functions which approximated some aspect of human movement, noise was added to these data. The function was differentiated directly to yield the true values of the first and second derivatives. These true values were then compared with the values estimated from the noisy data by the techniques under investigation. To evaluate the accuracy of data smoothing and differentiating techniques a graphical representation of both the noisy and filtered data is often used, but this does not provide an easily comparable criterion. Therefore the accuracies of the techniques were assessed by evaluating the percentage root mean square error between the true and estimated values of the signal. This gave a quantifiable criterion, and by using a percentage value it was possible to compare results across the different data sets used. Of the techniques compared the ordinary cross-validated quintic spline gave the most accurate results. This technique was computationally very slow, therefore a quicker alternative was used: the generalised cross validated spline, which was found to give slightly less accurate results compared with the ordinary cross-validated spline, but was superior to the other investigated techniques.

In applying a data smoothing and differentiation technique in biomechanics the difficulty is determining the amount of smoothing. This is equivalent to finding where the frequency components of the true signal are insignificant compared with those of the noise impinging on the signal. For many digital filtering techniques this requires the specification of a cut-off frequency and sometimes the number of filter terms, which will effectively specify the width of the pass-band. Truncated Fourier series are usually fitted by adjusting the number of terms until the difference between the input signal and the output signal is the same as some pre-determined error estimate for the sampled signal. For a spline, unless an automated technique is used, the degree of smoothing is normally specified by varying a smoothing parameter value (e.g. 'S') in accordance with the anticipated error in the signal. It is rarely the case in human movement

studies that one knows the precise frequency components of the true signal underlying a sampled signal, in which case some procedure must be adopted for the determination of the filter cut-off or other smoothing parameter. The techniques adopted to specify cut-off frequencies include using previously published values (e.g. Winter, Sidwall, and Hobson, 1974), and manual adjustment of the degree of smoothing after visual inspection of smoothed curves (e.g. Vaughan, 1982). For such biomechanical analysis to have genuine validity a repeatable process is required, where the degree of smoothing or filter cut-off is selected by a justifiable procedure which accounts for the peculiarities of each new data set, be that data set from another trial or another body landmark. The generalised cross-validated spline employs such a procedure. Whilst other techniques may be suggested which provide more accurate predictions of the true signal and derivative values, the technique cannot be considered complete unless it includes a procedure for determining how the degree of smoothing is selected.

The examination of data smoothing and differentiation techniques described in this study did not examine what was happening at the end points of the data sets. Visual inspection of the curves indicated that inaccuracies at the end of the data sets were proportional to the errors in the middle for the appropriate order spline, but these differences were not quantified. An assessment of data smoothing and differentiation techniques where end point accuracy is quantified may provide further insight into the suitability of the different techniques used to process biomechanical data

A further examination of the generalised cross-validated spline was undertaken, which illustrated that the accuracy of the spline is dependent on what order of spline is chosen, with the quintic spline being the most applicable for the purposes of this study. When designing a study, sample rate for cine-photogrammetric technique or similar opto-electronic technique must be selected prior to data collection, in which case the frequency components of the activity to be studied are not known. Using a numerical example it was shown that when using the generalized cross-validated quintic spline the accuracy of the results increased with sample rate. This accuracy was due to the effective cut-off frequency of the spline increasing with the sample rate, resulting in more of the true signal remaining in the smoothed signal. These results correspond to the formulae of Lanshammar (1980), which indicate increased accuracy in the estimation of derivatives with increasing sample rate. This illustrates that the noise levels of rigid body position and attitude estimates and their derivatives can be significantly reduced by sampling at rates much greater than twice the Nyquist frequency, even if the variance of the additive white noise remains constant.

Signal averaging was used to analyse the effectiveness of the spline routine. The results showed that the noise associated with each of the digitized points was different, and the spline was effective in removing this noise. The information gained from multiple digitizations of data was combined with information gained from frequency analyses of the signals and used to quantify the errors in the data. This analysis used the formulae of Lanshammar (1980).

The technique of Miller et al. (1980) determines the attitude and position of a rigid body directly from the digitizer coordinates of the markers on that rigid body. Three-dimensional data derived from three-

dimensional cine-photogrammetric techniques normally have a larger reconstruction error associated with one axis (the depth axis), this difference in errors between axes can introduce errors when estimating the position and attitude of a rigid body. The approach of Miller et al. (1980) has an advantage because the reconstruction of landmarks on the rigid body in an inertial reference frame prior to the estimation of the attitude and position of the rigid body is avoided, potentially reducing the influence of the error associated with one axis. Woltring (1981) has suggested a further extrapolation of this concept with the development of a state-space model of the whole process of determining rigid body kinematics. The usual procedure is to follow a sequence of steps: identify and measure images of body landmarks, locate body landmarks in three-dimensional reference frame, smooth data, determine rigid body position and attitude, estimate derivatives of position and attitude information. A state-space model could be defined which would permit all of these parameters to be estimated using a single computational procedure. Such state-space models are used in control engineering and navigation, e.g. Eykhoff (1974), but have not yet been used in biomechanics although future attempts to obtain more accurate data may hinge on such an approach.

Although more accurate cine-photogrammetric techniques are desirable, before this accuracy can be directly transferred into a more accurate description of limb kinematics there are a number of problems associated with determining limb kinematics which require further investigation. Specifically these are: the quantification of skin/marker movement; the definition of member reference frames; and the accurate smoothing and differentiation of data. Of these three areas the last has probably been the most thoroughly investigated. In this study it has also been shown that high sampling rates produce more accurate derivative estimates, so any cine-photogrammetric technique or similar opto-electronic technique which provides increased spatial resolution must not neglect temporal resolution.

7:3 MUSCLE MOMENT DETERMINATION

Techniques to determine the inertial parameters of body segments were reviewed in Chapter IV. The data for this were divided into three notional groups: cadaver data, measurements on live subjects, and the geometric modelling of body segments. The most recent initiative in this area of study has been the use of a variety of imaging techniques to measure the inertial properties of body segments. These imaging techniques include gamma mass scanning (Brooks and Jacobs, 1975; Zatsiorsky and Seluyanov, 1983, 1985), computerized tomography (CT) (Huang and Wu, 1976; Rodrigue and Gagnon, 1983), and magnetic resonance imaging (MRI) (Martin, Mungiole, Marzke, and Longhill, 1989). Measurements made using these techniques are not yet as accurate as measurements made on cadavers, but may have more face validity because a cadaver is not representative of a live subject. In the future these techniques may be the source of more inertial information, which at least will offer a new source of density data to be used as the input to geometric models of human body segments.

This study was concerned with elbow flexion and so the only body segment inertial parameters required were those of the forearm and hand; therefore a number of different techniques for computing these parameters were compared. The techniques compared were: scaling of data; the linear regression equations of Zatsiorsky and Seluyanov (1983); the linear regression equations of Hinrichs (1985); a new set of equations which attempted to relate pertinent physical dimensions of a segment to the segment's

moment of inertia; and finally modelling the segments as if they were geometric solids, for which the inertial parameters could be calculated. Sufficient information was given in the report of Chandler, Clauser, McConville, Reynolds, and Young (1975) on six cadavers, to allow each of these techniques to be used to estimate the inertial parameters of each of the cadaver's forearm and hand segments. The values estimated using each of these techniques were compared with the direct measurements made by Chandler et al. (1975).

The results for the scaling of the data of Dempster (1955) were not very accurate, even though the procedure used was found to give the most accurate results in the study of Forwood, Neal, and Wilson (1985). In the study of Forwood et al. (1985) the mean data of Chandler et al. (1975) were scaled back onto the individual cadavers in that study using various scaling techniques. In the present study a more rigorous assessment was performed as the data which were scaled were those of Dempster (1955) which were scaled onto the individual cadavers of Chandler et al. (1975). The regression equations of Zatsiorsky and Seluyanov (1983) also did not produce very accurate results, but this raised the problem of how different researchers define the body segments, particularly segment boundaries. For the remaining two sets of equations the regression equations of Hinrichs (1985) produced better results than the non-linear equations, but for extrapolation outside of the sample population the non-linear equations produced the more accurate results. It was suggested that this was because the non-linear relationships used to formulate the equations approximated more closely the relationship between body segment dimensions and moment of inertia, than the linear regression equations. The geometric models of the forearm and upper arm showed increased accuracy when more solids were used in the models, with the lack of accuracy in the volume estimation placing a limit on the accuracy of the moment of inertia predictions. It was suggested that if sufficient measurements had been available it would have been possible to model the limbs using more truncated cones (or other appropriate shapes), which could have resulted in greater accuracy in volume estimation, therefore potentially increasing moment of inertia estimation accuracy.

The regression equations of Hinrichs (1985) gave the best results on the data investigated to assess different anthropometric models. The geometric modelling techniques gave acceptable accuracy, but were limited in the number of solids used to model the segments. More solids could have resulted in better volume estimation, and consequently potentially better moment of inertia estimations. There would appear to be no limitation to the sample range with these techniques, and researchers are free to define segment boundaries which are most suitable for their study. Therefore the geometric modelling of body segments was used in this study. There is a need for further examination of the ways of determining accurate body segment inertia parameters, with imaging techniques, such as gamma mass scanning, CT, and MRI, perhaps providing the most promising avenue for research in the clarification of this important area.

Modelling the forearm as a series of truncated cones, each 0.02 m high, and the hand as a truncated cone and a hollow cylinder, see figure 4.2, resulted in a good estimate of their volume. It was not possible to directly assess further the accuracy of inertial parameters of the forearm and hand used to compute limb kinetics. It was assumed that the dumbell inertial parameters were accurately determined, so it was

possible to investigate the influence of errors in the inertial parameters of the hand and forearm on the whole system (forearm, hand, and dumbell). The system was most sensitive to errors in the location of the centre of mass. This parameter was dependent on the accuracy of volume estimation and the assumption of constant density. The effect of available variable density values on this parameter was shown to be small. As volume was accurately estimated, it was assumed that centre of mass location was well predicted in this study. Other work, e.g. Mungiole and Martin (1990) has shown that a variety of techniques, including modelling the segments as geometric solids, provide good estimates for the location of the centre of mass.

Resultant joint moments can be calculated for an activity given the appropriate kinematic and anthropometric data, and the external forces. These moments are computed by assuming that the body segments are rigid. The marker movements identified in Chapter II show that these segments are not truly rigid. The influence of the non-rigidity of the body segments has not been thoroughly investigated in human movement, although Denoth (1986) in a theoretical analysis showed that the "wobbling mass" was a significant variable contributing to ground reaction forces. There are branches of mechanics dealing specifically with the movement of non-rigid bodies, or pseudo-rigid bodies (e.g. Cohen and Muncaster, 1988) with improved measurement techniques these methods may be applied to the study of human body movement. If these moments are calculated, assuming the body is rigid, they represent the sum of the moments caused by the active muscular tension, and by the passive deformations of any tissues which may cross or surround the joint. All of these contributions must be accounted for if a resultant joint moment is to be called the muscle moment.

There was assumed to be only one articular contact point, which was assumed coincident with the pre-selected joint centre. There can of course be more than one effective articular contact point, but it is obviously difficult to determine these points of force application in vivo.

So that the resultant joint moments could be considered to represent the muscle moments about the joint, a number of assumptions were made, and have been discussed in Chapter IV. To allow for the moments caused by any passive structures crossing the joint, a model of passive visco-elasticity was used to estimate the values of the moments produced by these structures at the different joint angles, and these were subtracted from the resultant joint moments. There have been few studies which have quantified the passive visco-elastic moments about the elbow joint; three were reviewed in this study, a further quantification and analysis of these moments to provide a larger database on which to base future models would be valuable.

Estimates were made of the accuracy of the state variables and parameters used to compute the resultant joint moments. This information was used to make an estimate of the accuracy of these moments. Each state variable or parameter was varied in accordance with its estimated accuracy level, and then the resultant joint moments were computed. These new values were compared with the values obtained with the non-perturbated parameter or variable values. In this study the joint centre was selected based on its reported location in the literature, its position was then varied to see if this affected the moments. The

differences obtained were very small. The differences when the inertial parameters were varied were also small. For another activity the inertial parameters may have made a larger difference, but in this study the error levels were low because the dumbell, held in the subject's hand, dominated the values of the inertial parameters for the whole system (forearm, hand, and dumbell), and the inertial parameters for the dumbell were accurately determined. The moments estimated in this study were most sensitive to inaccuracies in the kinematic variables. This dependence on the accuracy of the kinematic data illustrates the need, as highlighted in section 7:3, for the further investigation of techniques with which to obtain more accurate kinematic data.

The procedures used in Chapters II, III, and IV to provide the necessary data for a sensitivity analysis of the muscle moments, are steps which should be seen as part of the accepted experimental protocol in this type of biomechanical analysis. By estimating the errors in parameters and state variables, it is possible to give an indication of the error in any variables derived from them.

The reviews of Chapters II, III, and IV have highlighted a number of problems in obtaining accurate biomechanical data. To determine the resultant joint moments it was necessary to combine information obtained from a number of techniques. The principal problems which impinge on calculating these moments are listed here:-

1. Limited accuracy in estimation of landmark locations.
2. Inability to precisely define member reference frames (in addition to problems due to marker movement).
3. Motion of skeleton measured from markers made on soft tissue.
4. Determining signal to noise ratio of sampled signal.
5. Selection of appropriate data smoothing and differentiation techniques.
6. Errors in the determination of the segmental inertial parameters.
7. Segments are not rigid.
8. Axes or centres of rotation are only estimates.

It can be seen that there is still much research to be performed in the area of determining accurate kinematics and kinetics of human movement.

7:4 MUSCLE MODELS

Chapter V focussed on the development and validation of a muscle model. Only three muscles were included in the model. These muscles were selected as a consequence of the size of their moment arms and cross-sectional areas as reported in the literature. Although other muscles may contribute to the flexion muscle moment at the elbow joint, their potential contributions were considered small enough to be ignored. To obtain the locations and insertions of the muscles osteometric scaling was used. The locations of the origins and insertions were measured on a dry bone specimen and then extrapolated to the experimental subject. To do this each muscle's attachments onto the skeleton had to be represented as a single point. The scaling was performed using a least-squares homogeneous scaling technique (Sommer, Miller, and Pijanowski, 1982). A non-homogeneous scaling technique may have been more

appropriate, but the technique currently available in the literature (Lewis, Lew, and Zimmerman, 1980) requires eight bony landmarks on a single bone, therefore in this study this technique was not applicable as this number of landmarks could not be clearly identified.

The lines of action of the muscles were modelled assuming that they acted in straight lines from origin to insertion. An alternative model was discussed, the centroid line model. In this model the line of action of the muscle is considered to be the line defined by the locus of the centre of the transverse cross-section of the muscle. No evaluations have been performed to assess the difference between using a centroid line or a straight line model in a muscle model. Jensen and Davy (1975) compared the two methods for estimating moment arms for the muscles crossing the hip, and found differences from one to 12 percent between the two representations. With increased availability of imaging techniques many of the drawbacks of the centroid line model may be obviated, and such data may be able to be readily incorporated in muscle models.

A model of pennated muscle was developed. This model was used to examine whether it was possible to ignore the degree of pennation in the short head of the biceps in the model of muscle used in this study; the results indicated that it was reasonable to do so. The degree of pennation in the short head of the biceps in the experimental subject was assumed to be equal to figures published in the literature (Amis, 1978). In the literature none of the other modelled elbow flexors were reported as being pennated. However in the future it may be possible to measure muscle pennation in vivo; Wagemans, Willems, and Marchal (1990) have presented details of how the angle of muscle fibre pennation can be determined in vivo using an ultrasound technique.

A model was developed of the mechanical properties of muscle, it was phenomenological in nature. It attempted to account for all the significant factors (linear and non-linear) which affect the force output of a muscle. Although it does not model the kinetics of muscular contractions at a molecular level, as for example the model of Huxley (1957) does, it attempts to reflect the consequences of these interactions as in evidence at a macroscopic level.

There have been a number of models presented in the research literature of the force-length and force-velocity relationships. In selecting the models for this study there were two considerations: how well does the model reflect observed phenomena, and are the parameters for the model determinable? Both models used are well supported by experimental evidence, and procedures were developed which permitted the model parameters to be determined experimentally.

Isolated muscle exhibits a force-length relationship even when not stimulated, due to the passive structures surrounding the muscle. This passive force can contribute to the moment acting at a joint. Joints also produce moments due to the passive structures surrounding the joint. A model of the moments produced by the passive structures crossing the elbow joint was developed which estimated the moment due to these sources for any given joint angle. This model was assumed to include the moments caused by the passive forces caused by the muscles. This relationship was only approximate as the passive force

exerted by the muscles depends on muscle length which is a function not only of joint angle but also of muscle force. The model was based on the data of Engin (1979), and Hayes and Hatze (1977). Further examination of these moments is required for all joints, particularly to determine variations between subjects and how the moment depends on the speed of movement of the limb.

The tension developed in the muscle fibres is transferred to the skeleton via the tendons in series with the fibres. Tendons are elastic, but the precise role of tendon in animal movement is unknown. It has been hypothesised that tendon has two potential roles in human movement: as a site of elastic energy storage (Ker, Dimery, Bibby, Kester, and Alexander, 1987), or as a way of allowing the muscle fibres to shorten at lower rates than the whole muscle-tendon complex, enabling the muscle fibres to exert higher forces due to the force-velocity relationship of muscle (Bobbert, Huijing, and van Ingen Schenau, 1986). Although the stress-strain relationship of tendon is non-linear, it was modelled using a linear relationship in this study. Recent studies have in fact suggested that between 20 and 80 percent of the maximum isometric force of a muscle the stress-strain relationship is linear (Baratta and Solomonow, 1991). It has been assumed by some researchers that during human activity the tendon can be considered inelastic (e.g. Pedotti, Krishnan, and Stark, 1978), whilst others have ignored the tendon in series with the muscle fibres and have modelled the activity of the whole model using models designed to represent the muscle fibres (e.g. Yoshihuku and Herzog, 1990). Further studies to investigate the validity of such assumptions would be valuable. If it could be demonstrated that making either of these assumptions gave an adequate representation of the mechanical behaviour of muscle in vivo, there would be advantages in such an approach because ignoring tendon elasticity would greatly simplify a muscle model.

Contrary to the suggestion that these simplified muscle models may provide sufficient insight into muscle behaviour at a macroscopic level, results of a recent study suggest that a more detailed model of muscle architecture is required. Recent research by Ettema and Huijing (1989) examined the lengthening of the tendon and aponeurosis during isometric contractions of an isolated muscle. Although in muscle models the aponeurosis is often considered to be stiff (e.g. Woittiez, Huijing, Boom, and Rozendal, 1984), or to have similar properties to the tendon (e.g. Otten, 1988), the work of Ettema and Huijing (1989) indicates that the lengthening of the aponeurosis is dependent on both muscle fibre force and muscle fibre length, whereas tendon length is only dependent on muscle fibre force. Such considerations may need to be incorporated into future models of pennated muscles, with Ettema and Huijing (1989) hypothesising that the different elastic properties of the aponeurosis gives similar advantages to muscle as tendon.

In a review of muscle activation, two mechanisms were identified by which the force of a voluntary contraction could be increased: either by recruiting more motor units, or by increasing the rate of discharge of the already active motor units (rate coding). A review of literature indicated that the mechanism for controlling the force output of the elbow flexors is generally recruitment rather than rate coding. Therefore the individual motor units were not modelled, but it was assumed that at any moment a certain proportion of the whole muscle was maximally active. This model of activation may not be appropriate when a muscle is fatigued but such conditions were not examined in this study.

The definition of the active state of a muscle was based on the relative concentration of calcium ions bound to the troponin. The model of the activation process developed considered the effect of stimulation on the active state, and the relationship between calcium concentration and muscle force.

As mentioned previously, the sub-models making up the model of the muscles were selected according to how well they reflected observed phenomena, and how easy it was to determine the parameters for the model. Some of the parameters were determined from the literature. As research into muscle continues, the database from which parameters for this type of model are derived will grow. With the increased availability of such information the accuracy and specificity of parameters for such models will increase. In this study the parameter based on the least information was the distribution of the different muscle fibre types in the muscles modelled.

The remaining parameters for the models were determined using an experimental procedure. This procedure was similar to that used by Hatze (1981d), although the procedure he used attempted to estimate more parameters. The model was validated using a simulation procedure. Given the rate of change of the length of the muscles, and assuming muscle activations were maximal, the forces of the muscles were estimated. Given the moment arms of these muscles it was possible to compare the model predicted muscle moments with those estimated using inverse dynamics. The model predicted moments fell within the anticipated accuracy range for the muscle moments as estimated using inverse dynamics. As this was a maximal dynamic activity it validated the muscle model, but did not validate the model for sub-maximal activity. As discussed in section 6:1 it is very difficult to obtain muscle forces during sub-maximal activity. Therefore it had to be assumed that as the muscle model was valid for maximal activity it would also be valid for the sub-maximal activities examined in Chapter VI.

Although not used for this purpose the validation procedure could have been used to further examine and provide insight into muscle during maximal activity. It would therefore be well suited to a range of sporting activities.

The model assumed that only three muscles were responsible for elbow flexion, although others may contribute to the flexion moment at the elbow joint. If other muscles did contribute to the moment their contribution would have been grouped with the three modelled muscles in the experimental procedure used to estimate the model parameters. The moment arms of the elbow flexors are dependent on the attitude of the forearm, therefore it is possible that other muscles may not have significantly contributed to the flexion moment during the static data capture that was used to initialise the muscle parameters, as the forearm was maintained in a supinated position. However during the dynamic data capture although predominantly held in a supinated position the forearm did vary from this position during some of the movement, in which case some muscles may have been able to contribute to the flexion moment, which were not accounted for in the experimental procedure used to determine some of the model parameters. The results of the validation procedure would seem to indicate that this was not the case. Due to the nature of the activities examined in this study it was assumed that throughout most of the range of movement no co-contraction of antagonists occurred.

The model also relied on a number of other variables: moment arms, lengths, and velocities of the muscles. If the moment arms had been inaccurately determined this would have introduced systematic error into the measurements, which would have been incorporated into the experimental determination of the model parameters. Given the recent advances in imaging techniques it may soon be possible to routinely determine the necessary details to describe muscle geometry in vivo, the work of Rugg, Gregor, Mandelbaum, and Chiu (1990) provides an example of such an approach. The same comments apply equally to the muscle length calculations. To obtain the velocity of the muscle it was necessary to differentiate the muscle length with respect to time. Such differentiation is a source of error as discussed in section 3:4.8. Again imaging techniques may soon provide a means of validating the modelling approach taken here to determine the moment arms and lengths of muscle in vivo.

The energetics of muscular actions were discussed and the equations presented which permitted the modelling of the initial heat associated with isometric and concentric muscle actions. A future development of this model would be to model the energetics of eccentric muscle actions which occur in most everyday and sporting movements.

As muscle models become more sophisticated it may be possible to gain further insight into the role of muscle in human movement; with the elucidation of the role of tendon, and biarticular muscles in human movement already being identified as areas of interest (e.g. Bobbert et al., 1986; van Ingen Schenau, 1990).

7:5 MUSCLE FORCE ESTIMATION

Chapter VI focussed on the procedures which have been used to estimate individual muscle forces in vivo. It is not possible to compute the individual muscle forces causing a movement using kinematic and kinetic information only, if the number of muscles is larger than the number of degrees of freedom at the joint. As this is generally the case, estimating these forces is a complex problem. Muscle forces have been measured directly by affixing force transducers to tendons (e.g. Komi, Salonen, Jarvinen, and Kokko, 1987), but such highly invasive procedures are not generally applicable. In the future direct measurement of muscle force in man may become technically more viable, at which time such measures could be used to validate other non-invasive, or at least less invasive, methods for estimating muscle forces.

Indirect procedures for estimating muscle forces include: models involving EMG, control models, dynamic optimization, and static optimization. EMG based procedures are invasive as electrodes must be affixed to the subject, and there are methodological problems associated with such procedures (e.g. Hof, 1984; Bigland-Ritchie, 1981). Control models attempt to model the way in which the body distributes the load between the muscles, there is no maximization or minimization of some function. In the simplest of these models muscle forces are distributed according to the estimated cross-sectional areas of the muscle (e.g. Amis, Dowson, and Wright, 1980). The more complex models, for example Pierrynowski and Morrison (1985a,b), incorporate a complex muscle model, and muscle forces are estimated based on the physiological properties of the muscles. The mechanism by which the human body recruits muscle to

produce a moment is not known, so these control models are hypothetical. In dynamic optimization studies the human body segment dynamics are modelled; the joint moments have to be found which cause the body segments to move in such a way that some performance criterion is maximised. In the more sophisticated models the joint moments are produced by muscle models. If the simulated activity compares well with the actual activity, in terms of kinematics and kinetics, then the muscle forces predicted by the model can be considered to reflect what the actual muscle forces are. These techniques are not generally applicable because it is difficult to formulate a performance criterion. For certain sporting activities a performance criterion may be obvious, but for everyday activities they are not so obvious. They therefore represent powerful tools for examining human muscular coordination for a limited range of activities.

Static optimization procedures were examined in detail in this study. A review of literature revealed that a large number of researchers had attempted to accurately estimate muscle forces using these procedures. These studies have led to there being a number of different objective functions which have been used to estimate individual muscle forces. Along with the application of these objective functions different constraints have been placed on either the muscle forces or the muscle stresses. The belief that some objective function, at least in part, reflects how the body recruits muscle is reflected in this quote from Chao and An (1978)

"However, in examining the voluntary functions of an anatomical structure, there is a striking ability for it to produce consistent functional activities. Such unique ability must be controlled by certain physiological laws based on which proper solutions to the redundant problem may be obtained. Consequently, it would be important for the biomechanicians to quantitate these laws, not only for the purpose of seeking basic understanding of how musculoskeletal systems function but also to establish workable models and theories for the analysis of abnormal functions in the hope of providing valuable clinical information." (page 159).

Whether the solution of this problem lies in the formulation of an appropriate objective function remains to be discovered. The human body is capable of a wide range of activities, and it is unlikely that the body recruits muscle using the same protocol for sprinting 100 metres as it would for running a marathon. If such criteria do exist there are perhaps different functions for different types of activity. But while researchers endeavour to uncover the truth, the problem of model validation provides a major obstacle to fruitful research.

There have been three methods used to validate the muscle forces estimated using objective functions: comparison of muscle activity as indicated by EMG signals with estimated muscle activity from the objective function; comparison of muscle forces predicted by the objective function with that predicted by a muscle model; and the use of muscle forces measured in vivo for evaluation. Unprocessed EMG information does not give a true indication of the relative or absolute activity of the muscles, only whether a muscle is active; further processing of EMG signals introduces many methodological problems. Validation using a muscle model requires a valid muscle model, and generally these can only provide good estimates of muscle activity during maximal activity, and therefore only validate the objective function for this limited case - maximal activity. The final method is limited as the number of studies where muscle forces have

been measured in vivo are small. If such data is used from the literature, model parameter estimation is more difficult and potentially less accurate, than it would be if the same researcher measures the muscle forces in vivo and tests the objective function. Such sources of data are generally highly invasive, in which case muscle recruitment patterns may be different from normal activity. It can therefore be concluded that data with which to validate objective functions and other alternative procedures used to predict muscle forces, are required.

As discussed it is not possible to validate fully one of these optimization procedures. To examine further a number of objective functions and constraints partial validation was sought. This was achieved by considering muscle activity as indicated by EMG signals, maximum muscle activity as indicated by the physiological properties of the muscles, and by comparing muscle force estimations with those predicted using the muscle model described in Chapter V.

For the linear objective functions examined there was no sharing of the load unless additional constraints were placed on the solution space. In these objective functions a single muscle was preferentially selected depending on either the moment arms or the cross-sectional areas of the muscles in the model, or the product of these two variables. The linear objective functions were limited because the number of active muscles predicted by a linear objective function depends on the number of constraints imposed. Therefore without the imposition of equality constraints none of the objective functions investigated predicted all the muscles to be simultaneously active under any of the conditions. One of the linear objective functions behaved slightly differently from the remainder; this function minimised the maximum stress experienced by the most stressed muscle. This meant the muscles were recruited in direct proportion to their respective cross-sectional areas. Of the linear objective functions examined this was the only one which predicted all three muscles to be simultaneously active without the imposition of additional constraints.

A number of non-linear objective functions were also examined. All of these functions predicted all the muscles to be active simultaneously. These were all concerned with the minimization of the sum of some function of: a) the muscle forces; b) the muscle stresses; or c) the relative muscle activities. As all the non-linear objective functions were solved analytically using a Lagrangian multiplier technique, it was possible to see how mathematically the solution to these objective functions was found. For the non-linear objective functions concerned with the sum of a function of the muscle forces, the way the load was shared between pairs of muscles was a function of the moment arms of the muscles and p, where p is the power to which the muscle force had been raised. However such a solution takes no account of physiological properties of the muscles. The objective functions which were a function of the muscle stresses predicted muscle forces which depended on the moment arms and cross-sectional areas of the muscles, and p. Again although these mechanical parameters are important there is no account taken of the physiological properties of the muscles. The final group of objective functions was concerned with the minimization of the sum of a function of the relative muscle forces. Analysis of the analytical solution to this group showed the results to be functions of the moment arm, the maximum force the muscle could exert, and p. This maximum muscle force was dependent on the muscle model used to predict it. For

most of the objective functions examined it was necessary to impose constraints on the muscle forces so that the predicted muscle forces did not exceed the physiological maxima. The objective functions examined were based on those reported in the literature, none of which could claim to have a genuine physiological basis. The force output of a muscle is a complex function of the length, velocity, and degree of activation of its fibres. By taking account of the previous or current states of the muscles, some knowledge of the mechanics of muscle could be incorporated into the model used to estimate muscle forces.

Most of the studies reviewed did not attempt to estimate or scale muscle parameters to their subjects, rather they used figures from the literature (e.g. McLaughlin and Miller, 1980). This procedure has the potential for producing errors in the estimated muscle forces, particularly for athletic subjects where certain muscle groups may be developed beyond the norm, and so for example would not match the cross-sectional data obtained from cadavers. Many of the objective functions were not based on the physiological properties of the muscles, the objective function of Hardt (1978) being a notable exception. A muscle model of some description provides a valid way of constraining the muscle forces, but very few studies have included a muscle model, exceptions being Pedotti et al. (1978), and Herzog (1987a,b).

A new objective function was formulated which attempted to take account of more of the physiological properties of muscle. It was hypothesised that the human body recruits muscles in such a way that the rate of energy expenditure to produce the current muscle moment is a minimum. An objective function was formulated to reflect this hypothesis. The rate of energy expenditure was modelled as a function of the length and velocity of the muscle fibres of each muscle, therefore these factors are accounted for in the objective function. The nervous systems control of the muscles is not instantaneous, a muscle is not turned on and off in an instant (bang-bang control) rather it takes time for force to develop, and time for it to reduce. To account for these delays a model of active state was used to give upper and lower active state levels for each time interval. Under three different conditions (sub-maximal isometric, sub-maximal dynamic, and maximal dynamic) this objective function estimated muscle forces which were physiologically realistic. Further assessment of the validity of the model was not possible because of lack of suitable criterion data.

The new objective function illustrated how more physiological properties of muscle could be incorporated into an objective function designed to estimate muscle forces. The objective function used was physiologically based, although it is not supported by direct experimental evidence. Unlike any other model reviewed, for static optimization studies, this model included aspects of the nervous control of the force output of a muscle. The forces exerted by the muscles were automatically within physiological maximum limits because the force-length and force-velocity relationships were included in the model. The tendons which lie in series with the muscle fibres of each muscle were also included in the model; the elastic properties of these tendons can influence the force-length and force-velocity properties of the whole muscle. Although it was not possible to validate this model, the muscle forces predicted by it were within the physiological maximum bounds which the muscle could exert. Examination of other objective functions showed this was not commonly the case.

The procedures adopted in this study differ from many of those in the literature. In particular the parameters required to describe the muscles in the study were experimentally determined. It is more common in static optimization studies to adopt muscle parameters from the literature, without trying to customise them to the experimental subject or validate them. The experimental determination of muscle model parameters does not necessarily make the muscle force predictions any more valid, but does make any constraints placed on these muscle forces based on these models more valid.

The most successful procedure examined for estimating individual muscle forces was the one described in section 5:5. The simulation model developed estimated the individual muscle forces during maximal activity, where the only input variable was the rate of change of the lengths of the muscles. As this procedure was successfully validated, by comparing estimated net muscle moments with those computed using inverse dynamics, the muscle force estimations can be viewed with some degree of confidence. Although this model is only applicable for maximal activity, it potentially offers the ability to obtain greater insight into muscular performance in athletic activity.

The dynamic optimization procedures discussed in section 6:2.3 have been used by relatively few researchers, and clearly warrant further study. They potentially offer insight into the coordination of muscles to produce a desired activity. In sporting activities where it is more likely that a clear performance criterion can be established, these methods, although complex, may greatly aid understanding of muscle recruitment patterns and the role of different muscles in influencing coordination of limbs.

For the examination of sub-maximal activity there is also a need for a means of validating procedures for estimating individual muscle forces. The measurement of the individual human muscle forces in vivo for all the muscles crossing a joint, for a range of activities, would provide a valuable contribution to this area of research. Such a validation would assume that the muscle forces measured under these conditions are reflective of the muscle forces under normal conditions.

The muscle force estimations analysed in this study were for movements where the intensity was near maximum. Many everyday movements are performed at a much lower intensity. Even if one of the current models was accurate for high intensity activity, it may not be appropriate for less intense activities. In section 5:3.5 movement specific motor unit recruitment was discussed. If this phenomenon does occur in muscles, where it may be possible to vary not only which muscles but also which motor units are active for different activities, individual muscle force estimation during sub-maximal activity becomes an even more complex task.

7:6 MODELLING

The basic methodology of this study has been underpinned by the extensive use of models. The problems of ensuring model validity have been examined at each stage of the modelling procedure. But the problem of a thorough validation of some of the models developed still remains, particularly the objective function designed to estimate individual muscle forces. Panjabi (1979) claimed

"After all, a mathematical model is only a set of equations. Its link to reality is via the physical properties

data of the system it is intended to simulate. Its success at simulation is not guaranteed but must be proven by suitable validation.....The basic dilemma in the process of validation may be stated in the following manner: a mathematical analogue can be validated only in a given number of known situations. Thus, no perfect validation is possible." (sic, page 238).

7:7 SUMMARY OF FINDINGS

The aim of this study was to develop and examine the methodology necessary to estimate the individual muscle forces causing elbow flexion. This section summarises the principal experimental findings of the study.

1. When employing the direct linear transformation for three-dimensional reconstruction of image coordinates the configuration of control points, used for camera calibration, was shown to have an influence on reconstruction accuracy in that having control points surrounding the calibrated space resulted in better reconstruction accuracy than having control points within that space.
2. There was a 20 percent reduction in accuracy when reconstructing points which were in the space equivalent in size and directly adjacent to the calibrated space.
3. The modelling and removal of lens distortions resulted in no increase in reconstruction accuracy.
4. Eight data smoothing and differentiation techniques were evaluated; the cross-validated quintic spline produced the most accurate results.
5. The accuracy of derivatives computed from displacement data using the generalised cross-validated quintic spline increased with increasing signal sample rate.
6. The accuracy of three groups of anthropometric methods (simple statistical models, complex statistical techniques, and geometric models) were compared. The linear regression equations of Hinrichs (1985) produced the most accurate estimates of moment of inertia values.
7. The linear regression equations of Hinrichs (1985) were not as accurate as a set of non-linear equations, when moment of inertia values were predicted for data which fell outside of the range of values in the data from which the equations were formulated.
8. The influence of the accuracy of the inertial parameters for the forearm, hand, and dumbell on the inertial parameters for the whole system was assessed using a sensitivity analysis. The inertial parameters for the whole system were most sensitive to errors in the centre of mass locations of the constituent parts of the whole system. These centre of mass locations were found to be well located with the techniques used.
9. A sensitivity analysis of the parameters and variables required to compute the resultant joint moments showed that these moments were most sensitive to errors in the kinematic data; suitable steps were taken to ensure high accuracy in these data.
10. A model was used to show that small amounts of muscle pennation may be ignored when modelling muscle architecture.
11. A model designed to examine the muscles causing elbow flexion, was shown to accurately simulate the activity of the muscles during a maximum dumbell curl.
12. Sixteen commonly used objective functions (e.g. minimisation of the sum of the muscle forces, and minimisation of the sum of the muscles stresses), each implemented with three different constraints, were

evaluated under three test conditions, and shown to estimate muscle forces which were physiologically unrealistic. The forces estimated by these objective functions were shown to be functions of the muscle cross-sectional areas and moment arms, but did not take account of the contractile properties of the muscles.

13. A new objective function was presented which both took account of the contractile properties of the muscles and minimised the energetic cost of producing the moment at a joint. This objective function, under the same test conditions with which the other objectives functions were evaluated, estimated physiologically realistic muscle forces.

7:8 SUMMARY

This study focussed on the development and examination of the procedures necessary to estimate individual muscle forces in vivo. These procedures included the measurement procedures required to determine the input parameters and variables required for the models used to estimate the muscle forces. The review, examination, and development of procedures undertaken in this study will hopefully increase understanding in this area, and increase the base from which future research will take place.

Individual muscle forces are of interest to researchers to provide insight into the etiology of injuries and the training of muscle for rehabilitation and sport. Such analyses may provide new insight into the limits of athletic performance, and facilitate the maximization of an athlete's abilities. In the exciting area of functional neuro-muscular stimulation, and the important area of optimization of worker performance, this information may also provide vital insight. New technologies may make the in vivo determination of individual muscle force more practicable and less invasive than direct assessment techniques. Models such as the ones developed here are the primary methods currently available to gain insight into these important phenenomena.

APPENDIX A

THE DIRECT LINEAR TRANSFORMATION

The Direct Linear Transformation (DLT) produces a direct linear relationship between the digitizer coordinates of a point and the object space coordinates of that point. Assuming the image (film frame, photograph) is a perfect plane, it represents a central projection of the object space onto the image plane. Given the coordinates of points known in the object space and their corresponding image coordinates the projective transformation matrix is (Ghosh, 1979):-

$$\begin{bmatrix} U_i - U_{io} \\ V_i - V_{io} \\ -C \end{bmatrix} = S.\,[M] \begin{bmatrix} X - X_o \\ Y - Y_o \\ Z - Z_o \end{bmatrix} \qquad [A.1]$$

Where:-

U_i, V_i - are the image coordinates of a point

U_{io}, V_{io} - are the image coordinates of the principal point

C - is the principal distance (or calibrated focal length)

S - is a scale factor

[M] - is a rotation matrix

X,Y,Z - are the object space coordinates of a point

and X_o, Y_o, Z_o are object space coordinates of the perspective centre

The principal point is the point of intersection of the image plane and the optical axis. The perspective centre is the common point on the optical axis at which the light rays are considered to intersect.

The image coordinates are not directly measured, instead the images are projected onto a digitizing tablet and measured from the projected image. If the image and its projection are parallel the following relationship between image coordinates and digitizer coordinates exists:-

$$U_i - U_{io} = S_u (U_d - U_{do} + \Delta U_d) \qquad [A.2]$$

$$V_i - V_{io} = S_v (V_d - V_{do} + \Delta V_d) \qquad [A.3]$$

Where:-

S_u, S_v - scale factor for the two axes

U_d, V_d - are the digitizer coordinates of a point

U_{do}, V_{do} - are digitizer coordinates of the principal point

and ΔU_d, ΔV_d are the errors associated with the coordinates

This relationship allows for correction for uniform and differential deformations in the image.

Expanding equation A.1:-

$$U_i - U_{io} = S\,[M_{11}(X-X_o) + M_{12}(Y-Y_o) + M_{13}(Z-Z_o)] \quad [A.4]$$

$$V_i - V_{io} = S\,[M_{21}(X-X_o) + M_{22}(Y-Y_o) + M_{23}(Z-Z_o)] \quad [A.5]$$

$$-C = S\,[M_{31}(X-X_o) + M_{32}(Y-Y_o) + M_{33}(Z-Z_o)] \quad [A.6]$$

Where:-

M_{ij} - are the elements of the rotation matrix [M]

Dividing equation A.4 by A.6 and multiplying both sides of the equation by -C gives:-

$$U_i - U_{io} = -C\,\frac{[M_{11}(X-X_o) + M_{12}(Y-Y_o) + M_{13}(Z-Z_o)]}{[M_{31}(X-X_o) + M_{32}(Y-Y_o) + M_{33}(Z-Z_o)]} \quad [A.7]$$

Similarly:-

$$V_i - V_{io} = -C\,\frac{[M_{21}(X-X_o) + M_{22}(Y-Y_o) + M_{23}(Z-Z_o)]}{[M_{31}(X-X_o) + M_{32}(Y-Y_o) + M_{33}(Z-Z_o)]} \quad [A.8]$$

Substitute A.2 and A.3 into A.7 and A.8 and simplify:-

$$U_d + \Delta U_d = \frac{AX + BY + CZ + D}{IX + JY + KZ + 1.0} \quad [A.9]$$

$$V_d + \Delta V_d = \frac{EX + FY + GZ + H}{IX + JY + KZ + 1.0} \quad [A.10]$$

Where:-

A -K - are the calibration coefficients

Re-arrangement of these equations allow them to be put into matrix form:-

$$A.x = b \quad [A.11]$$

Where:-

A - is a m*n matrix, composed of the object space coordinates of the control points, and the image coordinates of these points.

m - is twice the number calibration points

n - is the number of calibration coefficients (11)
x - is an n*1 unknown column matrix containing the camera specific calibration coefficients
and b is an m*1 column matrix containing the digitizer coordinates of the control points.

This system of equations requires at least six control points to make it determinant, but more control points can be accommodated. Solution of this system is performed using the linear least squares technique described in section 2:2.3. Once solved it yields the calibration coefficients. Comparison of equations A.7, A.8, A.9 and A.10 shows that given these coefficients it is also possible to calculate the variables contained in equation A.1.

LENS DISTORTION

The error in the digitizer coordinates is of two sources random and systematic. The removal of the random errors was discussed in section 3:4. One of the sources of systematic errors is lens distortion. The amount of radial lens distortion can be calculated from:-

$$\Delta U_{dr} = U_d'(K1.R^2 + K2.R^4 + K3.R^6) \qquad [A.12]$$

$$\Delta V_{dr} = V_d'(K1.R^2 + K2.R^4 + K3.R^6) \qquad [A.13]$$

Where:-
ΔU_{dr}, ΔV_{dr} . are the errors associated with radial lens distortion
K1, K2, and K3 - are constants
and
$U_d' = U_d - U_{do}$
$V_d' = Vd - V_{do}$
$R^2 = U'^2 + V'^2$
This model contains three parameters, additional parameters as used in section 2:3.4 are easily accommodated.

The amount of de-centering distortion (asymmetrical) can be calculated from:-

$$\Delta U_{da} = P1(R^2 + 2.U_d'^2) + 2.P2.U_d'.V_d' \qquad [A.14]$$

$$\Delta V_{da} = P2(R^2 + 2.V_d'^2) + 2.P1.V_d'.U_d' \qquad [A.15]$$

Where:-
ΔU_{da}, ΔV_{da} - are the errors associated with de-centering lens distortion
and P1 and P2 are constants.

Combining equations A.12, A.13, A.14, and A.15 gives:-

$$\Delta U_d = \Delta U_{dr} + \Delta U_{da} = U_d'(K1.R^2 + K2.R^4 + K3.R^6) + P1(R^2 + 2.U_d'^2) + 2.P^2.U_d'.V_d' \quad [A.16]$$

$$\Delta V_d = \Delta V_{dr} + \Delta U_{da} = V_d'(K1.R^2 + K2.R^4 + K3.R^6) + P2(R^2 + 2.V_d'^2) + 2.P1.V_d'.U_d' \quad [A.17]$$

Substitute these equations into A.9 and A.10 and re-arrange:-

$$-U/Q = -(AX + BY + CZ + D) / Q + U(IY + JY + KZ) / Q + \Delta U \quad [A.18]$$

$$-V/Q = -(EZ + FY + GZ + H) / Q + V(IX + JY + KZ) / Q + \Delta V \quad [A.19]$$

Where:-

$Q = IX + JY + KZ + 1.0$

These equations are put into matrix form, and solved to give the lens distortion coefficients, using the linear least squares technique described in section 2:2.3. To make the system of equations determinate at least eight control points are required. The digitizer coordinates of the principal point are also required. These can be calculated from the initial estimates of the calibration coefficients. Once this procedure has been implemented the digitizer coordinates can be corrected for lens distortion and (hopefully) an improved estimate of the calibration coefficients obtained. This procedure is repeated iteratively until no improvement is found in the locations of the points used for calibration, or until the accuracy in locating these points is no better than the accuracy to which they were measured originally.

SPACE INTERSECTION

The digitizer coordinates are first filtered to remove any random noise arising from the digitizing process. For the digitized control points the mean of ten digitizations is assumed to remove the random errors. The digitizer coordinates are then corrected for lens distortion. Re-arrangement of equations A.9 and A.10 gives:-

$$U_d = X(A - U_d.E) + Y(B - U_d.F) + Z(C - U_d.G) + D \quad [A.20]$$

$$V_d = X(H - V_d.E) + Y(I - V_d.F) + Z(J - V_d.G) + K \quad [A.30]$$

These equations can be put into matrix form, and given the digitizer coordinates of points in the object space from at least two camera images, the system of equations can be solved using linear least squares

to produce the object space coordinates of that point.

CAMERA LOCATION

Analysis of equations A.7, A.8, A.9, and A.10 leads to the following formulae:-

$$-D = AX_0 + BY_0 + CZ_0 \quad [A.31]$$

$$-1.0 = IX_0 + JY_0 + KZ_0 \quad [A.32]$$

$$-H = EX_0 + FY_0 + GZ_0 \quad [A.33]$$

In matrix form:-

$$\begin{bmatrix} A & B & C \\ I & J & K \\ E & F & G \end{bmatrix} \begin{bmatrix} X_0 \\ Y_0 \\ Z_0 \end{bmatrix} = \begin{bmatrix} -D \\ -1.0 \\ -H \end{bmatrix} \quad [A.34]$$

Solving this system of equations gives the location of the cameras perspective centre.

APPENDIX B

TEST FUNCTIONS

To evaluate the data smoothing and differentiation techniques in Chapter III a number of different data sets were used. These data sets were generated from test functions, which meant that true 'displacement' and first and second derivative values could be determined directly from these functions. Some of these functions were 'purely mathematical', whilst others attempted to model aspects of human movement. The functions are detailed in this appendix. The problems of deriving genuine data to test data smoothing and differentiation techniques were discussed in section 3:4.2; these functions enabled them to be circumvented.

Once the data had been generated from one of the functions, noise was added to the signal so that it approximated genuine noisy film derived data. The noise was white noise which means that the noise was stationary, uncorrelated, and with a mean value of zero. The noisy test data sets on which the smoothing and differentiating techniques had to operate on were generated from:-

$$g(t) = f(t) + e(t) \qquad [B.1]$$

Where:-
g(t) - is the noisy data set value at time t
f(t) - is the true signal value at time t
and e(t) is the value of the noise contaminating f(t) at time t.
For each data set the standard deviation (σ_e) of the noise is stated.

The test functions were initially implemented on the PRIME 750 Mainframe Computer, operating under the Salford University FORTRAN 77 compiler. The noise was added to the signals using a random number generator. When these programs were transferred to the Archimedes 440 microcomputer (Acorn), running an Acornsoft FORTRAN 77 compiler, a similar procedure was employed to generate the noise. Although every attempt was made to make these random number effects as similar as possible, there are some differences. All results therefore pertain to numerical studies carried out on the PRIME, unless otherwise stated.

DATA SET - **a**
This data set was a cosine wave. The following functions were used to obtain the criterion data:-

$$f(t) = \cos(t) \qquad [B.2]$$

$$f'(t) = -\sin(t) \qquad [B.3]$$

$$f''(t) = -\cos(t) \qquad [B.4]$$

$$t_i = (i - 1).\left(\frac{2\pi}{n - 1}\right) \qquad [B.5]$$

Where:-

$f(t)$, $f'(t)$, and $f''(t)$ - are the function and its first and second derivatives.
n - is the number of data points (n=101).

For the noisy data set generated from this function the noise had a standard deviation of 0.02, ($\sigma_e = 0.02$).

DATA SET - **b**

This was based on one of the functions presented by Cappozzo (1982). It was designed to model the displacement of the iliac crest tubercle of an amputee during level walking. The functions used to provide the criterion data were:-

$$f(t) = \sum_{i=1}^{13} a_i \sin(i\ w_0 t + \phi_i) \qquad [B.6]$$

$$f'(t) = \sum_{i=1}^{13} i\ w_0\ a_i \cos(i\ w_0\ t + \phi_i) \qquad [B.7]$$

$$f''(t) = -\sum_{i=1}^{13} (i\ w_0)^2\ a_i \sin(i\ w_0\ t + \phi_i) \qquad [B.8]$$

Where:-

$0 < t < 1.0$

$w_0 = 2\pi$

91 samples were used so $\Delta t = \frac{1}{90}$

The constants a_i, and ϕ_i are presented in table B.1

For the noisy data set generated from this function the noise had a standard deviation of 0.05, ($\sigma_e = 0.05$).

Table B.1 - Trigonometric constants.

i	a_i	ϕ_i
1	16.0	0.99
2	12.0	0.23
3	6.3	-2.97
4	0.5	0.0
5	1.2	-3.13
6	0.6	-0.84
7	0.3	2.14
8	0.2	0.58
9	0.1	1.15
10	0.09	0.17
11	0.04	-1.13
12	0.06	0.76
13	0.01	-1.21

DATA SET - **c**

This function was derived from a function of Felkel (1951). It was designed to model the displacement of the shank during walking. The functions used to produce the criterion data were:-

For $t < 0.85$ s

$$f(t) = -55.1\ t + 427\ t^3 - 342\ t^4 \quad [B.9]$$

$$f'(t) = -55.1 + 1281\ t^2 - 1368\ t^3 \quad [B.10]$$

$$f''(t) = 2562\ t - 4104\ t^2 \quad [B.11]$$

For $t > 0.85$ s

$$f(t) = 579.97 - 304.32\ t - 241.77\ t^{-1} \quad [B.12]$$

$$f'(t) = -304.32 + 241.77\ t^{-2} \quad [B.13]$$

$$f''(t) = 483.54\ t^{-3} \quad [B.14]$$

Where:-

$0 < t < 1.00$ s

$$\Delta t = \frac{1}{91}$$

For the noisy data set generated from this function the noise had a standard deviation of 0.5, ($\sigma_e = 0.5$).

DATA SET - **d**

This data set was generated from a function proposed by Trujillo and Busby (1983) for testing techniques

designed to differentiate noisy data. The criterion data were obtained from:-

For $0 < t < 4.0$

$$f(t) = \frac{1}{\pi^2} \sin(\pi t) \quad [B.15]$$

$$f'(t) = \frac{1}{\pi} \cos(\pi t) \quad [B.16]$$

$$f''(t) = -\sin(\pi t) \quad [B.17]$$

For $4.0 < t < 5.0$

$$f(t) = \frac{1}{\pi}(t - 4) \quad [B.18]$$

$$f'(t) = \frac{1}{\pi} \quad [B.20]$$

$$f''(t) = 0 \quad [B.19]$$

Where:-

$0 < t < 5.0$

$\Delta t = \frac{1}{40}$ $(n = 200)$

For the noisy data set generated from this function the noise had a standard deviation of 0.025, (σ_e = 0.025).

DATA SET - **e**

This data set was presented by Cappozzo (1982) and used part of the function presented for data set **b**. The criterion data were obtained from:-

$$f(t) = k\left(t - \frac{p}{2}\right)^2 + \sum_{i=1}^{13} a_i \sin\left(i\ w_o t + \phi_i\right) \quad [B.20]$$

$$f'(t) = (2\ k\ t) - (k\ p) + \sum_{i=1}^{13} i\ w_o\ a_i \cos\left(i\ w_o\ t + \phi_i\right) \quad [B.21]$$

$$f''(t) = (2k) - \sum_{i=1}^{13} \left(i\ w_o\right)^2 a_i \sin\left(i\ w_o\ t + \phi_i\right) \quad [B.22]$$

Where:-

$k = 0$

$0 < t < 1.0$ s

$$\Delta t = \frac{1}{91} \qquad n = 91$$

$$P = \Delta t \ (n - 1) - \frac{\Delta t}{2}$$

For the noisy data set generated from this function the noise had a standard deviation of 0.5, ($\sigma_e = 0.5$).

DATA SET - **f**

This data set was presented by Bar, Eden, Ishai and Seliktar (1979) for the investigation of numerical differentiation techniques. The criterion data were obtained from:-

$$f(t) = \cos(2.\pi.4.t) + 0.5 \ \sin(2.\pi.12.t) \qquad [B.23]$$

$$f'(t) = [(2.\pi.12).\cos(2.\pi.12.t)] - [(2.\pi.4).\sin(2.\pi.4.t)] \qquad [B.24]$$

$$f''(t) = [- (2.\pi.12)^2.\sin(2.\pi.12.t)] - [(2.\pi.4)^2.\cos(2.\pi.4.t)] \qquad [B.25]$$

Where:-

$$0 \leq t \leq 0.255 \ s$$

$$\Delta t = \frac{1}{400} \qquad (n = 101)$$

For the noisy data set generated from this function the noise had a standard deviation of 0.025, ($\sigma_e = 0.025$).

APPENDIX C

INERTIAL PROPERTIES OF GEOMETRIC SOLIDS

To determine the inertial properties of body segments these segments have been modelled as geometric solids. This appendix gives the formulae necessary to calculate the inertial properties of the geometric solids used in this study.

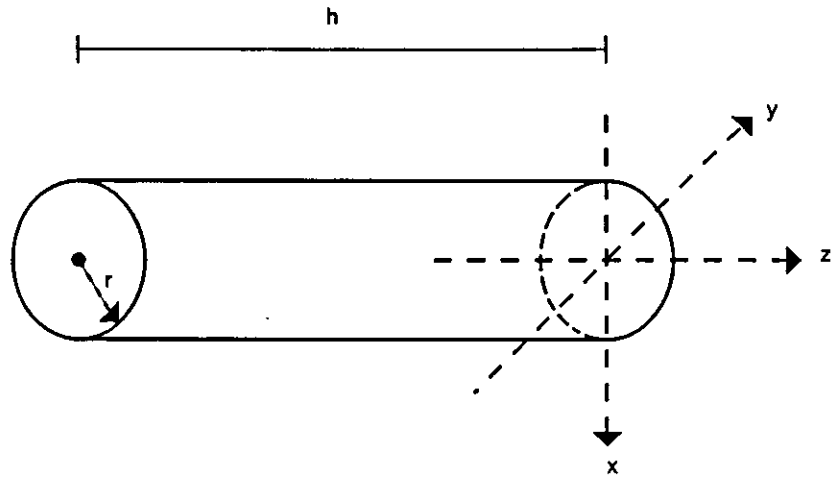

For this cylinder, the following equations apply:-

$$V = \pi.h.r^2 \qquad [C.1]$$

$$M = V.\rho \qquad [C.2]$$

$$\bar{x} = 0 \qquad [C.3]$$

$$\bar{y} = 0 \qquad [C.4]$$

$$\bar{z} = \frac{h}{2} \qquad [C.5]$$

$$I_x = I_y = \frac{M\,(3r^2 + h^2)}{12} \qquad [C.6]$$

$$I_z = \frac{M\,r^2}{2} \qquad [C.7]$$

Where:-

V - is the volume of the solid

r - is the radius of the cylinder

h - is the height of the cylinder

M - is the mass of the solid

ρ - is the density of the solid

$\bar{x}$, $\bar{y}$, $\bar{z}$ - are the locations of the centre of mass of the solid

I_x , I_y , I_z - are the moments of inertia about the x , y and z axes; with their origins passing through the mass centre

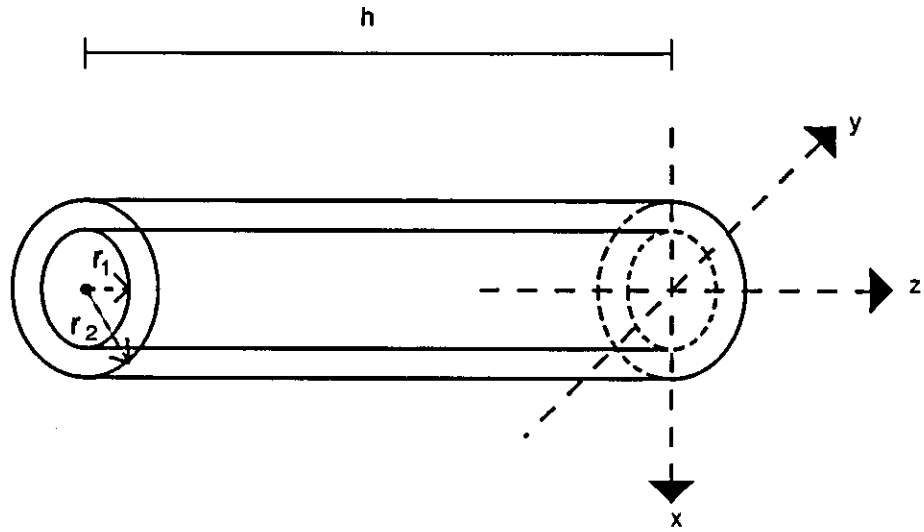

For this hollow cylinder the following equations apply:-

$$V = \pi.h\left(r_2^2 - r_1^2\right) \qquad [C.8]$$

$$M = V.\rho \qquad [C.9]$$

$$\bar{x} = 0 \qquad [C.10]$$

$$\bar{y} = 0 \qquad [C.11]$$

$$\bar{z} = \frac{h}{2} \qquad [C.12]$$

$$I_x = I_y = \frac{M\left(3.r_1^2 + 3.r_2^2 + h^2\right)}{12} \qquad [C.13]$$

$$I_z = \frac{M\left(r_1^2 + r_2^2\right)}{2} \qquad [C.14]$$

Where: -

r_1 - is the radius of the hollow

r_2 - is the radius of the outer cylinder

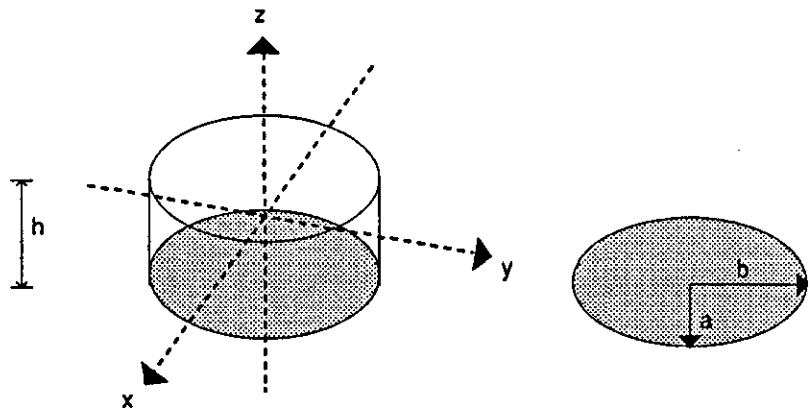

For an elliptical disc there are two radii: **a** is the semi-axis associated with the x axis, and **b** is the semi-axis associated with the y axis. If **a** is calculated as half the diameter and the perimeter of the disc is measured as U, then **b** can be calculated from:-

$$b = \left[\frac{1}{2}\left(\frac{U}{\pi}\right)^2 - a^2\right]^{\frac{1}{2}} \qquad [C.15]$$

$$V = \pi.a.b.h \qquad [C.16]$$

$$M = \rho.V \qquad [C.17]$$

$$\overline{x} = 0 \qquad [C.18]$$

$$\overline{y} = 0 \qquad [C.19]$$

$$\overline{z} = \frac{h}{2} \qquad [C.20]$$

$$I_x = \frac{M(3b^2 + h^2)}{12} \qquad [C.21]$$

$$I_y = \frac{M(3a^2 + h^2)}{12} \qquad [C.22]$$

$$I_z = \frac{M(a^2 + b^2)}{4} \qquad [C.23]$$

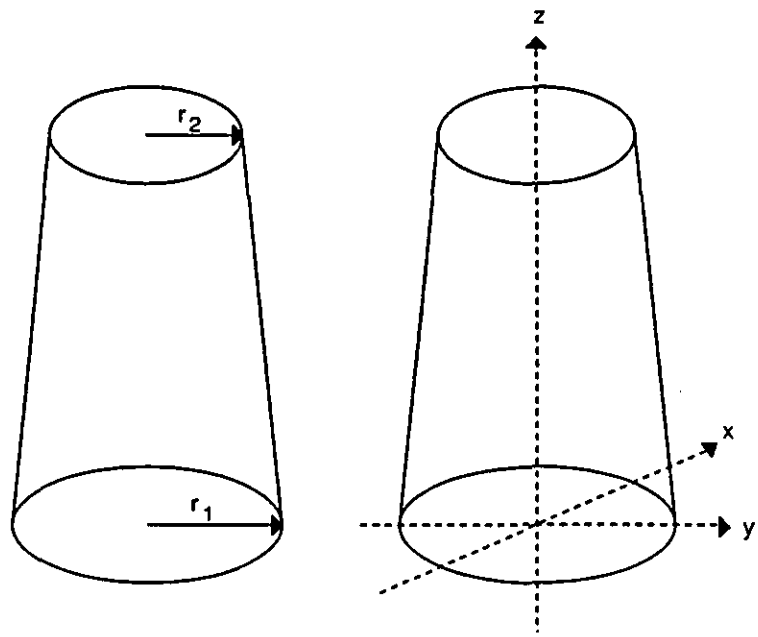

For this truncated cone, the following equations apply:-

$$V = \frac{\pi}{3} \cdot h.\left(r_1^2 + 2\, r_1\, r_2 + 3\, r_2^2\right) \qquad [C.23]$$

$$M = \rho.V \qquad [C.24]$$

$$\overline{x} = 0 \qquad [C.25]$$

$$\overline{y} = 0 \qquad [C.26]$$

$$\overline{z} = \frac{h}{4}\left[\frac{r_1^2 + 2\, r_1\, r_2 + 3\, r_2^2}{r_1^2 + r_1\, r_2 + r_2^2}\right] \qquad [C.27]$$

Let: $A = \frac{r_2}{r_1}$ $B = 1 + A + A^2$ [C.28] & [C.29]

$$I_x = I_y = M\left[\frac{9}{20\pi} \cdot \frac{1 + A + A^2 + A^3 + A^4}{B^2} \cdot \frac{M}{\rho h} + \frac{3h^2}{80} \cdot \frac{1 + 4A + 10A^2 + 4A^3 + A^4}{B^2}\right] \qquad [C.30]$$

$$I_z = \frac{3M}{10}\left[\frac{r_1^5 - r_2^5}{r_1^3 - r_2^3}\right] \qquad [C.31]$$

For each body segment a member reference frame is defined. The origin of this reference frame is originally at the proximal end of the segment, the precise definitions of these axes are given in section 3:2.5. The locations of the centres of mass of the sections making up the segment are all defined relative to the appropriate member reference frame. Once the location of the centre of mass of the whole system has been calculated the origin of the member reference frame is translated so that it is coincident with the centre of mass of the system. To determine the volume, mass, and location of the centre of mass these parameters are summed for all the solids used to represent the segment.

$$V = \sum_{j}^{n} \bar{v}_j \qquad [C.32]$$

Where:-

V - is the volume of the whole segment
n - is the number of solids used to represent the segment
and $\bar{v}_j$ - is the volume of the jth solid

$$M = \sum_{j}^{n} m_j \qquad [C.33]$$

Where:-

M - is the mass of the whole system
m_j - is the mass of the jth solid used to represent the segment

$$\bar{X} = \frac{\left(\sum_{j}^{n} m_j \bar{x}_j\right)}{M} \qquad [C.34]$$

$$\bar{Y} = \frac{\left(\sum_{j}^{n} m_j \bar{y}_j\right)}{M} \qquad [C.35]$$

$$\bar{Z} = \frac{\left(\sum_{j}^{n} m_j \bar{z}_j\right)}{M} \qquad [C.36]$$

Where:-

$\bar{X}, \bar{Y}, \bar{Z}$ - are the locations of centre of mass of the segment

$\bar{x}_j, \bar{y}_j, \bar{z}_j$ - are the locations the centre of mass of the jth solid used to represent the segment

To compute the moments of inertia of the segment about the principal axes, the moments of inertia of all the geometric solids must be summed using the parallel axis theorem.

$$I_x = \sum_j^n \left[\bar{I}_{xj} + M_j \left((\bar{y}_j - \bar{y})^2 + (\bar{z}_j - \bar{z})^2 \right) \right] \qquad [C.32]$$

$$I_y = \sum_j^n \left[\bar{I}_{yj} + M_j \left((\bar{x}_j - \bar{x})^2 + (\bar{z}_j - \bar{z})^2 \right) \right] \qquad [C.33]$$

$$I_z = \sum_j^n \left[\bar{I}_{zj} + M_j \left((\bar{x}_j - \bar{x}) + (\bar{y}_j - \bar{y})^2 \right) \right] \qquad [C.34]$$

Where:-

I_x, I_y, I_z - are the moments of inertia of the segment about the x , y , z axes respectively

$\bar{I}_{xj}$, $\bar{I}_{yj}$, $\bar{I}_{zj}$ - are the moments of inertia of the jth solid used to represent the segment

APPENDIX D

SOLUTION OF OBJECTIVE FUNCTIONS

In Chapters V and VI it was necessary to minimise a number of objective functions. This appendix gives the details of the procedures used to find the minimum solution to these objective functions.

The non-linear objective functions examined in section 6:4, were suitable to be solved using an analytical solution to the objective functions and associated constraints. It is possible using Lagrangian multipliers and forming the resultant Lagrangian Function, to find an analytical solution to the problem to be optimised (Bertsekas, 1976). Differentiation of the Lagrangian Function gives the minima points which can be, in some cases, analytically solved. Alternatively it forms a set of non-linear equations which can be solved eg. using Newton-Raphson method (Arora, 1989). The analytical solution for finding the minimum of the sum of the muscle forces, is presented.

The general problem is to find the minimum of:-

$$U(F_i) = \sum_{i=1}^{N} F_i^{\,p} \qquad [B.1]$$

Where:-
N - is the number of muscles
F_i - is the force in the i^{th} muscle
and p is the power to which the force is raised (p>1).

The minimum must be found subject to the constraint:-

$$g(F_i) = M - \sum_{i=1}^{N} R_i \cdot F_i = 0 \qquad [B.2]$$

Where:-
R_i - is the moment arm of the i^{th} muscle
and M is the net moment caused by all the muscles crossing a joint.

The Lagrangian Function is:-

$$L(F_i, \lambda) = U(F_i) + \lambda\, g(F_i) \qquad [B.3]$$

Where λ is a Lagrangian multiplier.

Differentiate to find the minimum:-

$$\frac{dL}{dF_i} = 0 \qquad [B.4]$$

From equation B.4, for i:-

$$\frac{dL}{dF_i} = p\,F_i^{p-1} + \lambda\,R_i = 0 \qquad [B.5]$$

Re-arrange to give:-

$$-\lambda = \frac{p\,F_i^{p-1}}{R_i} \qquad [B.6]$$

If i=j then:-

$$\frac{p\,F_j^{p-1}}{R_j} = \frac{p\,F_i^{p-1}}{R_i} \qquad [B.7]$$

Re-arrangement gives:-

$$F_i = \left[\frac{R_i}{R_j}\right]^{\left(\frac{1}{p-1}\right)} F_j \qquad [B.8]$$

Substitution of B.8 into B.2 after appropriate re-arrangement gives:-

$$F_j = M \cdot \left[R_j \cdot \sum_{i=1}^{N} \left\{\frac{R_i}{R_j}\right\}^{\frac{p}{p-1}} \right]^{-1} \qquad [B.9]$$

From B.9 the muscle forces can be calculated subject to B.1 and B.2. Equation B.8 shows that for non-linear problems (p>1) there is load sharing between the muscles. Although equation B.9 cannot be used to estimate the muscle forces for the linear case (p=1), equation B.8 indicates that in this case there is no load sharing between the muscles, because the muscle with the largest moment arm is recruited solely to produce the moment. The preceding formulation automatically constrains F_i to be greater than or equal to zero. To handle maximum and minimum constraints on the muscle forces equation B.9 is used and if one of the F_i's is above some constraint level the F_i is set to that constraint level, and the contribution of that muscle to the moment subtracted from the total moment, and the other muscle forces computed so as to satisfy the new moment. If another muscle exceeds a constraint the same procedure is repeated.

The preceding method has been used to compute the solution for the minimisation of the sum of the muscle forces, but if the sum of the muscle stress or relative muscle forces is to be minimised, the moment arm values have to be multiplied by the appropriate denominator in the objective function and a solution can then be found. The program, MUSCFOR, to compute the solution to these non-linear objective functions was coded in FORTRAN77.

SIMPLEX - was a program written to solve linear optimization problems. The FORTRAN77 code was based on that of Siddall (1982), and implements the revised simplex method. In the program slack variables were automatically introduced into the inequality constraints. The simplex algorithm was first

proposed by Dantzig (1963), and was designed to solve optimization problems with a linear objective function and linear constraints. The set of feasible solutions can be described graphically by a polyhedron (e.g. figure 6.1). The optimal solution must be at the corners of the polyhedron, therefore the simplex algorithm effectively finds the optimal solution by moving from one corner to the next until the lowest value for the objective function is obtained (assuming the function is to be minimised). The nature of the solution requires that the number of non-zero variables is less than the total number of constraints plus one. Therefore if in a two-dimensional study the only constraint is that the muscle moment should be satisfied by the predicted muscle forces, only one muscle will be predicted to be active. Therefore it is possible if sufficient constraints are not placed on a problem that the number of active muscles predicted will be a function of the mathematical technique not the objective function formulated.

SEEKER - was a program written to solve a number of non-linear optimization problems. A minimum solution was found to the objective function using the direct search method of Hooke and Jeeves (1961), with the computer program being adapted from the FORTRAN77 code of Siddall (1982). Given a feasible initial estimate of the solution the objective function is evaluated giving a value U. One of the variables is then increased by some predefined step size, if the value of U improves (i.e. becomes smaller if a minimum is required) then this value of the variable is retained if not then the variable value is reduced by the same step size, if this does not result in a improvement in U then the initial value is retained. This procedure is then repeated for the other variables. This results in a new base point, the whole procedure is repeated from new base points until a better set of values cannot be obtained. When this occurs, if the initial values are not changed then a smaller step size is used. The step size reduction continues until some user defined maximum reduction has occurred, or until a minimum is obtained. A minimum is defined as the lowest value for U found within the limits placed on number of searches and reductions in step size. The procedure which has just been described does not account for constraints, therefore running in conjunction with this routine is another routine which uses a penalty function to constrain the solution. The routine used was that of Fiacco and McCormick (1968), which if the search was tending toward using variables which defied a constraint, effectively changed the direction of the search to maintain the feasibility of the solution.

APPROXER - was a program written to solve non-linear optimization problems. The minimum for the objective function and associated constraints was found using the method of successive linear approximations (Griffith and Stewart, 1961). The computer program was based on the FORTRAN77 code of Siddall (1982). The objective function in this technique is modelled using a Taylor series approximation, in which only the linear terms are used. Once the objective function is in this linear form, a minimum for the objective function can be found using a linear programming technique. These linear approximations to the objective function are only valid close to the point for which they are formulated, so when a global minimum is sought successive linearisations of the objective function are performed. As the solution is found using a linear programming method constraints are directly considered in obtaining a solution (see notes for SIMPLEX), although the constraints may also need linearisation. Limits are placed on the number of successive linearisations, a minimum being the lowest value of U found.

APPENDIX E

RESULTS OF OBJECTIVE FUNCTIONS EVALUATION

It is the purpose of this appendix to present the results for the evaluation of the objective functions discussed in section 6:4.3. The objective functions were evaluated under three conditions, the details of these conditions are also presented in this appendix. For ease of reviewing the results, the objective functions and constraints are re-presented .

The objective functions were divided into three sets:-

Set I - the objective functions were:-

$$U1 = \sum_{i=1}^{NM} F_{Mi} \qquad U2 = \sum_{i=1}^{NM} \left(F_{Mi}\right)^2 \qquad U3 = \sum_{i=1}^{NM} \left(F_{Mi}\right)^3$$

$$U4 = \sum_{i=1}^{NM} \left(F_{Mi}\right)^{10} \qquad U5 = \sum_{i=1}^{NM} \left(F_{Mi}\right)^{100}$$

Where:-

NM - is the number of muscles

and F_{Mi} is the force produced by the i^{th} muscle.

Set II - the objective functions evaluated in this set were all concerned with the minimisation of the sum of some function of the individual muscle stresses; they were:-

$$U6 = \sum_{i=1}^{NM} \sigma_i \qquad U7 = \sum_{i=1}^{NM} (\sigma_i)^2 \qquad U8 = \sum_{i=1}^{NM} (\sigma_i)^3$$

$$U9 = \sum_{i=1}^{NM} (\sigma_i)^{10} \qquad U10 = \sum_{i=1}^{NM} (\sigma_i)^{100} \qquad U11 = \sigma$$

Where:-

σ_i - is the stress in the i^{th} muscle

$$\sigma_i = \frac{F_{Mi}}{CSA_i}$$

and CSA_i is the cross sectional area of the i^{th} muscle.

Objective function U11 was the function recommended by An et al. (1984), and requires the maximum muscle stress that is experienced by the most stressed muscles, to be minimized.

Set III - the objective functions in this set were concerned with the minimisation of the sum of the relative

muscle forces. The objective functions were:-

$$U12 = \sum_{i=1}^{NM} \frac{F_{Mi}}{F_{MMi}} \qquad U13 = \sum_{i=1}^{NM} \left[\frac{F_{Mi}}{F_{MMi}}\right]^2 \qquad U14 = \sum_{i=1}^{NM} \left[\frac{F_{Mi}}{F_{MMi}}\right]^3$$

$$U15 = \sum_{i=1}^{NM} \left[\frac{F_{Mi}}{F_{MMi}}\right]^{10} \qquad U16 = \sum_{i=1}^{NM} \left[\frac{F_{Mi}}{F_{MMi}}\right]^{100}$$

Where F_{MMi} is the maximum possible force, under current physiological conditions, of muscle i.

F_{MMi} was calculated by each of three methods; these methods were designated A, B, and C. In method A, F_{MMi} was calculated based on the force-length relationship of the muscles. In method B, F_{MMi} was calculated by considering the force-length and force-velocity relationships of the muscles, in this case using muscle fibre velocity. In method C, F_{MMi} was also calculated by taking into account the force-length and force-velocity relationships of the muscle, but in this case muscle velocity was used rather than muscle fibre velocity.

The three constraint conditions were:-
Constraint 1 - limiting muscle force so it was less than or equal to the maximum isometric force possible by the muscle (this occurs at the muscle fibres optimal length),
Constraint 2 - limiting the maximal muscle force by accounting for the current length of the muscle using the force-length model of muscle described in 5:2.2,
Constraint 3 - limiting the maximum force that the muscle can exert by taking into account the force-velocity model of muscle described in section 5:2.3. This constraint was not appropriate for condition A which was an isometric muscle action.

TABLE E.1 - Details for condition A, and results of muscle force estimation using different objective functions. (MU1 is the biceps, MU2 is the brachialis, and MU3 is the brachioradialis.)

MUSCLE	BICEPS	BRACHIALIS	BRACHIO-RADIALIS
Moment arm (m)	0.023	0.012	0.032
Constraint 1	600.6 N	1000.9 N	262.2 N
Constraint 2	556.3 N	878.8 N	92.5 N

N.B. - The maximum isometric muscle force values are used as constraint 1; constraint 2 is based on the maximum possible force the muscle can exert at its current length.

JOINT ANGLE = 130 degrees
JOINT MOMENT TO SATISFY= 20 N.m
MAXIMUM JOINT MOMENT = 34.2 N.m (based on maximum isometric force)
MAXIMUM JOINT MOMENT = 26.3 N.m (based on force-length relationship)

	MUSCLE FORCES (N)								
Objective	No Constraints			Constraint 1			Constraint 2		
Function	MU1	MU2	MU3	MU1	MU2	MU3	MU1	MU2	MU3
U1	0.0	0.0	**625.0**	504.8	0.0	**262.2**	556.3	353.8	92.5
U2	271.1	141.4	**377.1**	396.8	207.8	**262.2**	556.3	353.8	92.5
U3	288.1	208.1	**339.9**	366.6	264.8	**262.2**	538.1	388.7	92.5
U4	296.9	276.2	**308.0**	339.8	316.1	**262.2**	498.8	464.0	92.5
U5	298.4	296.4	**299.4**	332.4	330.3	**262.2**	488.0	484.8	92.5
U6	**869.6**	0.0	0.0	**600.6**	515.5	0.0	556.2	600.7	0.0
U7	409.2	593.0	**108.5**	409.2	593.0	**108.5**	421.9	611.3	92.5
U8	380.7	591.6	**129.5**	380.7	591.6	**129.5**	409.1	635.7	92.5
U9	357.7	587.0	**147.8**	357.7	587.0	**147.8**	399.1	654.9	92.5
U10	351.7	585.3	**152.8**	351.7	585.3	**152.8**	396.5	659.9	92.5
U11	351.1	585.1	**153.3**	351.1	585.1	**153.3**	396.3	660.4	92.5
U12a	**869.6**	0.0	0.0	**600.6**	515.5	0.0	556.3	600.4	0.0
U13a	271.1	141.4	**377.1**	396.8	207.0	**262.2**	556.3	353.8	92.5
U14a	288.1	208.1	**339.9**	366.6	264.8	**262.2**	538.1	388.7	92.5
U15a	296.9	276.9	**308.0**	339.8	316.1	**262.2**	498.8	464.0	92.5
U16a	298.4	296.4	**299.4**	332.4	330.3	**262.2**	488.0	484.8	92.5

N.B.- Where muscle forces are emboldened, they are greater than the physiological maximum, and where they are underlined they are equal to the physiological maximum.

TABLE E.2 - Details for condition B, and results of muscle force estimation using different objective functions. (MU1 is the biceps, MU2 is the brachialis, and MU3 is the brachioradialis.)

MUSCLE	BICEPS	BRACHIALIS	BRACHIO-RADIALIS
Moment arm (m)	0.023	0.012	0.032
Constraint 1	600.6 N	1000.9 N	262.2 N
Constraint 2	556.3 N	878.8 N	92.5 N
V_F ($m.s^{-2}$)	0.017	0.029	0.041
Constraint 3	480.0 N	572.2 N	68.1 N

N.B. - The maximum isometric muscle force values are used as constraint 1; constraint 2 is based on the maximum possible force the muscle can exert at its current length; and constraint 3 is based on the maximum possible force the muscle can exert at its current length and velocity.

JOINT ANGLE = 130 degrees
JOINT MOMENT TO SATISFY= 20 N.m
MAXIMUM JOINT MOMENT = 34.2 N.m (based on maximum isometric force)
MAXIMUM JOINT MOMENT = 26.3 N.m (based on force-length relationship)
MAXIMUM JOINT MOMENT = 20.1 N.m (based on force-velocity relationship)

Continued over page...

(TABLE 6.3 continued)

Objective	MUSCLE FORCES (N)											
	No Constraint			Constraint 1			Constraint 2			Constraint 3		
Function	MU1	MU2	MU3	MU1	MU2	MU3	MU1	MU2	MU3	MU1	MU2	MU3
U1										480.0	565.1	68.1
U2										480.0	565.1	68.1
U3										480.0	565.1	68.1
U4										480.0	565.1	68.1
U5										480.0	565.1	68.1
U6	FOR THESE VALUES SEE CONDITION A.									480.0	572.2	65.4
U7										476.3	572.2	68.1
U8										476.3	572.2	68.1
U9										476.3	572.2	68.1
U10										476.3	572.2	68.1
U11										476.3	572.2	68.1
U12a										480.0	572.2	65.4
U12b	**869.6**	0.0	0.0	**600.6**	515.5	0.0	556.3	**600.4**	0.0	480.0	572.2	65.4
U13a										480.0	572.2	65.4
U13b	**609.9**	452.2	17.1	**600.6**	468.3	17.7	**556.3**	545.5	20.6	480.0	572.2	65.4
U14a										480.0	572.2	65.4
U14b	**551.0**	518.0	34.7	**551.0**	518.0	34.7	**551.0**	518.0	34.7	480.0	572.2	65.4
U15a										477.2	572.2	67.4
U15b	**495.5**	560.4	58.7	**495.5**	560.4	58.7	**495.5**	560.4	58.7	480.0	572.2	65.4
U16a										476.3	572.2	68.1
U16b	479.6	569.0	66.9	479.6	569.0	66.9	479.6	569.0	66.9	479.6	569.0	66.9

N.B.- Where muscle forces are emboldened, they are greater than the physiological maximum, and where they are underlined they are equal to the physiological maximum.

TABLE E.3 - Details for condition C, and results of muscle force estimation using different objective functions. (MU1 is the biceps, MU2 is the brachialis, and MU3 is the brachioradialis.)

MUSCLE	BICEPS	BRACHIALIS	BRACHIO-RADIALIS
Moment arm (m)	0.036	0.020	0.053
Constraint 1	600.6 N	1000.9 N	262.2 N
Constraint 2	600.5 N	995.7 N	244.4 N
V_F ($m.s^{-2}$)	0.0376	0.000	0.1307
V_M ($m.s^{-2}$)	0.0323	0.0030	0.1451
Constraint 3	441.3 N	995.7 N	105.7 N

N.B. - The maximum isometric muscle force values are used as constraint 1; constraint 2 is based on the maximum possible force the muscle can exert at its current length; and constraint 3 is based on the force-velocity relationship of the muscles.

JOINT ANGLE = 90 degrees

JOINT MOMENT TO SATISFY= 41.4 N.m

MAXIMUM JOINT MOMENT = 55.5 N.m (based on maximum isometric force)

MAXIMUM JOINT MOMENT = 54.4 N.m (based on force-length relationship)

MAXIMUM JOINT MOMENT = 41.4 N.m (based on force-velocity relationship)

MAXIMUM JOINT MOMENT = 40.6 N.m (based on force-velocity data using muscle velocity rather than muscle fibre velocity)

	MUSCLE FORCES											
Objective	No Constraint			Constraint 1			Constraint 2			Constraint 3		
Function	MU1	MU2	MU3	MU1	MU2	MU3	MU1	MU2	MU3	MU1	MU2	MU3
U1	0.0	0.0	**781.1**	**600.6**	294.1	**262.2**	**600.5**	341.4	**244.4**	441.3	995.6	105.7
%	*100*	*100*	*638.98*	*36.10*	*-70.46*	*148.06*	*36.08*	*-65.71*	*131.22*	*0.00*	*-0.01*	*0.00*
U2	330.8	183.8	**487.1**	**583.8**	324.3	**262.2**	**600.5**	341.4	**244.4**	441.3	995.6	105.7
%	*-25.04*	*-81.54*	*360.83*	*32.29*	*-67.43*	*148.06*	*36.08*	*-65.71*	*131.22*	*0.00*	*-0.01*	*0.00*
U3	359.3	267.8	**436.0**	**540.3**	402.7	**262.2**	**558.8**	416.5	**244.4**	441.3	995.6	105.7
%	*-18.58*	*-73.10*	*312.49*	*22.43*	*-59.56*	*148.06*	*26.63*	*-58.17*	*131.22*	*0.00*	*-0.01*	*0.00*
U4	376.1	352.4	**392.7**	502.5	470.7	**262.2**	**519.7**	486.9	**244.4**	441.3	995.6	105.7
%	*-14.77*	*-64.61*	*271.52*	*13.87*	*-52.73*	*148.06*	*17.77*	*-51.10*	*131.22*	*0.00*	*-0.01*	*0.00*
U5	379.5	377.3	**381.0**	**492.2**	489.3	**262.2**	**509.1**	506.0	**244.4**	441.3	995.6	105.7
%	*-14.00*	*-62.11*	*260.45*	*11.53*	*-50.86*	*148.06*	*15.36*	*-49.18*	*131.22*	*0.00*	*-0.01*	*0.00*
U6	**1150.0**	0.0	0.0	**600.6**	988.9	0.0	**600.5**	989.1	0.0	441.3	995.6	105.7
%	*160.59*	*-100.00*	*-100.00*	*36.10*	*-0.68*	*-100.00*	*36.08*	*-0.66*	*-100.00*	*0.00*	*-0.01*	*0.00*
U7	**506.6**	781.6	**142.1**	**540.6**	**1000.9**	36.2	**543.2**	995.7	36.4	441.3	995.6	105.7
%	*14.80*	*-21.50*	*34.44*	*22.50*	*0.52*	*-65.75*	*23.09*	*0.00*	*-65.56*	*0.00*	*-0.01*	*0.00*

Continued:

	MUSCLE FORCES											
Objective	No Constraint			Constraint 1			Constraint 2			Constraint 3		
Function	MU1	MU2	MU3	MU1	MU2	MU3	MU1	MU2	MU3	MU1	MU2	MU3
U8	**478.0**	766.4	**167.3**	**505.0**	**1000.9**	60.4	**507.5**	995.7	60.7	441.3	995.6	105.7
%	*8.32*	*-23.03*	*58.28*	*14.43*	*0.52*	*-42.86*	*15.00*	*0.00*	*-42.57*	*0.00*	*-0.01*	*0.00*
U9	**454.6**	751.1	**188.9**	**471.5**	987.0	88.5	**471.5**	987.0	88.5	441.3	995.6	105.7
%	*3.01*	*-24.57*	*78.71*	*6.84*	*-0.87*	*-16.27*	*6.84*	*-0.87*	*-16.27*	*0.00*	*-0.01*	*0.00*
U10	**448.3**	746.6	**194.9**	**467.9**	966.2	98.7	**467.9**	966.2	98.7	441.3	995.6	105.7
%	*1.59*	*-25.02*	*84.39*	*6.03*	*-2.96*	*-6.62*	*6.03*	*-2.96*	*-6.62*	*0.00*	*-0.01*	*0.00*
U11	**447.7**	746.1	**195.5**	**447.7**	746.1	**195.5**	**447.7**	746.1	**195.5**	441.3	995.6	105.7
%	*1.54*	*-25.07*	*84.96*	*1.45*	*-25.07*	*84.96*	*1.45*	*-25.07*	*84.96*	*0.00*	*-0.01*	*0.00*
U12a	**1150.0**	0.0	0.0	**600.6**	988.9	0.0	**600.6**	989.1	0.0	441.3	995.6	105.7
%	*160.59*	*-100.00*	*-100.00*	*36.10*	*-0.68*	*-100.00*	*36.10*	*-0.66*	*-100.00*	*0.00*	*-0.01*	*0.00*
U12b	0.0	**2070.0**	0.0	**593.9**	**1000.9**	0.0	**596.8**	995.7	0.0	441.3	995.6	105.7
%	*-100.00*	*107.89*	*-100.00*	*34.58*	*0.52*	*-100.00*	*35.24*	*0.00*	*-100.00*	*0.00*	*-0.01*	*0.00*
U12c	0.0	**2070.0**	0.0	**593.9**	**1000.9**	0.0	**596.8**	995.7	0.0	441.3	995.6	105.7
%	*-100.00*	*107.89*	*-100.00*	*34.58*	*0.52*	*-100.00*	*35.24*	*0.00*	*-100.00*	*0.00*	*-0.01*	*0.00*
U13a	**520.9**	795.7	**127.0**	**520.9**	795.7	**127.0**	**520.9**	795.7	**127.0**	441.3	995.6	105.7
%	*18.04*	*-20.09*	*20.15*	*18.04*	*-20.09*	*20.15*	*18.04*	*-20.09*	*20.15*	*0.00*	*-0.01*	*0.00*
U13b	426.6	**1206.6**	36.0	**528.3**	**1000.9**	44.6	**530.8**	995.7	44.8	441.3	995.6	105.7
%	*-3.33*	*21.18*	*-65.94*	*19.71*	*0.52*	*-57.81*	*20.28*	*0.00*	*-57.62*	*0.00*	*-0.01*	*0.00*
U14a	**489.8**	779.5	**154.3**	**489.8**	779.5	**154.3**	**489.8**	779.5	**154.3**	441.3	995.6	105.7
%	*10.99*	*-21.71*	*45.98*	*10.99*	*-21.71*	*45.98*	*10.99*	*-21.71*	*45.98*	*0.00*	*-0.01*	*0.00*
U14b	440.1	**1111.9**	62.6	**491.1**	**1000.9**	69.9	**493.5**	995.7	70.2	441.3	995.6	105.7
%	*-0.27*	*11.67*	*-40.78*	*11.28*	*0.52*	*-33.87*	*11.83*	*0.00*	*-33.59*	*0.00*	*-0.01*	*0.00*
U14c	**478.7**	**1056.6**	57.2	**505.0**	**1000.9**	60.4	**507.5**	995.7	60.7	441.3	995.6	105.7
%	*8.47*	*6.12*	*-45.88*	*14.43*	*0.52*	*-42.86*	*15.00*	*0.00*	*-42.57*	*0.00*	*-0.01*	*0.00*
U15a	**463.9**	762.3	**178.4**	**463.9**	762.3	**178.4**	**463.9**	762.3	**178.4**	441.3	995.6	105.7
%	*5.12*	*-23.44*	*68.78*	*5.12*	*-23.44*	*68.78*	*5.12*	*-23.44*	*68.78*	*0.00*	*-0.01*	*0.00*
U15b	442.4	**1023.6**	94.4	**452.0**	**1000.9**	96.4	**454.2**	995.7	96.9	441.3	995.6	105.7
%	*0.25*	*2.80*	*-10.69*	*2.42*	*0.52*	*-8.80*	*2.92*	*0.00*	*-8.33*	*0.00*	*-0.01*	*0.00*
U15c	**471.5**	987.0	88.5	**465.4**	**1000.9**	87.4	**467.7**	995.7	87.7	441.3	995.6	105.7
%	*6.84*	*-0.87*	*-16.27*	*5.46*	*0.52*	*-17.31*	*5.98*	*0.00*	*-17.03*	*0.00*	*-0.01*	*0.00*
U16a	**457.0**	757.1	**185.0**	**457.0**	757.1	**185.0**	**457.0**	757.1	**185.0**	441.3	995.6	105.7
%	*3.56*	*-23.96*	*75.02*	*3.56*	*-23.96*	*75.02*	*3.56*	*-23.96*	*75.02*	*0.00*	*-0.01*	*0.00*
U16b	441.4	**998.2**	104.6	**441.4**	**998.2**	104.6	**442.4**	995.7	104.9	441.3	995.6	105.7
%	*0.02*	*0.25*	*-1.04*	*0.02*	*0.25*	*-1.04*	*0.25*	*0.00*	*-0.76*	*0.00*	*-0.01*	*0.00*
U16c	**467.9**	966.2	98.7	**456.4**	992.3	96.3	456.9	992.3	96.3	441.3	995.6	105.7
%	*6.03*	*-2.96*	*-6.62*	*3.42*	*-0.34*	*-8.89*	*3.54*	*-0.34*	*-8.89*	*0.00*	*-0.01*	*0.00*

N.B.- Where muscle forces are emboldened, they are greater than the physiological maximum, and where they are underlined they are equal to the physiological maximum. Figures in italics are percentage differences from criterion values.

REFERENCES

Abbott,B.C., and Aubert,X.M. (1951) Changes of energy during very slow stretches. ***Proceedings of the Royal Society***, Series B 139:104-117.

Abbott,B.C., Aubert,X.M., and Hill,A.V. (1951) The absorption of work by a muscle stretched during a single twitch or a short tetanus. ***Proceedings of the Royal Society***, Series B 139:86-104.

Abbott,B.C., and Howarth,J.V. (1973) Heat studies in excitable tissue. ***Physiological Review*** 53:120-158.

Abdel-Aziz,Y.I. (1974) Expected accuracy of convergent photos. ***Photogrammetric Engineering*** 40:1341-1346.

Abdel-Aziz,Y.I., and Karara,H.M. (1971) Direct linear transformation from comparator coordinates into object space co-ordinates in close range photogrammetry. In: ***ASP Symposium on Close Range Photogrammetry***, pp1-18, American Society of Photogrammetry, Falls, Church.

Ackland,T.R., Henson,P.W., and Bailey,D.A. (1988) The uniform density assumption: Its effect upon estimation of body segment inertial parameters. ***International Journal of Sport Biomechanics*** 4:146-155.

Adrian,E.D., and Bronk,D.W. (1929) The discharge of impulses in motor nerve fibres, Part II. The frequency of discharge in reflex and voluntary contractions. ***Journal of Physiology*** 67:119-151.

Alexander,R.M. (1968) ***Animal Mechanics***. Sidgwick and Jackson, London.

Alexander,R.S., and Johnson,P.D. (1965) Muscle stretch and theories of contraction. ***American Journal of Physiology*** 208:412-416.

Allen,D.G., Blinks,J.R., and Pendergast,F.G. (1977) Aequorin luminescence; Relation of light emission to calcium concentration - a calcium independent component. ***Science*** 195:996-998.

Amar,J. (1920) ***The Human Motor***. E.P.Dutton & Co., New York.

Amis,A.A. (1978) ***Biomechanics of the upper limb, and design of an elbow prosthesis***. Unpublished Ph.D. thesis, University of Leeds.

Amis,A.A., Dowson,D., Unsworth,A., Miller,J.H., and Wright,V. (1977) An examination of the elbow articulation with particular reference to variation of the carrying angle. ***Engineering in Medicine*** 6:3;76-80.

Amis,A.A., Dowson,D., and Wright,V. (1979) Muscle strengths and musculo-skeletal geometry of the upper limb. ***Engineering in Medicine*** 8:1;41-48.

Amis,A.A., Dowson,D., and Wright,V. (1980) Elbow joint force predictions for some strenuous isometric actions. ***Journal of Biomechanics*** 13:765-775.

Amis,A, Prochazka,A., Short,D., Trend,P.St.J., and Ward,A. (1987) Relative displacements in muscle and tendon during human arm movements. ***Journal of Physiology*** 389:37-44.

An,K.N., Hui,F.C., Morrey,B.F., Linscheid,R.L., and Chao,E.Y. (1981) Muscles across the elbow joints: A biomechanical analysis. ***Journal of Biomechanics*** 14:10;659-669.

An,K.N., Kaufman,K.R., and Chao,E.Y.S. (1989) Physiological considerations of muscle force through the elbow joint. ***Journal of Biomechanics*** 22:11/12;1249-1256.

An,K.N., Kwak,B.M., Chao,E.Y., and Morrey,B.F. (1984) Determination of muscle and joint forces: A new technique to solve the indeterminate problem. ***Journal of Biomechanical Engineering*** 106:364-367.

An,K.N., Morrey,B.F., and Chao,E.Y. (1985) Kinematics of the elbow. In: ***Biomechanics IX-A***, (Editors Winter,D.A., Norman,R.W., Well,R.P., Hayes,K.C., and Patla,A.E.), pp154-159, Human Kinetics Publishers, Champaign, Illinois.

Anderssen,R.S., and Bloomfield,P. (1974a) Numerical differentiation procedures for non-exact data. ***Numerische Mathematik*** 22:157-182.

Anderssen,R.S., and Bloomfield,P. (1974b) A time series approach to numerical differentiation. ***Technometrics*** 16:1;64-75.

Andrews,B.J., Cappozzo,A., and Gazzani,F. (1981) A quantitative method for assessment of differentiation techniques used for locomotion analysis. In: ***Computing in Medicine***, (Editors Paul,J.P., Jordan,M.M., Ferguson-Pell,M.W., and Andrews,B.J.), pp146-154, The MacMillan Press, London.

Angeles,J. (1986) Automatic computation of the screw parameters of rigid-body motions. Part I: Finitely-separated positions. ***Journal of Mechanisms, Transmissions, and Automation in Design*** 108:32-38.

Antonsson,E.K., and Mann,R.W. (1985) The frequency content of gait. **Journal of Biomechanics** 19:2;147-158.

Apkarian,J., Naumann,S., and Cairns,B. (1989) A three-dimensional kinematic and dynamic model of the lower limb. ***Journal of Biomechanics*** 22:2;143-155.

Ariano,M.A., Armstrong,R.B., and Edgerton,V.R. (1972) Hindlimb muscle fiber populations of five mammals. ***Journal of Histochemistry and Cytochemistry*** 21:51-55.

Aristotle (1955) ***Parts of Animals.*** (translation by Pech,A.L.), Harvard University Press, Cambridge, Mass.

Arora,J.S. (1989) ***Introduction to Optimum Design.*** McGraw-Hill Book Company, London.

Aubert,X.(1956) ***Le Couplage Energetique de la Contraction Musculaire.*** Arscia, Brussels.

Ayoub,M.A., Ayoub,M.M., and Ramsey,J.D. (1970) A stereometric system for measuring human motion. ***Human Factors*** 12:532-535.

Bagshaw,C.R. (1982) ***Muscle Contraction.*** Chapman and Hall, London.

Bagust,J., Knott,S., and Lewis,D.M. (1973) Isometric contractions of motor units in a fast twitch muscle of the cat. ***Journal of Physiology*** 231:87-104.

Bahill,A.T. (1981) ***Bioengineering: Biomedical, Medical and Clinical Engineering.*** Prentice-Hall, Englewood Cliffs, NJ.

Bahler,A.S. (1967) Series elastic component of mammalian skeletal muscle. ***American Journal of Physiology*** 213:1560-1564.

Bahler,A.S. (1968) Modelling of mammalian skeletal muscle. ***IEEE Transactions on Biomedical Engineering*** BME-15:249-257.

Baildon,R.W.A., and Chapman,A.E. (1983) Mechanical properties of a single equivalent muscle producing forearm supination. ***Journal of Biomechanics*** 16:10;811-819.

Baldwin,K.M., Winder,W.W., Terjung,R.L., and Holloszy,J.O. (1973) Glycolytic enzymes in different types of skeletal muscle: Adaptation to exercise. ***American Journal of Physiology*** 225:962-966.

Ball,K.R., and Pierrynowski,M.R. (1988) A modified direct linear transformation (DLT) calibration procedure to improve the accuracy of 3D reconstruction for large volumes. In: ***Biomechanics XI-B***, (Editors de Groot,G., Hollander,A.P., Huijing,P.A., and van Ingen Schenau,G.J.), pp1045-1050, Free University Press, Amsterdam.

Bankov,S., and Jorgensen,K. (1969) Maximum strength of elbow flexors with pronated and supinated forearm. ***Communications from the Danish National Association for Infantile Paralysis***, No.29.

Banus,M.G., and Zetlin,A. (1938) The relation of isometric tension to length in skeletal muscle. ***Journal of Cellular and Comparative Physiology*** 12:403-420.

Bar,A., Eden,G., Ishai,G., and Seliktar,R. (1979) A method for numerical differentiation of kinematic data. In: ***Biomechanics of Sports Games and Sports Activities***, (Editors Ayalon,A., and Natanya,A.), pp39-45, Wingate Institute for P.E. and Sport, Israel.

Baratta,R., and Solomonow,M. (1991) The effect of tendon performance viscoelastic stiffness on the dynamic performance of isometric muscle. ***Journal of Biomechanics*** 24:2;109-116.

Barbenel,J.C. (1983) The application of optimisation methods for the calculation of joint and muscle forces. ***Engineering in Medicine*** 12:1;29-43.

Barter,J.T. (1957) Estimation of the mass of body segments. ***WADC Technical Report 57-260***, Wright-Patterson Air-Force Base, Ohio.

Baskin,R.J., and Paolini,P.J. (1967) Volume change and pressure development in muscle during contraction. ***American Journal of Physiology*** 213:1025-1030.

Basmajian,J.V., and Latif,A. (1957) Integrated actions of the the chief flexors of the elbow. ***The Journal of Bone and Joint Surgery*** 39-A:5;1106-1118.

Bertsekas,D.P. (1976) Multiplier methods: A survey. ***Automatica*** 12:133-145.

Bigland-Ritchie,B. (1981) EMG/Force and fatigue of human voluntary contractions. ***Exercise and Sport Sciences Reviews*** 9:75-117.

Bean,J.C., and Chaffin,D.B. (1988) Biomechanical model calculation of muscle contraction forces: a double linear programming method. ***Journal of Biomechanics*** 21:1;59-66.

Bellemare,F., Woods,J.J., Johansson,R., and Bigland-Ritchie,B. (1983) Motor-unit discharge rates in maximal voluntary contractions of three human muscles. ***Journal of Neurophysiology*** 50:1380-1392.

Benidict,J.V., Walker,L.B., and Harris,E.H. (1968) Stress-strain characteristics and tensile strength of unembalmed human tendon. ***Journal of Biomechanics*** 1:53-63.

Bennet,M.B., Ker,R.F., Dimery,N.J., and Alexander,R.McN. (1986) Mechanical properties of various mammalian tendons. ***Journal of Zoology*** 209:537-548.

Bergemann,B.W. (1974) Three-dimensional cinematography: A flexible approach. ***Research Quarterly*** 45:302-309.

Bernstein,N.A. (1967) ***The Coordination and Regulation of Movements.*** Pergamon Press, Oxford.

Blanton,P.L., and Biggs,N.L. (1970) Ultimate tensile strength of fetal and adult human tendon. ***Journal of Biomechanics*** 3:181-189.

Blomstrand,E., and Ekblom,K.K. (1970) The needle biopsy technique for fibre type determination in human skeletal muscle - A methodological study. ***Acta Physiologica Scandinavica*** 116:437-442.

Bobbert,M.F., Brand,C., de Hann,A., Huijing,P.A., van Ingen Schenau,G.J., Rijnsburger,W.H., and Woittiez,R.D. (1986) Series elasticity of tendinous structures of the the rat EDL. ***Journal of Physiology*** 377:89P.

Bobbert,M.F., Huijing,P.A., and van Ingen Schenau,G.J. (1986) A model of the human triceps surae muscle-tendon complex applied to jumping. ***Journal of Biomechanics*** 19:11;887-898.

Bobbert,M.F., and van Ingen Schenau,G.J. (1990) Isokinetic plantar flexion: Experimental results and model calculations. ***Journal of Biomechanics*** 23:2;105-119.

van den Bogert,A.J., Hartmann,W., Schamhardt,H.C., and Sauren,A.H.J. (1988) In vivo relationship between force, EMG and length change in the deep digital flexor muscle of the horse. In: ***Biomechanics XI-A***, (Editors de Groot,G., Hollander,A.P., Huijing,P.A., and van Ingen Schenau,G.J.), pp 68-74 , Free University Press, Amsterdam.

van den Bogert,A.J., van Weeren,P.R., and Schamhardt,H.C. (1990) Correction for skin displacement errors in movement analysis of the horse. ***Journal of Biomechanics*** 23:1;97-101.

Borelli,A. (1680) ***De Motu Animalium.*** Angeli Bernabo, Rome.

Bouisset,S., and Pertuzon,E. (1968) Experimental determination of the moment of inertia of limb segments. In: ***Biomechanics***, (Editors Wartenweiler,J., Jokl,E., and Hebbelinck,M.), pp106-109, S.Karger, Basel, and University Park Press, Baltimore.

Brand,R.A., Crowninshield,R.D., Wittstock,C.E., Pedersen,D.R., Clark,C.R., and van Krieken,F.M. (1982) A model of lower extremity muscular anatomy. ***Journal of Biomechanical Engineering*** 104:304-310.

Brand,R.A., Pedersen,D,R., and Friederich,J.A. (1986) The sensitivity of muscle force predictions to changes in physiological cross-sectional area. ***Journal of Biomechanics*** 19:589-596.

Braune,W., and Fischer,O. (1987) ***The Human Gait.*** (Translation by Maquet,P., and Furlong,R.), Springer, Berlin.

Braune,W., and Fischer,O. (1889) Die rotationsmomente der beugemuskeln am ellenbogengelenk des menschen. ***Abh.d.,Konigisachs.Ges.,Mathem.-Phys.*** K1.15 (Cited by Pauwels, 1980).

Braune,W., and Fischer,C. (1889) ***The Centre of Gravity of the Human Body as Related to the Equipment of the German Infantry.*** S.Herzel Verlag, Leipzig.

Brett,J.R. (1965) The energetics of salmon. ***Scientific America*** 213:8;76-84.

Brooke,M.H., and Kaiser,K.K. (1970) Muscle fibre types: how many and what kind? ***Archives of Neurology*** 23:369-379.

Brooks,C.B., and Jacobs,A.M. (1975) The gamma mass scanning technique for inertial anthropometric measurement. ***Medicine and Science in Sports*** 7:290-294.

Brown,D.C. (1956) The simultaneous determination of the orientation and lens distortion of a photogrammetric camera. ***RCA Data Reduction Technical Report No.33*** AFMTC-TN-56-20, Astia Document No. 96626.

Brown,D.C. (1968) Advanced methods for the calibration of metric cameras. ***Paper for the U.S. Army Engineering Topographic Laboratories,*** No. DA-44-009-AMC-1457(X), DBA Systems Inc., Melbourne, Florida.

Brown,D.C. (1978) The bundle adjustment - progress and prospects. In: ***Proceedings of the Finnish Society of Photogrammetry*** 21:116-117.

Buchthal,F., and Scmalbruch,H. (1980) Motor unit of mammalian muscle. ***Physiological Reviews*** 60:1;90-142.

Buller,A.J., Eccles,J.C., and Eccles,R.M. (1960) Interactions between motoneurons and muscles in respect of the characteristic speeds of their responses. ***Journal of Physiology*** 150:417-439.

Burke,R.E. (1967) Motor unit types of cat triceps surae muscle. ***Journal of Physiology*** 193:141-160.

Burke,R.E. (1980) Motor unit types: Functional specification in motor control. ***Trends in Neurosciences*** 3:11;255-258.

Burke,R.E., and Edgerton,V.R. (1975) Motor unit properties and selective involvement in movement. ***Exercise and Sport Sciences Reviews*** 3:31-81.

Burke,R.E., Levine,D.N., Tsaris,P., and Zajac,F.E. (1973) Physiological types and histochemical profiles in motor units of cat gastrocnemius. ***Journal of Physiology*** 234:723-748.

Burrus,C.S., and Eschenbacher,P.W. (1981) An in-place in-order prime factor FFT algorithm. ***IEEE Transactions on Acoustic Speech and Signal Processing*** 29:806-816.

Busby,H.R., and Trujillo,D.M. (1985) Numerical experiments with a new differentiation filter. ***Journal of Biomechanical Engineering*** 107:293-299.

Calderdale,P.M., and Scelfo,G. (1987) A mathematical model of the locomotor apparatus. ***Engineering in Medicine*** 16:3;147-161.

Cappozzo,A. (1982) ***Head and trunk mechanics in level walking.*** Unpublished Ph.D. thesis, University of Strathclyde.

Cappozzo,A. (1983) Stereophotogrammetric system for kinesiological studies. ***Medical and Biological Engineering and Computing*** 21:217-223.

Cappozzo,A., and Gazzani,F. (1983) Comparative evaluation of techniques for the harmonic analysis of human locomotion. ***Journal of Biomechanics*** 8:5;307-320.

Cappozzo,A., Leo,T., and Pedotti,A. (1975) A general computing method for the analysis of human locomotion. ***Journal of Biomechanics*** 8:307-320.

Carlson,F.D., and Wilkie,D.W. (1974) ***Muscle Physiology.*** Prentice-Hall, Englewood Cliffs,N.J.

Cavagna, G.A., and Citterio,G. (1974) Effect of stretching on elastic characteristics and the contractile component of frog striated muscle. ***Journal of Physiology*** 239:1-14.

Cavanagh,P.R., and Gregor,R.J. (1974) The quick-release method for estimating the moment of inertia of the shank and foot. In: ***Biomechanics IV***, (Editors Nelson,R.C., and Morehouse,C.A.), pp524-530, University Park Press, Baltimore.

Cavanagh,P.R., and Williams,K.R. (1982) The effect of stride length variations on oxygen uptake during distance running. ***Medicine and Science in Sports and Exercise*** 14:30-35.

Chandler,R.F., Clauser,C.E., McConville,J.T., Reynolds,H.M., and Young,J.W. (1975) Investigation of the inertial properties of the human body. ***AMRL Technical Report 74-137***, Wright Patterson Air Force Base, Ohio.

Chao,E.Y.S. (1980) Justification af triaxial goniometer for the measurement of joint rotation. ***Journal of Biomechanics*** 13:989-1006.

Chao,E.Y., and An,K.N. (1978) Graphical interpretation of the solution to the redundant problem in

biomechanics. ***Journal of Biomechanical Engineering*** 100:159-167.

Chao,E.Y., and Morrey,B.F. (1978) Three-dimensional rotation of the elbow. ***Journal of Biomechanics*** 11:57-73.

Chapman,A.E. (1975) ***The investigation of mechanical models of muscle based on direct observations of voluntary dynamic human muscular contractions.*** Unpublished Ph.D thesis, University of London.

Chapman,A.E. (1985) The mechanical properties of human muscle. In: ***Exercise and Sport Sciences Reviews***, (Editor Terjung,R.L.), pp443-501, Collier MacMillan Publishers, London.

Chapman,A.E., Caldwell,G.E., and Selbie,S. (1984) Unpublished data referenced in Chapman (1985).

Civan,M.M., and Podolsky,R.J. (1966) Contraction kinetics of striated muscle fibers following quick changes in load. ***Journal of Physiology*** 184:511-534.

Clauser,C.E., McConville,J.T., and Young,J.W. (1969) Weight, volume and center of mass of segments of the human body. ***AMRL Technical Report 69-70***, Wright Patterson Air Force Base, Ohio.

Close,R. (1964) Dynamic properties of fast and slow skeletal muscles of the rat during development. ***Journal of Physiology*** 173:74-95.

Close,R.I. (1965) The relation between intrinsic speed of shortening and duration of the active state of muscle. ***Journal of Physiology*** 180:542-557.

Close,R.I. (1972) Dynamic properties of mammalian skeletal muscle. ***Physiological Reviews*** 52:129-197.

Cnockaert,J.C., Pertuzon,E., Goubel,F., and Lestienne,F. (1978) Series-elastic component in normal human muscle. In: ***Biomechanics VI-A***, (Editors Asmussen,E., and Jorgenson,K.), pp73-78, University Park Press, Baltimore.

Cohen,H., and Muncaster,R.G. (1988) ***Theory of Pseudo-Rigid Bodies.*** Springer, New York.

Cooley,J.W., and Tukey,J.W. (1965) An algorithm for the machine calculation of complex Fourier series. ***Maths of Computation*** 19:90;297-301.

Cooper,R.R., and Misol,S. (1970) Tendon and ligament insertion: A light and electron microscopic study. ***Journal of Bone and Joint Surgery*** 52A:1-20.

Cotes,J.E., and Meade,F. (1960) The energy expenditure and mechanical energy demand in walking. ***Ergonomics*** 3:97-119.

Cranfield,S.P. (1971) The mechanical properties of chicken latissimus dorsi muscles during tetanic contractions. ***Journal of Physiology*** 219:281-302.

Craven,P. and Wahba,G. (1979) Smoothing noisy data with spline functions: Estimating the correct degree of smoothing by the method of generalised cross-validation. ***Numerische Mathematik*** 31:377-403.

Crowninshield,R.D. (1978) Use of optimization techniques to predict muscle forces. ***Journal of Biomechanical Engineering*** 100:88-92.

Crowninshield,R.D., and Brand,R.A. (1981) A physiologically based criterion of muscle force prediction in locomotion. ***Journal of Biomechanics*** 14:2:793-801.

Crowninshield,R.D., Johnston,R.C., Andrews,J.G., and Brand,R.A. (1978) A biomechanical investigation of the human hip. ***Journal of Biomechanics*** 11:75-85.

Crowninshield,R.D., and Pope,M.H. (1975) An analytical model of the knee. In: ***A.S.M.E. 1975 Biomechanics Symposium***, (Editors Skalak,R., and Nerem,R.M.), A.S.M.E., New York.

Curtin,N.A., and Davies,,R.E. (1975) Very high tension with very little ATP breakdown by active skeletal muscle. ***Journal of Mechanochemistry and Cell Motility*** 3:147-154.

Curtin,N.A., and Woledge,R.C. (1978) Energy changes and muscular contraction. ***Physiological Reviews*** 58:690-761.

Dainis,A. (1980) Whole body and segment center of mass determination from kinematic data. ***Journal of Biomechanics*** 13:647-651.

Dale,W.C., and Baer,E. (1974) Fibre-buckling in composite systems: A model for the ultrastructure of uncalcified collagen tissues. ***Journal of Materials Science*** 9:369-382.

Dantzig,G.B. (1963) ***Linear Programming and Extensions***. Princeton University Press, Princeton, New Jersey.

Dapena,J. (1978) A method to determine the angular momentum of a human body about three orthogonal axes passing through its center of gravity. ***Journal of Biomechanics*** 11:251-256.

Dapena,J. (1979) ***A simulation method for predicting the effects of modifications in human***

airbourne movements. Unpublished Ph.D. thesis, University of Iowa.

Dapena,J., Harman,E.A., and Miller,J.A. (1982) Three-dimensional cinematography with control object of unknown shape. ***Journal of Biomechanics*** 15:11-19.

Davy,D.T., and Audu,M.L. (1987) A dynamic optimization technique for predicting muscle forces in the swing phase of gait. ***Journal of Biomechanics*** 20:2;187-201.

Davy,D.T., Kotzar,G.M., Brown,R.H., Heipe,K.G., Goldberg,V.M., Berilla,J., and Burstein,A.H. (1988) Telemetric force measurements across the hip after total arthroplasty. ***Journal of Bone and Joint Surgery*** 70-A:45-50.

Dempster,W.T. (1955) Space requirements of the seated operator. ***WADC Technical Report*** 55-159 , Aerospace Medical Research Laboratory, Wright-Patterson Air Force Base, Ohio.

Denier van der Gon,J.J., Ter Haar Romeny,B.M., and van Zuylen,E.J. (1985) Behaviour of motor units of human arm muscles: Differences between slow isometric contraction and relaxation. ***Journal of Physiology*** 359:107-118.

Denny-Brown,D. (1949) Interpretation of the electromyogram. ***Archives of Neurology and Psychiatry*** 61:99-128.

Denoth,J. (1986) The wobbling mass - a relevant variable in gait and load analysis. In: ***Proceedings of North American Congress on Biomechanics II***, pp213-214, Montreal, Quebec.

Denoth,J. (1988) Methodological problems in prediction of muscle forces. In: ***Biomechanics XI-A***, (Editors de Groot,G., Hollander,A.P., Huijing,P.A., and van Ingen Schenau,G.J.), pp 82-87 , Free University Press, Amsterdam.

Desmedt,J.E., and Godaux,E. (1977) Ballistic contractions in man: Characteristic recruitment pattern of single motor units of the tibialis anterior muscle. ***Journal of Physiology*** 264:673-693.

Dierckx,P. (1975) An algorithm for smoothing, differentiation and integration, of experimental data using spline Functions. ***Journal of Computational and Applied Mathematics*** 1:3;165-184.

Dierckx,P., and Piessens,R. (1977) Calculation of Fourier coefficients of discrete functions using cubic splines. ***Report TW 32, Applied Mathematics and Programming Division***, K.U Leuven, Belguim.

van Dijk,R., Huiskes,R., and Selvik,G. (1979) Roentgen stereophotogrammetric methods for the evaluation of the three dimensional kinematic behaviour and cruciate ligament length patterns of the human knee joint. ***Journal of Biomechanics*** 12:727-731.

Dohrmann,C.R. (1986) ***A dynamic programming approach to smoothing and differentiating data with spline functions.*** Unpublished Master's thesis, Ohio State University.

Dohrmann,C.R.,Busby,H.R., and Trujillo,D.M. (1988) Smoothing noisy data using dynamic programming and generalized cross-validation. ***Journal of Biomechanical Engineering*** 110:37-41.

Dostal,W.F., and Andrews,J.G. (1981) A three-dimensional biomechanical model of hip musculature. ***Journal of Biomechanics*** 14:11;803-812.

Drillis,R, Contini,R., and Bluestein,M. (1964) Body segment parameters. ***Artificial Limbs*** 8:1;44-66.

Dul,J., Johnson,G.E., Shiavi,R., and Townsend,M.A. (1984b) Muscle synergism - II. A minimum-fatigue criterion for load sharing between synergistic muscles. ***Journal of Biomechanics*** 17:9;675-684.

Dul,J., Townsend,M.A., Shiavi,R., and Johnson,G.E. (1984a) Muscle synergism - I. On criteria for load sharing between synergistic muscles. ***Journal of Biomechanics*** 17:9;663-673.

Ebashi,S., and Endo,M. (1968) Calcium ion and muscular contraction. ***Progress in Biophysics and Molecular Biology*** 18:125-183.

Edgerton,V.R., Roy,R.R., and Apor,P. (1986) Specific tension of human elbow flexor muscles. In: ***Biochemistry of Exercise VI***, (Editor Saltin,B.), pp 487-500, Human Kinetics Publishers, Champaign, Illinois.

Edman,K.A.P. (1979) The velocity of unloaded shortening and its relation to sarcomere length and isometric force in vertebrate muscle fibres. ***Journal of Physiology*** 291:143-159.

Edman,K.A.P.,Elzinga,G., and Noble,M.I.M. (1978) Enhancement of mechanical performance by stretching during tetanic contractions of vertebrate skeletal muscle fibres. ***Journal of Physiology*** 281:139-155.

Edman,K.A.P., Mulieri,L.A., and Scubon-Milieri,B. (1976) Non-hyperbolic force-velocity relationship in single muscle fibres. ***Acta Physiologica Scandinavica*** 98:143-156.

Eisenberg,E., Hill,T.L., and Chen,Y. (1980) Cross-bridge model of muscle contraction. ***Biophysics Journal*** 29:195-227.

Elliot,D.H., and Crawford,G.N.C. (1965) The thickness and collagen content of tendon relative to the strength and cross-sectional area of muscle. ***Proceedings of the Royal Society***, Series B 162:137-146.

Engin,A.E. (1979) Passive resistive torques about the long axes of the major human joints. ***Aviation,***

Space, and Environmental Medicine 50:1052-1057.

Engin,A.E., and Chen,S.M. (1987) Kinematic and passive resistive torques of human elbow joint complex. ***Journal of Biomechanical Engineering*** 109:318-323.

Ettema,G.J., and Huijing,P.A. (1989) Properties of tendinous structures and series elastic component of EDL muscle-tendon complex of the rat. ***Journal of Biomechanics*** 22:11/12;1209-1215.

Eykhoff,P. (1974) ***System Identification-Parameter and State Estimation.*** Wiley, New York

Faulkner,J.A., Clafin,D.R., and McCully,K.K. (1986) Power output of fast and slow fibers from human skeletal muscles. In: ***Human Muscle Power***, (Editors Jones,N.L., McCartney,N., and McComas,A.J.), pp81-94, Human Kinetics Publishers Inc., Champaign, Illinois.

Faulkner,J.A., Jones,D.A., Round,J.M., and Edwards,R.H.T. (1981) Dynamics of energetic processes in human muscle. In: ***Exercise Bioenergetics and Gas Exchange***, (Editors Ceretelli,P., and Whipp,B.J.), pp75-78, Elsevier Biomedical Press, Holland.

Felkel,E.O. (1951) Determination of acceleration from displacement-time data. ***Prosthetic Devices Research Project***, Series 11, Volume 16, Institute of Engineering Research, University of California, Berkeley.

Fenn,W.O. (1923) A quantitative comparison between the energy liberated and the work performed by the isolated sartorius muscle of the frog. ***Journal of Physiology*** 58:175-203

Fenn,W.O. (1924) The relation between the work performed and the energy liberated in muscular contraction. ***Journal of Physiology*** 58:373-395.

Fenn,W.O., Brody,H, and Petrilli,A. (1931) The tension developed by human muscles at different velocities of shortening. ***American Journal of Physiology*** 97:1-14.

Fenn,W.O., and Marsh,B.S. (1935) Muscular force at different speeds of shortening. ***Journal of Physiology*** 85:277-297.

Fiacco,A.V., and McCormick,G.P. (1968) ***Nonlinear Programming: Sequential Unconstrained Minimization Techniques***. Wiley, New York.

Fiehn,W., and Peter,J.B. (1971) Properties of the fragmented sarcoplasmic reticulum from fast and slow-twitch muscles. ***Journal of Clinical Investigation*** 50:570-573.

Fioretti,S., Germani,A., and Leo,T. (1985) Stereometry in very close-range stereophotogrammetry with

non-metric cameras for human movement analysis. ***Journal of Biomechanics*** 18:11;831-842.

Fioretti,S., and Jetto,L. (1989) Accurate derivative estimation from noisy data: a state-space approach. ***International Journal of Systems Science*** 20:1;33-53.

Fischer,O. (1909) Zur kinematik der gelenke vom typus des humeroradial gelenkes. ***Abh.D.Math-Phys.Cl.Sk.K.Sachs.Ges.*** 32:3-77.

Fischer,O. (1906) ***Theoretical Fundamentals for a Mechanics of Living Bodies, with Special Applications to Man.*** B.G.Teubner, Leipzig.

Fitzhugh,R. (1977) A model of optimal voluntary muscular control. ***Journal of Mathematical Biology*** 4:203-236.

Flitney,F.W., and Hirst,D.G. (1978) Cross-bridge detachment and sarcomere 'give' during stretch of active frog's muscle. ***Journal of Physiology*** 276:449-465.

Ford,L.E., Huxley,A.F., and Simmons,R.M. (1977) Tension responses to sudden length change in stimulated frog muscle fibres near slack length. ***Journal of Physiology*** 269:441-515.

Ford,L.E., Huxley,A.F., and Simmons,R.M. (1981) The relation of between stiffness and filament overlap in stimulated frog muscle fibres. ***Journal of Physiology*** 311:219-249.

Forsythe,G.E., Malcolm,M.A., and Moler,C.B. (1977) ***Computer Methods for Mathematical Computations.*** Prentice-Hall, Inc., Englewood Cliffs, New Jersey.

Forwood,M.R., Neal,R.J., and Wilson,B.D. (1985) Scaling segmental moments of inertia for individual subjects. ***Journal of Biomechanics*** 18:10;755-761.

Fraser,A. (1972) Comments on activation heat and its relation to activation. ***Cold Spring Harbor Symposia on Quantitative Biology*** 37:627-628.

Freund,H.J. (1983) Motor unit and muscle activity in voluntary motor control. ***Physiological Reviews*** 63:387-436.

Freund,H.J., Budingen,H.J., and Dietz,V. (1975) Activity of single motor units from human forearm muscles during voluntary isometric contractions. ***Journal of Neurophysiology*** 38:933-946.

Friberg,O. (1988) Computation of Euler parameters from multipoint data. ***Journal of Mechanisms, Transmissions, and Automation in Design*** 110:116-121.

Friederich,J.A., and Brand,R.A. (1990) Muscle fiber architecture in the human lower limb. ***Journal of Biomechanics*** 23:1;91-95.

Garnett,R.A.F., O'Donovan,M.J., Stephens,J.A., and Taylor,A. (1978) Motor unit organization of human medial gastrocnemius. ***Journal of Physiology*** 287:33-43.

Gagnon,M., and Rodrigue,D. (1979) Determination of physical properties of the forearm by anthropometry, immersion, and photographic methods. ***Research Quarterly*** 50:2;188-198.

van Gheluwe,B. (1974) A new three-dimensional filming technique involving simplified alignment and measurement procedures. In: ***Biomechanics IV***, (Editors Nelson,R.C., and Morehouse,C.A.), pp476-481, University Park Press, Baltimore.

van Gheluwe,B. (1975) Errors caused by mis-alignment of the cameras in cinematographical analysis. **Research Quarterly** 46:2;153-161.

van Gheluwe,B. (1978) Computerised three dimensional cinematography for any arbitrary camera set-up. In: ***Biomechanics VI-A***, (Editors Asmussen,E., and Jorgenson,K.), pp 343-348, University Park Press, Baltimore.

Ghosh,S.K. (1979) ***Analytical Photogrammetry***. Pergamon Press Inc., New York, U.S.A.

Gibbs,C.L. (1978) Cardiac energetics. ***Physiological Reviews*** 58:1;174-254.

Gillis,J.M., and Marechal,G. (1974) The incorporation of radioactive phosphorus-31 into ATP in glycerinated fibres stretched or released during contraction. ***Journal of Mechanochemistry and Cell Motility*** 3:55-68.

Gillis,J.M., Thomason,D., Lefevre,J., and Kretsinger,R.H. (1982) Paravalbumins and muscle relaxation: A computer simulation study. ***Journal of Muscle Research and Cell Motility*** 3:377-398.

Goldberg,L.J., and Derfler,B. (1977) Relationship among recruitment order, spike amplitude, and twitch tension of single motor units in human masseter muscle. ***Journal of Neurophysiology*** 40:879-890.

Gollnick,P.D., Piehl,K., and Saltin,B. (1974) Selective glycogen depletion pattern in human skeletal muscle fibres of man after exercise of varying intensity and varying pedal rates. ***Journal of Physiology*** 241:45-57.

Golub,G.H., Heath,M., and Wahba,G. (1979) Generalised cross-validation as a method for choosing a good ridge parameter. ***Technometrics*** 21:2;215-223.

Golub,G.H., and van Loan,C.F. (1983) ***Matrix Computations.*** North Oxford Academic Publishing Co. Ltd., Oxford.

Golub,G.H., and Reinsch,C. (1971) Singular value decomposition and least squares solutions. In: ***Handbook for Automatic Computations Vol. II: Linear Algebra,*** (Editors Wilkinson,J.H., and Reinsch,C.), pp131-154, Springer, Heidelberg.

Gordon,A.M., Huxley,A.F., and Julian,F.J. (1966) The variation in isometric tension with sarcomere length in vertebrate muscle fibres. ***Journal of Physiology*** 184:170-192.

Goubel,F., Bouisset,S., and Lestienne,F. (1971) Determination of muscular compliance in the course of movement. In: ***Medicine and Science in Sport Vol.6: Biomechanics II,*** (Editors Vredenbreght,J., and Wartenweiler,J.), pp154-158, Karger, Basel.

Goubel,F., and Pertuzon,E. (1973) Evaluation de l'elasticitie du muscle in situ par une methode de quick-release. ***Archives of Physiology and Biochemistry*** 81:697-707.

Greenwood,D.T. (1965) ***Principles of Dynamics.*** Pretice-Hall, Inc., Englewood Cliffs, New Jersey.

Grieg,H.W., Anson,B.,J., and Budinger,J.M. (1952) Variations in the form and attachments of the biceps brachii muscle. ***Quarterly Bulletin of Northwestern University Medical School,*** 26:241, (cited in Hollinshead, 1969).

Griffith,R.E., and Stewart,R.A. (1961) A nonlinear programming technique for the optimization of continuous processing systems. ***Management Science*** 7:4;379-392.

Grimby,L. (1984) Firing properties of single human motor units during locomotion. ***Journal of Physiology*** 346:195-202.

Grimby,L., and Hannerz,J. (1977) Firing rate and recruitment order of the toe extensor units in different modes of voluntary contraction. ***Journal of Physiology*** 264:865-879.

Grimby,L., Hannerz,J., and Hedman,B. (1981) The fatigue and voluntary discharge properties of single motor units in man. ***Journal of Physiology*** 316:545-554.

Grood,E.S., and Suntay,W.J. (1983) A joint coordinate system for the clinical description of three-dimensional motions: applications to the knee. ***Journal of Biomechanical Engineering*** 105:136-144.

Hagberg,M. (1979) The amplitude distribution of surface EMG in static and intermittent static muscular performance. ***European Journal of Applied Physiology*** 40:265-272.

Hahs,D.W., and Stiles,R.N. (1989) Buckle muscle tension tranducer: What does it measure ? ***Journal of Biomechanics*** 22:2;165-166.

Hall,S., and Depauw,K. (1982) A photogrammetrically based model for predicting total body mass centroid location. ***Research Quarterly*** 53:1;37-45.

Hamming,R.W. (1983) ***Digital Filters (Second Edition).*** Prentice-Hall international,Inc,London.

Hanavan,E.P. (1964) A mathematical model of the human body. ***AMRL Technical Report 64-102,*** Wright-Patterson Air Force Base, Ohio.

Hanson,R.J., and Norris,M.J. (1981) Analysis of measurements based on the singular value decomposition. ***SIAM Journal on Scientific and Statistical Computing*** 2:3;363-373.

Hardt,D.E. (1978) Determining muscle forces in the leg during normal human walking - an application and evaluation of optimiziation methods. ***Journal of Biomechanical Engineering*** 100:72-78.

Harkness,R.D. (1961) Biological functions of collagen. ***Biological Review*** 36:399-463.

Hatze,H. (1975) A new method for the simultaneous measurement of the moment of inertia, the damping coefficient and the location of the centre of mass of a body segment in situ. ***European Journal of Applied Physiology*** 34:217-226.

Hatze,H. (1976) The complete optimization of human motion. ***Mathematical Biosciences*** 28:99-135 (with correction in Math.Biosci. 37:279).

Hatze,H. (1977a) A myocybernetic control model of skeletal muscle. ***Biological Cybernetics*** 25:103-119.

Hatze,H. (1977b) The relative contribution of motor unit recruitment and rate coding to the production of static isometric muscle force. ***Biological Cybernetics*** 27:21-25.

Hatze,H. (1978) A general myocybernetic control model of skeletal muscle. ***Biological Cybernetics*** 28:143-157.

Hatze,H. (1979a) An algorithm for computing higher-order derivatives of noisy experimental data sequences. ***National Research Institute for Mathematical Sciences, Technical Report,*** TWISK 123, Pretoria, South Africa.

Hatze,H. (1979b) A model for the computational determination of parameter values of anthropomorphic segments. ***CSIR Technical Report, TWISK 79,*** Pretoria.

Hatze,H. (1980) A mathematical model for the computational determination of parameter values of anthropomorphic segments. ***Journal of Biomechanics*** 13:833-843.

Hatze,H. (1981a) The use of optimally regularized Fourier series for estimating higher-order derivatives of noisy biomechanical data. ***Journal of Biomechanics*** 14:1;13-18.

Hatze,H. (1981b) ***Myocybernetic Control Models of Skeletal Muscle.*** University of South Africa Press, Pretoria.

Hatze,H. (1981c) A comprehensive model for human motion simulation and its application to the take-off phase of the long jump. ***Journal of Biomechanics*** 14:3;135-142.

Hatze,H. (1981d) Estimation of myodynamic parameter values from observations on isometrically contracting muscle groups. ***European Journal of Applied Physiology*** 46:325-338.

Hatze,H. (1983) Computerized optimization of sports motions: An overview of possibilities, methods and recent developments. ***Journal of Sports Sciences*** 1:3-12.

Hatze,H. (1988) High-precision three-dimensional photogrammetric calibration and object space reconstruction using a modified DLT-approach. ***Journal of Biomechanics*** 21:7;533-538.

Hatze,H., and Buys,J,D. (1977) Energy-optimal controls on the mammalian neuromuscular system. ***Biological Cybernetics*** 27:9-20.

Hay,J.G. (1974) Moment of inertia of the human body. ***Kinesiology IV***, pp43-52, AAPHER, Washington.

Hay,J.G. (1987) Biomechanics of the long jump - and some wider implications. In: ***Biomechanics X-B***, (Editor Jonsson,B.), pp1193-1203, Human Kinetics Publishers Inc., Champaign, Illinois

Hay,J.G., Andrews,J.G., and Vaughan,C.L. (1983) Effects of lifting rate on elbow torques exerted during an arm curl exercise. ***Medicine and Science in Sport and Exercise*** 15:1;63-71.

Hay,J.G., and Reid,J.G. (1982) ***The Anatomical and Mechanical Bases of Human Motion.*** Prentice-Hall, Inc., Englewood Cliffs, New Jersey.

Hayes,K.C., and Hatze,H. (1977) Passive visco-elastic properties of structures spanning the the human elbow joint. ***European Journal of Applied Physiology*** 37:265-274.

Hellander,E., and Thulin,C.A. (1962) Isometric tension and myofilamental cross-sectional area in striated muscle. ***American Journal of Physiology*** 202:824-826.

Henneman,E., and Mendell,L.M. (1981) Functional organization of the motoneurone pool and its inputs. In: ***Handbook of Physiology Section 1, Volume II***, (Editor Brooks,V.B.), pp423-507, American Physiological Society, Bethesda, Maryland.

Henneman,E., Somjen,G., and Carpenter,D.O. (1965) Excitability and inhibitibility of motoneurons of different sizes. ***Journal of Neurophysiology*** 28:599-620.

Herzog,W. (1986) Influence of the amount of information about muscle properties in the cost function on the estimate of individual muscle forces. ***North American Congress on Biomechanics***, Montreal, Canada, 25-27 August.

Herzog,W. (1987a) Determination of muscle model parameters using an optimisation technique. In: ***Biomechanics X-B***, (Editor Jonsson,B.), pp1175-1179, Human Kinetics Publishers, Inc., Champaign, Illinois.

Herzog,W. (1987b) Considerations for predicting individual muscle forces in athletic movements. ***International Journal of Sports Biomechanics*** 3:128-141.

Herzog,W. (1987c) Individual muscle force estimations using non-linear optimal design. ***Journal of Neuroscience Methods*** 21:167-179.

Hill,A.V. (1938) The heat of shortening and dynamic constants of muscle. ***Proceedings of the Royal Society***, Series B 126:136-195 .

Hill,A.V. (1949a) The heat of activation and the heat of shortening in a muscle twitch. ***Proceedings of the Royal Society***, Series B 136:195-211.

Hill,A.V. (1949b) The abrupt transition from rest to activity in muscle. ***Proceedings of the Royal Society***, Series B 136:399-420.

Hill,A.V. (1950) The series elastic component of muscle. ***Proceedings of the Royal Society***, Series B 137:273-280.

Hill,A.V. (1964a) The effect of load on the heat of shortening muscle. ***Proceedings of the Royal Society***, Series B 159:297-318.

Hill,A.V. (1964b) The efficiency of mechanical power development during muscular shortening and its relation to load. ***Proceedings of the Royal Society***, Series B 159:319-324.

Hill,A.V. (1965) ***Trails and Trials in Physiology***. Edward Arnold (Pubs) Ltd., London.

Hill,A.V. (1970) ***First and Last Experiments in Muscle Mechanics.*** Cambridge University Press, Cambridge.

Hill,A.V., and Howarth,J.V. (1959) The reversal of chemical reactions in contracting muscle during an applied stretch. ***Proceedings of the Royal Society***, Series B 151:169-193 .

Hill,A.V., and Woledge,R.C. (1962) An examination of absolute values in myothermic measurements. ***Journal of Physiology*** 162:311-333.

Hill,D.K. (1968) Tension due to interaction between the sliding filaments in resting striated muscle. The effect of stimulation. ***Journal of Physiology*** 199:637-684.

Hill,T.L., Eisenberg,E., Chen,Y., and Podolsky,R.J. (1975) Some self-consistent two-state sliding filament models of muscle contraction. ***Biophysical Journal*** 15:335-372.

Hinrichs,R.N. (1985) Regression equations to predict segmental moments of inertia from anthropometric measurements. ***Journal of Biomechanics*** 18:8;621-624.

Hinrichs,R.N. (1990) Adjustments to the segment center of mass proportions of Clauser et al. (1969). ***Journal of Biomechanics*** 23:9;949-951.

Hof,A.L. (1984) EMG and muscle force: An introduction. ***Human Movement Science*** 3:119-153.

Hof,A.L., and van den Berg,J.W. (1977) Linearity between the weighted sum of of the EMGs of the human triceps surae and the total torque. ***Journal of Biomechanics*** 10:529-539.

Hof,A.L., and van den Berg,J.W. (1981a) EMG to force processing, I: An electrical analogue of the Hill muscle model. ***Journal of Biomechanics*** 14:747-758.

Hof,A.L., and van den Berg,J.W. (1981b) EMG to force processing, II: Estimation of the parameters of the Hill muscle model for the human triceps surae by means of a calf ergometer. ***Journal of Biomechanics*** 14:759-770.

Hof,A.L., and van den Berg,J.W. (1981c) EMG to force processing, III: Estimation of model parameters for the human triceps surae muscle and assessment of accuracy by means of a torque plate. ***Journal of Biomechanics*** 14:771-785.

Hof,A.L., and van den Berg,J.W. (1981d) EMG to force processing, IV: Eccentric-concentric contractions on a spring-flywheel set-up. ***Journal of Biomechanics*** 14:787-792.

Hof,A.L., Geelen,B.A., and van den Berg,Jw. (1983) Calf muscle moment, work and efficiency in level

walking; role of series elasticity. ***Journal of Biomechanics*** 16:525-537.

Hof,A.L., Pronk,C.N.A., and van Best,J,A. (1985) The moment of the calf muscles in walking and stepping. A comparison between EMG-to-force processing and kinetic analysis. In: ***Biomechanics IX-A***, (Editor Winter,D.A., Norman,R.W., Wells,R.P., Hayes,K.C., and Patla,A.E), pp478-483, Human Kinetics Publishers, Champaign, Illinois.

Hollinshead,W.H. (1969) ***Anatomy for Surgeons, Volume 3, The Back and Limbs.*** (2nd edition), Harper and Row, New York.

Holewijn,M., Plantinga,P., Woittiez,R.D., and Huijing,P.A. (1983) In vivo bundle length and the number of sarcomeres of the m.gastrocnemius of the rat. ***Journal of Anatomy*** 137:433-434.

Homsher,E. and Kean,C. (1978) Skeletal muscle energetics and metabolism. ***Annual Review of Physiology*** 40:93-131.

Homsher,E., Mommaerts,W.F.H.M., Ricchiuti,N.V., and Wallner,A. (1972) Activation heat, activation metabolism and tension-related heat in frog semitendinosus muscles. ***Journal of Physiology*** 220:601-625.

Hooke,R., and Jeeves,T.A. (1961) Direct search solution of numerical and statistical problems. ***Journal of Association for Computing Machinery*** 8:212-221.

Hu,C.L., and Schumaker,L.L. (1986) Complete spline smoothing. ***Numerische Mathematik*** 49:1;1-10.

Huang,H.K., and Wu,S.C. (1976) The evaluation of mass densities of the human body in vivo from CT scans. ***Computers in Biology and Medicine*** 6:337-343.

Hutchinson,M.F., and de Hoog,F.R. (1985) Smoothing noisy data with spline functions. ***Numerische Mathematik*** 47:99-106.

Huxley,A.F. (1957) Muscle structure and theories of contraction. ***Biophysics Journal*** 15:335-372.

Huxley,A.F. (1980) ***Reflections on Muscle.*** Liverpool University Press, Liverpool.

Huxley,A.F., and Simmons,R.M. (1971a) Mechanical properties of the cross-bridges of frog striated muscle. ***Journal of Physiology*** 218:59P-60P.

Huxley,A.F., and Simmons,R.M. (1971b) Proposed mechanism of force generation in striated muscle. ***Nature*** 233:533-538.

van Ingen Schenau,G.J. (1990) On the action of biarticular muscles, a review. ***Netherlands Journal of Zoology*** 40:3;521-540.

van Ingen Schenau,G.J., Bobbert,M.F., Ettema,G.J., de Graaf,J.B., and Huijing,P.A. (1988) A simulation of rat EDL force output based on intrinsic muscle properties. ***Journal of Biomechanics*** 21:10;815-824.

Jackson.K.M. (1979) Fitting of mathematical functions to biomechanical data. ***IEEE Transactions on Biomedical Engineering*** BME-26:2;122-124.

Jensen,R.K. (1976) Model for body segment parameters. ***Biomechanics V-B***, (Editor Komi,P.V.), pp380-386, University Park Press, Baltimore.

Jensen,R.K. (1978) Estimation of the biomechanical properties of three body types using a photogrammetric method. ***Journal of Biomechanics*** 11:349-358.

Jensen,R.H., and Davy,D.T. (1975) An investigation of muscle lines of action about the hip: a centroid line approach vs. the straight line approach. ***Journal of Biomechanics*** 8:103-110.

Jensen,R.H., and Metcalf,W.K. (1975) A systematic approach to the quantitative description of musculo-skeletal geometry. ***Journal of Anatomy*** 119:209-221.

Jetto,L. (1985) Small-computer procedure for optimal filtering of haemodynamic data. ***Medical and Biological Engineering and Computing*** 23:203-208.

Jewell,B.R., and Wilkie,D.R. (1958) An analysis of the mechanical components in frog's striated muscle. ***Journal of Physiology*** 143:515-540.

Johns,R.J., and Wright,V. (1962) Relative importance of various tissues in joint stiffness. ***Journal of Applied Physiology*** 17:5;824-828.

Johnson,M.A., Polgar,J., Weightman,D, and Appleton,D. (1973) Data on the distribution of fibre types in thirty-six human muscles. ***Journal of Neurological Sciences*** 18:111-129.

Julian,F.J. (1971) The effect of calcium on the force-velocity relation of briefly glycerinated frog muscle fibres. ***Journal of Physiology*** 218:117-145.

Julian,F,J., and Moss,R.L. (1981) Effects of calcium and ionic strength on shortening velocity and tension development in frog skinned muscle fibres. ***Journal of Physiology*** 311:179-199.

Julian,F.J., Moss,R.L., and Sollins,M.R. (1978) The mechanism for vertebrate striated muscle contraction. ***Circulation Research*** 42:1;2-14.

Julian,F.J., Rome,L.C., Stephenson,D.G., and Striz,S. (1986) The influence of free calcium on the maximum speed of shortening in skinned frog muscle fibres. ***Journal of Physiology*** 380:257-273.

Kapandji,I.A. (1970) ***The Physiology of the Joints. Volume 1.*** E & S Livingstone, Edinburgh and London.

Katch,V., Weltman,A., and Gold,E. (1974) Validity of anthropometric measurements and the segment-zone method for estimating segmental and total body volume. ***Medicine and Science in Sports*** 6:4;271-276.

Kaufman,K.R., An,K., and Chao,E.Y.S. (1989) Incorporation of muscle architecture into the muscle length-tension relationship. ***Journal of Biomechanics*** 22:8/9;943-948.

Kawai,M. (1982) Correlation between exponential processes and cross-bridge kinetics. In: ***Basic Biology of Muscle: A comparative approach.*** (Editor Twarog,B.M., Levine,R.J.C., and Dewey,M.M.), pp109-130, Raven Press, New York.

Kean,C., Homsher,E., Sarian-Garibian,V., and Zenplenyi,J. (1976) Phosphocreatine (PC) splitting by stretched frog muscle. ***Physiologist*** 19:250.

Kenefick,J.F.,Gyer,M.S., and Harp,B.F. (1972) Analytical selfcalibration. ***Photogrammetric Engineering*** 38:1117-1126.

Ker,R.F., Bennett,M.B., Bibby,S.R., Kester,R.C., and Alexander,R.McN. (1987) The spring in the arch of the human foot. ***Nature*** 325:147-149.

Ker,R.F., Dimery,N.J., and Alexander,R.McN. (1986) The role of tendon elasticity in hopping in a wallaby (Macropus rufogriseus). ***Journal of Zoology*** A208:417-428.

Kline,M. (1953) ***Mathematics in Western Culture.*** Oxford University Press, Oxford

Komi,P.V. (1973) Relationship between muscle tension EMG and velocity of contraction under concentric and eccentric work. In: ***New Developments in Electromyography and Clinical Neurophysiology,*** (Editor Desmedt,J.E.), Volume 1, pp596-606, Karger, Basel.

Komi,P.V., Salonen,M., Jarvinen,M., and Kokko,O. (1987) In vivo registration of Achilles tendon forces in man I: Methodological development. ***International Journal of Sports Medicine Supplement*** 8:3-8.

Koolstra,J.H., van Euden,T.M.G.J., Weijs,W.A., and Naeije,M. (1988) A three-dimensional mathematical model of the human masticatory system predicting maximum possible bite forces. ***Journal of Biomechanics*** 21:7:563-576.

Kukulka,C.G., and Clamman,H.P. (1981) Comparison of the recruitment and discharge properties of motor units in human bracial biceps and adductor pollicis during isometric contractions. ***Brain Research*** 219:45-55.

Lafortune,M.A., and Hennig,E.M. (1991) Contribution of angular motion and gravity to tibial acceleration. ***Medicine and Science in Sports and Exercise*** 23:3;360-363.

Lanczos,C. (1967) ***Applied Analysis.*** Pitman and Sons, London.

de Lange,A., Huiskes,R., and Kauer,J.M.G. (1990) Effects of data smoothing on the reconstruction of helical axis parameters in human joint kinematics. ***Journal of Biomechanical Engineering*** 112:107-113.

Lannergren,J., and Westerblad,H. (1987) The temperature dependence of isometric contractions of single, intact fibres dissected from a mouse foot muscle. ***Journal of Physiology*** 390:285-293.

Lanshammar,H. (1980) Precision Limits on Derivatives Obtained from Measurement Data. In: ***Biomechanics VII***, (Editors Fidelius,K. and Morecki,A.), pp586-592, Polish Publishers House and University Park Press, Baltimore.

Lanshammar,H. (1982) On precision limits for derivatives numerically calculated from noisy data. ***Journal of Biomechanics*** 15:6;459-470.

Lesh,M.D., Mansour,J.M., and Simon,S.R. (1979) A gait analysis subsystem for smoothing and differentiation of human motion data. ***Journal of Biomechanical Engineering*** 101:205-212.

Lew,W.D., and Lewis,J.L. (1977) An anthropometric scaling method with application to the knee joint. ***Journal of Biomechanics*** 10:171-181.

Lew,W.D., and Lewis,J.L. (1978) A method for calculating the in vivo ligament lengths with application to the human knee joint. ***Journal of Biomechanics*** 11:365-377.

Lewis,J.L., Lew,W.D., and Zimmerman,J.R. (1980) A nonhomogeneous anthropometric scaling method based on finite element principles. ***Journal of Biomechanics*** 13:815-824.

Lexell,J., Henriksson-Larsen,K., and Sjostrom,M. (1983) Distribution of different fibre types in human skeletal muscles 2. A study of cross-sections of whole m.vastus lateralis. ***Acta Physiologica Scandinavica*** 117:115-122.

Lippert,F.G. III (1973) The feasibility of photogrammetry as a clinical research tool. ***Journal of Biomechanics*** 6:459-473.

Lippold,O.C.J. (1952) The relation between integrated action potentials in a humna muscle and its isometric tension. ***Journal of Physiology*** 117:492-499.

London,J.T. (1981) Kinematics of the elbow. ***Journal of Bone and Joint Surgery*** 63A:529-535.

de Luca,C.J., Le Fever,R.S., McCue,M.P., and Xenakis,A.P. (1982) Behaviour of human motor units in different muscles during linearly varying contractions. ***Journal of Physiology*** 329:113-128.

Lyche,T., Schumaker,L.L., and Sepehrnoori,K. (1983) Fortran subroutines for computing smoothing and interpolating natural splines. ***Advances in Engineering Software*** 5:1;2-5.

Ma,S-P., and Zahalak,G.I. (1987) A simple self-consistent distribution-moment model for muscle: Chemical energy and heat rates. ***Mathematical Biosciences*** 84:211-230.

McClellan,J.H., Parks,T.W., and Rabiner,L.R. (1973) Program for designing optimum FIR linear phase filters. ***IEEE Transactions on Audio and Electroacoustics*** AU-21,506-526

MacConaill,M.A. (1967) The ergonomic aspects of articular mechanics. In: ***Studies on the Anatomy and Function of Bones and Joints***, (Editor Evans,F.G.), Springer Verlag, Berlin.

MacDougall,J.D., Sale,D.G., Alway,S.E., and Sutton,J.R. (1984) Muscle fiber number in biceps brachii in bodybuilders and control subjects. ***Journal of Applied Physiology*** 57:5;1399-1403.

McLaughin,T.M., Dillman,C.J., and Lardner,T.J. (1977) Biomechanical analysis with cubic splines. ***Research Quarterly*** 48:569-582.

McLaughlin,T.M., and Miller,N.R. (1980) Techniques for the evaluation of loads on the forearm prior to impact in tennis strokes. ***Journal of Mechanical Design*** 102:701-710.

Macleod,A., and Morris,J.R.W. (1987) Investigation of inherent experimental noise in kinematic experiments using superficial markers. In: ***Biomechanics X-B***, (Editor Jonsson,B.), pp1035-1039, Human Kinetics Publishers Inc., Champaign, Illinois.

McMahon,T.A., Valiant,G., and Frederick,E.C. (1987) Groucho running. ***Journal of Applied Physiology*** 62:6;2326-2337.

McPhedran,A.M., Wuerker,R.B., and Henneman,E. (1965) Properties of motor units in a homogenous red muscle (soleus) of the cat. ***Journal of Neurophysiology*** 28:71-84.

Marchand,F., Thiry,P.S., Sirois,J.P., Drouin,G., and Allard,P. (1983) Feasibility study for a 3-D bilateral motion analysis laboratory. In: ***Biomechanics IX-B***, (Editors Winter,D.A., Norman,R.W., Wells,R.P.,

Hayes,K.C., and Patla,A.E.), pp251-254, Human Kinetics Publ., Champaign, Illinois.

Martin,P.E., Mungiole,M., Marzke,M.W., and Longhill,J.M. (1989) The use of magnetic resonance imaging for measuring segment inertial properties. ***Journal of Biomechanics*** 22:4;367-376.

Martin,T.P., and Pongratz,M.B. (1974a) Mathematical correction for photographic perspective error. ***Research Quarterly*** 45:318-323.

Martin,T.P., and Pongratz,M.B. (1974b) Validation of a mathematical model for correction of photographic perspective error. In: ***Biomechanics IV***, (Editors Nelson,R.C., and Morehouse,C.A.), pp469-475, The MacMillan Press, U.S.A.

Marshall,R.N., Jensen,R.K., and Wood,G.A. (1985) A general Newtonian simulation of an n-segment open chain model. ***Journal of Biomechanics*** 18:359-367.

Marshall,R.N., Wood,G.A., and Jennings,L.S. (1989) Performance objectives in human movement: A review and application to the stance phase of normal walking. ***Human Movement Science*** 8:571-594.

Marzan,G.T., and Karara,H.M. (1975) A computer program for direct linear transformation solution of the collinearity condition and some applications of it. ***Symposium on Close Range Photogrammetric Systems***, pp420-476, American Society of Photogrammetry, Falls, Church.

Melzer,W., Rios,E., and Scneider,M.F. (1986) The removal of myoplasmic free calcium following calcium release in frog skeletal muscle. ***Journal of Physiology*** 372:261-292.

Miledi,R., Parker,I., and Scalow,G. (1977) Measurements of calcium transients in frog muscle by the use of arsenazo III. ***Proceedings of the Royal Society***, Series B 198:201-210.

Miller,D.I., and Nelson,R.C. (1973) **Biomechanics of Sport.** Henry Kimpton, London.

Miller,D.I., and Petak,K.L. (1973) Three-dimensional cinematography. In: ***Kinesiology III***, (Editor Widule,C.J.), pp14-19, American Association for Health, Physical Education, and Recreation, Washington D.C.

Miller,N.R., Shapiro,R., and McLaughlin,T.M. (1980) A technique for obtaining spatial kinematic parameters of segments of biomechanical systems from cinematographical data. ***Journal of Biomechanics*** 13:535-547.

Milner-Brown,H.S., Stein,R.B., and Lee,R.G. (1975) Synchronization of human motor units: Possible roles of exercise and supraspinal reflexes. ***Electroencephalography and Clinical Neurophysiology*** 38:245-254.

Milner-Brown,H.S., Stein,R.B., and Yemm,R. (1973a) The orderly recruitment of human motor units during voluntary isometric contractions. ***Journal of Physiology*** 230:359-370.

Milner-Brown,H.S., Stein,R.B., and Yemm,R. (1973b) Changes in firing rate of human motor units during linearly changing voluntary contractions. ***Journal of Physiology*** 230:371-390.

Mommaerts,W.F.H.M. (1969) Energetics of muscular contraction. ***Physiological Review*** 49:427-508.

Monster,A.W. and Chan,H. (1977) Isometric force production by motor units of extensor digitorum communis in man. ***Journal of Neurophysiology*** 40:1432-1443.

Morgan,D.L. (1977) Separation of active and passive components of short-range stiffness of muscle. ***American Journal of Physiology*** 232:C45-C49.

Morgan,D.L., Proske,U., and Warren,D. (1978) Measurement of muscle stiffness and the mechanism of elastic storage in hopping kangaroos. ***Journal of Physiology*** 282:253-261.

Morlock,M., and Yeadon,M.R. (1986) Regression equations for segmental inertia parameters. In: ***Proceedings of the North American Congress on Biomechanics II***, pp231-232, Montreal, Quebec.

Morrey,B.F., and An,K. (1983) Articular and ligamentous contributions to the stability of the elbow joint. ***The American Journal of Sports Medicine*** 11:5;315-319.

Morrison,J.B. (1970) The mechanics of the knee joint in relation to normal walking. ***Journal of Biomechanics*** 3:51-61.

Muhl,Z.F. (1982) Active length-tension relation and the effect of muscle pennation on fiber lengthening. ***Journal of Morphology*** 191:49-62.

Mungiole,M., and Martin,P.E. (1990) Estimating segment inertial properties: Comparison of magnetic resonance imaging with existing techniques. ***Journal of Biomechanics*** 23:10;1039-1046.

Nemeth,G., and Ohlsen,H. (1985) In vivo moment arm lengths for hip extensor muscles at different angles of hip flexion. ***Journal of Biomechanics*** 18:129-140.

Noble,M.L., and Kelley,D.L. (1969) Accuracy of tri-axial cinematographic analysis in determining parameters of curvilinear motion. ***Research Quarterly*** 40:3;643-645.

Nygaard,E., Houston,M., Suzuki,Y., Jorgensen,K., and Saltin,B. (1983) Morphology of the brachial biceps muscle and elbow flexion in man. ***Acta Physiologica Scandinavica*** 117:287-292.

Oguztoreli,M.N., and Stein,R.B. (1983) Optimal control of antagonistic muscles. ***Biological Cybernetics*** 48:91-99.

Olney,S.J., and Winter,D.A. (1985) Prediction of knee and ankle moments of force in walking from EMG and kinematic data. ***Journal of Biomechanics*** 19:9-20.

Otten,E. (1985) Morphometrics and force-length relations of skeletal muscles. In: ***Biomechanics IX-A***, (Editors Winter ,D,A., Norman,R.W., Wells,R.P, Hayes,K.C., and Patla,A.E.), pp27-32, Human Kinetics Publishers, Champaign Illinois.

Otten,E. (1987) ***A myocybernetic model of the jaw system of the rat.*** Orofacial Research Group, Bloemsingel 10,9712 KZ Groningen, The Netherlands.

Otten,E. (1988) Concepts and models of functional architecture in skeletal muscle. ***Exercise and Sport Sciences Reviews*** 16:89-137.

Panjabi,M. (1979) Validation of mathematical models. ***Journal of Biomechanics*** 12:238.

Patriarco,A.G., Mann,R.W., Simon,S.R., and Mansour,J.M. (1981) An evaluation of the approaches of optimization models in the prediction of muscle forces during human gait. ***Journal of Biomechanics*** 14:8:513-525.

Paul,J.P., and Berme,N. (1985) Significance of mathematical modelling. In: ***Biomechanics of Normal and Pathological Human Articulating Joints***, (Editors Berme,N., Engin,A.E., and da Silva,K.M.C.), pp 43-51, Martinus Nijhoff, Publishers, Dordrecht.

Pandy,M.G., and Berme,N. (1988) A numerical method for simulating the dynamics of human walking. ***Journal of Biomechanics*** 21:12;1043-1051.

Pandy,M.G., and Zajac,F.E. (1991) Optimal muscular coordination strategies for jumping. ***Journal of Biomechanics*** 24:1;1-10.

Pandy,M.G., Zajac,F.E., Sim,E., and Levine,W.S. (1990) An optimal control model for maximum-height human jumping. ***Journal of Biomechanics*** 23:12;1185-1198.

Pauly,J.E., Rushing,J.L., and Scieving,L.E. (1967) An electromyographic study of some muscles crossing the elbow joints. ***Anatomical Record*** 159:47-54.

Pauwels,F. (1980) ***Biomechanics of the Locomotor Apparatus.*** Translated by Maquet,P., and Furlong,R., Springer-Verlag, New York.

Pedersen,D.R., and Brand,R.A. (1989) Knee joint moment assumptions affect hip joint force calculations. In: ***Issues in the Modeling and Control of Biomechanical Systems***, (Editors Stein,J.L., Ashton-Miller,J.A., and Pandy,M.G.), pp1-3, American Society of Mechanical Engineers, New York.

Pedersen,D.R., Brand,R.A., Cheng,C., and Arora,J.S. (1987) Direct comparison of muscle force predictions using linear and non-linear programming. ***Journal of Biomechanical Engineering*** 109:192-199.

Pedotti,A., Krishnan,V.V., and Stark,L. (1978) Optimization of muscle-force sequencing in human locomotion. ***Mathematical Biosciences*** 38:57-76.

Penrod,D.D., Davy,D.T., and Singh,D.P. (1974) An optimization approach to tendon force analysis. ***Journal of Biomechanics*** 7:123-129.

Penrose,T., Wood,G., and Blanksby,B. (1976) The accuracy of positional data in tri-axial cinematography. ***Australian Journal for Health, Physical Education, and Recreation*** 71:7-12.

Person,R.S. (1958) An electromyographic investigation of co-ordination of the activity of antagonist muscles in man during the development of a motor habit. ***Pavlov Journal of Higher Nervous Activity*** 8:13-23.

Pettett,C.G., and Budney,D.R. (1981) On the calculation of derivatives from digital information. ***Proceedings of the Second International Symposium of Biomechanics Cinematography and High Speed Photography***, pp124-132, SPIE 291.

Pezzack,J.C.,Norman,R.W., and Winter,D.A. (1977) An assessment of derivative determining techniques used for motion analysis. ***Journal of Biomechanics*** 10:377-382.

Phillips,S.J., and Roberts,E.M. (1983) Spline solution to terminal zero acceleration problems in biomechanical data. ***Medicine and Science in Sports and Exercise*** 15:5;382-387.

Pierrynowski,M.R., and Morrison,J.B. (1985a) Estimating the muscle forces generated in the human lower extremity when walking: A physiological solution. ***Mathematical Biosciences*** 75:43-68.

Pierrynowski,M.R., and Morrison,J.B. (1985b) A physiological model for the evaluation of muscular forces in human locomotion: Theoretical aspects. ***Mathematical Biosciences*** 75:69-101.

Piessens.R. (1971) Calculation of Fourier coefficents of a function given a set of arbitrary points. ***Electronics Letters*** 7:681-682.

Plagenhoef,S.C. (1968) Computer program for obtaining kinetic data on human movement. ***Journal of***

Biomechanics 1:221-234.

Plagenhoef,S.C. (1971) ***Patterns of Human Motion.*** Prentice Hall, New jersey.

Podolsky,R.J., and Teichholz,L.E. (1970) The relation between calcium and contraction kinetics in skinned muscle fibres. ***Journal of Physiology*** 211:19-35.

Pollack,G.H. (1983) The cross-bridge theory. ***Physiological Reviews*** 63:3;1049-1113.

Powell,P.L., Roy,R.R., Kanim,P., Bello,M.A., and Edgerton,V.R. (1984) Predictability of skeletal muscle tension from architectural determinations in guinea pig hindlimbs. ***Journal of Applied Physiology*** 56:6;1715-1721.

Press,W.H., Flannery,B.P., Teukolsky,S.A., and Vetterling,W.T. (1986) ***Numerical Recipes: The Art of Scientific Computing.*** Cambridge University Press, Cambridge.

Rack,P.M.H., and Westbury,D.R. (1969) The effects of length and stimulus rate on tension in the isometric cat soleus muscle. ***Journal of Physiology*** 204:443-460.

Ragozin,D.L. (1983) Error bounds for derivative estimates based on spline smoothing of exact or noisy data. ***Journal of Approximation Theory*** 37:335-355.

Ranatunga,K.W. (1983) Temperature dependence of shortening velocity and rate of isometric tension development in rat skeletal muscle. ***Journal of Physiology*** 329:465-483.

Ranatunga,K.W. (1984) The force-velocity relation of rat fast- and slow-twitch muscles examined at different temperatures. ***Journal of Physiology*** 351:517-529.

Rau,G., and Vredenbreght,J. (1973) Surface Electromyography in relation to force, muscle length and endurance. In: ***New Developments in Electromyography and Clinical Neurophysiology,*** (Editor Desmedt,E.), pp607-622, S.Karger, Basel.

Rehunen,S., and Harkonen,M. (1980) High-energy phosphate compounds in human slow-twitch and fast-twitch muscle fibres. ***Scandinavian Journal of Clinical Laboratory Investigation*** 40:45-54.

Reinsch,C.H. (1967) Smoothing by spline functions. ***Numerische Mathematik*** 10:177-183.

Reuleaux,F. (1875) ***Theortische kinematik: Grundzuge einer Theorie des Maschinenwesens.*** F Vieweg, Braunschweig, The Kinematics of Machinery: Outline of a theory of Machines (Translated by Kennedy,A.B.W., 1963), MacMillan, London (1963)

Ridgway,E.B., and Gordon,A.M. (1975) Muscle activation: Effects of small length changes on calcium release in single fibers. ***Science*** 189:881-884.

Riemersa,D.J., and Lammertink,J.L.M.A. (1988) Calibration of the mercury-in-silastic strain gauge in tendon load experiments. ***Journal of Biomechanics*** 21:469-476.

Rodrigue,D., and Gagnon,M. (1983) The evaluation of forearm density with axial tomography. ***Journal of Biomechanics*** 16:11;907-913.

Rudel,R., and Taylor,S.R. (1973) Aequorin luminescence during contraction of amphibian skeletal muscle. ***Journal of Physiology*** 233:5P-6P.

Rugg,S.G., Gregor,R.G., Mandelbaum,B.R., and Chiu,L. (1990) In vivo moment arm calculations at the ankle using magnetic resonance imaging (MRI). ***Journal of Biomechanics*** 23:5;495-501.

Sandow,A., Taylor,S.R., and Preiser,H. (1965) Role of the action potential in excitation-contraction coupling. ***Federation Proceedings, American Society of Experimental Biology*** 24:116-1123.

Seireg,A., and Arvikar,J. (1973) A mathematical model for evaluation of forces in the lower extremities of the musculo-skeletal system. ***Journal of Biomechanics*** 6:313-326.

Seireg,A., and Arvikar,J. (1975) The prediction of muscular load sharing and joint forces in the lower extremities during walking. ***Journal of Biomechanics*** 8:89-102.

Selvik,G. (1974) ***A Roentgen stereophotogrammetric method for the study of the kinematics of the skeletal system.*** Thesis, Dept. of Anatomy, University of Lund, Lund, Sweden.

Selvik,G., Alberius,P., and Aronson,A.S. (1983) A Roentgen stereophotogrammetric system. ***Acta Radiologica Diagnosis*** 24:4;343-352.

Sexton,A.W., and Gerston,J.W. (1967) Isometric tension differences in fibers of red and white muscles. ***Science*** 157:199.

Shapiro,R. (1978) Direct linear transformation method for three-dimensional cinematography. ***Research Quarterly*** 49:197-205.

Siddall,J.N. (1982) ***Optimal Engineering Design.*** Marcel Dekker, Inc., New York.

Siegler,S., Chen,J., and Schneck,C.D. (1988) The three-dimensional kinematics and flexibility of the human ankle and subtalar joints - Part I: Kinematics. ***Journal of Biomechanical Engineering*** 110:364-373.

Siegler,S., Moskowitz,G.D., and Freedman,W. (1984) Passive and active components of the internal moment developed about the ankle joint during human ambulation. ***Journal of Biomechanics*** 17:647-652.

Simons,D., and Zuniga,E. (1970) Effect of wrist rotation on the X-Y plot of averaged biceps EMG and isometric tension. ***American Journal Physical Medicine*** 49:253-256.

Simpson,D. (1975) ***An examination of the design of an endoprothesis for the elbow.*** Unpublished M.Sc. thesis, University of Strathclyde, Glasgow.

Slepian,D. (1976) On bandwidth. ***Proceedings of the IEEE*** 64:292-300.

Smidt,G.L. (1973) Biomechanical analysis of knee flexion and extension. ***Journal of Biomechanics*** 6:79-92.

Smith,G. (1989) Padding point extrapolation techniques for the Butterworth digital filter. ***Journal of Biomechanics*** 22:8/9;967-971.

Smith,I.C.H. (1972) Energetics of activation in frog and toad muscle. ***Journal of Physiology*** 220:583-599.

Sommer,H.J., Miller,N.R., and Pijanowski,G.J. (1982) Three-dimensional osteometric scaling and normative modelling of skeletal segments. ***Journal of Biomechanics*** 15:3;171-180.

Sonnenblick,E. (1964) Series elastic and contractile elements in heart muscle: changes in muscle length. ***American Journal of Physiology*** 207:1330-1338.

Soudan,K., and Dierckx,P. (1979) Calculation of derivatives and Fourier coefficients of human motion data, while using spline functions. ***Journal of Biomechanics*** 12:21-26.

Spector,S.A., Gardiner,P.F., Zernicke,R.F., Roy,R.R., and Edgerton,V.R. (1980) Muscle architecture and force-velocity characteristics of cat soleus and medial gastrocnemius: Implications for motor control. ***Journal of Neurophysiology*** 44:951-960.

Spoor,C.W. (1984) Explanation, verification and application of helical-axis error propagation formulas. ***Human Movement Science*** 3:95-117.

Spoor,C.W., and Veldpaus,F.E. (1980) Rigid body motion calculated from spatial co-ordinates of markers. ***Journal of Biomechanics*** 13:391-393.

Sprigings,E.J., Burko,D.B., Watson,L.G., and Laverty,W.H. (1987) A evaluation of three segmental

methods used to predict the location of the total body CG for human airborne movements. ***Journal of Human Movement Studies*** 13:57-68.

Stearns,S.D. (1975) ***Digital Signal Analysis.*** Hayden Book Company Inc., New Jersey.

Stein,R.B., Oguztoreli,M.N., and Capaday,C. (1986) What is optimized muscular movements ?. In: ***Human Muscle Power***, (Editors Jones,N.L., McCartney,N., and McComas,A.J.), pp131-150, Human Kinetics Publishers Inc., Champaign, Illinois.

Steindler,A. (1970) ***Kinesiology of the Human Body Under Normal and Pathological Conditions.*** Charles C Thomas Publisher, Springfield, Illinois.

Stephens,J.A., Reinking,R.M., and Stuart,D.G. (1978) The motor unit of cat medial gastrocnemius: Electrical and mechanical properties as a function of muscle length. ***Journal of Morphology*** 146:495-512.

Stephenson,D.G., and Williams,D,A. (1981) Calcium activated force responses in fast- and slow-twitch skinned muscle fibres of the rat at difference temperatures. ***Journal of Physiology*** 317:281-302.

Stevens,J.A., and Usherwood,T.P. (1977) The mechanical properties of human motor units with special reference to their fatigability and recruitment threshold. ***Brain Research*** 125:91-97.

Stevens,J.C., Dickinson,V., and Jones,N.B. (1980) Mechanical properties of human skeletal muscle form in vitro studies of biopsies. ***Medical and Biological Engineering and Computing*** 18:1-9.

Stienen,G.J.M. Blangé,T., and Shnerr,M.C. (1978) Tension responses of frog sartorius muscle to quick ramp-shaped shortenings and some effects of metabolic inhibition. ***Pflugers Archives*** 376:97-104.

Street,S.F., and Ramsey,R.W. (1965) Sarcolemma: Transmitter of active tension in frog skeletal muscle. ***Science*** 149:1379-1380.

Sugi,H. (1972) Tension changes during and after stretch in frog muscle fibres. ***Journal of Physiology*** 225:237-253.

Taylor,C.P.S. (1969) Isometric muscle contraction and the active state: An analog computer study. ***Biophysical Journal*** 9:759-780.

Ter Haar Romeny,B.M., Denier van der Gon,J.J., and Gielen,C.A.M. (1982) Changes in recruitment order of motor units in the human biceps muscle. ***Experimental Neurology*** 40:771-783.

Ter Haar Romeny,B.M., Denier van der Gon,J.J., and Gielen,C.A.M. (1984) Relation between location of

the motor unit in the human biceps brachii and its critical firing levels for different tasks. ***Experimental Neurology*** 85:631-650.

Thames,M.D., Teichholz,L.E., and Podolsky,R.J. (1974) Ionic strength and the contraction kinetics of skinned muscle fibres. ***Journal of General Physiology*** 63:509-530.

Thorstensson,A., Sjodin,B., Tesch,P., and Karlsson,J. (1977) Actomyosin, ATPase, myokinase, CPK and LDH in human fast and slow twitch muscle fibres. ***Acta Physiologica Scandinavica*** 99:225-229.

Trujillo,D.M., and Busby,H.R. (1983) Investigation of a technique for the differentiation of empirical data. ***Journal of Dynamic Systems, Measurement, and Control*** 105:200-202.

Utreras,F. (1980) Sur le choix de parametre d'adjustement dans le lissage par fonctions spline. ***Numerische Mathematik*** 34:15-28.

Vaughan,C.L. (1982) Smoothing and differentiation of displacement-time data: An application of splines and digital filtering. ***International Journal of Bio-Medical Computing*** 13:375-385.

Vaughan,C.L., Andrews,J.G., and Hay,J.G. (1981) Selection of body segment parameters by optimization methods. ***Journal of Biomechanical Engineering*** 104:38-44.

Veldpaus,F.E., Woltring,H.J., and Dortmans,L.J.M.G. (1988) A least-squares algorithm for the equiform transformation from spatial marker co-ordinates. ***Journal of Biomechanics*** 21:1;45-54.

Verstraete,M.C., and Soutas-Little,R.W. (1990) A method for computing the three-dimensional angular velocity and acceleration of a body segment from three-dimensional position data. ***Journal of Biomechanical Engineering*** 112:114-118.

da Vinci,L. (1883) **The Literary Works of Leonardo da Vinci.** (translation by Richter,J.P.), Sampson, Low, Marston, Searle, and Rivington, London.

Wagemans,E., Willems,E.J., and Marchal,G.J. (1990) Determination of muscle fiber angle in vivo by means of ultra sound. In: ***Biomechanics of Human Movement: Applications in Rehabilitation, Sports, and Ergonomics***, (Editors Berme,N., and Cappozzo,A.), pp176-178, Bertec Corporation, Ohio.

Wagman,I.H., Pierce,D.S., and Burges,R.E. (1965) Proprioceptive influence in volitional control of individual motor units. ***Nature*** 207:957-958.

Wahba,G. (1975) Smoothing noisy data with spline functions. ***Numerische Mathematik*** 10:177-183.

Wahba,G., and Wold,S. (1975) A completely automatic french curve: Fitting spline functions by cross

validation. ***Communications in Statistics*** 4:1;1-17.

Walmsley,B., Hodgson,J.A., and Burke,R.E. (1978) Forces produced by the medial gastrcnemius and soleus muscles during locomotion in freely moving cats. ***Journal of Neurophysiology*** 41:1203-1216.

Walton,J.S. (1981) ***Close-range cine-photogrammetry: A generalised technique for quantifying gross human movement.*** Unpublished Ph.D thesis, College of Health, Physical Education, and Recreation, The Pennsylvania State University.

Wani,A.M., and Guha,S.K. (1975) A model for gradation of tension-recruitment and rate coding. ***Medical and Biological Engineering*** 13:870-875.

Weinbach,A.P. (1938) Contour maps, center of gravity, moment of inertia and surface area of the human body. ***Human Biology*** 10:356-371.

Wells,J.B. (1965) Comparison of mechanical properties between slow and fast mammalian muscles. ***Journal of Physiology*** 178:252-269.

Wendt,I.R., and Gibbs,C.L. (1973) Energy production of rat extensor digitorum longus muscle. ***American Journal of Physiology*** 224:1081-1086.

Wendt,I.R., and Gibbs,C.L. (1974) Energy production of mammalian fast and slow-twitch muscles during development. ***American Journal of Physiology*** 226:465-483.

White,S.C., Yack,H.J., and Winter,D.A. (1989) A three-dimensional musculoskeletal model for gait analysis. Anatomical variability estimates. ***Journal of Biomechanics*** 22:8/9;885-893.

Whitsett,C.E. (1963) Some dynamic response characteristics of weightless man. ***AMRL TR-63-18,*** Wright-Patterson Air Force Base, Ohio.

Wilkie,D.R. (1950) The relation between force and velocity in human muscle. ***Journal of Physiology*** 110:249-280.

Wilkie,D.R. (1956) Measurement of the series elastic component at various times during a single muscle twitch. ***Journal of Physiology*** 134:527-530.

Wilson,B.D., and Hay,J.G. (1974) Comparison of three methods for determining the angular momentum of the human body. In: ***Biomechanics V-B***, pp467-475, (Edited by Komi,P.V.), University Park Press, Baltimore.

Winter,D.A. (1979) ***Biomechanics of Human Movement.*** John Wiley and Sons, Chichester.

Winter,D.A., Sidwall,H.G., and Hobson,D.A. (1974) Measurement and reduction of noise in kinematics of locomotion. ***Journal of Biomechanics*** 7:157-159.

Winters,J.M., and Stark,L. (1985) Analysis of fundamental human movement patterns through the use of in-depth antagonistic muscle models. ***IEEE Transactions on Biomedical Engineering*** BME-32:10;826-839.

Wittenburg,J. (1977) ***Dynamics of Systems of Rigid Bodies.*** B.G.Teubner, Stuttgart.

Witzmann,F.A., Kim,D.H., and Fitts,R.H. (1983) Effect of hindlimb immobilization on the fatigability of skeletal muscle. ***Journal of Applied Physiology*** 54:5;1242-1248.

Woittiez,R.D., Huijing,P.A., Bobbert,M.F., Rozendal,R.H., and Rijnsburger,W.H. (1987) The power and force of slow and fast muscles during concentric and eccentric contractions. In: ***Biomechanics X-A***, (Editor Jonsson,B.), pp529-533, Human Kinetics Publishers, Champaign, Illinois.

Woittiez,R.D., Huijing,P.A., Boom,H.B.K., and Rozendal,R.H. (1984) A three-dimensional muscle model: A quantified relation between form and function of skeletal muscle. ***Journal of Morphology*** 182:95-113.

Wold,S. (1974) Spline functions in data analysis. ***Technometrics*** 16:1;1-11.

Woledge,R.C. (1961) The thermoelastic effect of change of tension in active muscle. ***Journal of Physiology*** 155:187-208.

Woledge,R.C. (1968) The energetics of tortoise muscle. ***Journal of Physiology*** 197:685-707.

Woledge,R.C. (1971) Heat production and chemical change in muscle. ***Progress in Biophysics and Molecular Biology*** 22:39-74.

Woltring,H.J. (1978) Simultaneous multiframe analytical calibrations (SMAC) by recourse to oblique observations of planar control distributions. In: ***Proceedings of the NATO Symposium Applications of Human Biosterometrics***, (Editor Herron,R.E.), 166:124-135.

Woltring,H.J. (1980) Planar control in multi-camera calibration for three-dimensional gait studies. ***Journal of Biomechanics*** 13:39-48.

Woltring,H.J. (1981) Comment on the paper "A technique for obtaining spatial kinematic parameters of segments of biomechanical systems from cinematographical data". ***Journal of Biomechanics*** 14:4;227.

Woltring,H.J. (1982) Estimation and precision of 3-D kinematics by analytical photogrammetry. In: ***Computing in Medicine***, (Editors Paul,J.P., Jordan,M.M., Ferguson-Pell,M.W., and Andrews,B.J.),

pp232-241, The MacMillan Press, London.

Woltring,H.J. (1985) On optimal smoothing and derivative estimation from noisy displacement data in biomechanics. ***Human Movement Science*** 4:3;229-245.

Woltring,H.J. (1986) A Fortran package for generalized, cross-validatory spline smoothing and differentiation. ***Advances in Engineering Software*** 8:2;104-113.

Woltring,H.J., and Huiskes,R. (1985) A statistically motivated approach to instantaneous helical axis estimation from noisy, sampled landmark coordinates. In: ***Biomechanics IX-B***, (Editors Winter,D.A., Norman,R.W., Well,R.P., Hayes,K.C., and Patla,A.E.), pp274-279, Human Kinetics Publishers, Champaign, Illinois.

Woltring,H.J., Huiskes,R., de Lange,A., and Veldpaus,F.E. (1985) Finite centroid and helical axis estimation from noisy landmark measurements in the study of human joint kinematics. ***Journal of Biomechanics*** 18:5;379-389.

Woltring,H.J., de Lange,A., Kauer,J.M.G., and Huiskes,R.,(1987) Instantaneous helical axis estimation via natural cross-validated splines. In: ***Biomechanics: Basic and Applied Research***, (Editors Bergmann,G., Kobler,A., and Rohlmann,A.), pp121-128, Martinus Nijhoff Publishers, Dordrecht.

Woltring,H.J., McClay,I.S., and Cavanagh,P.R. (1989) 3-D photogrammetric camera calibration without calibration structure. In: ***Proceedings of the XIIth International Congress of Biomechanics***, (Editors Gregor,R.J., Zernicke,R.F., and Whiting,W.C.), Abstract No. 197, Department of Kinesiology, University of of California, Los Angeles.

Wood,G.A. (1975) Computer models for human motion analysis. ***Australian Journal of Health, Physical Education, and Recreation*** 76:35-42.

Wood,G.A., and Jennings,L.S. (1979) On the use of spline functions for data smoothing. ***Journal of Biomechanics*** 12:477-479.

Wood,G.A., and Marshall,R.N. (1986) The accuracy of DLT extrapolation in three-dimensional film analysis. ***Journal of Biomechanics*** 19:9;781-785.

Wuerker,R.B., McPhedran,A.M., and Henneman,E. (1965) Properties of motor units in the heterogeneous pale muscle (m.gastrocnemius) of the cat. ***Journal of Neurophysiology*** 28:85-99.

Yamada,H. (1970) ***Strength of Biological Materials.*** Williams and Wilkins, Baltimore.

Yeadon,M.R. (1984) ***The mechanics of twisting somersaults.*** Unpublished Ph.D. thesis,

Loughborough University of Technology.

Yeadon,M.R., and Morlock,M. (1989) The appropriate use of regression equations for the estimation of segmental inertia parameters. ***Journal of Biomechanics*** 22:6/7;683-689.

Yellin,H. (1967) Neural regulation of enzymes in muscle fibers of red and white muscle. ***Experimental Neurology*** 1:179-194.

Yemm,R. (1977) The orderly recruitment of motor units of the masseter and temporal muscles during voluntary isometric contraction in man. ***Journal of Physiology*** 265:163-174.

Yeo,B.P. (1976) Investigations concerning the principle of minimal total muscular force. ***Journal of Biomechanics*** 9:413-416.

Yoon,Y.S., and Mansour,J.M. (1982) The passive elastic moment at the hip. ***Journal of Biomechanics*** 15:905-910.

Yoshihuku,Y., and Herzog,W. (1990) Optimal design parameters of the bicycle-rider system for maximal power output. ***Journal of Biomechanics*** 23:10;1069-1079.

Youm,Y., and Yoon,Y.S. (1978) Analytical development in the investigation of wrist kinematics. ***Journal of Biomechanics*** 12:613-621.

Youm,Y., Dryer,R.F., Thambyrajah,K., Flatt,A.E., and Sprague,B.L. (1979) Biomechanical analyses of forearm pronation-supination and elbow flexion-extension. ***Journal of Biomechanics*** 12:245-255.

Zahalak,G.I. (1981) A distribution-moment model approximation for kinetic theories of muscular contraction. ***Mathematical Biosciences*** 55:89-114.

Zahalak,G.I. (1986) A comparison of the mechanical behaviour of the cat soleus with a distribution-moment model. ***Journal of Biomechanical Engineering*** 108:131-140.

Zajac,F.E., Wicke,R.W., and Levine,W.S. (1984) Dependence of jumping performance on muscle properties when humans use only calf muscles for propulsion. ***Journal of Biomechanics*** 17:7;513-523.

Zatsiorsky,V., and Seluyanov,V. (1983) The mass and inertial characteristics of the main segments of the human body. In: ***Biomechanics VIII-B***, pp1152-1159, (Edited by Matsui,H., and Kobayashi,K.), University Park Press, Baltimore.

Zatsiorsky,V., and Seluyanov,V. (1985) Estimation of the mass and inertia characteristics of the human body by means of the best predictive regression equations. In: ***Biomechanics IX-B*** pp233-239, (Edited

by Winter,D.A., Norman,R.W., Wells,R.P., Hayes,K.C., and Patla,A.E.), Human Kinetics Publishers, Champaign, Illinois.

Zernicke,R.F., Caldwell,G., and Roberts,E.M. (1976) Fitting biomechanical data with cubic spline functions. ***Research Quarterly*** 47:9-19.

Zheng,Y., Hemami,H, and Stokes,B.T. (1984) Muscle dynamics, size principle, and stability. ***IEEE Transactions on Biomedical Engineering*** BME-31:7;489-497.

van Zuylen,E.J., van Velzen,A., and Denier van der Gon,J.J. (1988) A biomechanical model for flexion torques of human arm muscles as a function of elbow angle. ***Journal of Biomechanics*** 21:3;183-190.